

ANALYSIS OF RESIDENTIAL BUILDING ENERGY CODE COMPLIANCE FOR
NEW AND EXISTING BUILDINGS BASED ON BUILDING ENERGY
SIMULATION

A Dissertation

by

SUNGKYUN JUNG

Submitted to the Office of Graduate and Professional Studies of

Texas A&M University

in partial fulfillment of the requirements for the degree of

DOCTOR OF PHILOSOPHY

Chair of Committee,	Jeff S. Haberl
Committee Members,	Juan-Carlos Baltazar
	Wei Yan
	David E. Claridge
Head of Department,	Gregory A. Luhan

December 2020

Major Subject: Architecture

Copyright 2020 Sungkyun Jung

ABSTRACT

Currently, the International Energy Conservation Code (IECC) is the most widely-used residential building energy code in the United States. Either the IECC or IECC with amendments has been adopted by 33 states. The latest version of the IECC contains three compliance requirements, including: mandatory, prescriptive, and performance paths for compliance. The performance path includes specifications for the standard house design and the proposed design to be analyzed using whole-building energy simulations. In the performance path, the annual simulated energy cost of the proposed house must be less than the annual energy cost (or source energy usage) of the standard reference house.

Unfortunately, most of the whole-building energy simulation programs are too complicated to be used by building energy code officials or homeowners without special training. To resolve this problem, simplified simulation tools have been developed that require fewer user input parameters. Such simplified software tools have had a significant impact on the increased use of the performance-based code compliance path for residential analysis. However, many of the simplified features may not represent the energy efficient features found in an existing residence. This may mis-represent the potential energy saving when/if a house owner decides to invest in a retrofit to reduce their annual energy costs.

Currently, there are building energy simulation validation methods developed by ASHRAE, and RESNET including: ASHRAE Standard-140, IEA BESTEST, HVAC

BESTEST, and BESTEST-EX. These tests have been developed to test the algorithms of building energy performance simulation, which require complex inputs and outputs to view the test results. Unfortunately, even though two different building simulation validation programs may produce the necessary inputs/outputs for certification, they are rarely tested side-by-side or on actual residences. Furthermore, results from a simplified analysis of a building is rarely compared against a detailed simulation of an existing building. Therefore, there is a need to compare the results of a simplified simulation versus a detailed simulation of an existing residence to better determine which parameters best represent the existing house so more accurate code-compliant simulations can be performed on existing structures.

The purpose of this study is to develop an accurate, detailed simulation model of an existing single-family residence that is compared with a simplified building energy simulation of the same residence to help determine which on-site measurements can be made to help tune the simplified model so it better represents the existing residence. Such an improved building energy simulation can be used to better represent annual energy cost savings from retrofits to an existing building.

DEDICATION

I dedicate this dissertation to my father, mother, wife, and my son who loved me and helped me in many ways.

ACKNOWLEDGEMENTS

This dissertation was completed with the support and encouragement of many people, for whom I'm grateful. First of all, I would like to sincerely thank Professor Jeff Haberl for guiding me as my committee chair. He has been patiently and consistently providing the guidance I need for all the years I have studied at Texas A&M University and has supported and encouraged me to complete my doctoral study. My special thanks also to Professor Juan-Carlos Baltazar for his expert advice on IC3 modeling and many other aspects of building energy analysis. I would also like to thank Professor Wei Yan and Professor David Claridge for providing valuable advice on my dissertation as committee members.

This study utilized several resources developed by the Texas Emissions Reduction Program (TERP). In this context, I am grateful to the TERP team, which includes staff and students of the Energy Systems Laboratory for helping with this study in various ways. Finally, and most importantly, I am deeply grateful for the love, support, patience, and encouragement of my family. My father, mother, wife, and son helped me overcome many obstacles and achieve my goals.

TABLE OF CONTENTS

	Page
ABSTRACT	ii
DEDICATION.....	iv
ACKNOWLEDGEMENTS	v
TABLE OF CONTENTS	vi
LIST OF FIGURES.....	x
LIST OF TABLES.....	xvi
1. INTRODUCTION.....	1
1.1. Background	1
1.2. Purpose and Objectives.....	7
2. LITERATURE REVIEW	8
2.1. History of Residential Building Energy Codes and Standards.....	8
2.2. International Energy Conservation Code (IECC) Compliance Paths for Residential Buildings.....	13
2.3. Performance-based Residential Building Code-Compliance Software	15
2.3.1. Ekotrope	16
2.3.2. EnergyGauge USA	16
2.3.3. The International Code Compliance Calculator (IC3)	17
2.3.4. REM/Rate.....	17
2.3.5. REScheck	18
2.3.6. Summary	19
2.4. Testing Simplified Residential Building Energy Simulation Tools	19
2.4.1. IEA BESTEST.....	20
2.4.2. ASHRAE Standard 140 - 2014	24
2.4.3. Procedures for the Verification of International Energy Conservation Code (IECC) Performance Path Calculation Tools (by RESNET)	27
2.4.4. Procedures for Verification of RESNET Accredited HERS Software Tools.....	30
2.4.5. Building Energy Simulation Test (BESTEST).....	34

2.5.	Empirical Test.....	34
2.5.1.	Oak Ridge National Laboratory	35
2.5.2.	Lawrence Berkeley National Laboratory	36
2.5.3.	National Renewable Energy Laboratory	36
2.5.4.	Argonne National Laboratory.....	36
2.6.	Input Specifications for Building Energy Simulation	38
2.6.1.	International Energy Conservation Code (IECC).....	38
2.6.2.	Mortgage Industry National Home Energy Rating Systems Standards	39
2.6.3.	Building America House Simulation Protocols.....	40
2.6.4.	Prototype Residential Building Designs for Energy and Sustainability Assessment	40
2.7.	Previous Studies about Result Differences between Building Performance Simulation Tools for Building Energy Rating and Code Compliance.....	41
2.8.	Summary of Literature Review	44
3.	SIGNIFICANCE AND LIMITATIONS.....	47
3.1.	Significance of the Study	47
3.2.	Limitations of the Study.....	47
4.	RESEARCH METHODOLOGY	49
4.1.	Development of a Detailed Case-study House Simulation Model.....	53
4.1.1.	Information of the Case-study House.....	54
4.1.2.	Monthly Utility Billing Data	58
4.1.3.	Weather Data	61
4.1.4.	Eave Depth and Window Setback	71
4.1.5.	Indoor Temperatures.....	73
4.1.6.	Domestic Water Heater Inlet and Outlet Temperatures.....	84
4.1.7.	Ground Heat Transfer.....	88
4.1.8.	Trees	88
4.1.9.	Fence	92
4.1.10.	Detailed Calibrated Case-Study House Simulation.....	92
4.2.	Development of a 2015 IECC Simplified Uncalibrated House Simulation Model.....	117
4.2.1.	2009 IECC Simplified Uncalibrated Residential Base-Case Simulation Model with Air Source Heat Pump System	117
4.2.2.	2015 IECC Simplified Uncalibrated Residential Base-Case Simulation Model with Natural Gas System.....	120
4.3.	Development of a Simplified Case-study House Simulation ModelAnalysis of the Simplified Uncalibrated House Simulation Model	138

4.4.	Comparison of the Detailed and Simplified Model	138
5.	RESULTS OF THE DETAILED CALIBRATED CASE STUDY HOUSE SIMULATION MODEL	140
5.1.	Analysis of the Impact of Shading	140
5.1.1.	Window Setback.....	140
5.1.2.	Eaves	140
5.1.3.	Trees	141
5.1.4.	Fences.....	141
5.1.5.	Results of the Impact of Shading	141
5.2.	Analysis of the Impact of Unconditioned Space	144
5.2.1.	Garage	144
5.2.2.	Roof Type	145
5.2.3.	Results of the Impact of Unconditioned Space	145
5.3.	Analysis of the Impact of Domestic Hot Water Heater: Inlet and Outlet Water Temperatures.....	148
5.3.1.	Inlet Water Temperature	148
5.3.2.	Outlet Water Temperature (Tank Temperature).....	149
5.3.3.	Results of the Impact of DHW Outlet Water Temperature.....	149
5.3.1.	Results of the Impact of DHW Inlet Water Temperature	151
5.4.	Analysis of the Impact of Ground Heat Transfer	153
5.4.1.	Winkelmann’s Ground Heat Transfer.....	153
5.4.2.	Ground Heat Transfer through the Entire Surface.....	153
5.4.3.	Without Ground Heat Transfer.....	153
5.4.4.	Results of the Impact of Ground Heat Transfer	154
5.5.	Comparison of the Detailed Calibrated Model and the Simplified Uncalibrated Model.....	157
5.6.	Selected Calibrations for Improving the Accuracy of a Simplified Model	159
6.	RESULTS OF THE IECC-COMPLIANT HOUSE SIMULATION MODEL.....	164
6.1.	Analysis of the Impact of Fenestration	164
6.1.1.	Window Glazing.....	164
6.1.2.	Window Frame	187
6.2.	Shading (Roof Eave and Window Setback)	192
6.2.1.	Roof Eave.....	192
6.2.2.	Window Setback.....	195
6.3.	Ground Heat Transfer.....	197
6.4.	Attic and the Duct Model.....	203
7.	SUMMARY AND FUTURE RECOMMENDATIONS	207
7.1.	Summary of the Case-Study House Simulation Analysis	207

7.2.	Summary of the IECC House Simulation Analysis	208
7.3.	Summary of the Comparison of the Detailed Calibrated Model and the Simplified Uncalibrated Model	209
7.4.	Summary of the Selected Calibrations for Improving the Accuracy of a Simplified Model.....	209
7.5.	Recommendations for Future Research	210
REFERENCES.....		212

LIST OF FIGURES

	Page
Figure 2.1: Building Energy Codes and Standards.....	12
Figure 4.1: Overall Methodology- Phase I: Analysis of Case-Study House Simulation.....	51
Figure 4.2: Overall Methodology- Phase II: Analysis of the IECC House Simulation.....	52
Figure 4.3: Front View (Southwest) of the Case-study House	54
Figure 4.4: Back View (Northwest) of the Case-study House	55
Figure 4.5: Side View (Northwest) of the Case-study House.....	55
Figure 4.6: Side View (Northeast) of the Case-study House.....	56
Figure 4.7: Monthly Electricity Use for the Case-study House	59
Figure 4.8: Average Billing Period Outdoor Temp. vs. Monthly Average Daily Electricity Use	59
Figure 4.9: Monthly Natural Gas Use for the Case-study House.....	60
Figure 4.10: Average Billing Period Outdoor Temp. vs. Monthly Average Daily Natural Gas Use.....	61
Figure 4.11: Solar Test Bench.....	62
Figure 4.12: Webpage of NCEI	63
Figure 4.13: Hourly Dry Bulb Temperature (8/1/2018 through 7/8/2019).....	68
Figure 4.14: Hourly Wet Bulb Temperature (8/1/2018 through 7/8/2019).....	68
Figure 4.15: Hourly Dew Point Temperature (8/1/2018 through 7/8/2019).....	69
Figure 4.16: Hourly Wind Speed (8/1/2018 through 7/8/2019)	69
Figure 4.17: Hourly Global Solar Radiation (8/1/2018 through 7/8/2019).....	70
Figure 4.18: Hourly Direct Normal Solar Radiation (8/1/2018 through 7/8/2019)	70

Figure 4.19: Eave Depth of the Case-study House: 1.5 ft	71
Figure 4.20: Window Setback of the Case-study House: 3 inches.....	73
Figure 4.21: Measured DHW Closet, Garage, Attic, House (Room) Temperatures	74
Figure 4.22: Measured 15-minute DHW Closet, Garage, Attic, House (Room) Temperatures from 3/5/19 to 3/16/19	74
Figure 4.23: Measured 15-minute DHW Closet, Garage, Attic, House (Room) Temperatures from 3/19/19 to 3/27/19	75
Figure 4.24: Measured 15-minute DHW Closet, Garage, Attic, House (Room) Temperatures from 7/15/19 to 7/24/19	75
Figure 4.25: Measured 1-minute DHW Closet, Garage, Attic, House (Room) Temperatures from 11/5/19 to 11/9/19.....	76
Figure 4.26: Measured 15-minute Attic Temperature with Measured Outdoor Temperature and Solar Radiation from 3/8/19 to 3/14/19	77
Figure 4.27: Measured 15-minute Attic Temperature with Measured Outdoor Temperature and Solar Radiation from 7/16/19 to 7/22/19	77
Figure 4.28: Measured DHW Closet Temperature Versus the Corresponding Outside Air Temperature (From 3/5/19 to 11/9/19).....	79
Figure 4.29: Measured Garage Temperature Versus the Corresponding Outside Air Temperature (From 3/5/19 to 11/9/19)	79
Figure 4.30: Measured Attic Temperature Versus the Corresponding Outside Air Temperature (From 3/5/19 to 11/9/19)	80
Figure 4.31: Measured House Temperature Versus the Corresponding Outside Air Temperature (From 3/5/19 to 11/9/19)	80
Figure 4.32: Comparison of Measured DHW Closet Temperature and the Predicted Temperature	82
Figure 4.33: Comparison of Measured Garage Temperature and the Predicted Temperature	82
Figure 4.34: Comparison of Measured Attic Temperature and the Predicted Temperature	83

Figure 4.35: Comparison of Measured House Temperature and the Predicted Temperature	83
Figure 4.36: Measurement Sensors for Domestic Hot Water Heater	84
Figure 4.37: Measured DHW Inlet Water, DHW Outlet Water (Water Tank), DHW Closet, and Outdoor air Temperatures and Solar Radiation	85
Figure 4.38: Measured DHW Inlet Water, DHW Outlet Water (Water Tank), DHW Closet, and Outdoor air Temperatures and Solar Radiation for Eight Days (5/12/2020 to 5/20/2020)	85
Figure 4.39: Comparison of Selected Inlet Water Temperatures	86
Figure 4.40: 5-minute Continuous Inlet Water Temperatures	87
Figure 4.41: Daily Maximum Temperatures of Measured Outlet Water Temperatures.....	87
Figure 4.42: Example of Trees in the Case-Study House.....	89
Figure 4.43: Tree Types and Locations in the Case-study House	90
Figure 4.44: Tree Modeling of DOE-2.1E Building Energy Simulation.....	90
Figure 4.45: Tree Shading (Solar Transmittance) Schedules	91
Figure 4.46: Fence Modeling of DOE-2.1E Building Energy Simulation	92
Figure 4.47: Monthly Average Daily Electricity Usage Versus Monthly Average Outdoor Temperature	94
Figure 4.48: Simulated Electricity Usage Versus Measured Electricity Usage.....	94
Figure 4.49: Monthly Average Daily Natural Gas Usage Versus Monthly Average Outdoor Temperature.....	95
Figure 4.50: Simulated Natural Gas Usage Versus Measured Natural Gas Usage.....	95
Figure 4.51: Room Temperature for Heating Season (before Calibration)	98
Figure 4.52: Room Temperature for Cooling Season (before Calibration).....	98
Figure 4.53: Room Temperature for Heating Season (after Calibration).....	99
Figure 4.54: Room Temperature for Cooling Season (After Calibration).....	99

Figure 4.55: DHW Closet Temperature for Heating Season (before Calibration)	100
Figure 4.56: DHW Closet Temperature for Cooling Season (before Calibration)	100
Figure 4.57: DHW Closet Temperature for Heating Season (after Calibration)	101
Figure 4.58: DHW Closet Temperature for Cooling Season (after Calibration)	101
Figure 4.59: Garage Temperature for Heating Season (before Calibration)	102
Figure 4.60: Garage Temperature for Cooling Season (before Calibration)	102
Figure 4.61: Garage Temperature for Heating Season (after Calibration)	103
Figure 4.62: Garage Temperature for Cooling Season (after Calibration)	103
Figure 4.63: Attic Temperature for Heating Season (before Calibration)	104
Figure 4.64: Attic Temperature for Cooling Season (before Calibration)	104
Figure 4.65: Attic Temperature for Heating Season (after Calibration)	105
Figure 4.66: Attic Temperature for Cooling Season (after Calibration)	105
Figure 4.67: Monthly Average Daily Electricity Usage Versus Monthly Average Outdoor Temperature for the Billing Period	106
Figure 4.68: Simulated Electricity Usage Versus Measured Electricity Usage	106
Figure 4.69: Monthly Average Daily Natural Gas Usage Versus Monthly Average Outdoor Temperature for the Billing Period	107
Figure 4.70: Simulated Natural Gas Usage Versus Measured Natural Gas Usage	107
Figure 4.71: Monthly Avg. Daily Electricity Usage vs. Monthly Average Outdoor Tempemrautre for the Billing Period	109
Figure 4.72: Simulated Electricity Usage vs. Measured Electricity Usage	109
Figure 4.73: Monthly Average Daily Natural Gas Usage vs. Monthly Average Outdoor Tempemrautre for the Billing Period	110
Figure 4.74: Simulated Natural Gas Usage vs. Measured Natural Gas Usage	110
Figure 4.75: Monthly Average Daily Electricity Usage Versus Monthly Average Outdoor Tempemrautre for the Billing Period	112

Figure 4.76: Simulated Electricity Usage Versus Measured Electricity Usage.....	112
Figure 4.77: Monthly Average Daily Natural Gas Usage Versus Monthly Average Outdoor Temperature for the Billing Period.....	113
Figure 4.78: Simulated Natural Gas Usage Versus Measured Natural Gas Usage.....	113
Figure 4.79: Monthly Average Daily Electricity Usage Versus Monthly Average Outdoor Temperature for the Billing Period.....	115
Figure 4.80: Simulated Electricity Usage Versus Measured Electricity Usage.....	115
Figure 4.81: Monthly Average Daily Natural Gas Usage Versus Monthly Average Outdoor Temperature for the Billing Period.....	116
Figure 4.82: Simulated Natural Gas Usage Versus Measured Natural Gas Usage.....	116
Figure 4.83 2009 IECC simplified residential base-case model	118
Figure 4.84 Calculation example for stud and non-stud portions of the exterior wall ...	122
Figure 4.85 Layers of underground surface for the U-effective method (Winkelmann, 2002)	124
Figure 4.86 Reference window in the base-case model	127
Figure 4.87 The dimensioning of a window with a frame.....	128
Figure 4.88 Concept of the equivalent frame width	130
Figure 4.89 2009 IECC base case model Vs. 2015 IECC base case model	131
Figure 5.1: Shading Impact Analysis Result (MMBtu).....	143
Figure 5.2: Example of Building Thermal Envelope	144
Figure 5.3: Example of the Roof Omission in a Simplified Building Energy Modeling.....	145
Figure 5.4: Example of Cases for Unconditioned Space Analysis	146
Figure 5.5: Unconditioned Space Analysis Results (MMBtu)	147
Figure 5.6: DHW Outlet Water Temperature Analysis Results (MMBtu).....	150
Figure 5.7: DHW Inlet Water Temperature Analysis Results (MMBtu)	152

Figure 5.8: Example of Cases for Ground Heat Transfer Analysis	154
Figure 5.9: Ground Heat Transfer Analysis Results (MMBtu)	155
Figure 5.10: Site Energy Usage for the Comparison of the Detailed Calibrated Model and the Simplified Uncalibrated Model (MMBtu).....	158
Figure 5.11: Site Energy Usage for the Comparison of the Simplified Uncalibrated Model and the Simplified Selected Calibrated Model (MMBtu)	162
Figure 6.1: Solar heat gains for January 7 (south facing).....	167
Figure 6.2: Solar heat gains for January 7 (north facing).....	168
Figure 6.3: Solar heat gains for January 7 (east facing)	168
Figure 6.4: Solar heat gains for January 7 (west facing)	169
Figure 6.5: Solar heat gains for August 3 (south facing).....	174
Figure 6.6: Solar heat gains for August 3 (north facing).....	175
Figure 6.7: Solar heat gains for August 3 (east facing)	175
Figure 6.8: Solar heat gains for August 3 (west facing)	176
Figure 6.9: Monthly solar heat gain (south facing)	180
Figure 6.10: Monthly solar heat gain (north facing)	182
Figure 6.11: Monthly solar heat gain (east facing).....	183
Figure 6.12: Monthly solar heat gain (west facing)	185
Figure 6.13: Annual building energy performance (BEPS) report.....	186
Figure 6.14: Annual building energy performance (BEPS) report.....	191
Figure 6.15: Annual building energy performance (BEPS) report.....	194
Figure 6.16: Annual building energy performance (BEPS) report.....	196
Figure 6.17: Annual building energy performance (BEPS) report.....	201
Figure 6.18: Annual building energy performance (BEPS) report.....	202
Figure 6.19: Annual building energy performance (BEPS) report.....	206

LIST OF TABLES

	Page
Table 4.1: Building Characteristics of the Case-study House	57
Table 4.2: Monthly Electricity Utility Billing Data for the Case-study House	58
Table 4.3: Monthly Natural Gas Utility Billing Data for the Case-study House.....	60
Table 4.4: Summary of Sensors Installed at the Solar Test Bench	62
Table 4.5: Regression Model Coefficients.....	81
Table 4.6 Summary of input parameters for the 2009 IECC simplified residential base case model	119
Table 4.7 Details of exterior wall thermal properties (Insulation part)	121
Table 4.8 Details of exterior wall thermal properties (Stud part)	121
Table 4.9 Perimeter conduction factors for concrete slab-on-grade (Winkelmann, 2002)	126
Table 4.10 Development procedure for the 2015 IECC residential base case model from the 2009 IECC model (RUN 30)	136
Table 4.11: Input Specifications of the Detailed and Simplified Case-study House Simulation Models.....	139
Table 5.1: List of Cases for Shading Analysis.....	142
Table 5.2: Shading Impact Analysis Result (%).....	143
Table 5.3: List of Cases for Unconditioned Space Analysis.....	146
Table 5.4: Unconditioned Space Analysis Results (%)	147
Table 5.5: List of Cases for DHW Outlet Water Temperature Analysis	149
Table 5.6: DHW Outlet Water Temperature Analysis Results (%).....	150
Table 5.7: List of Cases for DHW Inlet Water Temperature Analysis.....	151
Table 5.8: DHW Inlet Water Temperature Analysis Results (%)	152

Table 5.9: List of Cases for Ground Heat Transfer Analysis.....	154
Table 5.10: Ground Heat Transfer Analysis Results (%).....	155
Table 5.11: Input Specifications for the Comparison of the Detailed Calibrated Model and the Simplified Uncalibrated Model.	157
Table 5.12: Source Energy Usage for the Comparison of the Detailed Calibrated Model and the Simplified Uncalibrated Model (MMBtu).....	158
Table 5.13: Source Energy Percentage Difference for the Comparison of the Detailed Calibrated Model and the Simplified Uncalibrated Model (%).....	158
Table 5.14: Input Specifications for the Comparison of the Simplified Uncalibrated Model and the Simplified Selected Uncalibrated Model.....	161
Table 5.15: Source Energy Usage for the Comparison of the Simplified Uncalibrated Model and the Simplified Selected Calibrated Model (MMBtu).....	162
Table 5.16: Source Energy Percentage Difference for the Comparison of the Simplified Uncalibrated Model and the Simplified Selected Calibrated Model (%).....	162
Table 6.1: Properties of the Selected Glazing (source: DOE-2 BDL Summary, Version 2.1E, P.126).....	165
Table 6.2: Solar heat gain difference between the shading coefficient and the window library methods for January 7 (single clear window)	170
Table 6.3: Solar heat gain difference between the shading coefficient and the window library methods for January 7 (double clear window).....	171
Table 6.4: Solar heat gain difference between the shading coefficient and the window library methods for January 7 (double low-E window).....	172
Table 6.5: Solar heat gain difference between the shading coefficient and the window library methods for August 3 (single clear window)	177
Table 6.6: Solar heat gain difference between the shading coefficient and the window library methods for August 3 (double clear window).....	178
Table 6.7: Solar heat gain difference between the shading coefficient and the window library methods for August 3 (double low-E window).....	179

Table 6.8: Monthly solar heat gain difference between the shading coefficient and the window library methods (south facing)	181
Table 6.9: Monthly solar heat gain difference between the shading coefficient and the window library methods (north facing)	182
Table 6.10: Monthly solar heat gain difference between the shading coefficient and the window library methods (east facing)	184
Table 6.11: Monthly solar heat gain difference between the shading coefficient and the window library methods (west facing)	185
Table 6.12: Annual building energy performance (BEPS) report difference between the shading coefficient and the window library methods	186
Table 6.13: Thermal properties of window frames.....	188
Table 6.14: Frame width by frame type.....	188
Table 6.15: Reference window size and window shape	189
Table 6.16: Test cases for window frame analysis	189
Table 6.17: Annual building energy performance (BEPS) report difference between the window frame type, width, and shape	191
Table 6.18: Test cases for roof eave analysis.....	192
Table 6.19: Annual building energy performance (BEPS) report difference between the roof eaves.....	194
Table 6.20: Test cases for window setback analysis.....	195
Table 6.21: Annual building energy performance (BEPS) report difference between the window frame type, width, and shape	196
Table 6.22: Preliminary tests for ground heat transfer analysis	198
Table 6.23: Test cases for ground heat transfer analysis	199
Table 6.24: Annual building energy performance (BEPS) report difference between ground heat transfer analysis	201
Table 6.25: Annual building energy performance (BEPS) report difference between ground heat transfer analysis	202

Table 6.26: Test cases for duct model analysis.....	203
Table 6.27: Annual building energy performance (BEPS) report difference between duct model analysis.....	206

1. INTRODUCTION

1.1. Background

The concept of building code has been in use for thousands of years. The Code of Hammurabi (1800 B.C.) is generally recognized as the world's first building code. It stated that if a residence disintegrated and led to the death of the people that lived there, the builder would get the death penalty (IBHS, 2015). In the U.S., the great fires of history led to new regulations. For example, the great Chicago fire in 1871 killed 250 people, destroyed 17,000 structures and left nearly 100,000 people homeless (IBHS, 2015). Four years later, the city enacted a new building code and a fire-prevention ordinance. As is often the case, the beginning of building codes was preceded by tragedies that motivated the creation of the building codes to prevent future occurrences of such tragedies (IBHS, 2015).

In the U.S. building energy codes began shortly after the oil embargoes (i.e., fuel shortages) of the 1960s and 1970s. The first oil embargo occurred in 1967 as a result of the war between the Arabs and Israeli from June 5 to 12 in 1967 (i.e., the Six-Day War) (Crowder & Foster, 1998; Mann, 2013). Although the oil embargo in 1967 did not significantly decrease the amount of oil available in the United States, the second oil embargo in 1973 did and it became an energy security issue that initiated many of today's energy efficiency efforts (Crowder et al., 1998; Mann, 2013). The second oil embargo occurred as a result of the 1973 Arab-Israeli War. This caused an immediate increase in the cost of crude oil and its derivative products, including gasoline, home

heating oil, and fuel oil. This also caused a re-evaluation of building energy codes with the eventual inclusion of energy efficiency requirements that produced the first ASHRAE building energy Standard 90-75 in 1975 and the Model Code for Energy Conservation in New Buildings (MCEC) in 1977 (Heldenbrand, 2001; Horner, 2011). After ASHRAE Standard 90-75 was published, in 1980, the American National Standard Institute (ANSI) approved a jointly sponsored revision, ANSI/ASHRAE/IES 90A-1980, as an American National Standard. Standard 90A-1980 that was a revision of Sections 1 through 9 (e.g., Purpose, Scope, Definitions, Exterior Envelope Requirements, HVAC Systems, HVAC Equipment, Service Water Heating, Energy Distribution Systems, and Lighting Power Budget Determination Procedures) of ASHRAE 90-75 (Heldenbrand, 2001). In 1983 - 1984, the ASHRAE 90 committee was reorganized into two committees - 90.1, covering commercial and high-rise residential buildings, and 90.2, covering low-rise residential buildings (Hunn, 2010). The first ASHRAE Standard 90.2 -1993 for low-rise residential buildings appeared in 1993, and 2001, 2004, and 2007 versions of Standard 90.2 were published.

During the same time as the publications of the ASHRAE Standards 90-75, 90.1 and 90.2, the U.S. Department of Energy (DOE) funded an effort by the National Conference of States on Building Codes and Standards (NCSBCS) to develop a building energy code to regulate the design of building envelopes and the design of mechanical, electrical, and illumination systems and equipment. The resulting document, the Model Code for Energy Conservation in New Buildings (MCEC), was published in 1977. This effort essentially put the technical criteria of ASHRAE 90-75 into code language that

could be adopted and enforced by state and local governments (Crowder et al., 1998; Heldenbrand, 2001). After the MCEC in 1977, the Council of American Building Officials (CABO) published the first Model Energy Code (MEC), which was a subsequent revision of MCEC in 1983. The MEC applied to all new residential and commercial buildings, and it was revised and published again in 1986, 1989, 1992, 1993, and 1995. In 1998, the International Code Council (ICC) replaced it with the 1998 IECC, which was updated in 2000, 2003, 2006, 2009, 2012, 2015, and 2018 (Crowder et al., 1998; Halverson et al., 2002; Heldenbrand, 2001). Since the MEC and IECC were developed or affected by ASHRAE Standards, they are closely related to each other. In addition, the IECC or the IECC with amendments was the main building energy code in many states, and the IECC or the IECC with amendments was adopted by 33 states in the U.S. (DOE, 2016).

Currently, the latest version of the IECC (2018 IECC) contains two compliance paths including the prescriptive path (i.e., mandatory plus prescriptive requirements) and performance path (i.e., mandatory plus performance requirements) for low-rise residential buildings (DOE, 2012; ICC, 2015, 2018). The mandatory requirements are compliance requirements that must be fulfilled for every building design regardless of which compliance path is selected. Prescriptive requirements are compliance requirements that either must be fulfilled for the building being designed, or if the compliance requirement is not fulfilled, a tradeoff must be applied that is equivalent to the prescriptive requirement. The performance approach requirement is also called the whole-building tradeoff approach. This is a compliance path that can trade envelope

components and system components to fulfill the whole-building energy performance requirements of the building energy code using annual energy analysis.

Since 2006, in the IECC the Simulated Performance Alternative (Performance) method of the IECC was the only performance compliance method until the 2012 IECC. To comply with the simulated performance alternative, the IECC required that a proposed design simulation model be shown to have an annual energy cost that is less than or equal to the annual energy cost of the standard reference design simulation model where the input parameters for the proposed design simulation model can be decided by users. The input parameters for reference design simulation models were defined by the building energy code to represent the maximum energy cost of a house that meets the code (ICC, 2012).

The Energy Rating Index compliance alternative (ERI) method was added to the 2015 IECC as another performance path method. To comply with this ERI method, an ERI reference design simulation model shall be shown to have an index value that is less than or equal to the maximum energy rating indexes for the climate zone in which the building is located (ICC, 2015). The major difference between the traditional performance path and the ERI performance path is that the ERI performance path allows equipment trade-offs for the energy cost saving calculation.

Performance path methods, such as the performance path or, the ERI performance path in the IECC enable more flexible building design and construction options, which can result in innovative design or financial savings (DOE, 2013). Currently, a whole-building energy simulation tool is necessary to comply with the

performance path methods. However, there are many different simulation tools that can be used to perform this analysis. Unfortunately, the results of different simulation programs that simulate the same building can range from good agreement to very little agreement (Hui, 2003). To obtain more consistent results between residential energy simulation tools for IECC code compliance using the Simulated Performance Alternative, the Residential Energy Services Network (RESNET) developed the Procedures for Verification of International Energy Conservation Code Performance Path Calculation Tools. Even if there is no software certification for the IECC currently, prior to 2016, there were five RESNET accredited IECC performance verification software tools; Ekotrope v.1.9.0 and v.2.1.0 (RESNET, 2016c), EnergyGaugeUSA v.5.1 and 4.0 (RESNET, 2016c), IC3 v4.01 (RESNET, 2016c), REM/Rate REM/Design v.14.6.4 and v.5.2 (RESNET, 2016c), and Right-Energy® IECC (RESNET, 2016c).

Despite the effort of RESNET and the software vendors, major differences still remain between the certified simulation tools. According to the Energy Systems Laboratory (ESL) in their 2013 report, the ESL compared the simulation result differences between IC3 (v.3.12.1), REM/Rate (v.13), and EnergyGauge (v.2.8.05) and showed that although these programs agreed when the parameters that were compared represented code-compliance. However, there were major differences between the results when these same parameters were changed to represented values above code (Mukhopadhyay et al., 2013). Therefore, this study will analyze and compare simplified, uncalibrated simulations versus detailed, calibrated simulation of a case-study house to

determine how accurate the simplified models can be and which measurements can be the most useful for improving the accuracy of the model.

1.2.Purpose and Objectives

The purpose of this study is to compare analyzed results from the detailed building energy simulation model of an existing single-family residence versus the results from the simplified building energy simulation model of the same residence to determine which parameters that represent an existing house. The objectives of this study are:

- 1) To review: the history of residential building energy codes and standards; the IECC code compliance for residential buildings; the performance-based code-compliant software for residential buildings; test suites of building energy simulation tools; and input specifications for building energy simulation.
- 2) To identify a case-study house using calibrated installed sensors;
- 3) To develop a detailed case-study house simulation model;
- 4) To develop a simplified case-study house simulation model;
- 5) To compare the difference between the detailed and the simplified models; and
- 6) To summarize an analysis of the detailed and simplified code-compliant residential simulation model with the case-study house simulation model.

2. LITERATURE REVIEW

For this study, a literature review was performed on the following areas of interest: 1) the history of residential building energy codes and standards; 2) the International Energy Conservation Code Compliance Paths for Residential Buildings (e.g., prescriptive, performance path, and ERI path); 3) Performance-based Code-Compliant Software for Residential Buildings; 4) Test Suites for Building Energy Simulation Tools; 5) Input Specifications for Building Energy Simulation; 6) Calibrated Simulation; and 7) Summary of Literature Review.

2.1. History of Residential Building Energy Codes and Standards

The earliest versions of the existing residential building energy codes and standards began shortly after the oil embargoes (i.e., fuel shortages) of the 1960s and 1970s. By the end of the 1960s, a series of energy crises appeared that are commonly referred to as the Arab oil embargoes, which led to the development of the first modern day building energy codes (Adelman, 2004; Horner, 2011). The first oil embargo occurred in 1967, when oil prices increased because of the war between the Arabs and Israel from June 5 - 12 in 1967 (i.e., the Six-Day War). Although this first oil embargo lasted only a few days, it resulted in higher oil prices. However, the higher prices fell back quickly with the swift Arab defeat (Adelman, 2004; Horner, 2011). A second, more prolonged oil embargo appeared in 1973. During the 1973 Arab-Israeli War, Arab members of the Organization of Petroleum Exporting Countries (OPEC) created an oil

embargo against the United States in retribution for the U.S. decision to support the Israeli military (Historian, 2016). This 1973 oil embargo had the immediate impact of raising the cost of crude oil and its related products, including: gasoline, home heating oil, and fuel oil used to generate electricity at power generators (Crowder et al., 1998).

This caused renewed interest in building energy codes and the consequent support of energy efficiency requirements that produced ASHRAE Standard 90-75 (i.e., residential and commercial). Since this standard, building energy codes and standards have begun to develop. Figure 2.1 shows a diagram of how the building energy codes and standards developed.

ASHRAE Standard 90-75 covered Energy Conservation in New Building Design. It was created and published by the American Society of Heating, Refrigerating, and Air-Conditioning Engineers (ASHRAE) with the technical support of the Illuminating Engineering Society of North America (IESNA) (Heldenbrand, 2001; Horner, 2011). In 1980, the American National Standard Institute (ANSI) approved a jointly-sponsored revision, which was called ANSI/ASHRAE/IES Standard 90A-1980, which became an American National Standard (ANS). Standard 90A-1980¹ was a revision of ASHRAE Standard 90-75 (Heldenbrand, 2001). The update did not substantially change the energy conservation levels that were published in ASHRAE 90-75 (Hunn, 2010). Prior to this, the standard covered both commercial buildings and residential buildings in the ASHRAE Standard 90A-1980. However, during the 1983 –

¹ The name of 90A-1980 comes from the ASHRAE/IES Standard 90-1980. The ASHRAE/IES Standard 90-1980 was comprised of three sections. The section about the energy requirements for commercial and residential buildings was contained in section A.

1984 period, ASHRAE 90 Standard was being subdivided into two sections for commercial and residential buildings, and the ASHRAE 90 Standard committee was reorganized into two committees - 90.1, covering commercial and high-rise residential buildings; and 90.2, covering low-rise residential buildings (Hunn, 2010). In 1993, ASHRAE Standard 90.2-1993 (Energy Efficient Design of Low-Rise Residential Buildings) was published. This standard is the first version of ASHRAE Standard 90.2 that covered only residential buildings. Since then ASHRAE Standards 90.2 – 2001, 2004, and 2018 have been published.

During the development of ASHRAE Standards 90.1 and 90.2, other efforts began which resulted in additional building energy codes. In 1977, the Department of Energy (DOE) funded the National Conference of States on Building Codes and Standards (NCSBCS) to develop a building energy code to regulate the design of building envelopes and the mechanical and electrical systems and equipment. The NCSBCS developed and published a model energy code named the Model Code for Energy Conservation in New Buildings (MCEC) in 1977. The MCEC added code language to the technical criteria of the ASHRAE 90-75. So States and local governments could adopt the MCEC as a building energy code (Crowder et al., 1998; Heldenbrand, 2001).

With regard to the MCEC, in 1983, the Council of American Building Officials (CABO) published the first Model Energy Code (MEC), which was a revision of the 1978 MCEC. The MEC applied to all new residential and commercial buildings. It was maintained by CABO through a series of annual public code hearings. This code was

updated on a 3-year cycle by the CABO until the International Codes Council (ICC)'s International Energy Conservation Code (IECC) replaced it in 1998 (Crowder et al., 1998; Halverson et al., 2002; Heldenbrand, 2001). The ICC was established in 1994 by three model code organizations, which include the Southern Building Code Congress International (SBCCI), the Building Officials and Code Administrators International (BOCA), and the International Conference of Building Officials (ICBO). The ICC transferred CABO's one and two family dwelling building energy code and the Model Energy Code to the IECC. The ICC is currently developing new editions of the IECC (Crowder et al., 1998; ICC, 2016).

Today, there is one main national energy code for residential buildings under continuous development: the IECC by the International Code Council (ICC). Currently, the 2009 – 2018 IECC or code with amendments are the most commonly adopted residential building energy codes in the U.S. (31 states, 62%). Seven states, such as California, have developed their own energy codes. However, most energy codes have been developed to include or are based on the IECC series for residential buildings (DOE, 2016).

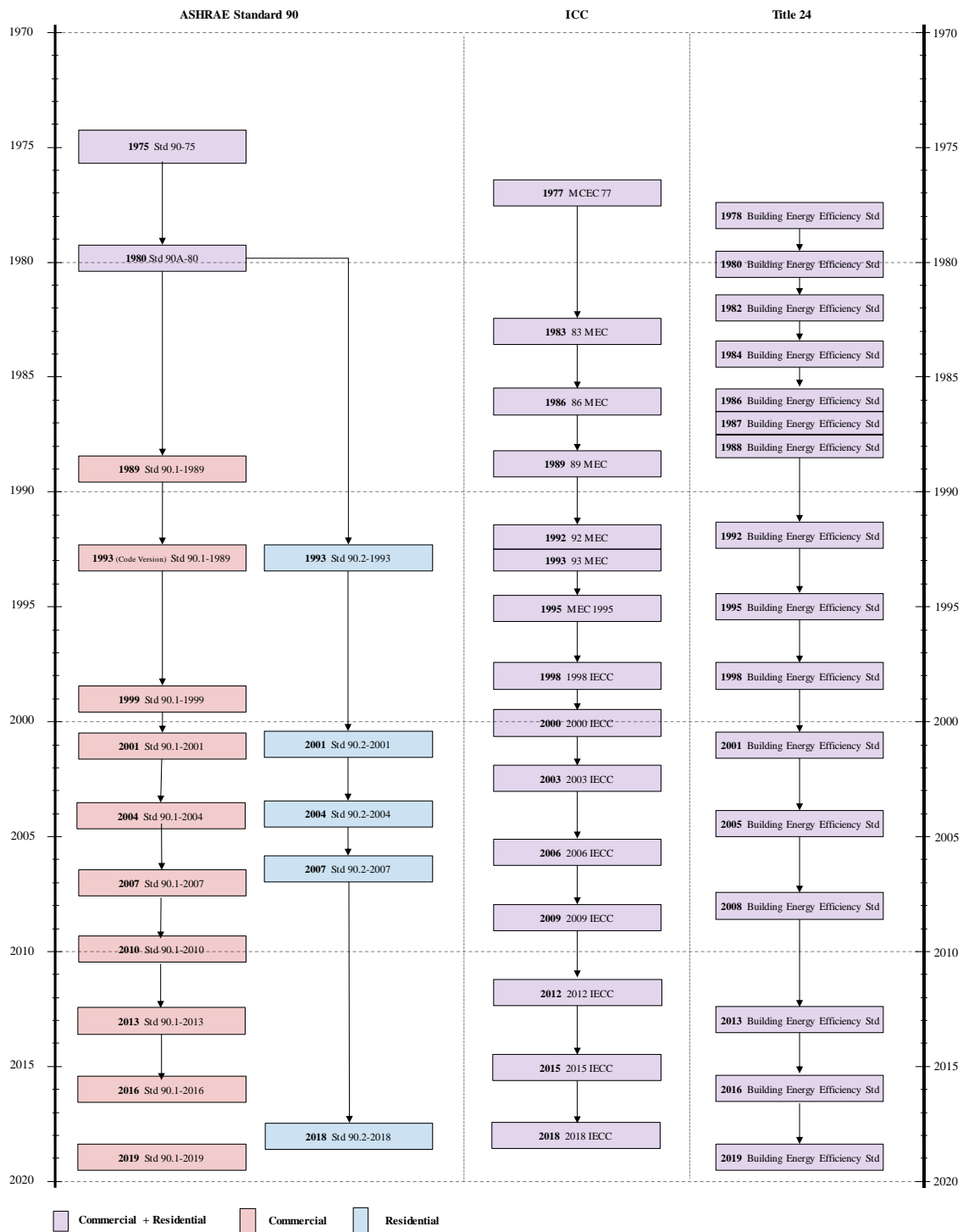


Figure 2.1: Building Energy Codes and Standards

2.2. International Energy Conservation Code (IECC) Compliance Paths for Residential Buildings

The International Code Council (ICC) is one of several organizations that have developed minimum building energy codes for residential buildings in the U.S. The ICC publishes new versions of the building energy code for residential and commercial buildings periodically. Currently, the latest version of the IECC (2018 IECC), contains mandatory requirements and two compliance paths: prescriptive and performance. The mandatory requirements must be followed regardless of which compliance path is selected. The prescriptive compliance path gives users selected options to choose that meet the minimum requirements to satisfy the code for each building component. The performance compliance path requires the proposed design to have an annual energy cost that is less than or equal to the standard (prescriptive) design of the same building using an authorized building energy code-compliant simulation program (Hui, 2003; Taylor & Lucas, 2010).

While the prescriptive path limits the flexibility of the building design by using pre-defined prescriptive options, the performance-based code compliance paths provide more design choices, which can lead to different building energy saving measures. In the 2018 IECC, there are two performance-based code compliance paths for residential buildings. The Simulated Performance Alternative in Section R405 and the Energy Rating Index Compliance (ERI) Alternative in Section R406 (ICC, 2018). The Simulated Performance Alternative compliance path is the traditional performance path in the IECC that requires building energy performance simulation software to calculate the annual

energy costs of the proposed design and of the reference design. The proposed design describes the desired house, while the reference design defines the maximum energy performance a house is allowed that meets the code. The energy costs are calculated by simulating the hourly annual building energy performance of the two houses (i.e., proposed and reference houses) to show the proposed house has less annual energy cost than the reference house. With the release of the 2015 IECC, the Energy Rating Index Compliance Alternative (ERI) method became a new performance path method to obtain code compliance. The ERI method requires an ERI score based on an analysis that uses a HERS index scoring procedure (RESNET, 2016b). In the analysis, two houses are used to rate the design and ERI reference design to calculate the ERI score. Both are very similar with the proposed and reference design in the Simulated Performance Alternative compliance path. The rated design is a description of the proposed house. The ERI reference design describes a house, that is equivalent to a house, but that complies with the 2006 IECC.

Using the two house models, the ERI score is calculated as a numerical score where 100 is equivalent to a level of the 2006 IECC, and 0 score is equivalent to zero energy house (i.e., a house that requires zero annual energy use). The score is calculated using the total annual energy use of the rated design relative to the total energy use of the ERI reference design (RESNET, 2016b).

Although the use of the performance path is more complicated than the use of prescriptive path because of the use of a whole-building energy simulation, the performance path has advantages that enable more flexible design and construction

options (Taylor et al., 2010). In the performance path, however, the simulation software's role is very important and needs to be carefully evaluated to ensure consistent results, because the results of the software have a significant impact on the code compliance.

2.3. Performance-based Residential Building Code-Compliance Software

According to the IECC, different whole-building energy simulation tools can be used for performance-based residential building code compliance (ICC, 2015). However, most of these tools are complicated to use when evaluating building energy code compliance because the software can require hundreds of input parameters in order to run. In addition, some of the software may not have an easy-to-use user interface and may have input parameters that are difficult for the average user to understand, which can lead to input errors by untrained users. To solve this problem, simplified and easy-to-use simulation tools for building energy code compliance have been developed. In addition, some of these tools have even been evaluated with RESNET's test cases for consistent code compliance results (RESNET, 2016c).

Four software tools have been certified by RESNET, including: Ekotrope (version 1.9.0, 2.1, 2.2, 3.0 and 3.1), EnergyGaugeUSA (version 4.1, 4.1, 6.0 and 6.1), REM/Rate (version 14.6.4, 15.2, 15.3, 15.4, 15.5, 15.6 and 15.7) and Right-Energy HERS. In this study, these four software tools were reviewed. In addition, the IC3 and REScheck were reviewed in the following section although they are not certified by RESNET.

2.3.1. Ekotrope

Ekotrope was developed by an MIT startup company in October of 2011 (Determan, 2014). Ekotrope version 1.9, 2.1, 2.2, 3.0 and 3.1 were accredited by RESNET in 2017 as HERS Software tools. Ekotrope contains three building simulation tools, including: RATER, OPTIMIZER, and True Cost of Ownership (TCO) (ekotrope, 2016). OPTIMIZER software helps to find the optimized designs to meet energy goals and cost targets for builders. TCO provides information about the cost to own houses for home buyers, sellers, and lenders. This set of web-based software tools can conduct building energy and cost analysis using different building energy components such as envelope and system, which are defined by Ekotrope software or by users. Since Ekotrope provides the building thermal envelope library data of most common types of walls, floors and roofs in the market, users can utilize this software more easily than other software that requires detailed descriptions of the building's thermal envelope.

2.3.2. EnergyGauge USA

The Florida Solar Energy Center (FSEC) developed a residential building energy and economic analysis software called EnergyGauge USA. This software also provides code compliance and ratings of energy use (Fairey et al., 2012). EnergyGauge USA is a building energy performance tool that uses the DOE-2.1e energy simulation program, and it is a RESNET-certified IECC software tool (RESNET, 2016c). For the IECC performance path code compliance, EnergyGauge USA is an accredited rating software program by RESNET.

2.3.3. The International Code Compliance Calculator (IC3)

The International Code Compliance Calculator (IC3) is an easy-to-use, web-based, code compliance simulation developed by the Energy Systems Laboratory at Texas A&M University. IC3 was developed using the DOE-2.1e program to provide easy-to-use web-based software for builders, home energy raters, and code officials to analyze building energy code compliance for new single-family residential buildings in Texas. The user interface of IC3 was designed to ensure simple and fast input using a simplified user input. In addition, IC3 provides simplified outputs that report the code compliance as a percent above or below code for 254 counties in Texas (ESL, 2016).

2.3.4. REM/Rate

REM/Rate is a user-friendly, residential energy analysis, code compliance and Home Energy Rating (HERS) software developed by the Architectural Energy Corporation (AEC) specifically for the needs of HERS Providers and Home Energy Raters (AEC, 2016; NORESO, 2016a, 2016b). Currently, NORESO is developing and maintaining REM/Rate since NORESO purchased the Architectural Energy Corporation (AEC) in 2014 (AEC, 2016; NORESO, 2016a). The REM/Rate software calculates heating, cooling, domestic hot water, lighting, and appliance energy loads, consumption and costs for new and existing single and multi-family homes.

REM/Rate, which contains algorithms from the SERI/RES program (Polly et al., 2011), has many unique features including: a simplified input procedure; extensive component libraries; automated energy efficient improvement analysis; a duct condition and leakage analysis; latent and sensible coding analysis; lighting and appliance audit; and active and passive solar analysis (NORESO, 2016b; Polly et al., 2011). REM/Rate

software is widely used by organizations to conduct Home Energy Rating Systems (HERS) Ratings (NORESO, 2016b). REM/Rate (v.16.0) is one of the accredited HERS software tools by RESNET (RESNET, 2020a).

2.3.5. REScheck

REScheck was developed by the Pacific Northwest National Laboratory (PNNL) for the US DOE. In the US DOE, the Building Energy Code Program (BECF) supports building energy code development, adoption, implementation, and enforcement processes to promote energy efficiency with cost-effective improvements (DOE, 2015a). REScheck began in 1997 when the first building energy code compliance software, MECcheck was developed by PNNL for single-family and low-rise multi-family residential buildings to help builders, state and local code officials for complying with the Model Energy Code (MEC) and IECC requirements (Bartlett et al., 2012). In November 2002, MECcheck was renamed REScheck since the "MEC" in MECcheck was outdated since the MEC was changed into the IECC (Bartlett et al., 2012). Currently, REScheck is available in a web-based version and a downloadable desktop version, and provides compliance checking with the IECC and the ANSI/ASHRAE/IESNA Standard 90.2 codes, which are the basis for most state building energy codes (DOE, 2015b, 2015c).

2.3.6. Summary

In summary, hourly building energy simulation tools are being used for building energy performance rating and code compliance. However, even when they've been certified by RESNET, they can still have significant simulation result differences for different simulation programs. According to Mukhopadhyay (Mukhopadhyay et al., 2013), the performance-based compliance results of the RESNET-certified software did not show a huge difference when specific parameters were tested, which resulted in a code-compliant simulation. However, when the energy performance of the building elements were tested parametrically, the results for different simulation programs were found to be significantly different for values that yielded above-code simulations (Mukhopadhyay et al., 2013).

2.4. Testing Simplified Residential Building Energy Simulation Tools

Currently, there are three building energy simulation tests, including: a) Building Energy Simulation Test (BESTEST) (Neymark & Judkoff, 2008), b) ASHRAE Standard 140-2017 (ASHRAE, 2017), and c) RESNET Procedures for Verification of RESNET Accredited HERS Software Tools (RESNET, 2017, 2020b). Within those tests, there are three approaches to validate building energy performance simulation tools, including: a comparative testing; an analytical verification; and an empirical validation. Comparative testing involves a direct comparison of the results obtained from two or more building energy analysis simulations that comply with standard procedures using equivalent inputs. Analytical verification checks the outputs from the fundamental algorithms in the

simulation tools (i.e., isolated heat transfer mechanisms) to find intrinsic problems. Empirical Validation compares measured data from a real building or a test cell with outputs from a simulation tool. (Judkoff, 2008).

Currently, for testing simplified residential building energy simulation models, comparative verifications are used that certain procedures for the verification of the International Energy Conservation Code (IECC) performance path calculation tools and procedures for verification of RESNET accredited HERS software tools.

2.4.1. IEA BESTEST

The International Energy Agency Building Energy Simulation Test and the Diagnostic Method (IEA BESTEST) were developed in 1995 (R Judkoff & J Neymark, 1995). The National Renewable Energy Laboratory (NREL) developed the Building Energy Simulation Tests (BESTEST) jointly with the International Energy Agency (IEA) experts. This group was organized under the Solar Heating and Cooling (SHC) Programme, Task 12 Subtask B, and the Energy Conservation in Building and Community Systems (BCS) Programme, Annex 21 Subtask C (R Judkoff et al., 1995). The purpose of Task 12 was to develop actual implementation procedures and data for the overall IEA verification methodology developed by NREL since 1981. This methodology consists of a combination of empirical verifications, analytical verifications, and comparative analysis techniques (R Judkoff et al., 1995).

2.4.1.1. HERS BESTEST

The Home Energy Rating System Building Energy Simulation Test (HERS BESTEST) is a method of assessing the reliability of building energy software used by Home Energy Rating Systems (HERS). HERS BESTEST was also published by NREL in 1995, and was intended to test simplified building simulation tools commonly used for residential buildings. HERS BESTEST provides more realistic test cases, but less diagnostic cases than the IEA BESTEST procedure for simplified building simulation tools (Neymark et al., 2008).

HERS BESTEST procedures were developed to certify the accuracy of building energy analysis tools used to determine energy efficiency ratings. HERS BESTEST was developed as a response to the Energy Policy Act of 1992 (Title I, Subtitle A, Section 102, Title II, Part 6, Section 271), which promoted uniformity regarding systems for rating the annual energy efficiency of residential buildings. Accordingly, the HERS BESTEST method provides test cases and acceptance ranges for certifying the accuracy of building energy performance tools used to determine energy efficiency ratings. The test cases are divided into Tier 1 and Tier 2 tests for certification of building energy rating tools. The Tier 1 tests were designed using a basic house with typical windows and insulation. Tier 2 tests were designed to test passive solar design features (R. Judkoff & J. Neymark, 1995a, 1995b).

Using these test case results, the HERS BESTEST provides the results of annual heating loads for Colorado Springs, Colorado, and annual cooling loads for Las Vegas, Nevada. Each annual heating and cooling load results from simulation test cases by three

simulation tools, including: BLAST 3.0 Level 215, DOE2.1e-W54, and SERIRES/SUNCODE 5.7. The results are used for reference results that define the acceptance ranges of each test case. For a software to pass the HERS BESTEST, the annual heating and cooling loads and the results from sensitivity tests must be within the acceptance range of the test cases (R. Judkoff et al., 1995a, 1995b).

2.4.1.2. Florida-HERS BESTEST

The Home Energy Rating System Building Energy Simulation Test for Florida (Florida-HERS BESTEST) is a specific version of HERS BESTEST. Specifically, the Florida-HERS BESTEST was developed by National Renewable Energy Laboratory at the requested by the Florida Solar Energy Center (FSEC) to the Department of Energy (DOE) since Florida Building Energy Efficiency Rating Act stipulated that Florida's rating system must be compatible with the standard Federal rating system (Judkoff & Neymark, 1997a, 1997b).

Florida-HERS BESTEST is the same as the original HERS BESTEST except for the envelope thermal properties of the basecase building and weather files. The Florida-HERS BESTEST has slightly improved the performance of building envelope than the HERS BESTEST. For example, while the HERS BESTEST tests use the Colorado Springs weather file for heating loads and Las Vegas weather file for cooling loads, The Florida-HERS BESTEST uses an Orlando weather file to test the cooling and heating loads (Judkoff et al., 1997a, 1997b).

2.4.1.3. *HVAC BESTEST*

Since IEA BESTEST has limited test cases for residential mechanical equipment, and the HERS BESTEST and Florida-HERS BESTEST did not have test cases for the equipment, the HVAC BESTEST was developed for testing space conditioning equipment. The HVAC BESTEST test cases consist of a number of equipment performance parameters with controlled sensible and latent internal gains to test the space conditioning equipment loads in a highly simplified near-adiabatic building envelope (Henninger et al., 2004; Neymark & Judkoff, 2002, 2004).

2.4.1.4. *BESTEST-EX*

The Building Energy Simulation Test for Existing Homes (BESTEST-EX) is another method for testing home energy audit software and the associated calibration methods that were developed by NREL on behalf of the U.S. Department of Energy (DOE). BESTEST-EX contains two types of test cases, including: building physics tests and a utility bill calibration tests. (Judkoff et al., 2011) The BESTEST-EX building physics test cases provide inputs necessary to model existing home and retrofits. BESTEST-EX contains the results of an average retrofit energy savings prediction using state-of-the-art detailed simulation programs such as EnergyPlus, DOE2.1E, and SUNREL. BESTEST-EX was developed so that the retrofit energy savings predictions could be referenced to compare with other audit software tools (Judkoff et al., 2017). For example, the utility bill calibration test cases have averaged reference simulation results for bills from EnergyPlus, DOE2.1E, and SUNREL. These average simulation results

are then compared to the results of the audit software providers' tools (Judkoff et al., 2011; Judkoff et al., 2017).

In summary, the BESTEST test suites (i.e., IEA BESTEST, HVAC BESTEST, and BESTEST-EX) have been developed to test the algorithms in the building energy performance simulation under specific conditions. To accomplish this, the tests require complex inputs and outputs to view the test results. To date, the tests developed have been well suited to determine the differences in the algorithms in different simulation tools. However, these are limited tests for simplified simulation tools developed for building energy codes or building energy rating systems.

2.4.2. ASHRAE Standard 140 - 2014

The National Renewable Energy Laboratory (NREL) has developed the Building Energy Simulation Test (BESTEST), which is a methodology to verify the accuracy of whole-building energy simulation tools. This methodology can find and analyze differences of simulation results that are caused by simulation modeling, algorithms, coding, or inputs errors. This methodology has been adopted by ANSI/ASHRAE Standard 140, Method of Test for Evaluation of Building Energy Analysis starting in 2001. Since 2001 ANSI/ASHRAE Standard 140 has undergone updates every three years through 2017 (2001, 2004, 2007, 2011, 2014, and 2017) (ASHRAE, 2011, 2017).

The ASHRAE Standard 140 has two test classes, Class I and Class II, to meet the different levels of software modeling details. The Class I test cases consist of detailed

diagnostic tests designed for simulation software capable of hourly or more frequent simulation time steps. In contrast, Class II test cases are somewhat simplified tests cases developed for simplified simulation tools to test residential building simulation models(ASHRAE, 2011, 2017).

Class I test cases have been categorized into three tests including: a) building thermal envelope and fabric load tests, b) space-cooling equipment performance tests, and c) space-heating equipment performance tests. The building thermal envelope and thermal fabric load tests have basic test cases and in-depth test cases. The basic test cases in the building thermal envelope and thermal fabric load tests include: shading, window orientation, thermostat setback, night ventilation, sunspace, and free-float (no mechanical heating or cooling of buildings) tests for low mass and high mass building models. The in-depth tests for the building thermal envelope and fabric load tests contain: interior infrared radiation, exterior infrared radiation, surface convection/infrared radiation, infiltration, internal gains, exterior shortwave absorptance, solar gains, cavity albedo, shading, window orientation, and thermostat tests.

Space-cooling and heating equipment performance tests can be classified into analytical verification test cases and comparative test cases. Analytical verification test cases are designed to test each detailed mechanical equipment performance by changing specific input parameters, comparative test cases are designed to test overall equipment performance with realistic house models. The analytical verification test cases in space-cooling equipment performance tests contain tests for the outdoor dry-bulb temperature

test, the thermostat set-point, part-load ratio test, latent load test, sensible heat ratio test, and sensible load test. The comparative test cases in space-cooling equipment performance tests contain tests for infiltration, latent gain, outdoor air fraction, the infiltration fraction, thermostat tests, undersized system test, economizer test, and test concerning no outdoor air cases. For the space-heating equipment performance tests, Standard 140 contains efficiency tests, steady part-load tests, no load tests, varying part-load tests, circulating fan tests, cycling circulating fan tests, and draft fan tests in its analytical test cases. The comparative test cases include realistic weather data test, setback thermostat test, and undersized furnace test cases.

Class II test cases were adapted from the HERS BESTEST, which were developed by the National Renewable Energy Laboratory. This set of test cases are classified the Tier 1 and Tier 2 tests for certification of residential energy performance analysis tools (ASHRAE, 2011; Haddad & Beausoleil-Morrison, 2001). Tier 1 cases test typical building configurations by changing one or more components from a basecase. Tests for the infiltration, wall and ceiling insulation, window performance, window area, overhang, internal load, solar absorptance, and floor types are contained in the Tier 1 cases. Tier 2 cases have additional test cases to test passive solar design, and focus on testing shading and windows. The Tier 2 test cases consist of vertical fins, overhangs, no glazing, and evenly distributed windows for low mass and high mass interior walls.

In the case of Class I tests, hourly and monthly energy consumption results are required to evaluate the test suites. This means that certain simplified software cannot be tested with the Class I test suites because they have simplified inputs and outputs. Since

Class II tests (i.e, ASHRAE standard version of the HERS BESTEST) were developed to test the simplified software such as the Home Energy Rating System (HERS) software, they require fewer inputs and outputs to test. For this reason, the Procedures for Verification of International Energy Conservation Code Performance Path Calculation Tools were developed by RESNET, which include the procedures in the HERS BESTEST. In addition to these limitations, the current RESNET test suites do not test capabilities such as: the interactions with the attic and foundation which is covered in the IECC code compliance.

Currently, ASHRAE Standard Project Committee 140 (SSPC 140) is maintaining and developing ASHRAE Standard 140. According to the agenda of SSPC 140 (July 16, 2020), several tasks about the building energy simulation tests are underway include: 140-2017 Addendum a: Update Sec. 5.2 (BESTEST thermal fabric, 1995), DOE Empirical Validation Activities, and Tool Accreditation.

2.4.3. Procedures for the Verification of International Energy Conservation Code (IECC) Performance Path Calculation Tools (by RESNET)

The Simulated Performance Alternative method in the IECC requires simulated energy performance analysis using compliance software tools. Compliance software tools for the IECC are required to have four minimum capabilities, including : auto generation of the standard reference design defined by the IECC; calculation of heating and cooling equipment sizes; calculation of heating, cooling, and ventilating performance based on climate and equipment sizing, the generation of inspection checklist of the proposed design components characteristics for code officials to

determine; and the ability to simulate the difference between the standard reference design and the proposed design.

To verify the accuracy of residential energy simulation software tools to determine for the International Energy Conservation Code (IECC) compliance using the Simulated Performance Alternative method, the Procedures for Verification of IECC Performance Path Calculation Tools were developed by the Residential Energy Services Network (RESNET) (ICC, 2009; RESNET, 2016d). The RESNET procedures are based on a comparative analysis, which uses several computer simulation software to compare reference building performance results.

The RESNET certification supports the 2006 and 2009 IECC performance-path methods (RESNET, 2016c). The certification includes five tests: 1) Building Load Tests, 2) IECC Code Standard Reference Design auto-generation tests, 3) HVAC tests, 4) Duct distribution system efficiency tests, and 5) Hot water system performance tests. Each test category has its own test suite and acceptance criteria. The details of the tests are described below.

a. Building Loads Tests: The purpose of these tests are to verify building load calculations between different residential energy simulation tools to accomplish the ANSI/ASHRAE Standard 140-2011, Class II, Tier 1 test process. The Standard 140-2011 test processes were adopted and applied to the building loads tests and the acceptance criteria. These tests are performed by testing specific residential building modeling cases that have varied selective input parameters

related to the building envelope performance such as: infiltration, insulation, and varying window types for heating and cooling loads.

b. IECC Standard Reference Design Auto-Generation Tests: These tests are designed for testing the IECC Standard Reference Design auto-generation capability with only the information of the Proposed Design. These tests also test the ability to report minimum values of the Reference Home building components and requires the calculation of the energy using an e-Ratio, which is the value of Proposed Home annual energy use divided by Standard Reference Design annual energy use.

c. HVAC Tests : These tests are performed using the L100 building case described by the HERS BESTEST procedures (RESNET, 2016d). For each test case, acceptance criteria are provided. These criteria are based on reference results from six building energy simulation tools, including: two DOE-2.1e tools, two DOE-2.2 tools, the Micropas version 6.5 software, and TRNSYS version 15, which are capable of detailed hourly building simulation and HVAC modeling computations (RESNET, 2016d).

d. Duct Distribution System Efficiency (DSE) Test: The Duct Distribution System Efficiency (DSE) tests are designed to ensure that the impact of duct insulation, duct air leakage and duct location are properly accounted for in the software. The acceptance criteria for these tests were established using ASHRAE Standard 152-2004 (RESNET, 2016d).

e. Hot Water System Performance Tests: Hot water system tests are designed to

determine if IECC performance compliance software tools accurately account for both the hot water usage rate (i.e., gallons per day) and the climate impacts (i.e., inlet water temperatures) of hot water systems. The tests are limited to standard gas-fired hot water systems and cannot be used to evaluate solar hot water systems, heat pump hot water systems, hot water systems that recover heat from air conditioner compressors, or other types of hot water systems. The acceptance criteria for these tests are based on reference results from three software tools; TRNSYS Version 15, DOE-2.1e (v.120) as used by EnergyGauge USA Version 2.5, and REM/Rate Version 12 (RESNET, 2016d).

The RESNET verification methods are referenced as part of the BESTEST. However, since BESTEST requires many input parameters, it is hard to apply it directly to easy-to-use simulation tools that have a GUI or a web-based input because many of the required input parameters cannot be accessed. In addition, the five tests evaluate mostly a static condition defined in the test cases, whereas more dynamic tests are needed.

2.4.4. Procedures for Verification of RESNET Accredited HERS Software Tools

Since Home Energy Rating Systems (HERS) Index is calculated by a building energy performance comparison based on the Rated Home as compared with the HERS Reference Home, building energy performance simulation software is required. In order to ensure the accuracy and comparability of HERS tools, software vendors seeking

RESET accreditation shall comply with the procedures prescribed by the RESNET document (RESNET, 2013, 2020b). The ERI path was developed using the HERS Index, and the HERS procedures can be directly applied for the IECC ERI path. The Energy Rating Index (ERI) performance path in the IECC requires building energy performance simulation tools such as the Simulated Performance Alternative method mentioned above. The test procedures include six test sets: a. ANSI/ASHRAE Standard 140-2017, Class II, Tier 1 tests, b. HERS Reference home auto-generation tests, c. HERS method tests, d. HVAC tests, e. Duct distribution system efficiency tests, and f. Hot water system performance tests. The details of the test sets are described below (RESNET, 2020b).

a. ANSI/ASHRAE Standard 140-2017, Class II, Tier 1 Tests: RESNET adopted the Class II, Tier 1, test sets from ANSI/ASHRAE Standard 140-2017. The ASHRAE test set was developed from the HERS BESTEST for testing the accuracy of building loads calculations for simplified building energy simulation software. This test set is same with the test set in Procedures for Verification of International Energy Conservation Code (IECC) Performance Path Calculation Tools. These tests verify building heating and cooling loads by varying infiltration, insulation, and window types (RESNET, 2017, 2020b).

b. HERS Reference Home auto-generation Tests: Building energy simulation tools for HERS or the ERI paths simulate two different house models for HERS or for ERI index scores. First, the simulation tools generate the rated home inputs prepared by user inputs and the specifications in ANSI/RESNET/ICC Standard

301-2014. Then, the software generate the reference home inputs using the information of the rated home (RESNET, 2016a, 2017). Since the reference home must be generated automatically according user inputs and the standard home specifications, the HERS reference home auto-generation tests are required. This test set tests the auto-generated reference home inputs by giving predicted user inputs for heating and cooling system efficiency, weather files, mechanical ventilation type, and the number of bedrooms.

c. HERS Method Tests: This test set is intended to determine the ability of HERS software to calculate a precise HERS Index score. Since the HERS Index calculation needs input parameters such as Reference Home End User Loads (REUL), Reference Home End Use Energy Consumptions (EC_r), Rated Home End Use Energy Consumptions (EC_X), and the applicable manufacturers equipment performance ratings (MEPR), this test set evaluates these parameters whether they are calculated correctly or not (RESNET, 2017).

d. HVAC Tests : This test set uses building geometry information using the L100 building case described by the HERS BESTEST procedures for its HVAC tests (RESNET, 2017). During these tests, building energy usage for heating and cooling systems are calculated as the efficiency of the system changes.

Acceptance criteria are provided for the tests. The criteria were developed based on reference results from six building energy simulation tools, including: two DOE-2.1e tools, two DOE-2.2 tools, the Micropas version 6.5 software, and TRNSYS version 15 (R. Judkoff et al., 1995a, 1995b; RESNET, 2017).

e. Duct Distribution System Efficiency Test: Distribution System Efficiency (DSE)

tests are developed to assure the impact of duct insulation, duct air leakage, and duct location in building energy performance simulation (RESNET, 2017).

f. Hot Water System Performance Tests: Hot water system tests are developed to

test the amount of hot water usage and the climate impacts of inlet water temperatures. The RESNET provides the calculation of the hot water usage per day which covers distribution losses and other features associated with hot water distribution systems in ANSI/RESNET/ICC Standard 301-2014 Addendum A-2015. HERS building energy performance software must apply this calculation method to pass these tests. Acceptance criteria for these tests are developed based on reference results from four different building energy simulation tools; REM/Rate v15.3, EnergyGauge USA Version 5.1, Ekotrope v2.2, and BEopt/EnergyPlus 2.6. Minimum and maximum acceptance criteria for each result are determined by the range of results from the reference tools (RESNET, 2016a, 2017).

These test procedures are similar with the procedures for the IECC performance path, with selected differences. These differences include the HERS index calculations, domestic hot water energy calculations, and appliance energy calculations.

2.4.5. Building Energy Simulation Test (BESTEST)

The purpose of the Building Energy Simulation Test (BESTEST) is to increase the consistency of the use of building energy simulation software tools by developing test procedures for the software. These building simulation test procedures were developed to validate, diagnose, and improve the current building simulation software tools by presenting standardized input parameters and reference simulation outputs (EERE, 2017; Haddad et al., 2001). Currently, several versions of BESTEST have been published, including: IES BESTEST (R Judkoff et al., 1995), HERS BESTEST (R. Judkoff et al., 1995a, 1995b), Florida-HERS BESTEST (Judkoff et al., 1997a, 1997b), HVAC BESTEST (Neymark et al., 2002, 2004), and BESTEST-EX (Judkoff et al., 2011; Judkoff et al., 2017).

2.5. Empirical Test

The U.S. Department of Energy (DOE) is supporting for ASHRAE Standard 140 to develop empirical validation test suites. Ongoing projects include: the small commercial building prototype at Oak Ridge National Laboratory's Flexible Research Platforms (FRPs), a zone in Lawrence Berkeley National Laboratory's FLEXLAB, and performance mapping of several high-efficiency commercial rooftop unitary air-conditioning systems in cooling mode at the NREL Flow-Through Test Loop. At the same time, Argonne National Laboratory is working on the theory and application of uncertainty in empirical validation exercises. ASHRAE Standing Standard Project Committee (SSPC) 140 is responsible for these projects, and they will integrate these

empirical validation test suites into Standard 140 if the uncertainty analysis indicates the tests are meaningful (ASHRAE, 2017).

2.5.1. Oak Ridge National Laboratory

The ORNL Flexible Research Platforms (FRP) consist of residential and light commercial building research platforms. For the residential platforms, ORNL and their industry partners built unoccupied and owner-occupied research houses to evaluate residential energy efficiency technologies and collect energy performance data before and after retrofits (ORNL, 2019). For the light commercial building research platforms, there is a single-story FRP with a footprint of 40 by 60 ft (2,400 sqft), and a two-story FRP with a footprint of 40 by 40 ft (3,200 sqft). These two types of FRPs are designed to imitate common light commercial buildings in the U.S. for commercial building energy performance research (Im et al., 2016). For the research at the FRP, occupancy is emulated by controlling of lighting, humidifiers for human-based latent loading, and a heater for miscellaneous electrical loads. To reduce the uncertainty in building modeling input data from ground heat transfer, ONRL installed 12" Geofoam EPS46 (R.4.6 per inch - RSI 0.76 per inch) insulation to the floor of the FRPs. Additionally, piping around the perimeter is also provided so that the cold or water can be circulated through these pipes to maintain the desired ground temperature.

2.5.2. Lawrence Berkeley National Laboratory

LBNL has a facility for building energy experiments called FLEXLAB located in Berkeley, CA. FLEXLAB provides researchers with a facility to study building energy efficiency for building energy components such as HVAC, lighting, fenestration, facade, control systems (Birru et al., 2013; McNeil et al., 2014). The facility includes eight test cells to test individual or integrated systems for a building facade, fenestration, HVAC, lighting, control, and plug loads. Since FLEXLAB specialized on testing the performance of a specific building configuration, this facility is specially equipped to verify building energy performance simulation with comparative studies for different building components and equipment (McNeil et al., 2014; Peng et al., 2017).

2.5.3. National Renewable Energy Laboratory

The National Renewable Energy Laboratory (NREL) develops and validates model inputs for building energy performance simulation. The effort includes "Performance Mapping" of inputs to better understand their impact. NREL's Performance Maps project develops EnergyPlus model inputs to accurately estimate building energy performance in various conditions (Christensen, 2014).

2.5.4. Argonne National Laboratory

Argonne National Laboratory is working to better understand the uncertainties involved in building energy modeling and the building energy saving estimations. Researchers in the laboratory is analyzing and assessing input parameters of energy models along with the energy models themselves, with the goal of developing tools for

calibrating the estimation of building energy models to measured utility use to reduce the uncertainty of building energy modeling. The Argonne methods start with the assumption that certain model parameters are uncertain, and use Bayesian statistics to reduce the uncertainty so that the predicted output best matches the measured energy use. Their method allows almost automatic calibration of the building energy models. The methods and software tools are being intergrated into the Open Source OpenStudio building energy modeling platform being developed by researchers at the NREL, Argonne, Lawrence Berkeley National Laboratory and Oak Ridge National Laboratory (ANL, 2019).

2.6. Input Specifications for Building Energy Simulation

Building simulations usually require a large number of inputs, and whole-building energy simulation tools require skilled experience and understanding of the inputs as well as the underlying algorithms and procedures upon which the program are built. Otherwise, easy-to-use simulation tools do not require many input parameters in the user interface since the tool developers previously defined the inputs and provide default values. To define the required input parameters, there are four input specification for building energy simulation including: the International Energy Conservation Code, the Mortgage Industry National Home Energy Rating Systems Standards, the Building America House Simulation Protocols, and the Prototype Residential Building Designs for Energy and Sustainability Assessment.

2.6.1. International Energy Conservation Code (IECC)

The IECC provides a performance-based compliance path in Section R405: Simulated Performance Alternative. This section provides information about mandatory requirements, definitions, calculate procedures, and calculation software tools for performance-based compliance. In the performance-based compliance, the annual energy cost of the proposed residence (proposed design) must be less than or equal to the annual energy cost of the standard reference design in order to pass performance-based compliance requirements (ICC, 2015). In other words, the user needs to simulate two designs (i.e., the proposed design, and the standard reference design). To do this, the user

needs to know about how to create the inputs of the proposed design and the standard reference design respectively. The IECC's Table R405.5.2 states that input specifications should be included in the standard reference design and the proposed design for each building component. However, it does not indicate which inputs should be entered if complex input configurations are possible, such as roof types or foundation types. This problem may be a problem for users or software developers in constructing inputs to compare the proposed design with the standard reference design.

2.6.2. Mortgage Industry National Home Energy Rating Systems Standards

The purpose of this standard is to produce accurate and consistent home energy rating such as the Home Energy Rating System index (HERS index). The HERS index is represented by a score of 0 to 100, where a house without any net annual energy purchases has an index value of 0. In contrast if a house is the same as the HERS Reference Home, which is the HERS index baseline, it has an index value of 100. This index value is calculated using the results of a comparison of the Rated Home and Reference Home models (RESNET, 2013).

Chapter Three of this document provides a detailed HERS Rating calculation method. In particular, Table 303.4.1 provides a table of input parameters that make up the HERS Reference Home and the Rated Home in a manner similar to Table R405.5.2 of the IECC mentioned above.

2.6.3. Building America House Simulation Protocols

Building America (BA) is an industry-led research program sponsored by the U.S. Department of Energy (DOE). Building America is primarily a program committed to facilitating the development and application of advanced building energy technologies. As the size of the home building and retrofit industries grew, Building America needed accurate and consistent methods to analyze them (Wilson et al., 2014).

Accordingly, the Building America House Simulation Protocols have been developed to facilitate accurate and consistent analysis of new and existing, single-family and multifamily buildings across different simulation analysis programs. These specifications define a consistent reference building and provide simulation input standards for building envelope, cooling and heating equipment, distribution system, domestic hot water, air infiltration, mechanical ventilation, lighting, appliances and miscellaneous electric loads.

2.6.4. Prototype Residential Building Designs for Energy and Sustainability Assessment

This study was conducted by the Applied Economics Office (AEO) in the Engineering Laboratory at the National Institute of Standards and Technology (NIST). It created two “prototypical” residential building models to provide a basis for predicting energy, life cycle cost, and sustainability of new and existing buildings for research in the residential building sector concerned with energy efficiency and sustainability. The two houses were used as a baseline to predict energy savings and sustainability impacts. The two prototype detached residential house simulation models (a one-story building

and a two-story building) were developed based on the 2009 IECC. These prototypes will be used as a framework for developing additional prototypes designs (Kneifel, 2012). However, this study only covered the reference house models, so it is difficult to use for the building energy code which needs both a proposed house and a reference house model. Furthermore, since this study only considers two types of buildings, it is not possible to analyze other building types (i.e., multi-family, etc.).

In the study it recommended that input specifications must be uniform, and prepared for both the proposed (rated) and standard (reference) houses to use for building performance rating and code compliance. The uniform input specifications should lead to the same results between users or simulation tools. The uniform input specifications will also help define default values when developing an improved easy-to-use simulation tool which has a lot of pre-defined input values for building performance rating and code compliance.

2.7. Previous Studies about Result Differences between Building Performance

Simulation Tools for Building Energy Rating and Code Compliance

Currently, hourly building energy performance simulation tools are used for building energy rating and code compliance. The role of simulation is very important for their accurate and consistent results. However, there are differences between the simulations for building energy performance ratings and code compliance when the results from different software are used to evaluate the same building under the same weather conditions. Such problems of inconsistency have been identified in selected

papers and reports, such as: Raslan et al. (2009), Raslan and Davies (2010), Mukhopadhyay et al (2009), and Schwartz and Raslan (2013).

Raslan et al. (2009) tested eight building energy performance simulation tools, certified by Approved Document Part L2a (ADL2A), which allows for the use of a variety of accredited simulation tools in the UK. In this study, they found that the different simulation tools resulted in a lack of consistency in providing a pass/fail outcome for the same building. The inconsistent results were drawn from: a) limitations in the scope of the applicability of the accredited tools, b) a lack of input data standardization, and c) variability between tool results in building energy simulation. To solve these issues, they recommended: a) extending the applicability of simulation tools, b) the development of more rigorous accreditation procedures, and c) the need for measures to increase the validity and consistency of results (Raslan et al., 2009).

Raslan and Davies (2010) conducted a wide-scale industry survey of simulation-based compliance methodologies for the UK building regulations. Despite the fact that simulation tools were accredited by the Approved Document Part L2A, which allows for the use of a variety of accredited simulation tools in the UK, results from a wide-scale industry survey found that in the majority of cases where multiple tools were used, respondents reported significant differences and frequent inconsistencies in results (Raslan & Davies, 2010).

In the report by Mukhopadhyay et al. (Mukhopadhyay et al., 2013), an analysis was conducted that explored the differences in results obtained from four code-compliant programs (IC3 Ver.3.12.1, REM/Rate Ver.13.00, EnergyGauge Ver.2.8.05 and

REScheck Ver.4.4.3.1), which were certified to comply with the 2009 IECC by RESNET. The study compared the building annual energy consumption and percentage above-code results obtained from the four hourly building energy simulation programs used the 2009 IECC. To accomplish this, special user input parameters for IC3 Ver.3.12.1, REM/Rate Ver.13.00, EnergyGauge Ver.2.8.05 and REScheck Ver.4.4.3.1 were developed for the 2009 IECC. Sensitivity tests were then conducted on the house size, window size, exterior insulation, window SHGC, window U-value, and slab insulation. According to the analysis results, there were no significant differences in the results between the software for the basecase model that met code compliance. However, significant differences were found when certain parameters were above or below code-compliance varied, for example window-to-wall ratios, window u-values, wall, ceiling and floor insulation levels, etc.

Schwartz and Raslan (2013) conducted a case-study analysis to determine how the results from different building energy performance simulation tools varied for different performance rating systems. In this study, three different building performance simulation tools (Tas-EDSL Ver.9.2.1, EnergyPlus Ver.7.1, and IES-VE Ver.6.4.0.10) were used for two different rating systems (BREEAM 2011 and LEED 2009). Results of the case-study showed that different simulation tools resulted in different energy consumption, for the following reasons: a) The difference in the way the tools interpret the construction element area, b) the use of different weather files in the simulations, c) simulation algorithm differences, d) differences in the required input data, and e) human error. However, the different building performance simulation results had only a minor

effect on the BREEAM and LEED's ratings. This is because both BREEAM and LEED express 'performance improvement' as a ratio between the performances of the 'Designed' building against a 'Basecase' building, which helps reduce the magnitude of any differences (Schwartz & Raslan, 2013).

2.8. Summary of Literature Review

The earliest residential building energy codes and standards began shortly after the oil embargoes of the 1960s and 1970s. These caused the re-evaluation of building energy codes and the consequent support of energy efficiency requirements that produced the first minimum building energy code, ASHRAE Standard 90-75 (Hunn, 2010).

In 1977, the first residential model energy code, the Model Code for Energy Conservation in New Buildings (MCEC), was developed into code language using portions of the technical criteria of the ASHRAE 90-75. In 1983, the Model Energy Code (MEC), a subsequent revision of the 1978 MCEC was published. Finally, in 1998, the Model Energy Code was replaced by the International Codes Council (ICC)'s International Energy Conservation Code (IECC).

Currently, the International Energy Conservation Code (IECC) is the most widely-used residential building energy code in the United States. Either the IECC or the IECC with amendments has been adopted by 33 states in the U.S. (DOE, 2016). The latest version of the IECC (2018 IECC) contains three compliance requirements: mandatory, prescriptive, and performance elements. In the IECC, the mandatory

requirement is the basic standard that must be met, regardless of the compliance path selected. The prescriptive aspects give users different ways of meeting the minimum requirements for each building component. The performance criteria include specifications for the standard references and proposed designs used in whole-building energy simulations (Hui, 2003; Taylor et al., 2010). Although the necessity of using whole-building energy simulations makes the performance path more complicated than the prescriptive path, the performance path has substantial advantages that allow for more flexible design and construction options (Taylor et al., 2010).

Even if different whole-building energy simulation tools can be used for the IECC performance-based residential building code compliance (ICC, 2015), most of simulation programs are too complicated for use by building energy code officials or homeowners who have not had time to learn how to use the programs. To resolve this problem, simplified simulation tools, which have an easy-to-use user interface that require fewer user input parameters have been developed. Such software tools have had a significant impact on the increased use of the building performance-based code compliance. However, this has also increased the number of complaints about the differences in code-compliance results from one software to the next, in spite of industry efforts to test software programs.

Currently, there are several building energy simulation validation methods, including: BESTEST, ASHRAE Standard-140, and the RESNET Procedures (ASHRAE, 2017; R Judkoff et al., 1995; RESNET, 2016d, 2020b). The current test methods, which include: IEA BESTEST, HVAC BESTEST, BESTEST-EX, and Class I test cases in

ASHRAE Standard-140 have been developed to test the algorithms of building energy performance simulation (ASHRAE, 2017; R Judkoff et al., 1995; Judkoff et al., 2011; Neymark et al., 2002, 2004, 2008) . Since these tests require complex inputs and multiple outputs to view the test results, they cannot be used with a simplified simulation program without modification. In addition, even though the HERS BESTEST, Florida-HERS BESTEST, or the Class II test in ASHRAE Standard-140, or the RESNET Procedures for Verification of International Energy Conservation Code Performance Path Calculation Tools were developed for simplified simulation tools, these still require additional testing for several missing building energy components such as attic types and foundation types. To solve this problem, it is necessary to provide clearly defined input parameters for the reference house and the designed house.

Finally, according to Mukhopadhyay, the performance-based compliance results of the various RESNET-certified software did not show significant differences when the parameters tested fell within the range of the code-compliant values. However, when the energy performance of the building parameters were systematically changed and tested, the results across the different software were found to be significantly different for parameter values that yielded above-code simulations (Mukhopadhyay et al., 2013). Thus, sensitivity testing of the building energy components should also be used to verify the building energy simulation models for the IECC performance-based compliance method for both code-compliance, and for values above or below code compliance.

3. SIGNIFICANCE AND LIMITATIONS

3.1. Significance of the Study

The purpose of this study is to compare analyzed results from the detailed building energy simulation model of an existing single-family residence versus the results from the simplified building energy simulation model of the same residence to determine which parameters that represent an existing house.

This study is expected to provide the following benefits toward the analysis of residential building energy code compliance based on building energy simulation:

- a. Analysis of a simplified residential building energy simulation model for code compliance; and
- b. Analysis of residential building input specifications for code-compliant simulation.

3.2. Limitations of the Study

Limitations to this study include:

- a. This study is focused solely on single-family residential building code-compliance simulation and its validation methods;
- b. This study was performed using a single-family, IECC code-compliant detached house in Texas (a hot and humid climate);
- c. This study is focused on a one-story case-study house, a slab-on-grade house with a gas furnace for the heating and domestic water heating and an electric air-conditioner for the cooling;
- d. This study is focused on the simplified simulation represented by the ESL's IC3

simulation model; and

e. This study is focused on the DOE-2.1e building energy simulation program.

4. RESEARCH METHODOLOGY

This chapter explains the methodology used in this research. The purpose of this methodology is to help develop improved IECC-compliant building energy simulation models of new and existing residences that are accurate, consistent, and easy-to-use. This chapter describes a simplified house simulation model for the IECC code compliance, a case-study house simulation model, measurements of selected parameters, a calibrated simulation model, and an analysis of the 2015 International Energy Conservation Code (IECC) compliance residential simulation models. The methodology in this research includes five major tasks 1) Development of case-study house simulation models, 2) Analysis of the case-study house simulation models, 3) Development of a detailed and a simplified house simulation models for the IECC, 4) Analysis of the IECC simulation house models, and 5) Summary of the methodology.

The overall procedure for the improved IECC residential simulation model analysis in this study is shown in Figure 4.1 and Figure 4.2. In this study, two major analyzes were conducted. The first is the case-study house simulation analysis. For the case-study house analysis, a simplified and detailed case-study house simulation models were developed. To develop the case-study simulation models, case-study house information, monthly utility billing data, weather data, and measured house temperature data were used. However, because some of the input parameters of the simulation model cannot be measured or information is not available, those input parameters were taken from a simplified house simulation model developed in Ch 4.2. During the simulation

model development, the monthly utility data was used to calibrate the detailed simulation model. The characteristics of the simplified building simulation model include external shading, unconditioned space, domestic hot water heater, and ground heat transfer were tested on the developed detailed calibrated case-study house simulation model. The second is the analysis of the IECC simulation models. For this analysis, a 2015 IECC simplified and detailed simulation models were developed. With the models, the features in the case-study house were tested. Detailed descriptions of it are shown in the corresponding sections.

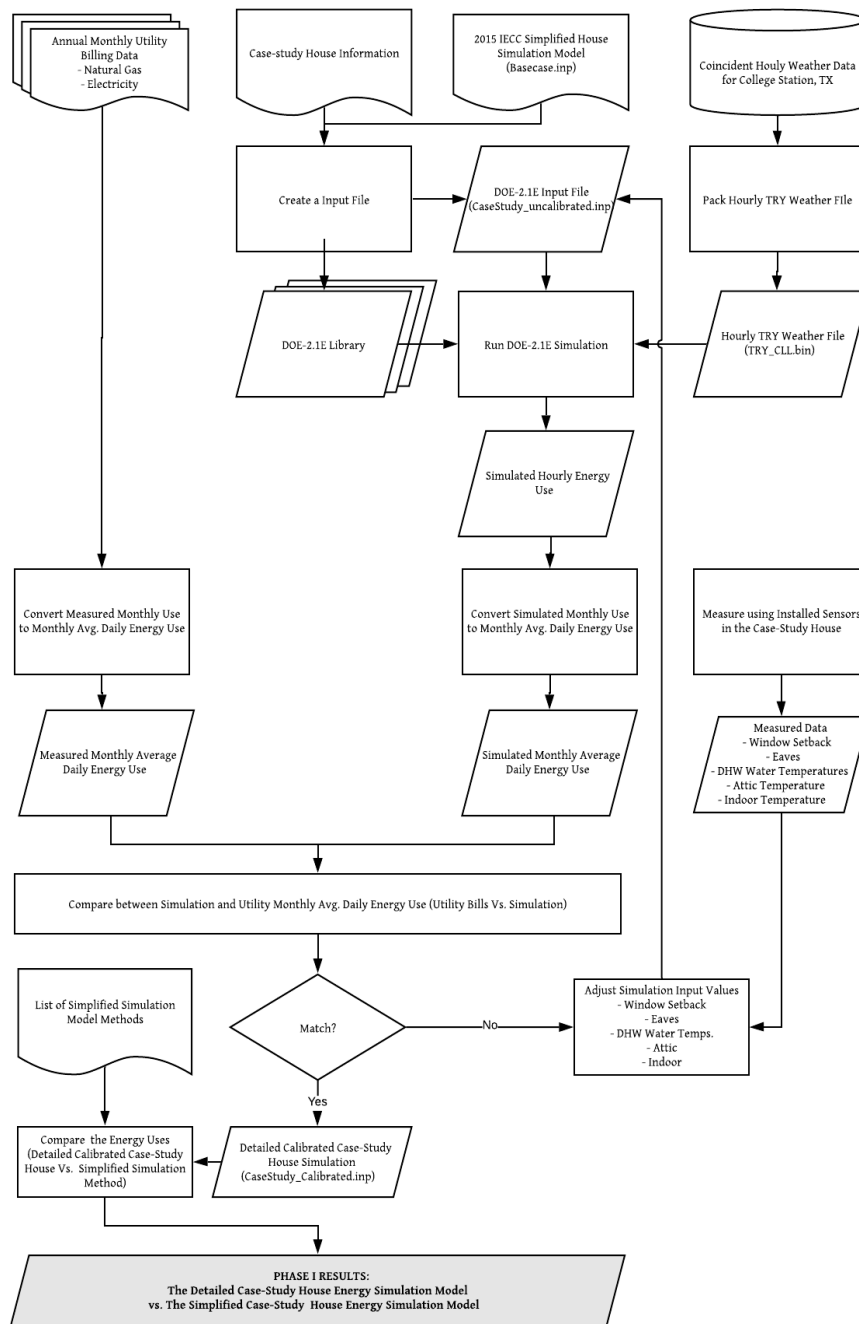


Figure 4.1: Overall Methodology- Phase I: Analysis of Case-Study House Simulation

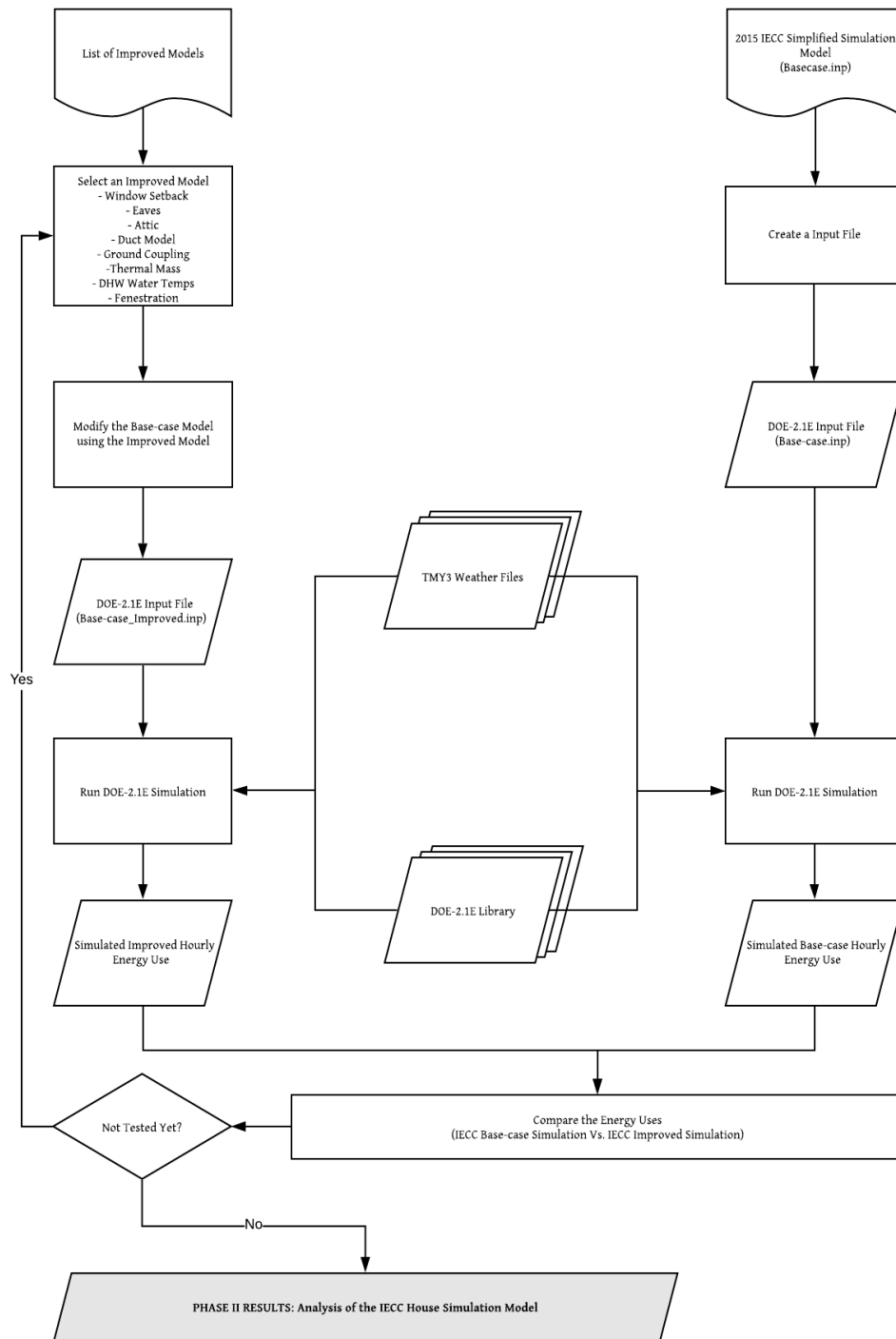


Figure 4.2: Overall Methodology- Phase II: Analysis of the IECC House Simulation

4.1. Development of a Detailed Case-study House Simulation Model

A detailed case-study house simulation model of a house in College Station, TX, was developed to validate the existing simplified case-study house simulation model. At the case-study house, attic temperatures were measured, the inlet, outlet water temperatures of the domestic hot water system, and closet space that contained the DHW heater were measured. In addition, the indoor air temperature of the house was measured, and the attached garage temperature was measured and compared with the simulated results.

This section describes the case study house information, inputs for the case study house simulation, monthly utility billing data, weather data, simplified house simulation model, and validation method that was used. It also presents a discussion of how the detailed case-study house simulation was calibrated to the measured data.

The detailed house simulation analysis was divided into two stages. In the first stage, the simulation was run using the basic building specification. In the second stage, the detailed house simulation models were improved using specific measured data to obtain more accurate results. After the first stage simulation, a more accurate detailed house simulation model was created using selected data measured on-site, including: window setback, roof eaves, attic temperatures, DHW closet temperatures, indoor temperatures, DHW outlet water temperatures, and DHW inlet water temperatures.

4.1.1. Information of the Case-study House

In this section, information about the case-study house is presented. The case-study house is a single-story, single-family residence located in College Station, Texas. Building characteristics and photos were collected from the homeowner. The building characteristics were also partially taken from the summary of the building characteristics in previous study (Im, 2003). Figure 4.3 through Figure 4.19 shows the four orientations of the case-study house. The case study house uses natural gas for heating and domestic hot water, and electricity for cooling and other electric end-uses for the 2,391 sqft. residence. Detailed information is provided in Table 4.1. This information was used to complete the as-built house simulation model together with the simplified house simulation model. Table 4.1 shows a summary of the building characteristics.



Figure 4.3: Front View (Southwest) of the Case-study House



Figure 4.4: Back View (Northwest) of the Case-study House



Figure 4.5: Side View (Northwest) of the Case-study House



Figure 4.6: Side View (Northeast) of the Case-study House

Table 4.1: Building Characteristics of the Case-study House

Component		Case-study House	
Envelope	Exterior Wall	Wall Color	Dark
		Average Wall Height	9 ft
		Insulation R-Value	R-13
		Stud Spacing	16"
	Windows	Grass Area	234 ft ²
		Gazing Type	Clear Double Pane
		Frame Type	Aluminum
		U-Value	0.87
		SHGC	0.66
		Setback	3 inch
	Roof/Attic	Roof Color	Dark
		Ceiling Type	Ceiling with Attic Above
		Insulation R-Value	R-29.6 (8" insulation depth)
		Eaves	1.5 ft
Slab Floor	Gross Area	2,391 ft ²	
	Slab Perimeter R-Value	R-0	
Systems	Heating	Fuel	Natural Gas
		System Type	Furnace
		Efficiency (AFUE or HSPF)	66%
		Manufacturer	Lennox
		System Location	Attic
	Cooling	System Type	Air Conditioner, Air Cooled
		Efficiency (SEER)	10
		Manufacturer	Lennox
		System Location	Unconditioned Area
	Domestic Water Heater	Fuel	Gas
		Capacity	50 Gallon
		Energy Factor	0.594
		Burner Capacity	38,000 Btu/h
		Type	Storage
Tank Location		Unconditioned Area	
Manufacturer		Rheem	
Tank Temperature	135.3 F		

4.1.2. Monthly Utility Billing Data

One year of monthly utility bills for the electricity and natural gas use for the period Aug 2018 through July 2019 were collected from the homeowner. Table 4.2 and Table 4.3 show the monthly electricity and natural gas utility billing data, and the calculated monthly average daily use.

Table 4.2: Monthly Electricity Utility Billing Data for the Case-study House

Date of Service		Days in the Billing Periods	Monthly Elec. Usage (kWh)	Monthly Avg. Daily Elec. Use (kWh/day)	Average Daily Temp. of Billing Period (F)
From	to				
8/11/2018	9/11/2018	32	2491	77.8	84.18
9/12/2018	10/10/2018	29	1716	59.2	77.51
10/11/2018	11/8/2018	29	903	31.1	64.79
11/9/2018	12/10/2018	32	795	24.8	51.74
12/11/2018	1/10/2019	31	1007	32.5	52.85
1/11/2019	2/8/2019	29	722	24.9	52.86
2/9/2019	3/11/2019	31	723	23.3	53.21
3/12/2019	4/9/2019	29	780	26.9	63.36
4/10/2019	5/9/2019	30	1171	39.0	70.45
5/10/2019	6/10/2019	32	1994	62.3	78.84
6/11/2019	7/10/2019	30	2402	80.1	81.79
7/11/2019	8/9/2019	30	2691	89.7	84.54

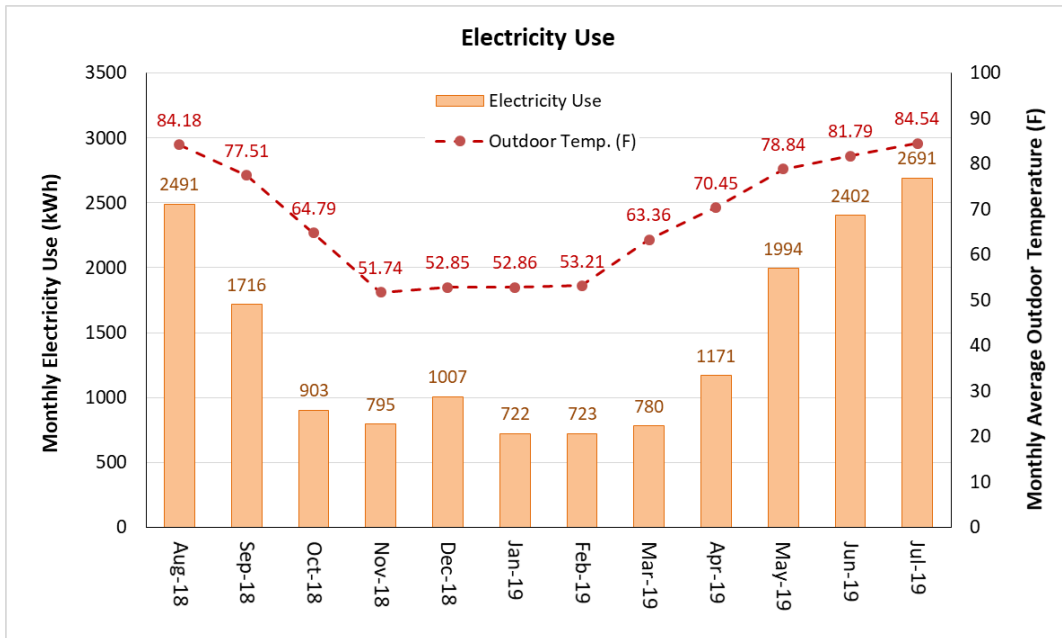


Figure 4.7: Monthly Electricity Use for the Case-study House

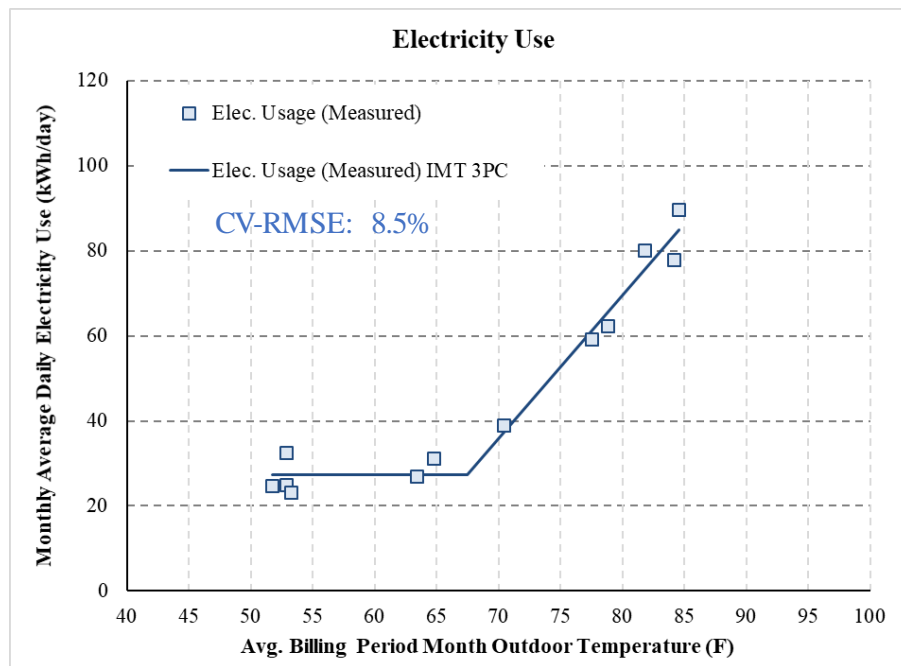


Figure 4.8: Average Billing Period Outdoor Temp. vs. Monthly Average Daily Electricity Use

Table 4.3: Monthly Natural Gas Utility Billing Data for the Case-study House

Date of Service		Days in the Billing Periods	Monthly N.G. Usage (MCF)	Monthly N.G. Usage (MMBtu)	Monthly Avg. Daily N.G. Usage (MMBtu/day)	Average Daily Temp. of Billing Period (F)
From	to					
8/17/2018	9/19/2018	34	2.3	2.3	0.068	82.94
9/20/2018	10/15/2018	26	1.7	1.7	0.065	75.33
10/16/2018	11/14/2018	30	4.4	4.4	0.147	59.82
11/15/2018	12/14/2018	30	6.8	6.8	0.227	53.45
12/15/2018	1/16/2019	33	8.0	8.0	0.242	52.2
1/17/2019	2/14/2019	29	8.2	8.2	0.283	53.1
2/15/2019	3/15/2019	29	7.3	7.3	0.252	55.0
3/16/2019	4/15/2019	31	3.4	3.4	0.110	64.0
4/16/2019	5/15/2019	30	1.3	1.3	0.043	71.1
5/16/2019	6/17/2019	33	3.6	3.6	0.109	80.7
6/18/2019	7/16/2019	29	2.0	2.0	0.069	83.0
7/17/2019	8/19/2019	34	2.3	2.3	0.068	84.6

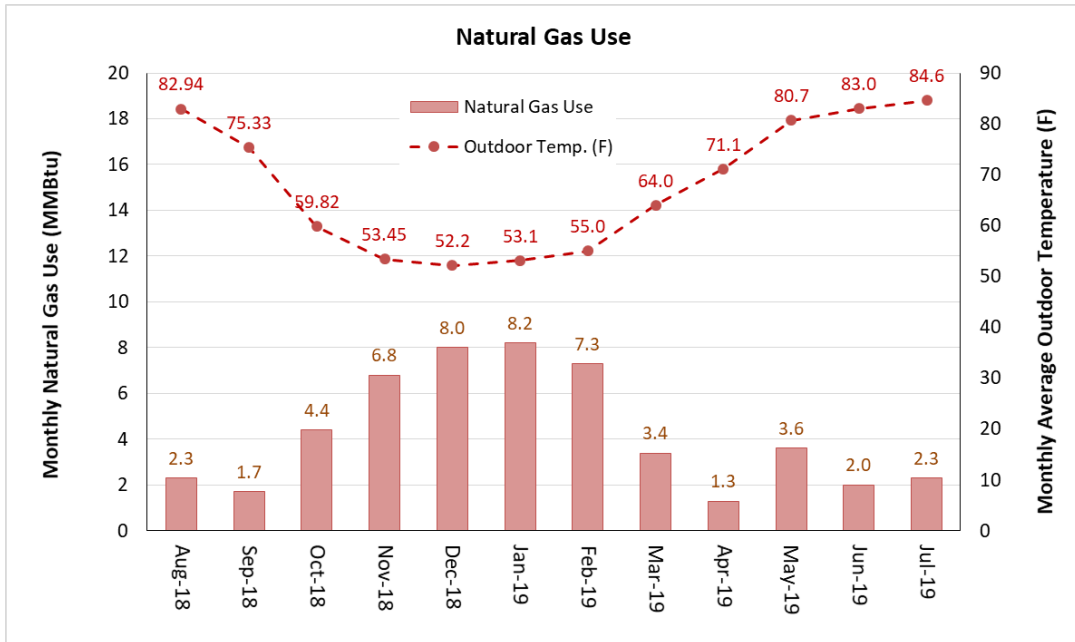


Figure 4.9: Monthly Natural Gas Use for the Case-study House

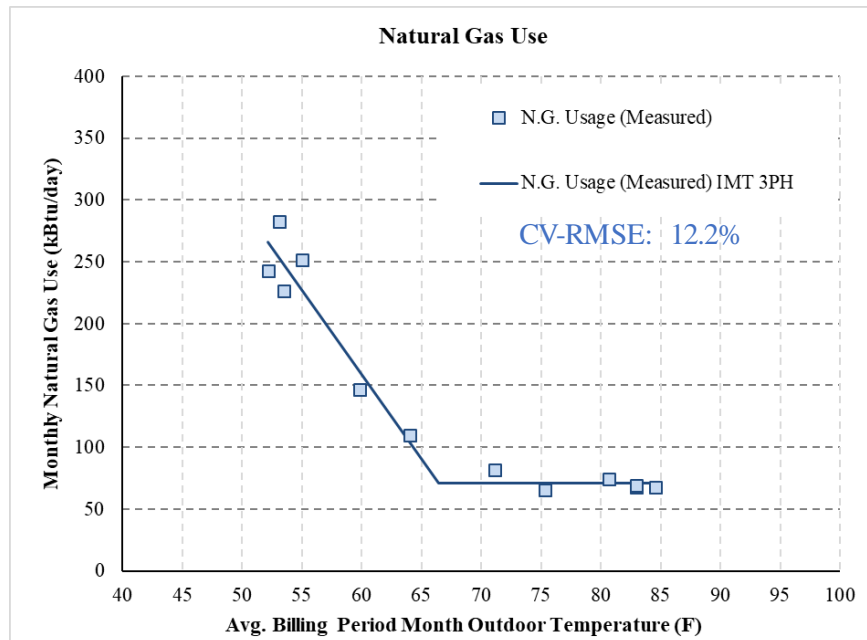


Figure 4.10: Average Billing Period Outdoor Temp. vs. Monthly Average Daily Natural Gas Use

4.1.3. Weather Data

4.1.3.1. Measured Weather Data from Nearby Solar Test Bench

For the case-study house simulation model, the global solar radiation data were obtained from the nearby Solar Test Bench (STB) at Energy Systems Laboratory of Texas A&M University. The STB is located on the roof of the Langford A Architecture Building at the Texas A&M University’s main campus, College Station, TX. Outdoor air temperature, relative humidity, wind speed and direction, and beam and diffuse solar radiation are measured at the STB. The STB measures one-minute interval data, which was converted to hourly data for use in this study.

Table 4.4: Summary of Sensors Installed at the Solar Test Bench

Sensor	Number of Sensors	Type	Manufacturer / Model
Temperature and Relative Humidity	2	Temperature and Relative Humidity	Vaisala / HMP45A
Anemometer	2	Wind Speed and Wind Direction	Metone / 034B
Pyranometer (LICOR)	3	Global Solar Radiation	Li-cor / LI200
Normal Incidence Pyrheliometer (NIP)	2	Normal Incidence Solar Radiation	Eppley / NIP
Precision Spectral Pyranometer (PSP)	2	Global Solar Radiation	Eppley / PSP
Black and White Pyranometer (B/W)	2	Diffused Solar Radiation	Eppley / 8-48
Ultraviolet Radiometer (TUVR)	2	UV radiation	Eppley / TUVR

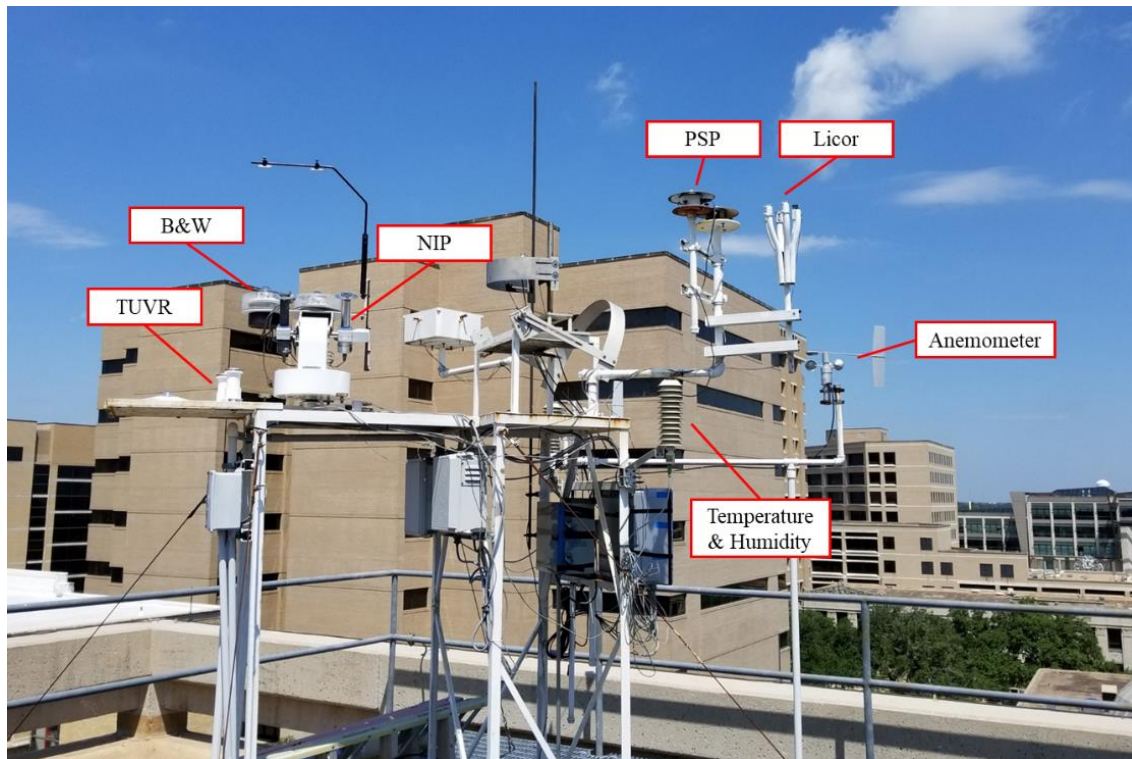


Figure 4.11: Solar Test Bench

4.1.3.2. National Centers for Environmental Information

For this study weather data was also obtained from the National Oceanic and Atmospheric Administration (NOAA) National Centers for Environmental Information (NCEI), formerly the National Climatic Data Center (NCDC), which included: dry bulb temperatures, relative humidity, wind direction, and wind speed. Figure 4.12 shows the hourly data that was available for downloading at the NCEI webpage. The Local Climatological Data (LCD) for Easterwood Airport, College Station, TX was also used to cross-check the measured data from the STB.

The screenshot displays the NOAA National Centers for Environmental Information (NCEI) website. The header includes the NOAA logo, the text "NOAA NATIONAL CENTERS FOR ENVIRONMENTAL INFORMATION", and "NATIONAL OCEANIC AND ATMOSPHERIC ADMINISTRATION". Below the header, there is a navigation menu with links for Home, Climate Information, Data Access, Customer Support, Contact, and About. A search bar is located on the right side of the menu. The main content area is titled "Local Climatological Data (LCD)" and provides information about the data, including a list of quick links and a description of the data format and availability.

NOAA NATIONAL CENTERS FOR ENVIRONMENTAL INFORMATION
NATIONAL OCEANIC AND ATMOSPHERIC ADMINISTRATION
Formerly the National Climatic Data Center (NCDC)... [more about NCEI](#)

Home Climate Information Data Access Customer Support Contact About Search

Home > Data Access > Land-Based Station > Datasets > Local Climatological Data (LCD)

Quick Links

Land-Based Station

Datasets

LCD

COOP

Climate Normals

USHCN

GHCN

GSOD

USCRN

GOSIC

ASOS

AWOS

Solar Radiation

Local Climatological Data (LCD)

Local Climatological Data (LCD) consist of hourly, daily, and monthly summaries for approximately 1,600 U.S. locations.

- Local Climatological Data (LCD)
Data are available based on when the station began until present. Please note, there may be a 48-hour lag in the availability of the most recent data.
- LCD Sample
The LCD product consists of four forms. Each of these forms is also available in comma separated values (CSV) format. Follow these links to view LCD sample before accessing the data.
- QCLCD ASCII Files
QCLCD ASCII, or plain text, data files provide monthly summaries of observations for all stations. Files between 2005 and 2007 may not match the same information presented in the QCLCD web form, and the Hourly Wind Speed is represented in knots (kts) rather than miles per hour (mph) for this period. The QCLCD ASCII data are available as compressed zip files. To download them, right click on the filename and select Save As. Then decompress the files using WinZip (Microsoft Windows/NT environment) or standard UNIX gunzip/tar.

Figure 4.12: Webpage of NCEI

4.1.3.3. *Hourly Weather Data Preparation for the TRY Weather File*

In order to develop a calibrated simulation of the case-study house using the monthly utility billing data, actual weather data that corresponds to the specific utility billing periods of natural gas and electricity use was used. For this study, a Test Reference Year (TRY) format weather file containing the actual weather data was prepared (Kim & Baltazar, 2010). Hourly weather data was also collected from the Solar Test Bench (STB) at the Energy Systems Laboratory at Texas A&M University and data were collected from the National Centers for Environmental Information (NCEI), formerly the National Climatic Data Center for cross-checking purposes and for filling in missing data. The hourly weather parameters for the weather file are shown below:

- Dry bulb temperature (°F),
- Wet bulb temperature (°F),
- Dew point temperature (°F),
- Wind speed (knots),
- Wind direction (°),
- Global solar radiation (Btu/hr-ft²),
- Calculated Direct normal solar radiation (Btu/hr-ft²), and
- Station pressure (inHg).

For the calculation for the direct normal solar radiation using the measured global solar radiation, The Erbs correlation method was used (Duffie & Beckman, 2014). The calculation of direct normal solar radiation (I_b) uses the following equations.

$$\frac{I_d}{I} = 1.0 - 0.09K_T \quad \text{For } K_T \leq 0.22 \quad (4.1)$$

$$\frac{I_d}{I} = 0.9511 - 0.1604K_T + 4.388K_T^2 - 16.638K_T^3 + 12.336K_T^4 \quad \text{For } 0.22 < K_T \leq 0.8 \quad (4.2)$$

$$\frac{I_d}{I} = 0.165 \quad \text{For } K_T > 0.8 \quad (4.3)$$

Where $K_T = \text{Hourly clearness index} = \frac{I}{I_o}$,

$I_d = \text{Hourly diffuse solar radiation}$,

$I = \text{Hourly measured global solar radiation}$, and

$I_o = \text{Hourly extraterrestrial radiation}$

The hourly extraterrestrial solar radiation (I_o) was calculated using

$$I_o \cong G_o = G_{SC} \left(1 + 0.033 \cos \frac{360n}{365}\right) \times (\cos \phi \cos \delta \cos \omega + \sin \phi \sin \delta) \quad (4.4)$$

Where $G_o = \text{Hourly extraterrestrial radiation between sunrise and sunset}$,

$G_{SC} = \text{Solar constant} = 1,367 \frac{W}{m^2}$,

$n = n^{\text{th}} \text{ day of the year}$,

$\phi = \text{Latitude in degree}$,

$\delta = \text{Solar declination} = 23.45 \sin 360 \frac{284-n}{365}$, and

$\omega = \text{Hourly angle at the midpoint of the hour in degree}$

$$I_d = \left(\frac{I_d}{I}\right) \times I \quad (4.5)$$

$$I_b = \left\{1 - \left(\frac{I_d}{I}\right)\right\} \times I \quad (4.6)$$

4.1.3.4. *Weather Conditions*

This section provides additional detail about the hourly weather data used for the corresponding period of the utility bills. The data was prepared (i.e., packed) for the TRY weather file format for use with the DOE-2.1e calibrated simulation. The list of the figures and the corresponding weather data is shown below.

- Hourly dry bulb temperature,
- Hourly wet bulb temperature,
- Hourly dew point temperature,
- Hourly wind speed,
- Global solar radiation, and
- Direct normal solar radiation.

Data at 1-minute intervals from Aug 1st, 2018 to July 8th, 2019, which correspond to the period of the utility bills for one year. The building energy simulation program in this study requires hourly weather data, therefore this 1-min interval data was converted into hourly data. In addition, all of the above data except for direct normal solar radiation were obtained using the STB. The hourly direct normal solar radiation was calculated using the equations shown in Equation 4.1 to Equation 4.6 in Ch. 4.1.3.3. Figure 4.13 shows the hourly dry bulb temperature. In the cooling season, the outside temperature has risen to about 100 F, and it has decreased to about 70 F. In the heating season, the temperature has decreased to about 30 F, and it has increased to about 80 F. Moreover, the temperature difference between the days became larger than the cooling season.

Figure 4.14 shows the hourly web bulb temperature. The web bulb temperature had a similar tendency to the dry bulb temperature. This is also related to the dew point temperature. Figure 4.15 shows the hourly dew point temperature. The dew point temperature also showed the same tendency as the dry and wet bulb temperatures. Figure 4.16 shows the hourly wind speed. The wind speed varied regardless of the seasons, different from the temperatures, and was obtained with a wind speed sensor in the STB. Wind speed is very important weather data in a simulation because it is closely related to the calculation of heat loss of the building envelope such as walls and windows. Figure 4.17 shows the hourly global solar radiation. The global solar radiation was obtained using an LI-COR pyranometer. The global solar radiation was generally high in summer and low in winter compared to summer. Using this global solar radiation, hourly direct normal solar radiation was calculated. Figure 4.18 shows the hourly direct normal solar radiation. The hourly direct normal solar radiation calculation equation using the global solar radiation is shown in Equation 4.1 to Equation 4.6 in Ch. 4.1.3.3.

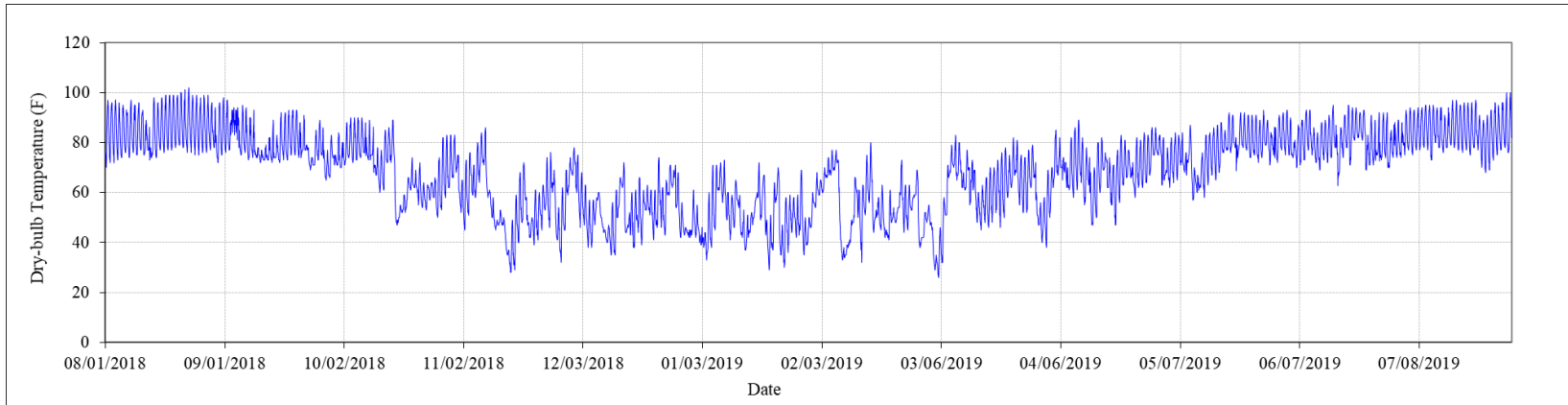


Figure 4.13: Hourly Dry Bulb Temperature (8/1/2018 through 7/8/2019)

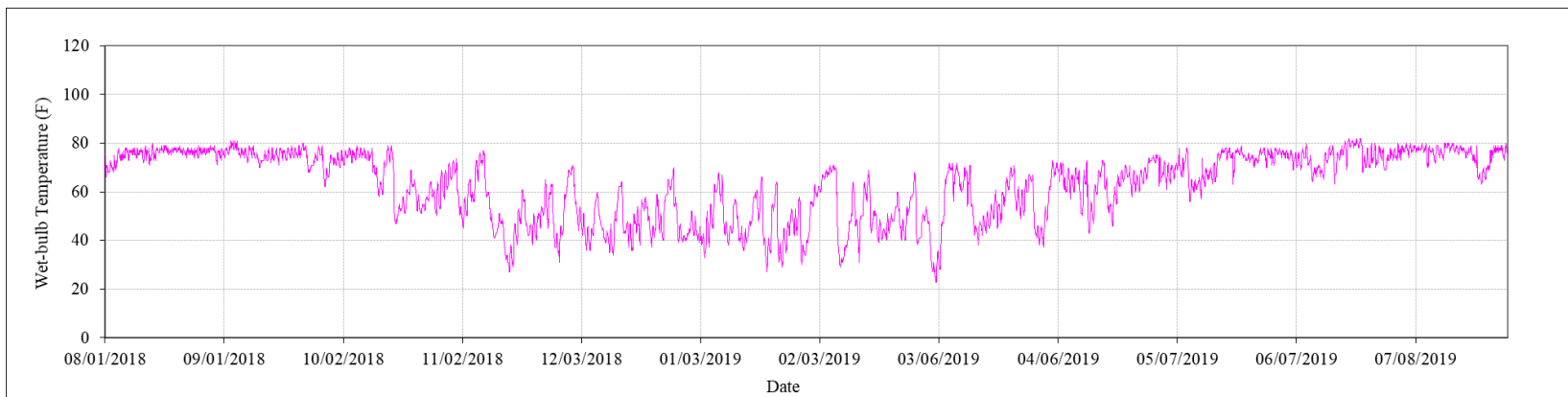


Figure 4.14: Hourly Wet Bulb Temperature (8/1/2018 through 7/8/2019)

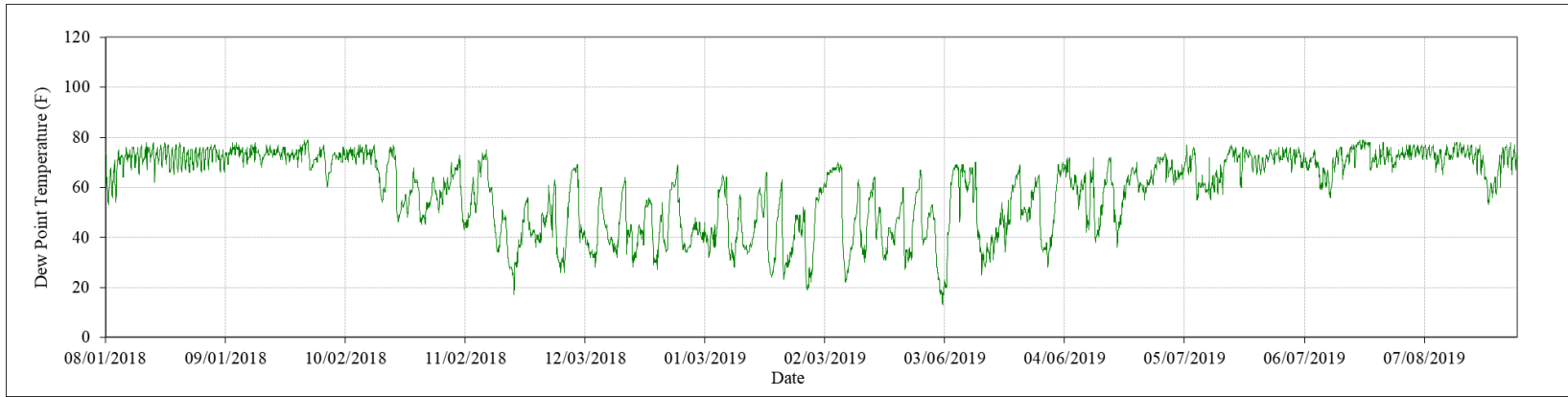


Figure 4.15: Hourly Dew Point Temperature (8/1/2018 through 7/8/2019)

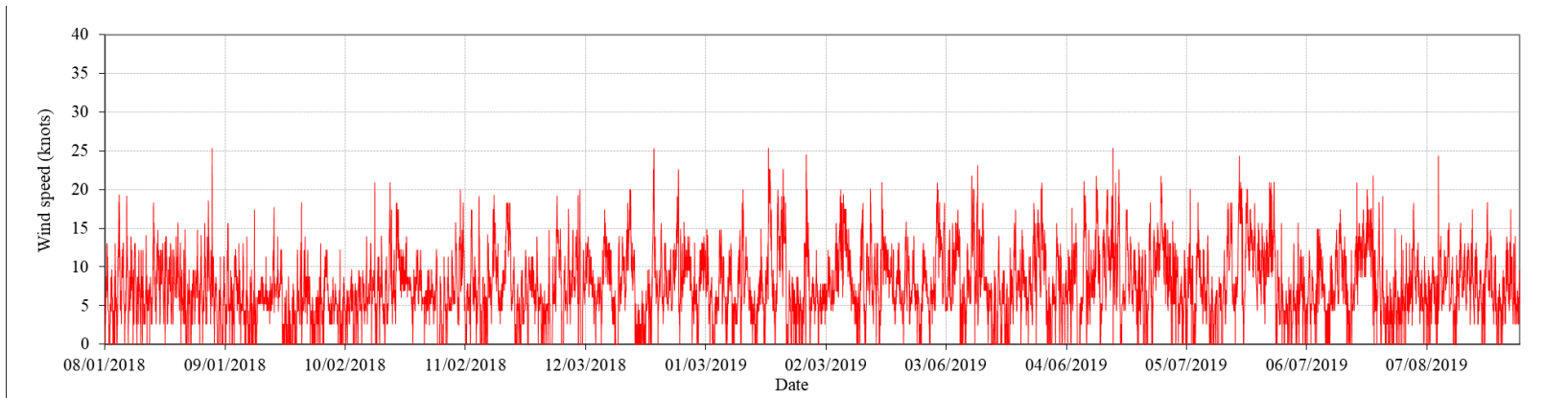


Figure 4.16: Hourly Wind Speed (8/1/2018 through 7/8/2019)

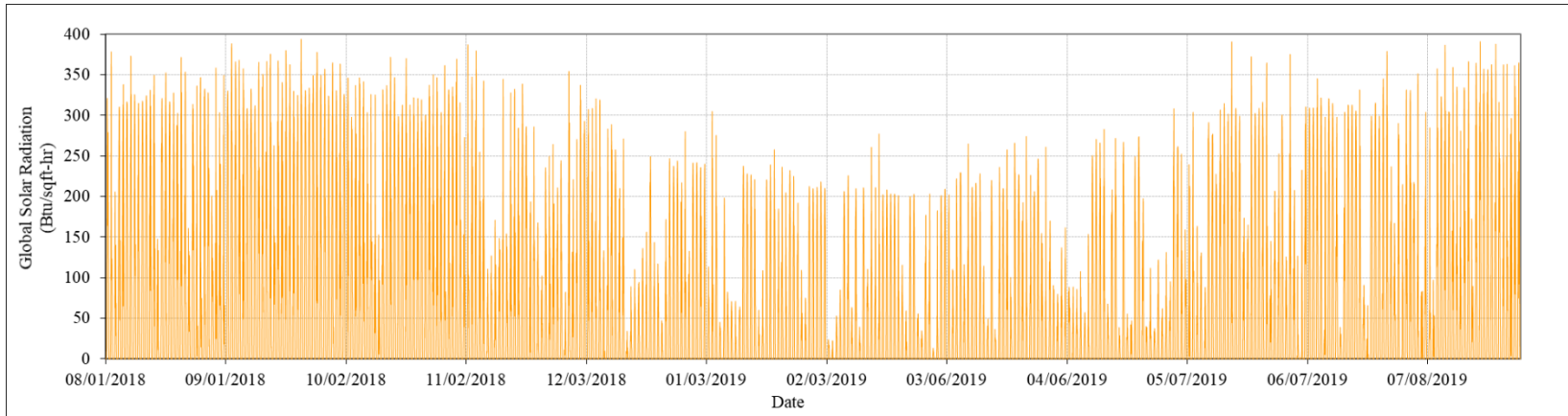


Figure 4.17: Hourly Global Solar Radiation (8/1/2018 through 7/8/2019)

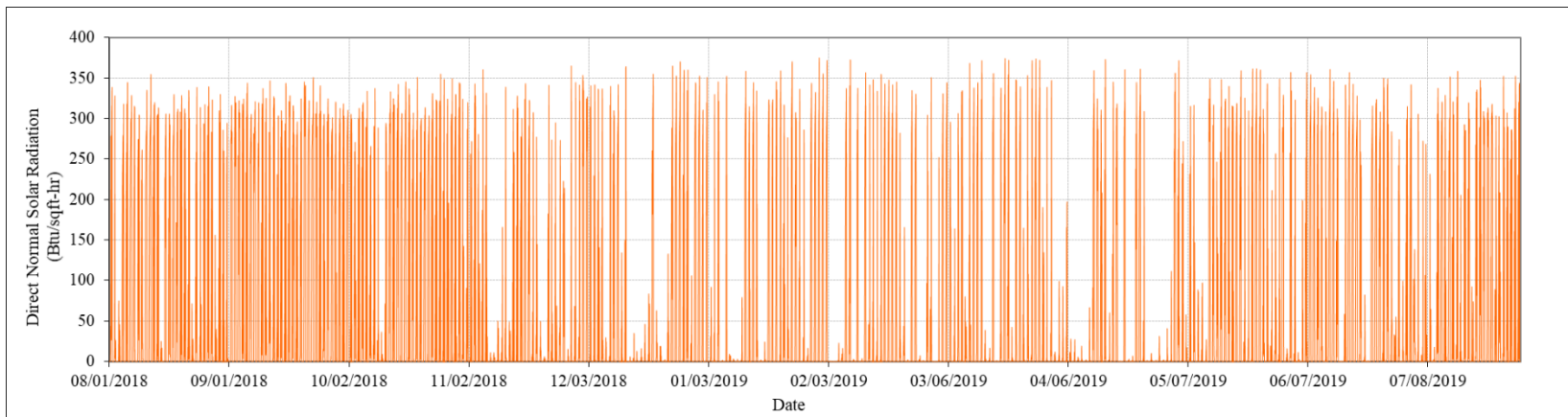


Figure 4.18: Hourly Direct Normal Solar Radiation (8/1/2018 through 7/8/2019)

4.1.4. Eave Depth and Window Setback

To develop a detailed case-study house model, eave depth and window setback were measured. Eaves are the edges of the roof that protrude from the wall and usually protrude beyond the side of the building. The case-study house also had eaves, a common element in real residences. The main function of the eaves is to block rainwater from the wall and prevent water from penetrating at the junction between the roof and the wall. Eaves can also protect passages around buildings from rain, prevent erosion of walls when rain hits the ground. While this does not seem to be related to building energy use, eaves can also affect building energy use while controlling solar penetration. Therefore, the eave depth of the case-study house was measured, which was 1.5ft. Figure 4.19 shows the eave depth measured. This eave depth provides shading to the case-study house windows.



Figure 4.19: Eave Depth of the Case-study House: 1.5 ft

Window setback means that the depth of the window from the exterior wall to the inside. The case-study house has a 3-inch window setback. Figure 4.20 shows the window setback of the case-study house. These window setbacks may or may not be present depending on the window installation method. However, when the exterior is made of thick bricks like a case-study house, window setback may inevitably occur. This can also play the role of shading like eaves, so it is thought that it will affect building energy consumption.



Figure 4.20: Window Setback of the Case-study House: 3 inches

4.1.5. Indoor Temperatures

To develop a case-study house simulation model, the DHW closet, garage, attic, and room temperatures were measured. Figure 4.21 shows the measured DHW closet, garage, attic, and room temperatures along with outdoor and solar radiation. In this study, the temperatures were measured four times for five days to two weeks. The first measurement was taken from March 5 to March 16 at 15-minute intervals. The second measurement measured data at 15-minute intervals from March 19 to March 27. The third measurement measured data at 15-minute intervals from July 15th to July 24th. The fourth measurement measured data at 1-minute intervals from November 5 to November 9. Figure 4.22 to Figure 4.25 show the four measurements.

Figure 4.26 shows the attic temperature measured with outdoor temperature and solar radiation during the heating season. The attic temperature of the case-study house is affected by solar radiation and outdoor temperature. As outdoor temperature and solar radiation increased, the attic temperature also increased, and as they decreased, the attic temperature decreased. The attic temperature during the heating season rose to about 100 F at its and dropped to about 60 F during the evening. The fluctuation of attic temperature in the heating season was larger than that in the cooling season. Figure 4.27 shows the attic temperature measured with outdoor temperature and solar radiation during the cooling season.

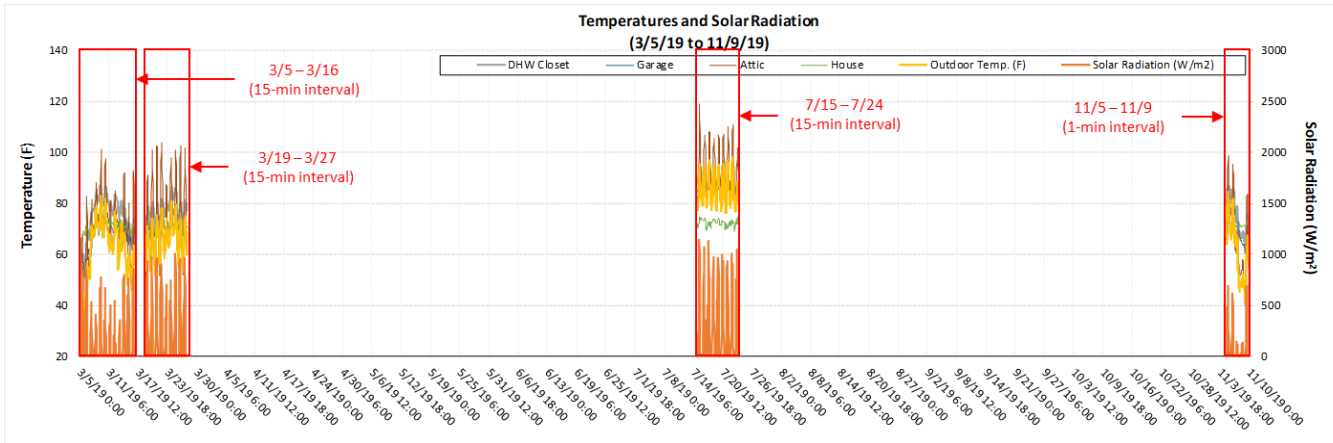


Figure 4.21: Measured DHW Closet, Garage, Attic, House (Room) Temperatures

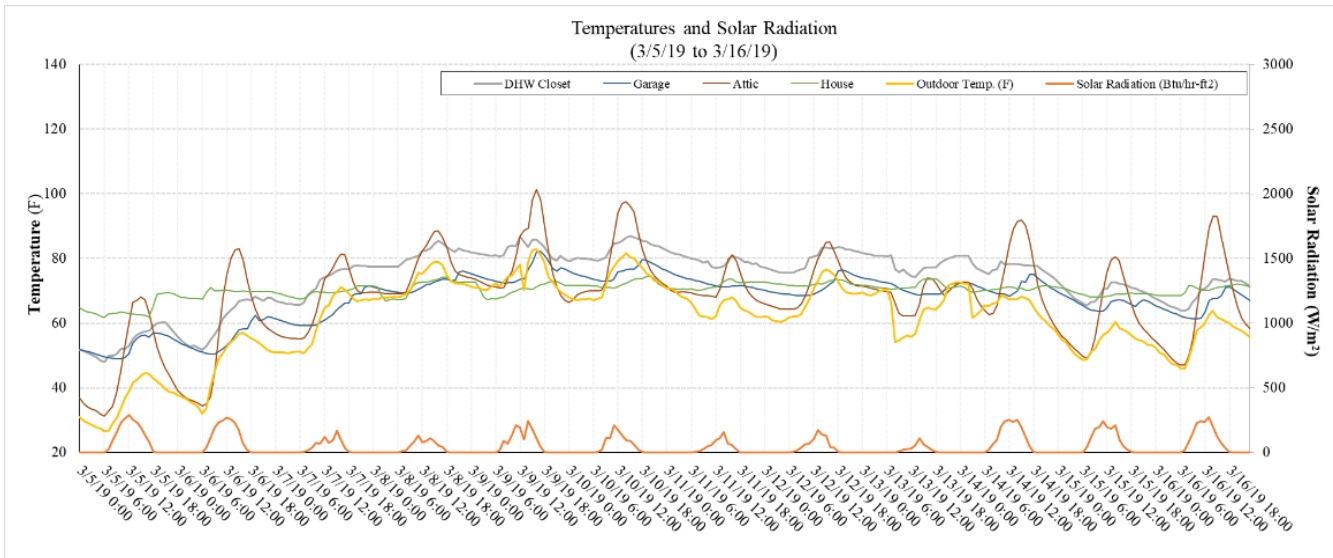


Figure 4.22: Measured 15-minute DHW Closet, Garage, Attic, House (Room) Temperatures from 3/5/19 to 3/16/19

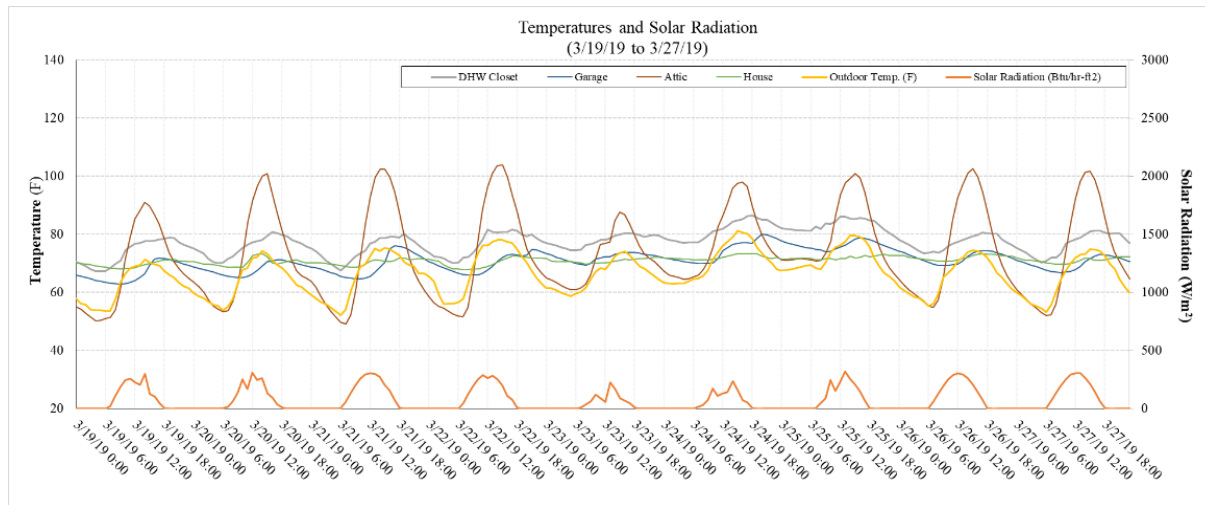


Figure 4.23: Measured 15-minute DHW Closet, Garage, Attic, House (Room) Temperatures from 3/19/19 to 3/27/19

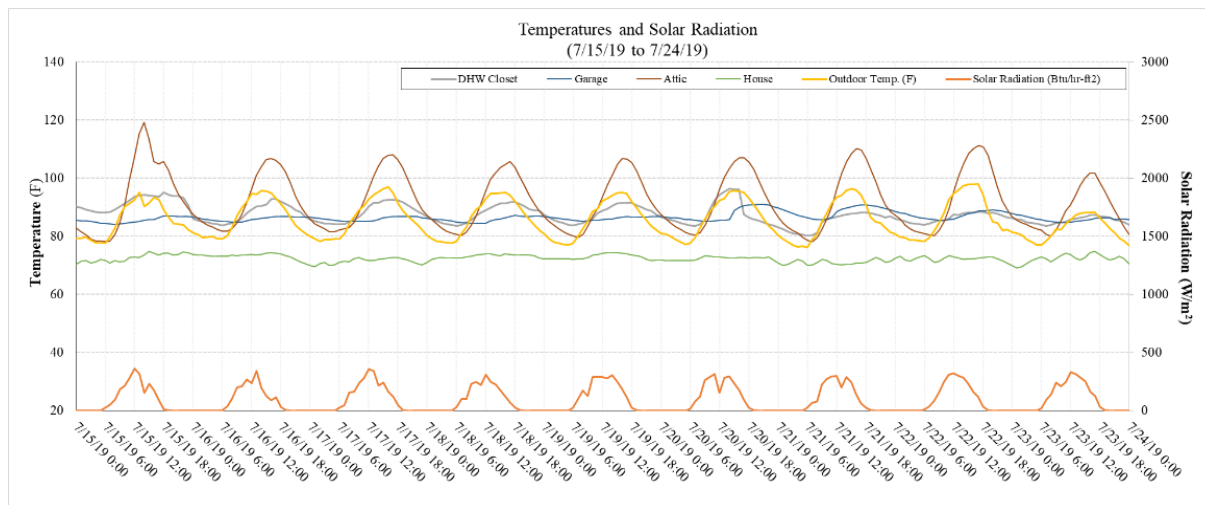


Figure 4.24: Measured 15-minute DHW Closet, Garage, Attic, House (Room) Temperatures from 7/15/19 to 7/24/19

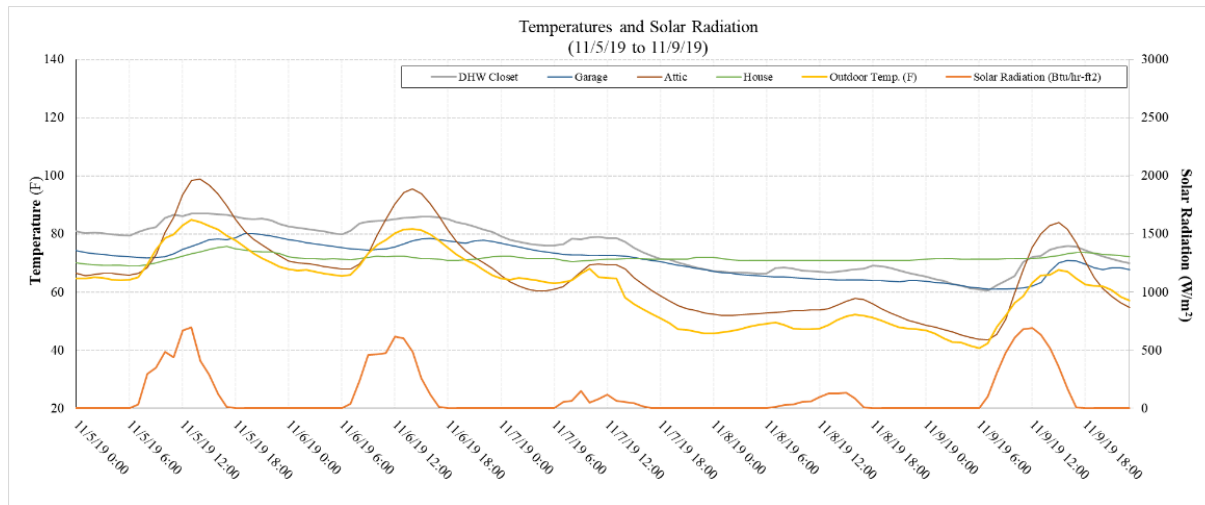


Figure 4.25: Measured 1-minute DHW Closet, Garage, Attic, House (Room) Temperatures from 11/5/19 to 11/9/19

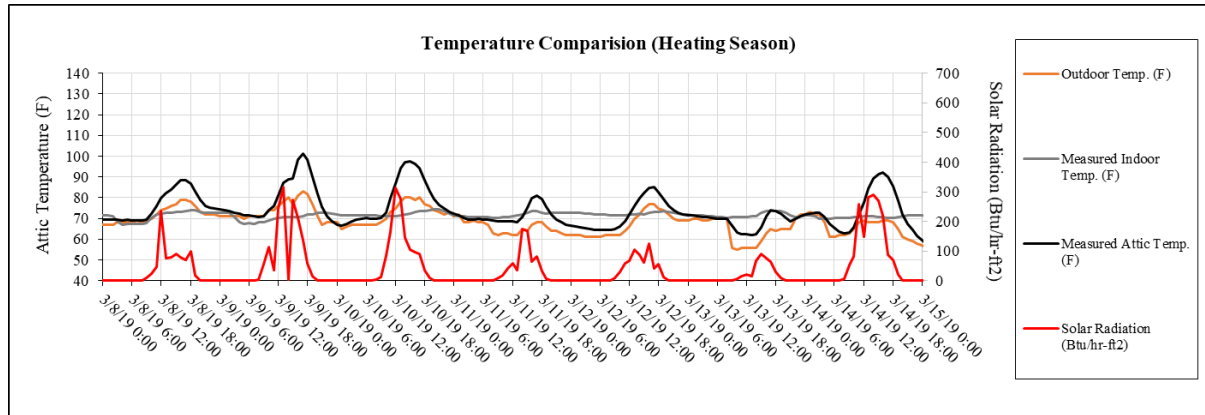


Figure 4.26: Measured 15-minute Attic Temperature with Measured Outdoor Temperature and Solar Radiation from 3/8/19 to 3/14/19

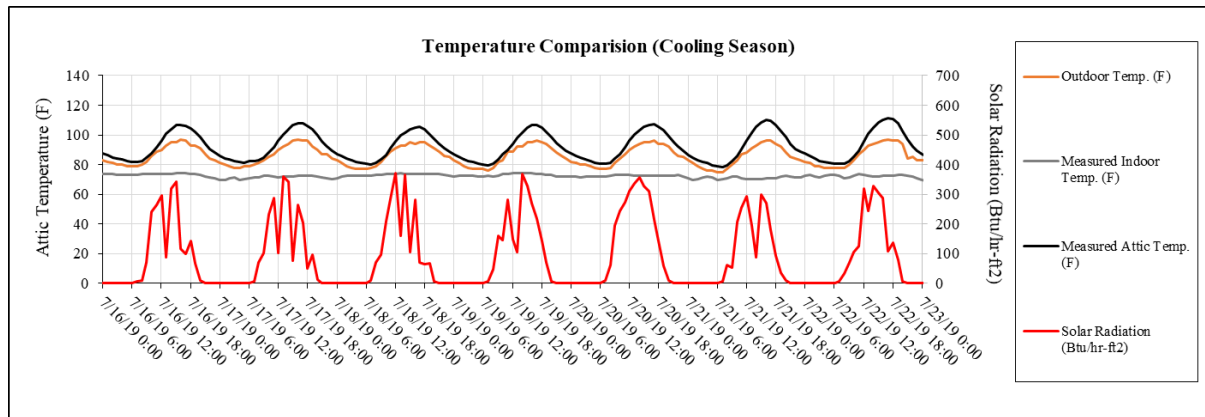


Figure 4.27: Measured 15-minute Attic Temperature with Measured Outdoor Temperature and Solar Radiation from 7/16/19 to 7/22/19

The DHW closet temperature, garage temperature, attic temperature, and room temperatures were plotted against the outside temperature are shown in Figure 4.28 to Figure 4.31 to determine if there were any predictable relationships between the outside temperature and each indoor temperature. Figure 4.28 shows the measured DHW closet temperature versus outside air temperature. At ambient temperatures less than 90 F, the DHW closet temperature was higher than the outdoor temperature. Figure 4.29 shows the measured garage temperature versus the outdoor air temperature. The garage temperature was also higher than the outdoor temperature because it is next to the house and often had a car parked in it. It also had an uninsulated, metal garage door facing southwest. Figure 4.30 shows the measured attic temperature versus the outdoor air temperature. The attic temperature tracked the outdoor temperature. However, the attic temperature fluctuated 30 F degrees due to the influence of solar radiation. Figure 4.31 shows the measured room temperature versus the outdoor air temperature. The room temperature was about 73.9 F during the cooling season, and 67.7 F during the heating season.

The DHW closet, garage, and attic temperatures were affected by outdoor temperature and solar radiation. Therefore, to better predict the temperatures, regression models were developed using outdoor temperature and solar radiation. Table 4.5 shows the regression model coefficients calculated.

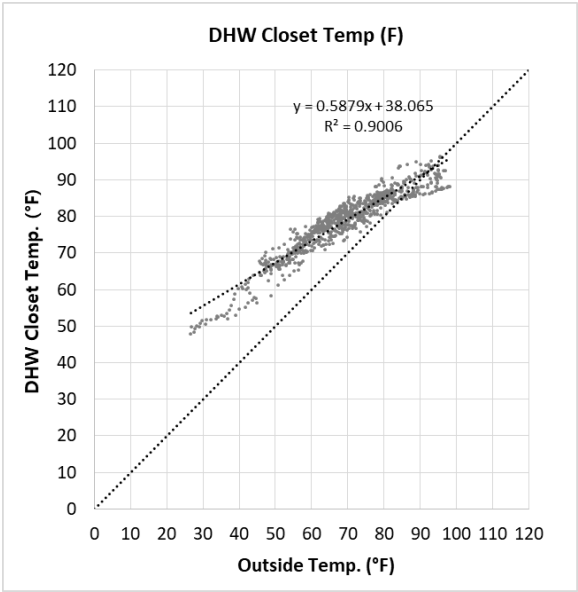


Figure 4.28: Measured DHW Closet Temperature Versus the Corresponding Outside Air Temperature (From 3/5/19 to 11/9/19)

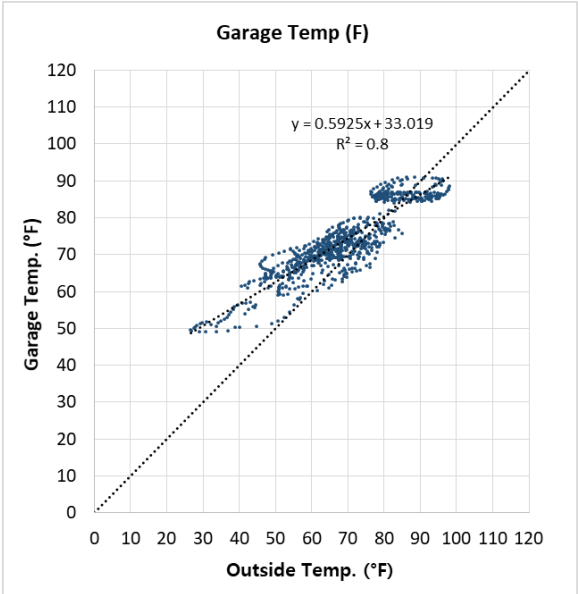


Figure 4.29: Measured Garage Temperature Versus the Corresponding Outside Air Temperature (From 3/5/19 to 11/9/19)

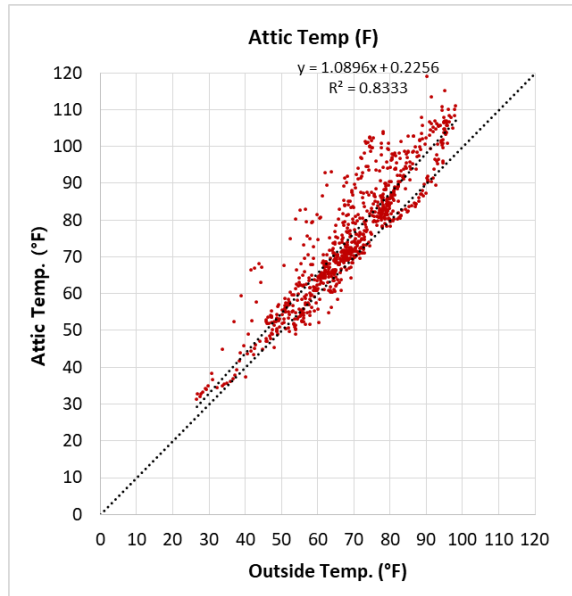


Figure 4.30: Measured Attic Temperature Versus the Corresponding Outside Air Temperature (From 3/5/19 to 11/9/19)

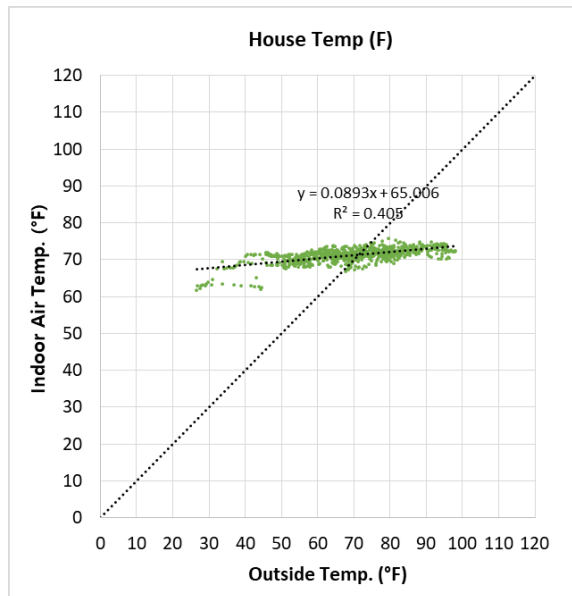


Figure 4.31: Measured House Temperature Versus the Corresponding Outside Air Temperature (From 3/5/19 to 11/9/19)

Table 4.5: Regression Model Coefficients

	DHW Closet	Garage	Attic	House
Intercept	37.087	31.091	1.830	64.801
Outdoor Temp (F)	0.614	0.645	1.046	0.095
Solar Radiation (Btu/hr-ft²)	-0.011	-0.021	0.018	-0.002

DHW Closet Temperature (Modeled) = 37.087 + 0.614 × Measured Outdoor Temp (F) – 0.011 × "Measured Solar Radiation (Btu/hr – sqft)"

Garage Temperature (Modeled) = 31.091 + 0.645 × Measured Outdoor Temp (F) – 0.021 × "Measured Solar Radiation (Btu/hr – sqft)"

Attic Temperature (Modeled) = 1.830 + 1.046 × Measured Outdoor Temp (F) + 0.018 × "Measured Solar Radiation (Btu/hr – sqft)"

House Temperature (Modeled) = 64.801 + 0.095 × Measured Outdoor Temp (F) – 0.002 × "Measured Solar Radiation (Btu/hr – sqft)"

These measured temperatures were compared against the simulated temperatures to determine how well the model worked. Figure 4.32 shows the comparison of measured DHW closet temperatures and the predicted temperatures. Figure 4.33 shows the comparison of measured garage temperatures and the predicted temperatures. Figure 4.34 shows the comparison of measured attic temperatures and the predicted temperatures. Figure 4.35 shows the comparison of the measured house (room) temperatures and the predicted temperatures. In all cases except the attic, the predicted temperatures using the regression models were similar to the measured temperatures.

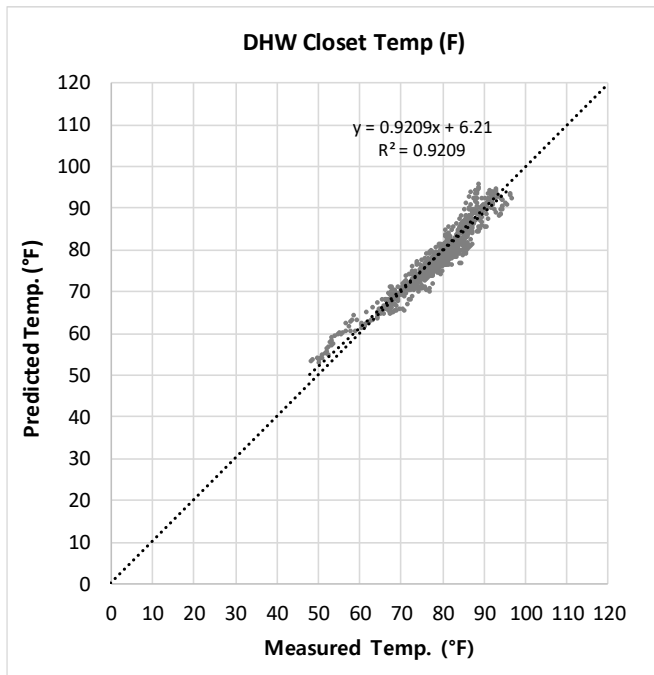


Figure 4.32: Comparison of Measured DHW Closet Temperature and the Predicted Temperature

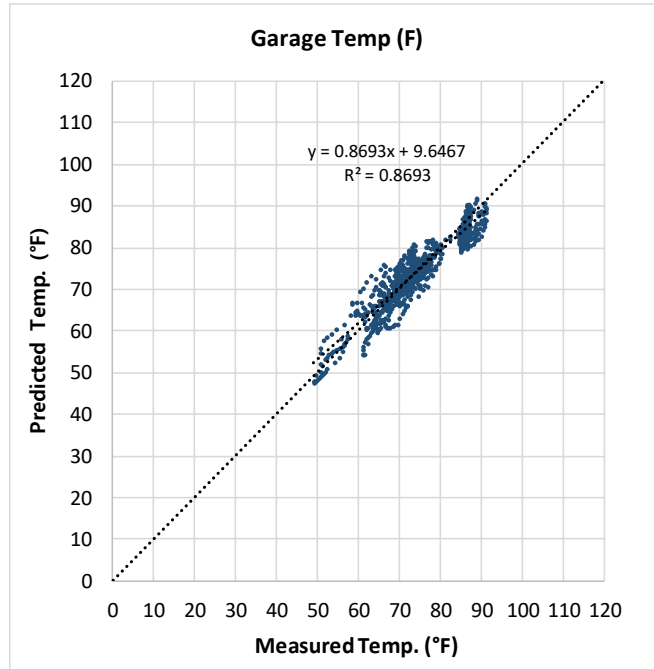


Figure 4.33: Comparison of Measured Garage Temperature and the Predicted Temperature

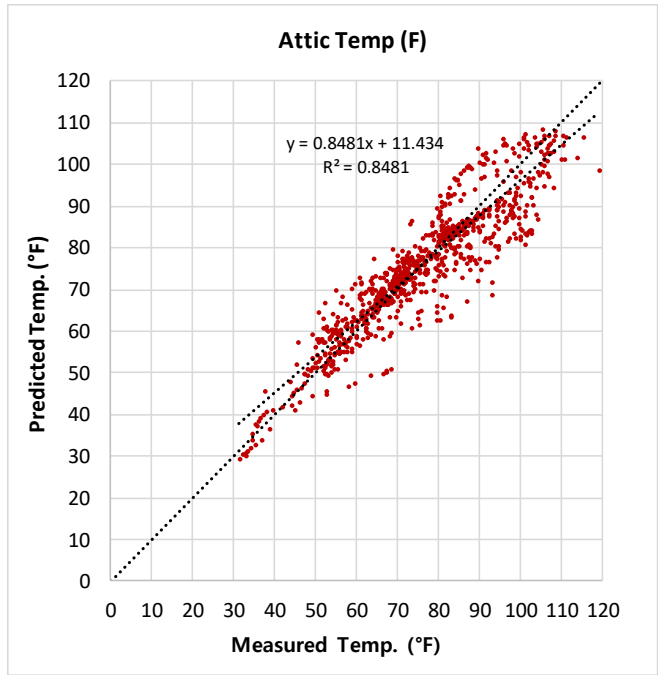


Figure 4.34: Comparison of Measured Attic Temperature and the Predicted Temperature

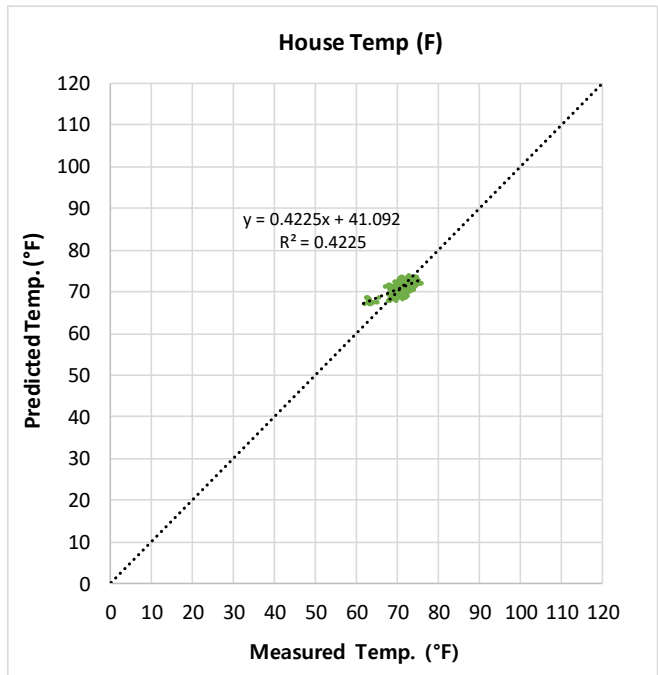


Figure 4.35: Comparison of Measured House Temperature and the Predicted Temperature

4.1.6. Domestic Water Heater Inlet and Outlet Temperatures

To develop a more-accurate case-study house simulation model, inlet and outlet temperatures of the domestic hot water heater were measured. To measure these conditions, sensors were installed at 3 points. Figure 4.36 shows the measurement sensors and their installation.

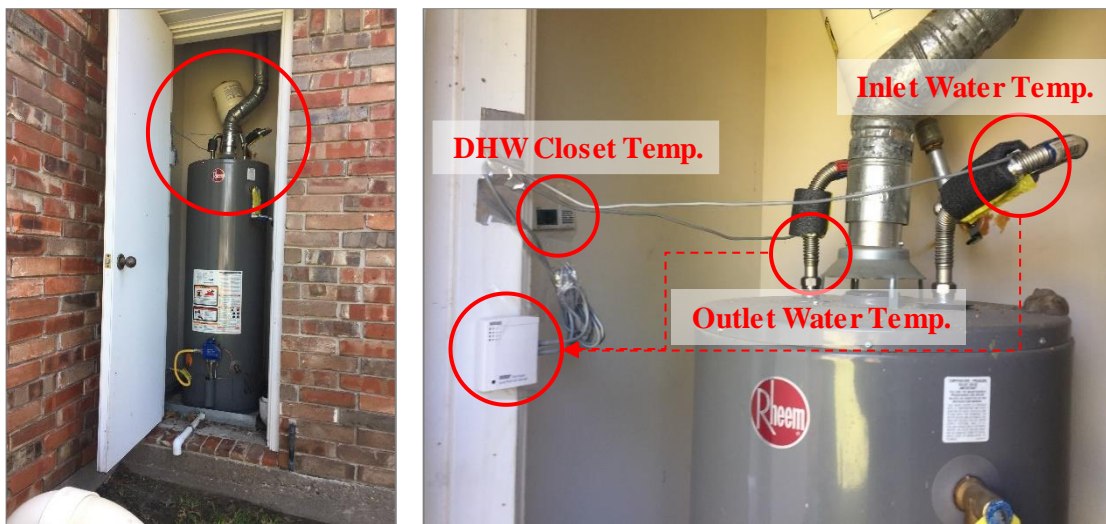


Figure 4.36: Measurement Sensors for Domestic Hot Water Heater

The temperatures were measured from October 27th, 2019 to August 2nd, 2020 at 1-minute intervals. Figure 4.37 shows the DHW inlet and outlet water temperature measured data. Coincident solar radiation and outdoor temperatures from June 8th, 2020 to July 8th, 2020 were not measured due to malfunction of the STB. The gaps in the data represent where the losses were being occurred. Figure 4.38 shows more detail of the measured DHW inlet and outlet water temperature over eight days.

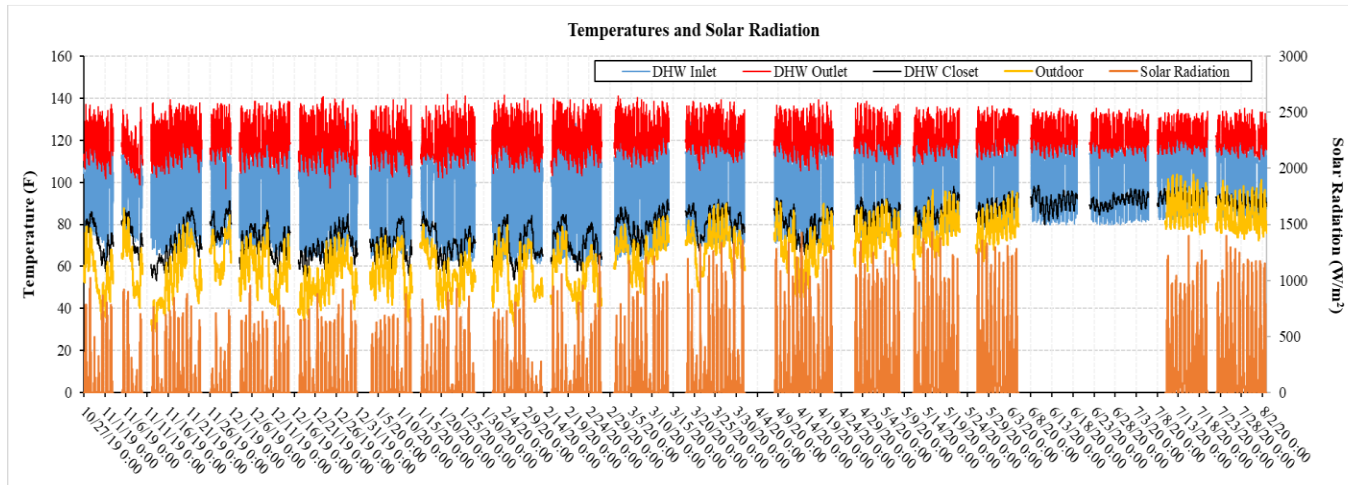


Figure 4.37: Measured DHW Inlet Water, DHW Outlet Water (Water Tank), DHW Closet, and Outdoor air Temperatures and Solar Radiation

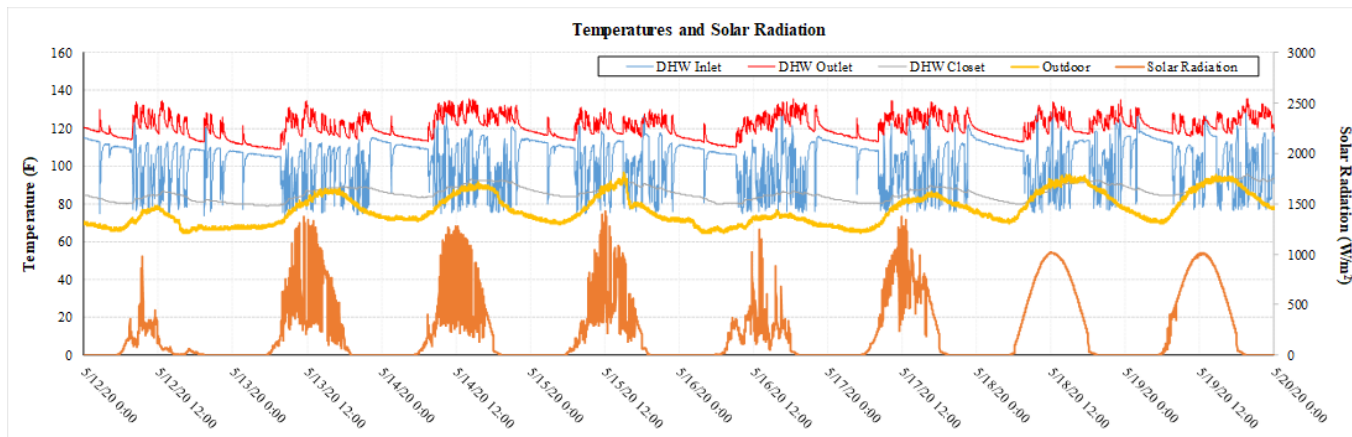


Figure 4.38: Measured DHW Inlet Water, DHW Outlet Water (Water Tank), DHW Closet, and Outdoor air Temperatures and Solar Radiation for Eight Days (5/12/2020 to 5/20/2020)

4.1.6.1. Inlet Water Temperature

The inlet water temperature represents the temperature of water entering the DHW. As shown in Figure 4.38, the measurement of inlet water temperature was affected by the heat of the closet and nearby DHW tank temperature, therefore when the DHW water was not used, the temperature increased rapidly. A review of the data showed continuous temperatures that lasted for 3 minutes or 5 minutes were indicating the low inlet temperature and were selected as the inlet water temperature. Figure 4.39 shows a comparison of selected inlet water temperatures. Since it was impossible to predict the inlet water temperatures with regression models, 3-minute continuous and 5-minute continuous inlet water temperature models were developed using the Building America's inlet water temperature model equations. In addition, for this study, the monthly water temperature was obtained from the College Station pump station.

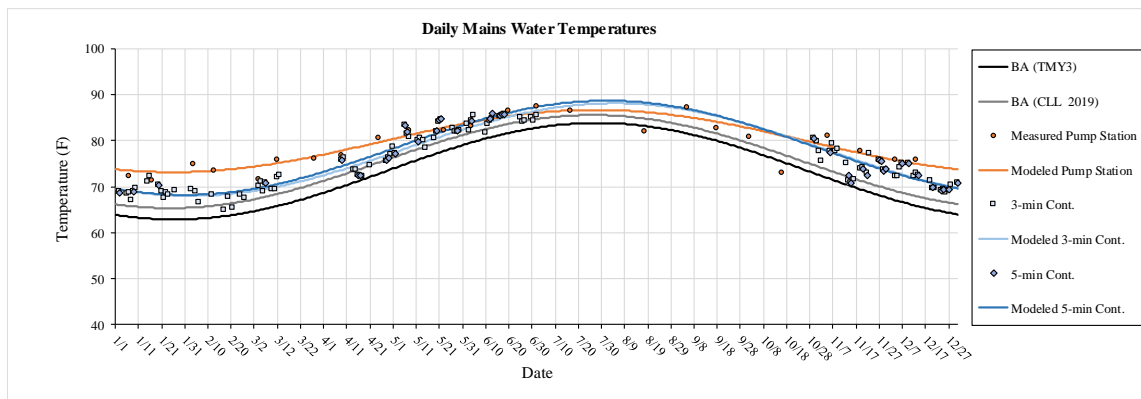


Figure 4.39: Comparison of Selected Inlet Water Temperatures

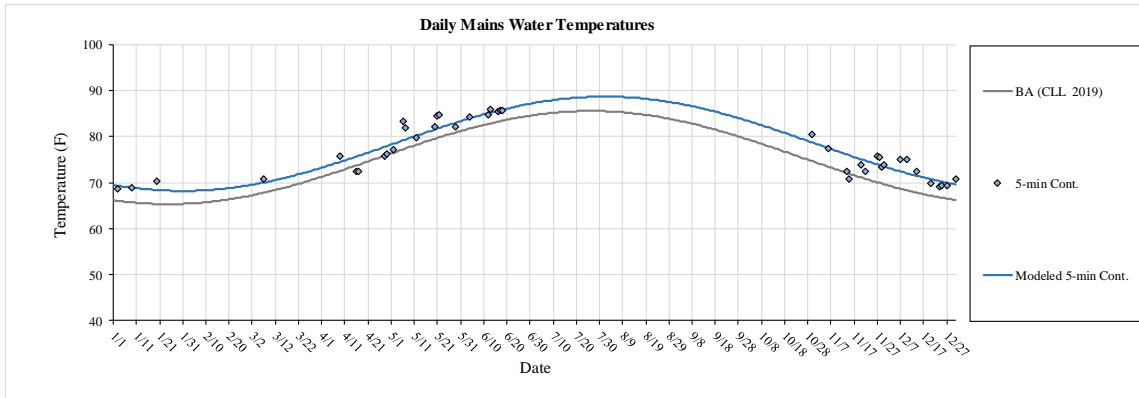


Figure 4.40: 5-minute Continuous Inlet Water Temperatures

4.1.6.1. Outlet Water Temperature

Outlet water temperature is the temperature of the water leaving the DHW. As shown in Figure 4.38, the max outlet water temperatures only occurred when water flowed from the tank. Therefore, to select only the actual outlet water temperature from the total data, the daily maximum temperature of the measured outlet water temperatures was used. Finally, the average value of the daily maximum temperatures, 135.6F, was selected as the outlet water temperature.

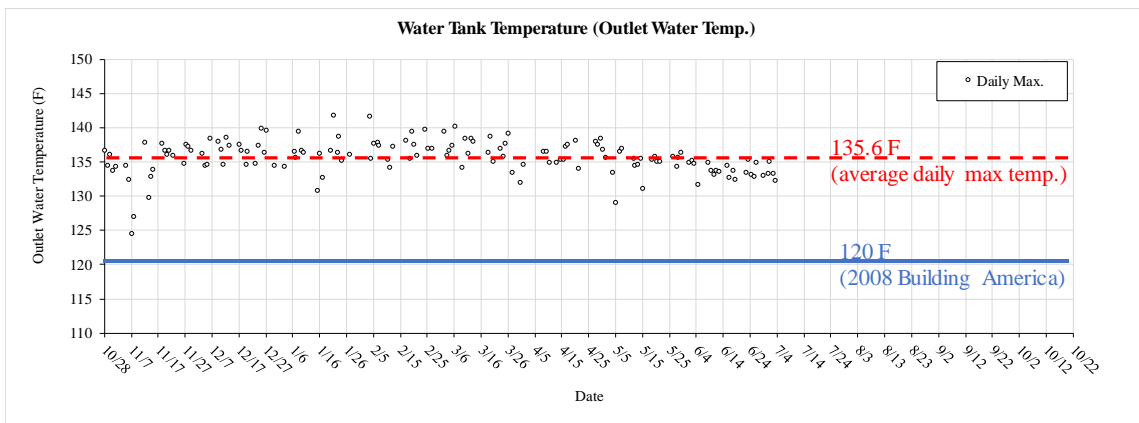


Figure 4.41: Daily Maximum Temperatures of Measured Outlet Water Temperatures

4.1.7. Ground Heat Transfer

The Winkelmann-Huang (W-H) ground heat transfer method was used for the case-study house model. This method is more accurate than the standard DOE-2.1E's ground heat transfer model (Huang et al., 1988).

The W-H method was developed using a finite difference foundation model. The finite difference foundation model was incorporated by Huang et al. (Huang et al., 1988) in 1988. This was revised by Fred Winkelmann in 1998, corrected and revised again in 2002 (Winkelmann, 2002). The Winkelmann-Huang method assumes that heat transfer occurs mainly in the exposed surroundings of the subterranean surface because this area has a relatively short path of heat flow to the outdoor air. In the standard DOE-2.1E's ground heat transfer model, the DOE-2.1E simulation program calculates using a one-dimensional layer with thermally linked to the ground. Unfortunately, this calculation overestimates the ground heat transfer calculation as the ground heat transfer occurs over the entire floor. Therefore, in this study, the W-H method was used for a more accurate calculation for the case-study house model.

4.1.8. Trees

The case-study house is also surrounded by trees. Figure 4.42 shows the trees around the case-study house, and Figure 4.43 shows the tree types and locations in the case-study house. Unfortunately, the duration of tree shading depends on the type of trees since not all the trees lose their leaves at the same time. The case-study house had five types of trees: post oak, elm, crape myrtle, juniper, and live oak. The post oak, elm, and crape myrtle are deciduous trees, and they shed leaves seasonally, usually in the

autumn (Patterson, 2020). The juniper and live oak trees are classified as evergreen trees, but the two slightly different types. The needles on the juniper tree leafs do not fall off and it remains evergreen, year around (Lyons et al., 2020). However, the live oak tree leafs fall-off during 3 weeks in mid-March before new leafs appear (CTTC, 2020; TPDDL, 2020). Figure 4.43 shows the tree modeling of DOE2.1E building energy simulation, and Figure 4.45 shows the tree shading schedules used in the model.



Figure 4.42: Example of Trees in the Case-Study House



Figure 4.43: Tree Types and Locations in the Case-study House

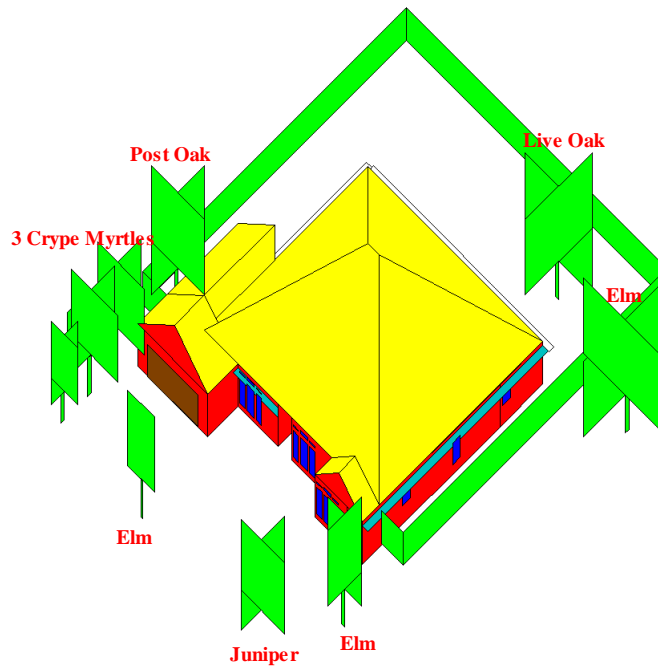


Figure 4.44: Tree Modeling of DOE-2.1E Building Energy Simulation

```

$ TREE SHADING SCHEDULE: Transmittance 0 to 1

$ Post Oak Tree (Deciduous) Shading Schedule
T-SH-1 = SCHEDULE
    THRU MAR 31 (ALL) (1,24) (0.7)
    THRU OCT 31 (ALL) (1,24) (0.1)
    THRU DEC 31 (ALL) (1,24) (0.7) ..

$ Elm Tree (Deciduous) Shading Schedule
T-SH-2 = SCHEDULE
    THRU MAR 31 (ALL) (1,24) (0.7)
    THRU OCT 31 (ALL) (1,24) (0.1)
    THRU DEC 31 (ALL) (1,24) (0.7) ..

$ Crape Myrtle Tree (Deciduous) Shading Schedule
T-SH-3 = SCHEDULE
    THRU MAR 31 (ALL) (1,24) (0.7)
    THRU OCT 31 (ALL) (1,24) (0.1)
    THRU DEC 31 (ALL) (1,24) (0.7) ..

$ Live Oak Tree (Evergreen) Shading Schedule
T-SH-4 = SCHEDULE
    THRU MAR 15 (ALL) (1,24) (0.1)
    THRU APR 21 (ALL) (1,24) (0.7)
    THRU DEC 31 (ALL) (1,24) (0.1) ..

$ Juniper Tree (Evergreen) Shading Schedule
T-SH-5 = SCHEDULE
    THRU DEC 31 (ALL) (1,24) (0.1) ..

```

Figure 4.45: Tree Shading (Solar Transmittance) Schedules

4.1.9. Fence

The case-study house has fences around the backyard, which creates shading on the left and right sides windows. Figure 4.46 shows the fence modeling of DOE-2.1E building energy simulation.

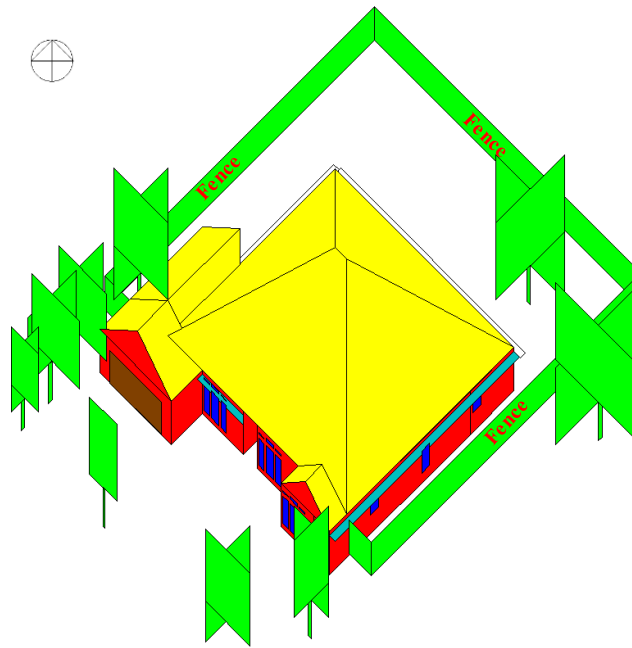


Figure 4.46: Fence Modeling of DOE-2.1E Building Energy Simulation

4.1.10. Detailed Calibrated Case-Study House Simulation

To develop a calibrated DOE-2.1E simulation of the case-study house, a series of simulations were prepared. The calibration process included adjusting: zone temperatures, lighting and equipment energy uses, the cooling system efficiency, and the domestic hot water use. The objective of the calibration process was to improve the match in the simulated versus measured environmental data and energy use data.

4.1.10.1. Uncalibrated Simulation

An uncalibrated simulation was created using the house information in Ch.4.1.1. to Ch.4.1.9. Figure 4.47 shows the monthly average daily electricity usage versus the average outdoor temperatures for the billing period. The result of the uncalibrated simulation was that the baseload of simulated electricity usage was higher than the measured data. In general, the simulated electricity use modeled the measured electricity use reasonably well. However, the simulated electricity usage became slightly less than the actual usage as the outdoor temperature increase in the cooling season. Figure 4.48 shows the simulated electricity usage versus measured electricity usage, which shows that the electricity usage of the uncalibrated simulation differed slightly from the measured electricity usage data.

Figure 4.49 shows the monthly average daily natural gas usage versus monthly average outdoor temperatures for the billing period. The result of the uncalibrated simulation showed that the baseload of the simulated natural gas usage was less than the measured data. Figure 4.50 shows the simulated natural gas usage versus measured natural gas usage, which shows that the natural gas usage of the uncalibrated simulation had a constant difference from the measured natural gas usage data.

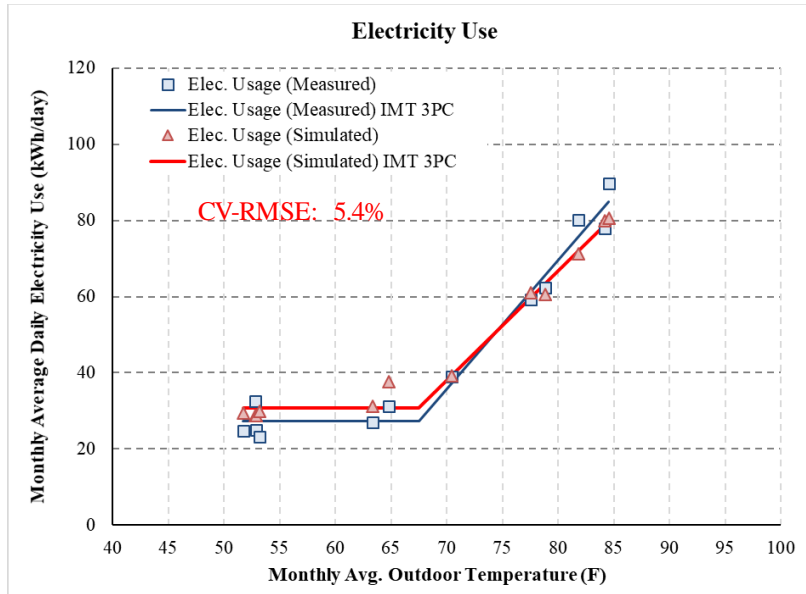


Figure 4.47: Monthly Average Daily Electricity Usage Versus Monthly Average Outdoor Temperature

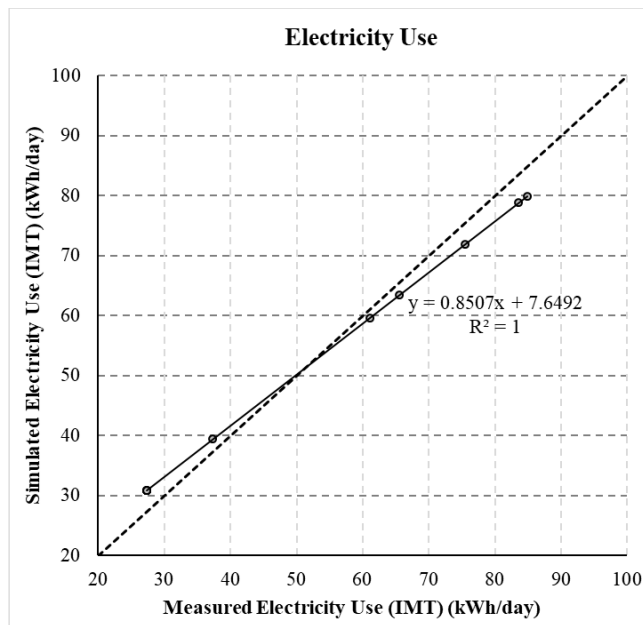


Figure 4.48: Simulated Electricity Usage Versus Measured Electricity Usage

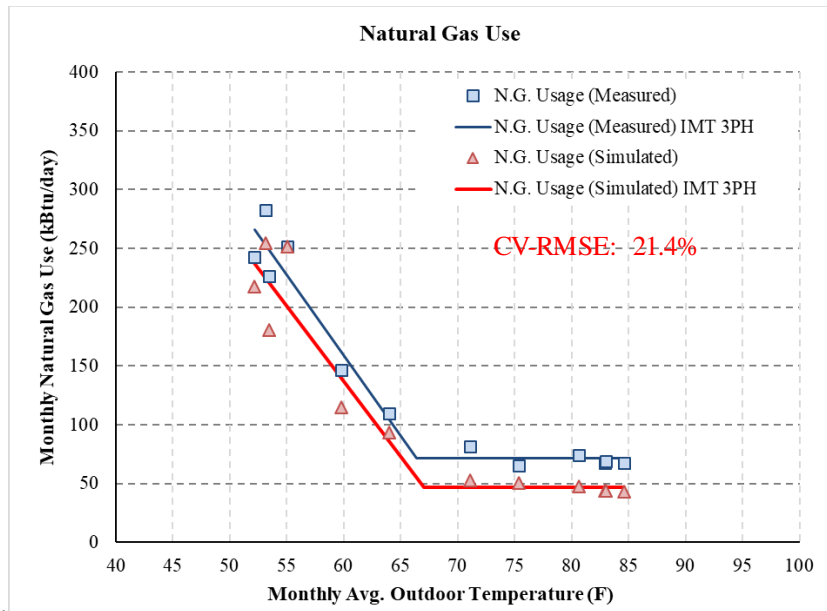


Figure 4.49: Monthly Average Daily Natural Gas Usage Versus Monthly Average Outdoor Temperature

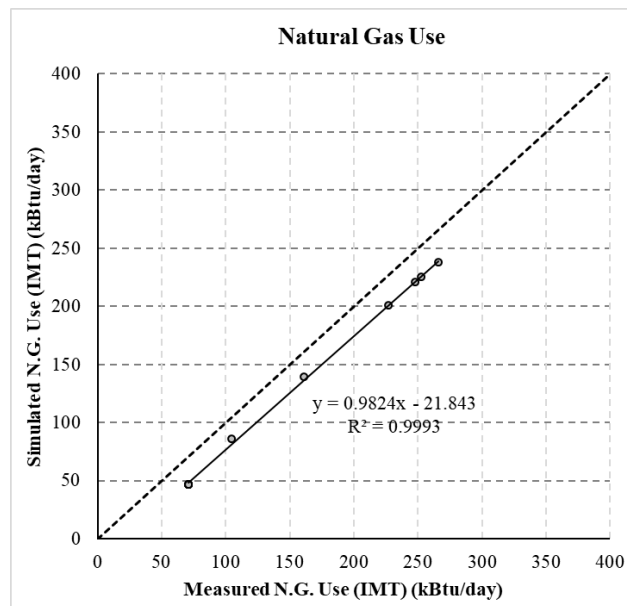


Figure 4.50: Simulated Natural Gas Usage Versus Measured Natural Gas Usage

4.1.10.2. Calibration #1: Zone Temperatures

Measured zone temperatures such as room, DHW closet, garage, and attic temperatures were used to calibrate the model. Figure 4.51 through Figure 4.66 show measured and simulated zone temperatures before calibration and after calibration. The measured and simulated room temperatures were similar even without calibration. However, some changes occurred while calibrating the other zone temperatures. The measured and simulated DHW closet temperatures were different than the uncalibrated simulation. In order to calibrate the simulated temperature, heat was added to the zone of the DHW closet, which represented 1,600 Btu/hr. After the temperature calibration, the difference in the measured and simulated DHW closet temperatures were reduced.

The measured and simulated garage temperatures were similar in the heating season, but they were different in the cooling season. In order to calibrate against the simulated temperatures, the floor weight of the attic was changed. To perform this adjustment, the floor weight was changed from using Custom Weighting Factors to a floor weight of to 35 lb/sqft. The measured and simulated attic temperatures were also calibrated since there were differences. To calibrate the simulated attic temperature, the floor weight of the attic was changed from the use of Custom Weighting Factors to 5 lb/sqft. After the calibration, the temperature difference between measured and simulated was reduced.

Figure 4.67 shows the monthly average daily electricity usage versus monthly average outdoor temperatures for the billing period after the calibrations for the zone temperatures. The result of this calibrated simulation resulted in the baseload of

simulated electricity usage still being larger than the measured data. The simulated electricity usage became less than the actual usage as the outdoor temperature increase in the cooling season. Figure 4.68 shows the simulated electricity usage versus measured electricity usage, where shows that the electricity usage of the simulation differing from the measured electricity usage data, where it was above the use at cold temperatures, and below at higher temperatures.

Figure 4.69 shows the monthly average daily natural gas usage versus monthly average outdoor temperatures. The result of this calibrated simulation showed that the simulated natural gas usage was less than the measured data by a constant amount. Figure 4.70 shows the simulated natural gas usage versus measured natural gas usage, and this shows that the natural gas usage of the simulation differed from the measured natural gas usage data by a constant amount.

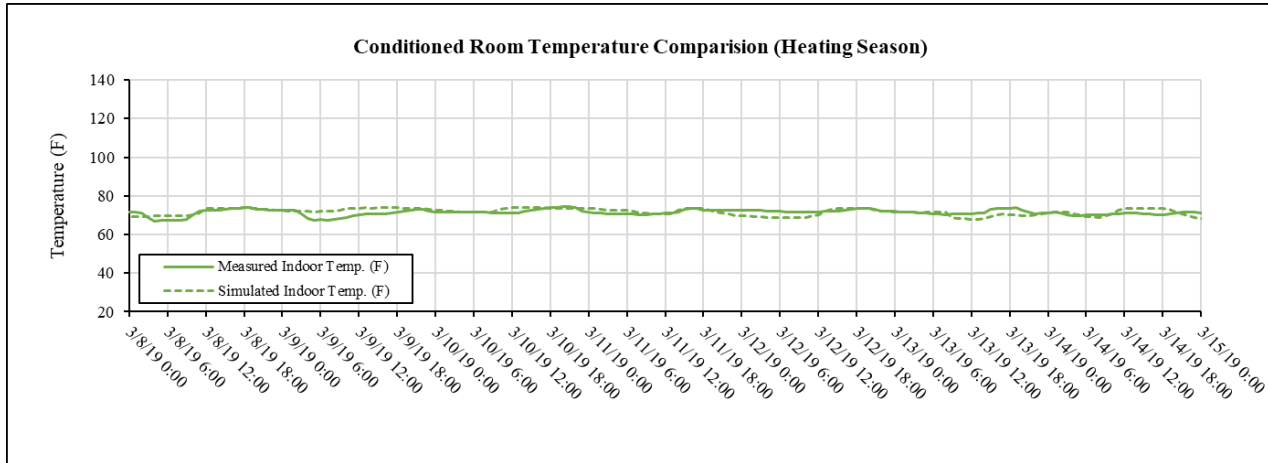


Figure 4.51: Room Temperature for Heating Season (before Calibration)

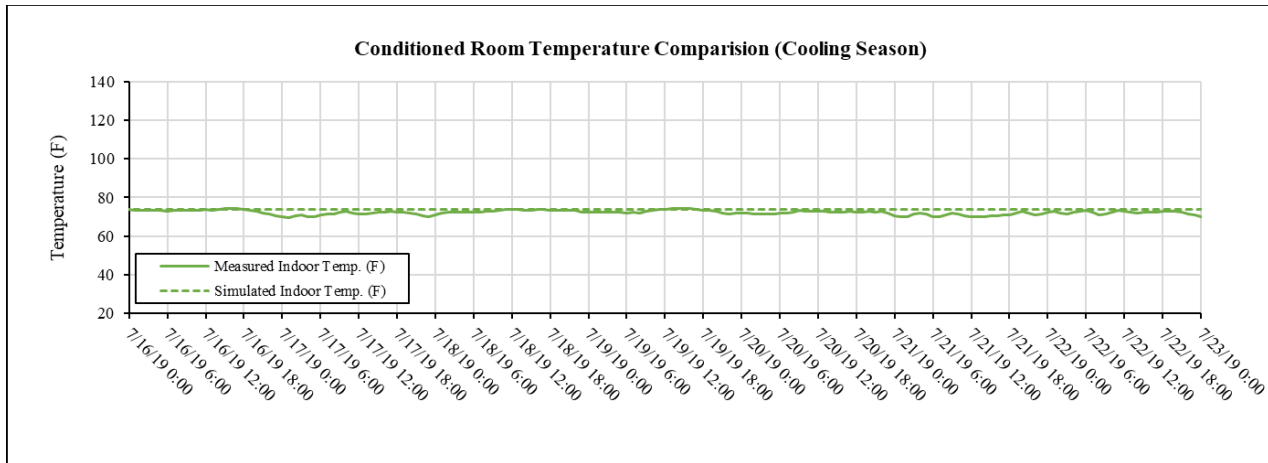


Figure 4.52: Room Temperature for Cooling Season (before Calibration)

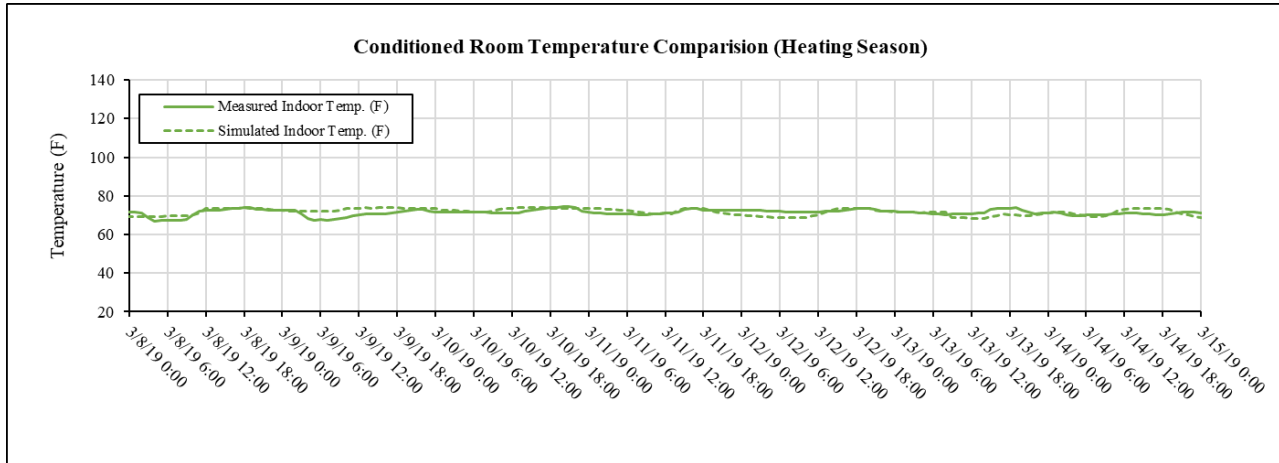


Figure 4.53: Room Temperature for Heating Season (after Calibration)

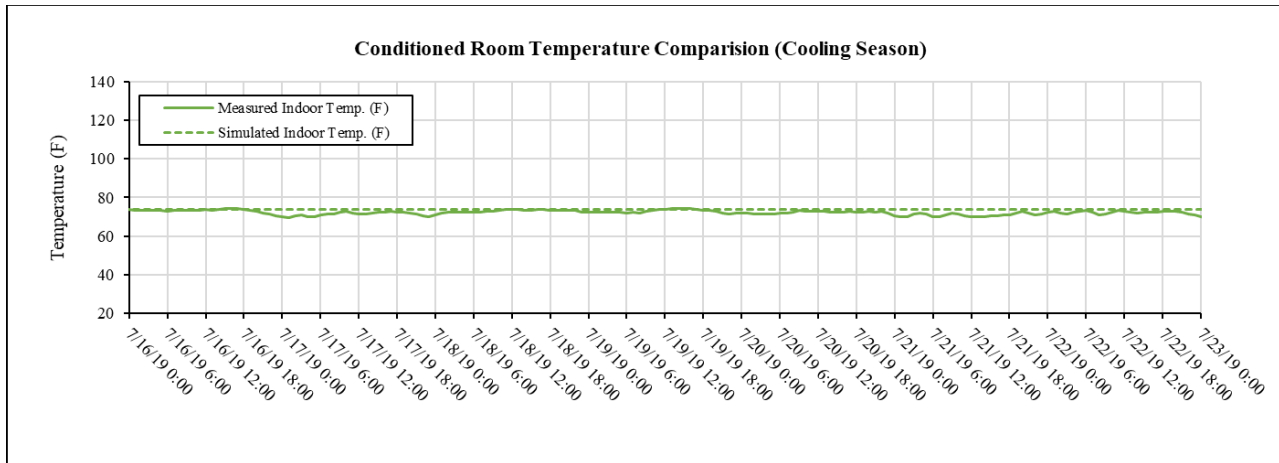


Figure 4.54: Room Temperature for Cooling Season (After Calibration)

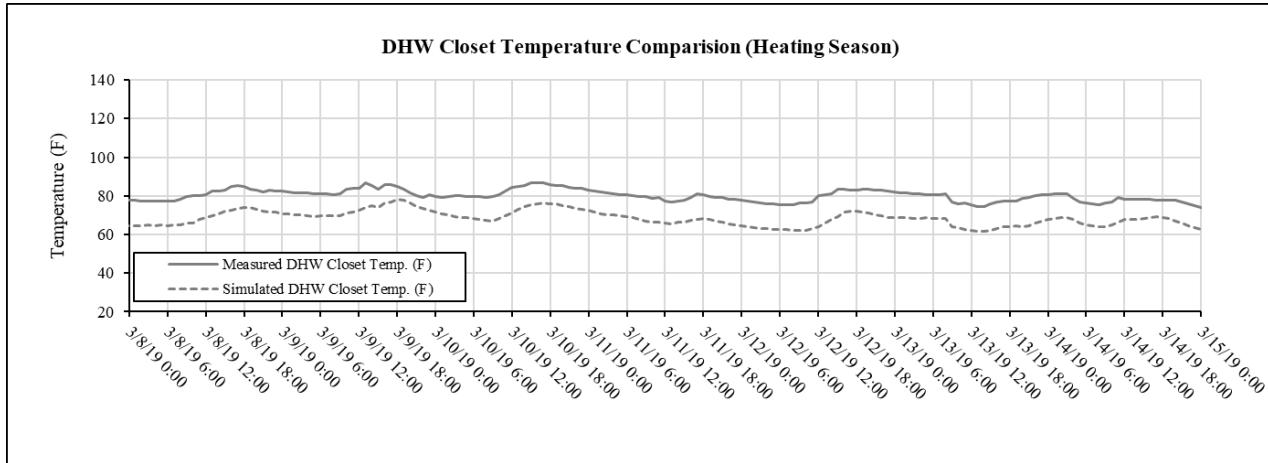


Figure 4.55: DHW Closet Temperature for Heating Season (before Calibration)

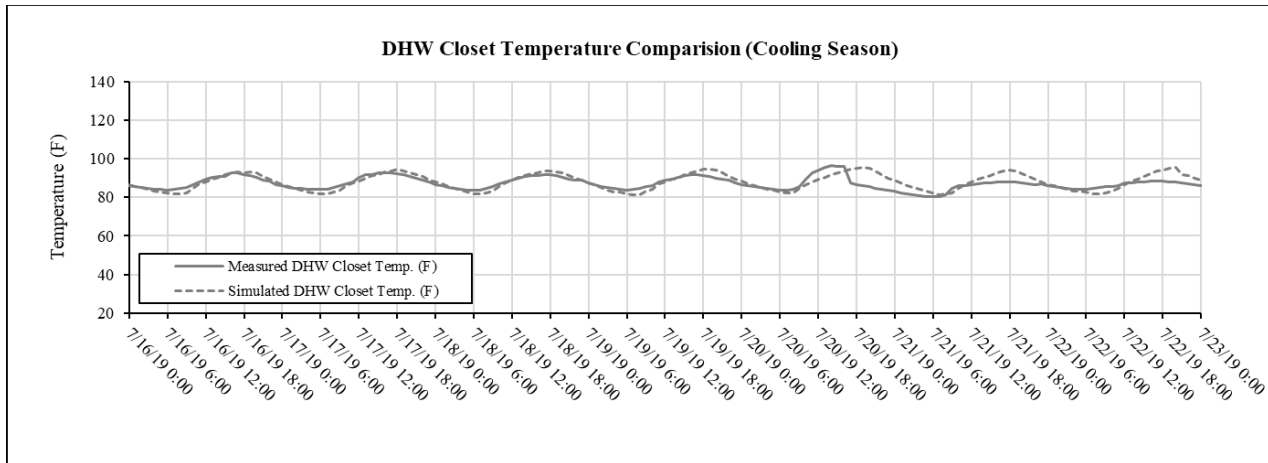


Figure 4.56: DHW Closet Temperature for Cooling Season (before Calibration)

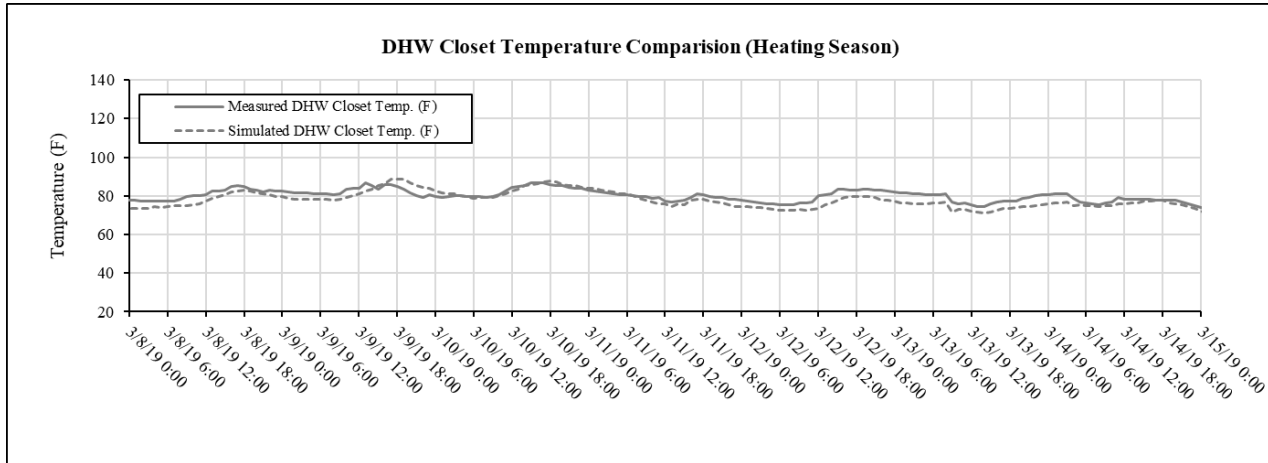


Figure 4.57: DHW Closet Temperature for Heating Season (after Calibration)

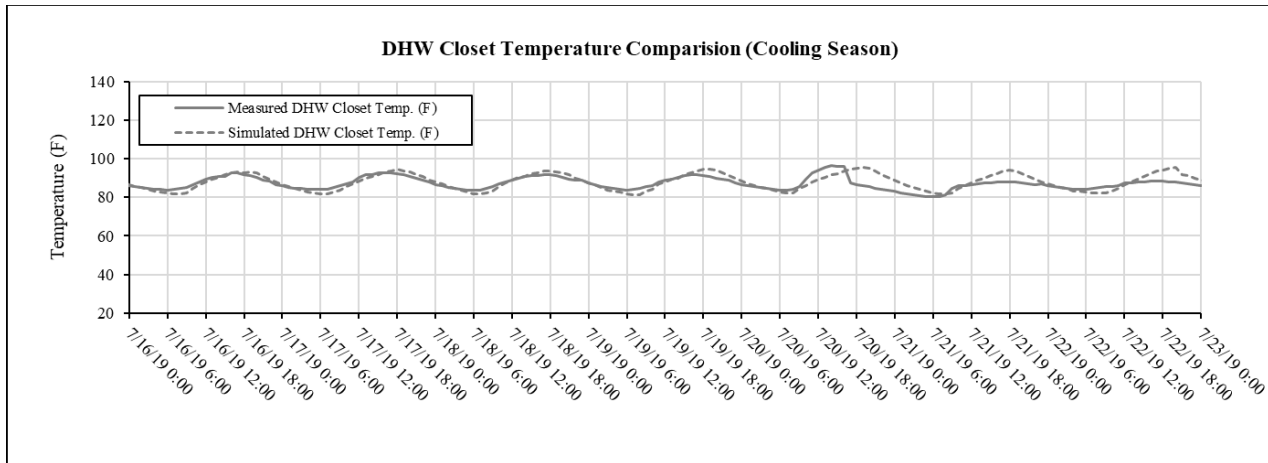


Figure 4.58: DHW Closet Temperature for Cooling Season (after Calibration)

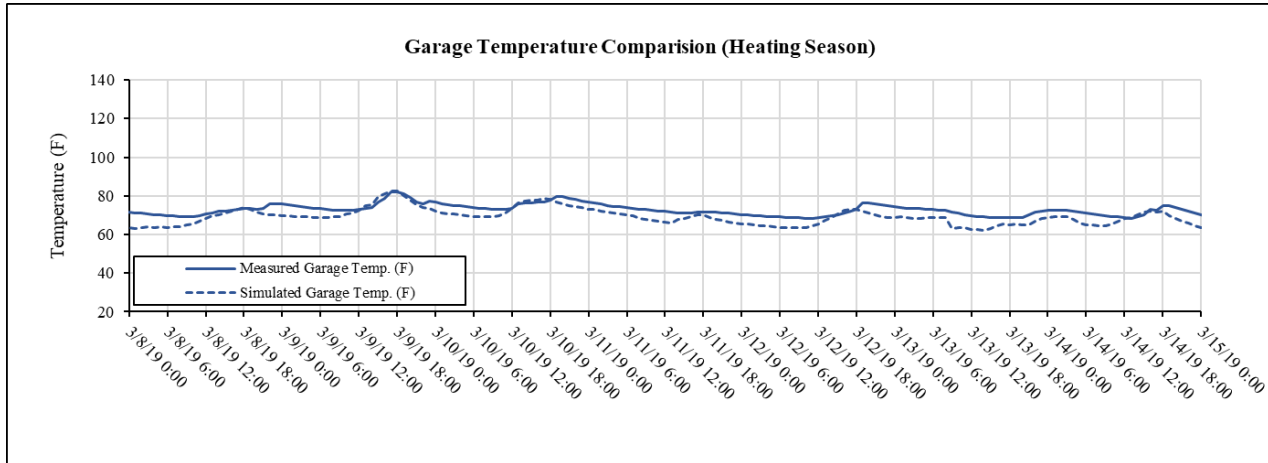


Figure 4.59: Garage Temperature for Heating Season (before Calibration)

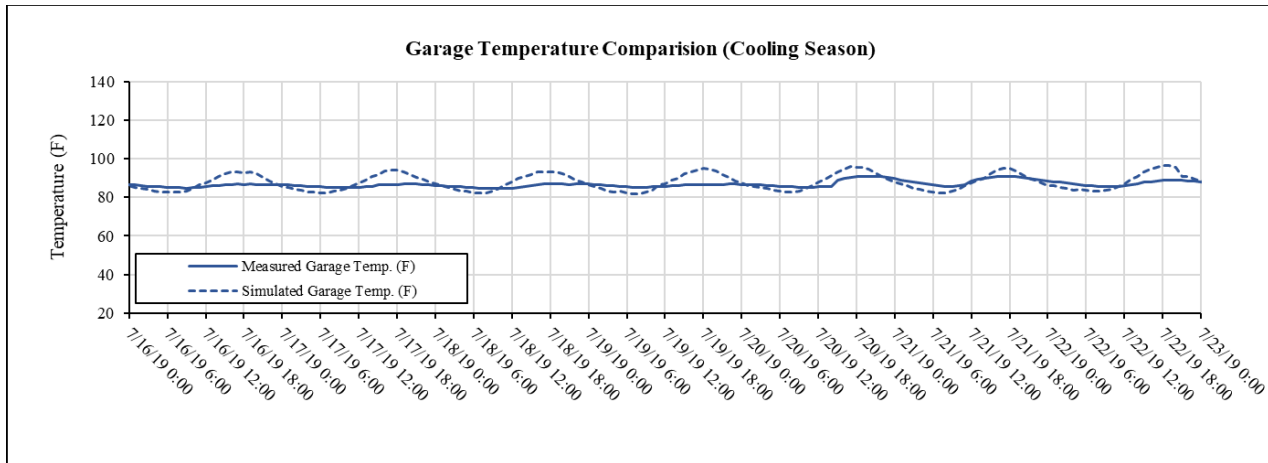


Figure 4.60: Garage Temperature for Cooling Season (before Calibration)

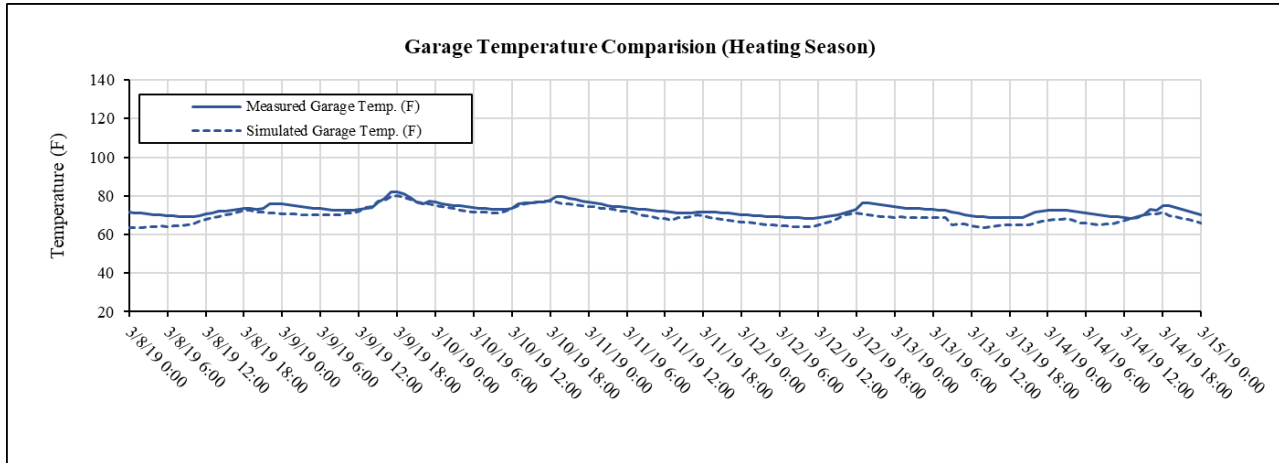


Figure 4.61: Garage Temperature for Heating Season (after Calibration)

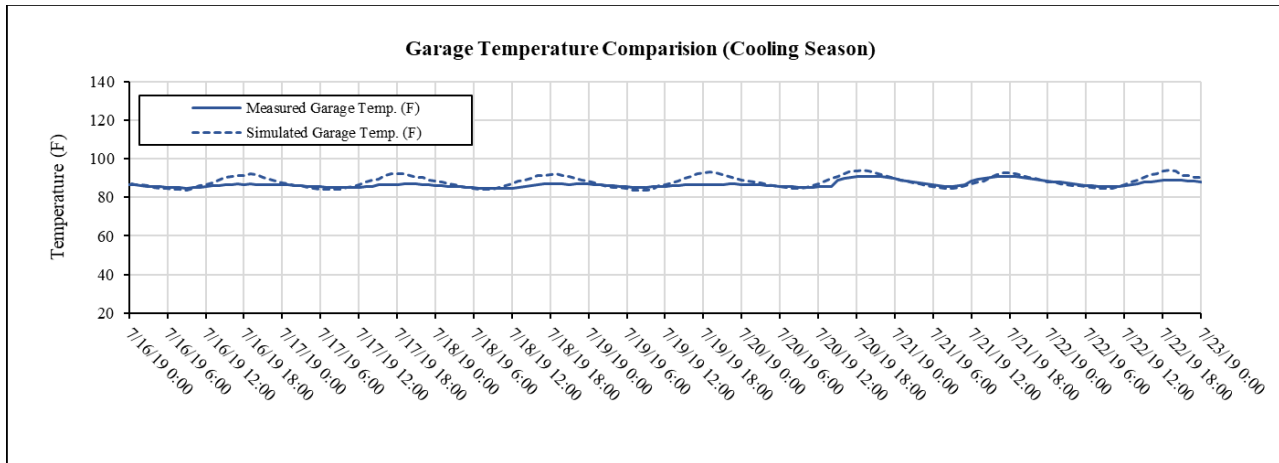


Figure 4.62: Garage Temperature for Cooling Season (after Calibration)

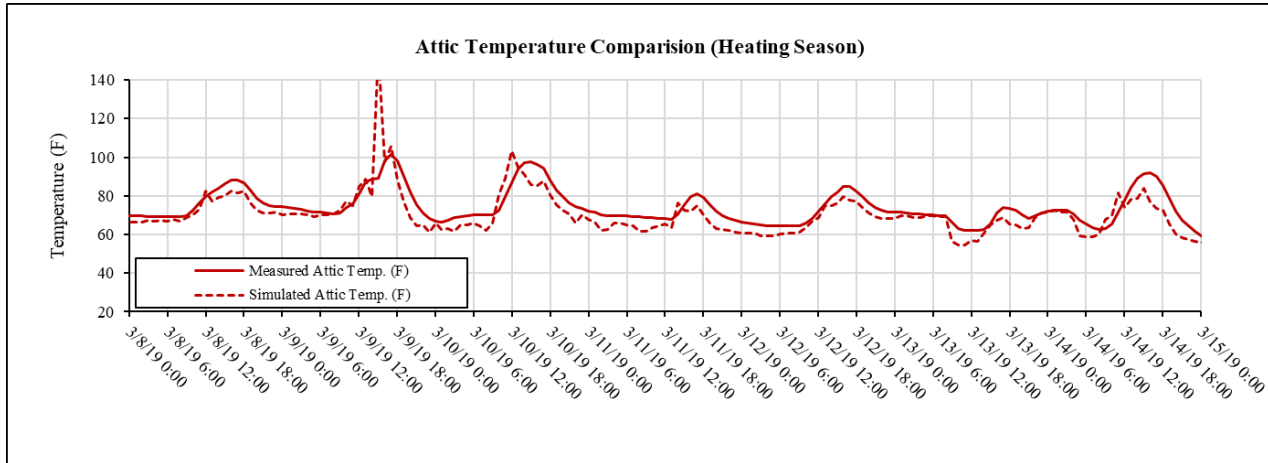


Figure 4.63: Attic Temperature for Heating Season (before Calibration)

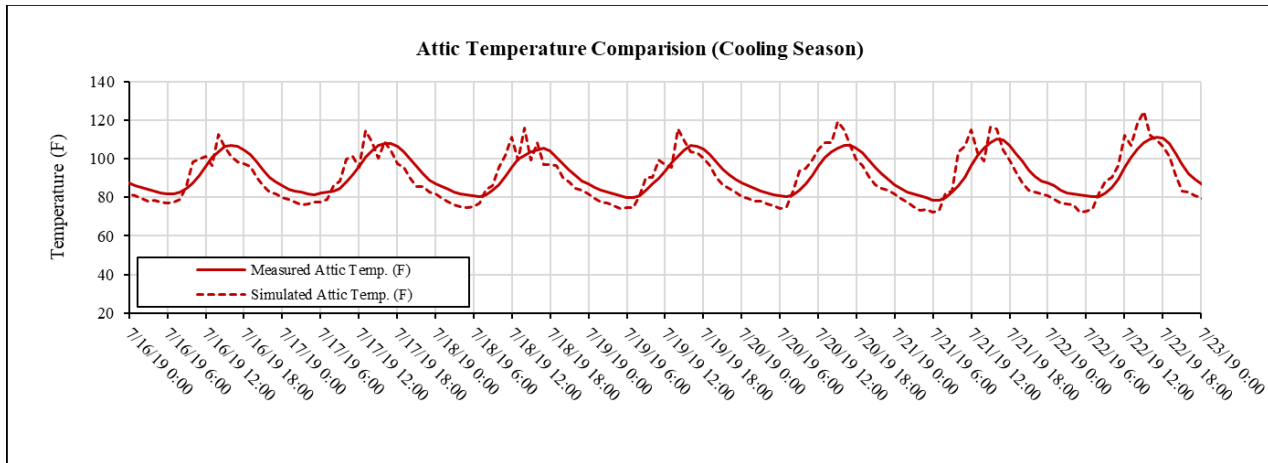


Figure 4.64: Attic Temperature for Cooling Season (before Calibration)

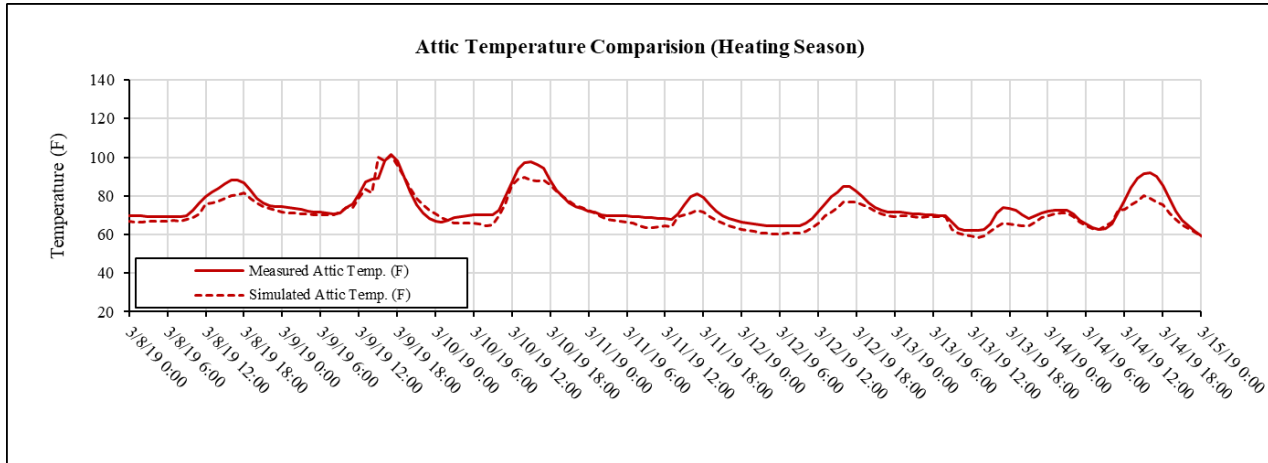


Figure 4.65: Attic Temperature for Heating Season (after Calibration)

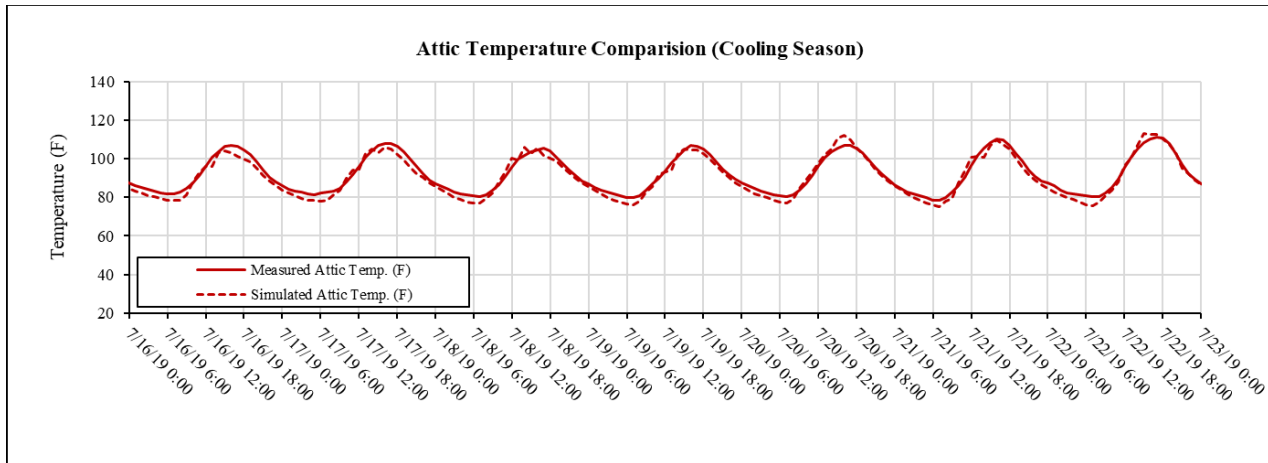


Figure 4.66: Attic Temperature for Cooling Season (after Calibration)

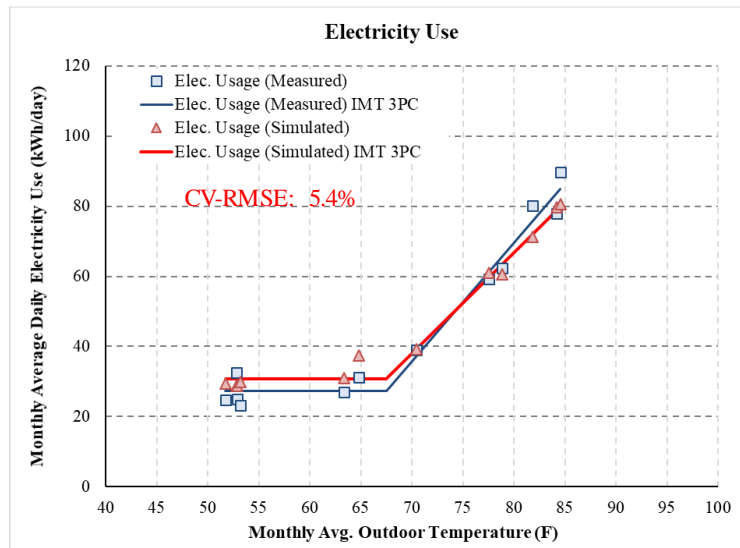


Figure 4.67: Monthly Average Daily Electricity Usage Versus Monthly Average Outdoor Temperature for the Billing Period

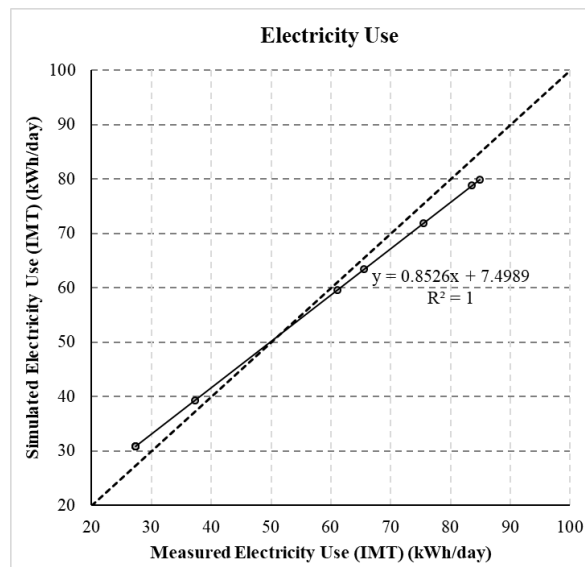


Figure 4.68: Simulated Electricity Usage Versus Measured Electricity Usage

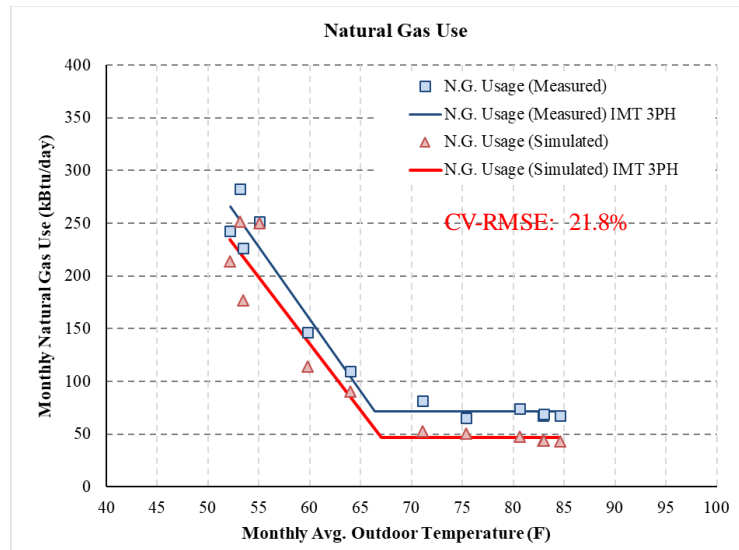


Figure 4.69: Monthly Average Daily Natural Gas Usage Versus Monthly Average Outdoor Temperature for the Billing Period

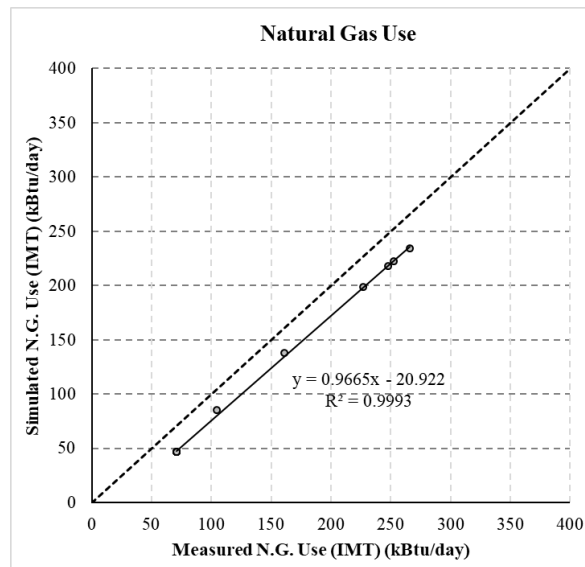


Figure 4.70: Simulated Natural Gas Usage Versus Measured Natural Gas Usage

4.1.10.3. Calibration #2: Lighting&Equipment

The lighting and equipment electricity usage was also calibrated in the simulation process. The results show the simulated electricity usage was decreased since the simulated electricity usage baseload was larger than measured (Figure 4.47). So, the electricity consumption of lighting and equipment was reduced from 1.1 kW to 0.9 kW.

Figure 4.71 shows the monthly average daily electricity usage versus monthly average outdoor temperatures after calibration of the lighting and equipment electricity usage. The result of the calibrated simulation showed that the baseload of simulated electricity usage was now close-to the measured data after this calibration. However, the simulated electricity usage was still less than the actual usage in the cooling season. Figure 4.72 shows the simulated electricity usage versus measured electricity usage, which shows that the electricity usage of the simulation still differed from the measured electricity usage data.

Figure 4.73 shows the monthly average daily natural gas usage versus monthly average outdoor temperatures. The result of the initial simulation showed that the baseload of simulated natural gas usage was less than the measured data, and the simulated natural gas usage was less than the actual usage in the heating season. However, after this calibration, the results of the simulation were similar to the actual measured usage compared to previous results. Figure 4.74 shows the simulated natural gas usage versus measured natural gas usage after the calibration.

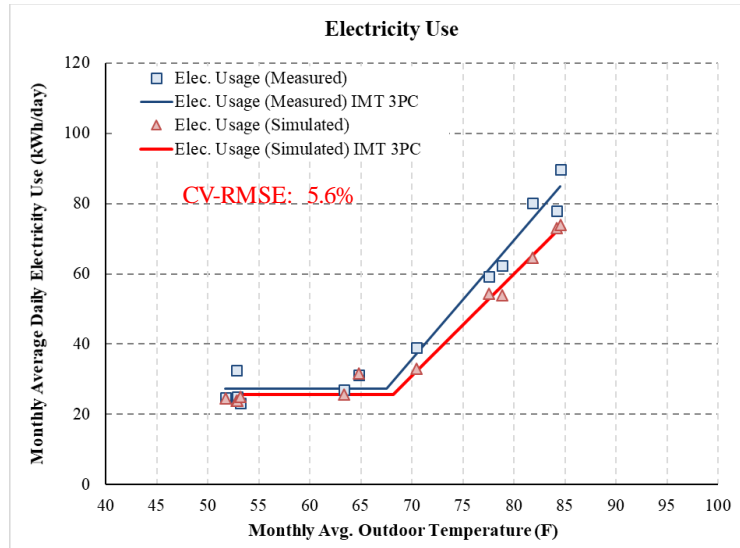


Figure 4.71: Monthly Avg. Daily Electricity Usage vs. Monthly Average Outdoor Temperature for the Billing Period

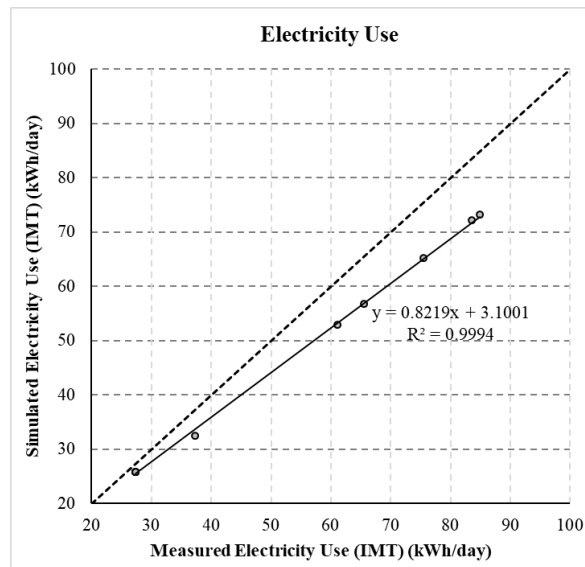


Figure 4.72: Simulated Electricity Usage vs. Measured Electricity Usage

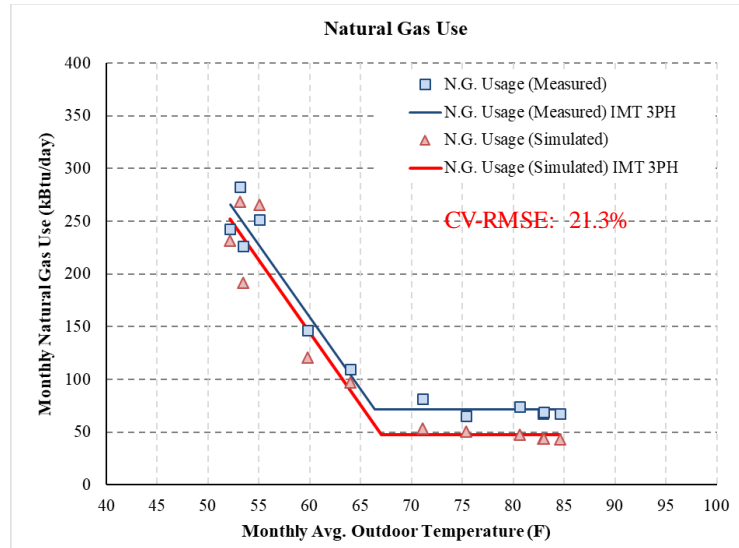


Figure 4.73: Monthly Average Daily Natural Gas Usage vs. Monthly Average Outdoor Temperature for the Billing Period

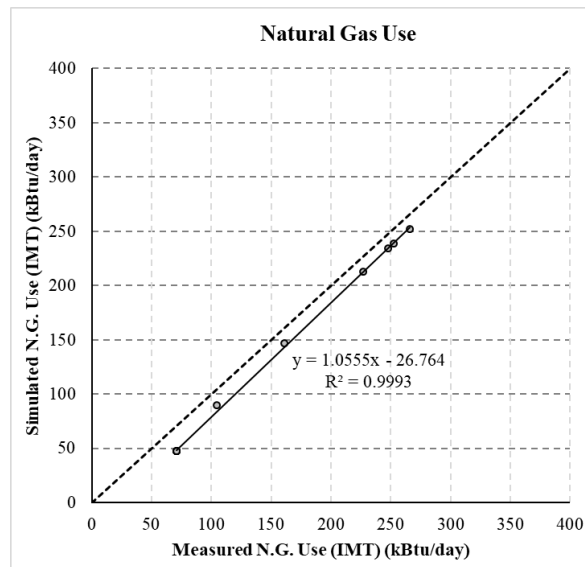


Figure 4.74: Simulated Natural Gas Usage vs. Measured Natural Gas Usage

4.1.10.4. Calibration #3: SEER

The SEER was calibrated in this chapter. The SEER was adjusted to match the energy consumption during the cooling season. So, the SEER was reduced from 10 to 8.

Figure 4.75 shows the monthly average daily electricity usage versus monthly average outdoor temperatures after calibration of the SEER. The result of simulation is that the base load of simulated electricity usage was matched with the measured data after this calibration. The simulated electricity usage was also matched with the actual usage in the cooling season. Figure 4.76 shows the simulated electricity usage versus measured electricity usage, which shows that the electricity usage of the simulation is similar to the measured electricity usage data.

Figure 4.77 shows the monthly average daily natural gas usage versus monthly average outdoor temperatures. The result of simulation is that the base load of simulated natural gas usage is still less than the measured data. The simulated natural gas usage is still less than the actual usage in the heating season. Figure 4.78 shows the simulated natural gas usage versus measured natural gas usage, and this shows that the natural gas usage of the simulation still differs from the measured natural gas usage data.

The difference in natural gas usage between measured and simulated was almost unchanged in Calibration #2 of Ch.4.1.10.3.

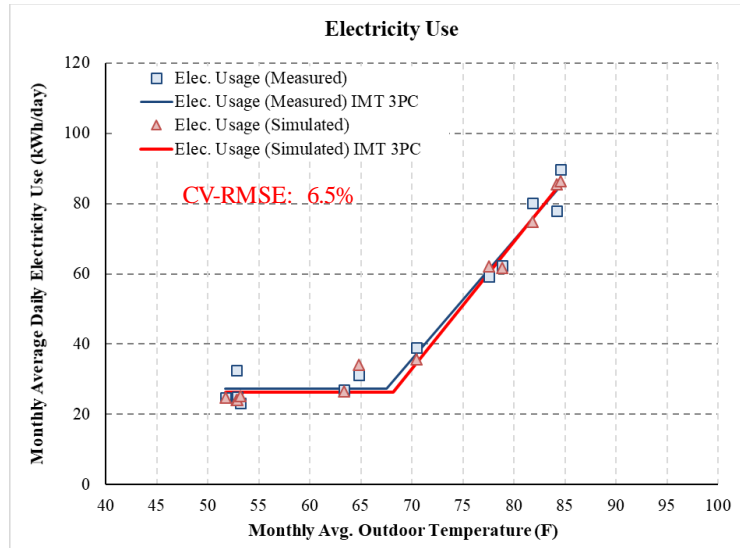


Figure 4.75: Monthly Average Daily Electricity Usage Versus Monthly Average Outdoor Temperature for the Billing Period

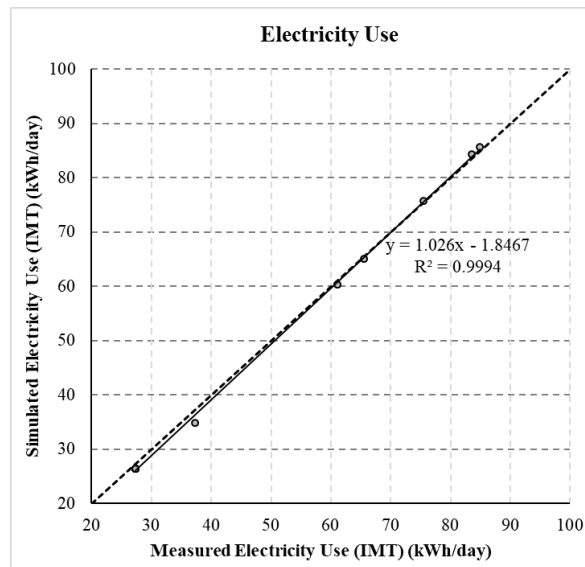


Figure 4.76: Simulated Electricity Usage Versus Measured Electricity Usage

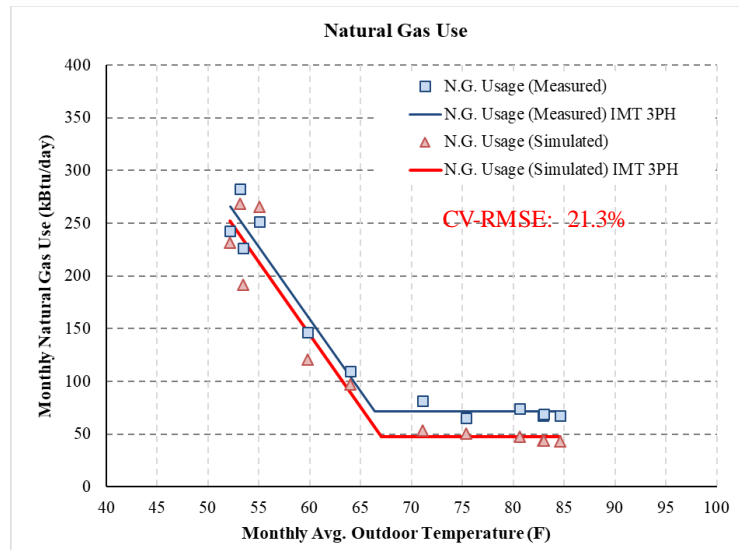


Figure 4.77: Monthly Average Daily Natural Gas Usage Versus Monthly Average Outdoor Temperature for the Billing Period

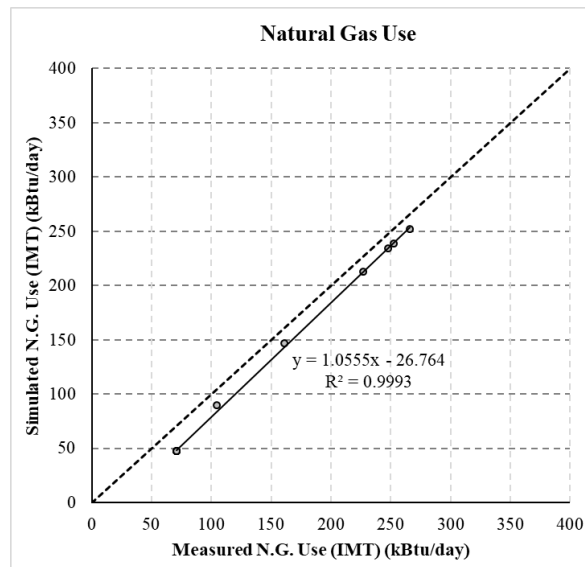


Figure 4.78: Simulated Natural Gas Usage Versus Measured Natural Gas Usage

4.1.10.5. Calibration #4: Hot Water Use

The hot water use was calibrated in this chapter. The hot water use was adjusted to match the natural gas consumption during the heating season. So, the hot water use was increased from 50 gal/day to 85 gal/day.

Figure 4.79 shows the monthly average daily electricity usage versus monthly average outdoor temperatures. The electricity usage was not changed by the hot water use changed. The result of simulated electricity usage was matched with the measured data in the calibration of the SEER in Ch.4.1.10.4. Figure 4.80 shows the simulated electricity usage versus measured electricity usage, which shows that the electricity usage of the simulation is similar to the measured electricity usage data.

Figure 4.81 shows the monthly average daily natural gas usage versus monthly average outdoor temperatures. The result of simulated natural gas usage was matched with the measured data by changing the hot water use. Figure 4.82 shows the simulated natural gas usage versus measured natural gas usage, and this shows that the natural gas usage of the simulation was similar with the measured natural gas usage data.

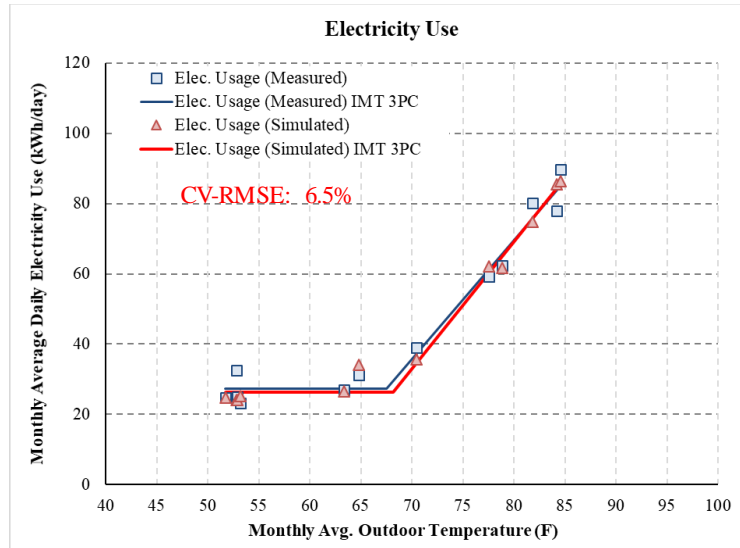


Figure 4.79: Monthly Average Daily Electricity Usage Versus Monthly Average Outdoor Temperature for the Billing Period

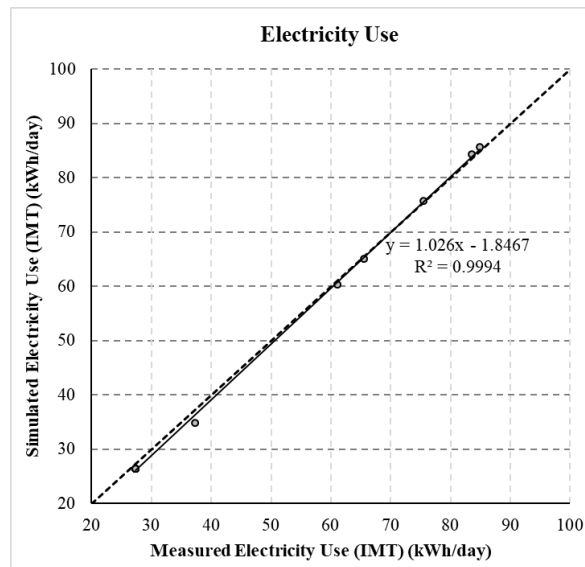


Figure 4.80: Simulated Electricity Usage Versus Measured Electricity Usage

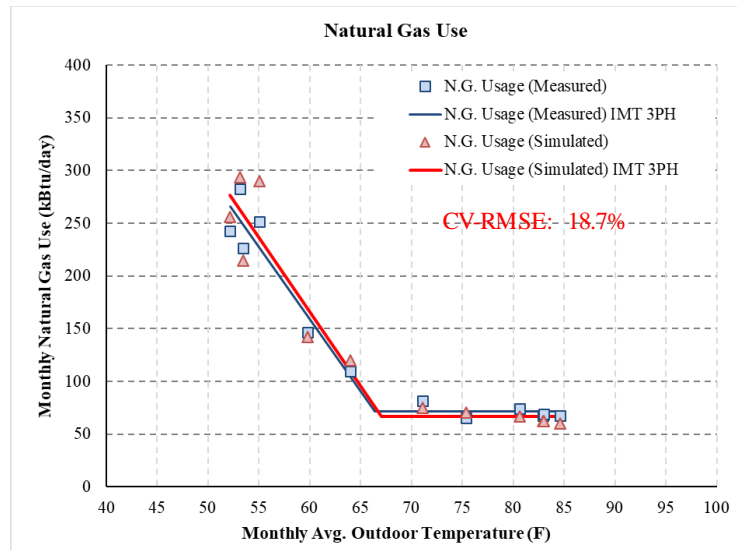


Figure 4.81: Monthly Average Daily Natural Gas Usage Versus Monthly Average Outdoor Temperature for the Billing Period

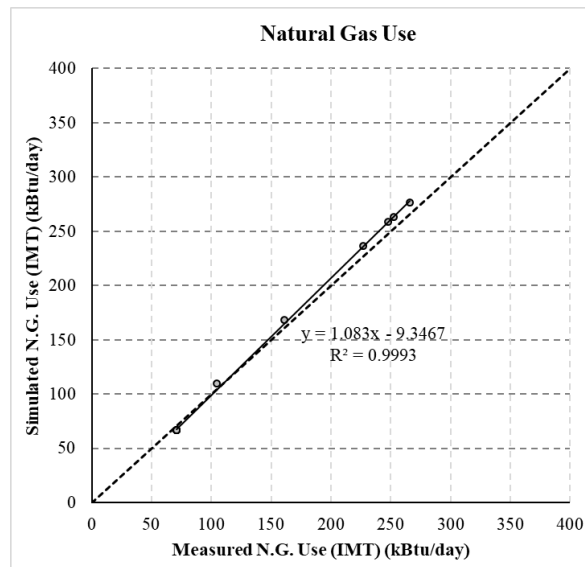


Figure 4.82: Simulated Natural Gas Usage Versus Measured Natural Gas Usage

4.2. Development of a 2015 IECC Simplified Uncalibrated House Simulation Model

This section provides the procedure to develop a simplified uncalibrated residential model in College Station, TX. The base-case model is based on the standard reference design and specifications as defined in Section R405 of the 2015 IECC and specifications of the IC3. First, this study used a 2009 IECC simplified residential air source heat pump (ASHP) base case simulation model for Houston (Do & Choi, 2013). Then, using the 2009 IECC simplified model, a 2015 IECC residential base-case simulation model with natural gas (NG) system for College Station was developed by modifying input parameters using the 2015 IECC and IC3 specifications.

4.2.1. 2009 IECC Simplified Uncalibrated Residential Base-Case Simulation Model with Air Source Heat Pump System

A 2009 IECC simplified uncalibrated residential base case model was developed in 2013 based on the standard reference design and requirements as determined from the climate-specific characteristics in Chapter 4 of the 2009 IECC. During the study, a building description language (BDL) file (RUN30.inp) was developed for DOE-2.1e program. This simulation model has an air source heat pump (ASHP) system for heating and cooling, and an electric water heater for domestic hot water. The residential simulation model has a flat roof, and does not have an attic space (Do et al., 2013).

For this study, the 2015 IECC base-case model was developed using the step-by-step procedure from the 2009 IECC base-case model (RUN30.inp) using the step-by-step procedure, which was verified with IC3, and REM/Rate v 14.3 program in 2013 (Do et al., 2013).

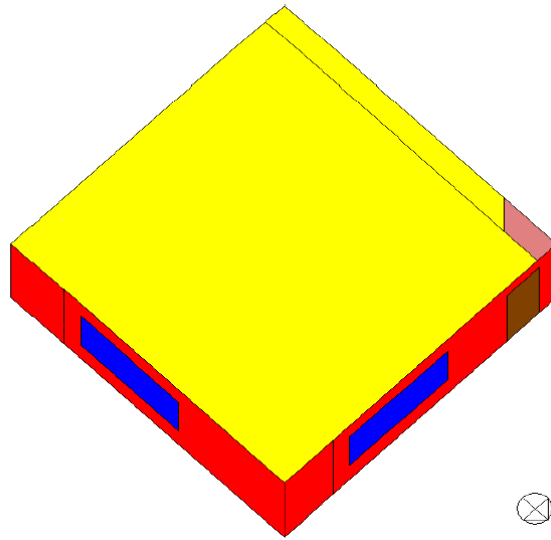


Figure 4.83 2009 IECC simplified residential base-case model

Table 4.6 Summary of input parameters for the 2009 IECC simplified residential base case model

Input	2009 IECC Simplified Residential Base Case Model
# of Space	1
Area	2500
Window-to-floor Ratios (WFR)	15%
Overhang	No
Azimuth	0
# of People	0
Plenum	Removed
Return-Air-Path	Direct
Door Location	Single (N)
System Type	RESYS
SEER	13
HSPF	7.7
Fan Schedule	Always
Thermostat Heat	72 F
Thermostat Cool	75 F
Air Flow Rate	1800 cfm
Floor U-Value (Slab-on-Grade)	0.088
Roof U-Value	0.035
Roof Absorptance	0.75
Wall U-Value	0.082
Door U-Value	0.65
Glazing U-Value	0.65
Window Frame	Frame
Glazing SHGC	0.3
Infiltration ACH	0.35
GND Reflec.	0.24
Lighting (w/sqft)	0.1951
Equipment (w/sqft)	0.2632
Lighting	Always
Equipment	Always
Infiltration	Always
Interior Shading	Schedule (Summer = 0.70, Winter=0.85)
DHW System	DHW

4.2.2. 2015 IECC Simplified Uncalibrated Residential Base-Case Simulation Model with Natural Gas System

The 2015 IECC model was developed with the College Station climate and a natural gas system for space heating and water heating, which is different than the previous 2009 IECC model that was an all-electric. This new revision was created to facilitate a comparison with the case-study house described in the next chapter. A systematic input change procedure is used to develop the new 2015 IECC base-case model with natural gas heating and DHW systems located in College Station, TX. The procedure starts with the RUN 30, 2009 IECC ASHP base-case model, to develop the 2015 IECC NG base-case model by modifying selected input parameters, including: system type, system efficiency, roof type, roof U-value, exterior wall U-value, door U-value, glazing U-value, glazing SHGC, infiltration, and interior shading. In addition the house-type was changed from the flat roof to a gable roof. The gable roof was also applied to better match the case study house and a duct model was added in the attic space of the gable roof. The detailed description of the 2015 IECC model is provided in the following sections.

4.2.2.1. *Exterior Wall*

The U-value of the exterior wall, which was 0.082 Btu/h-ft²-F, in Houston (Climate Zone 2) in the 2009 IECC, was changed to 0.084 Btu/h-ft²-F in the 2015 IECC. The method of applying the U-value is as follows. The exterior walls of the base case

house were constructed with 2 x 4 studs placed 16 inches on center. The exterior wall has 25 percent of the total area as studs and the remaining 75 percent are the insulation portion. As mentioned above, according to the 2015 IECC, the U-value of the wall was changed to 0.084 Btu/h-ft²-F in College Station (Climate Zone 2). The wall insulation thickness was calculated to match the U-value (Btu/h-ft²-F). The detailed exterior wall construction is as follows.

Table 4.7 Details of exterior wall thermal properties (Insulation part)

Insulation Part (65%)					
Material Description	Materials in DOE-2	Conductivity (Btu-ft/h-ft ² -F)	Thickness (ft)	Conductance (Btu/h-ft ² -F)	Resistance (h-ft ² -F/Btu)
Ext. Air Film		-	-	-	0.170
Brick (3 inch Face)	BK04	0.758	0.250	3.030	0.330
Air Layer	AL21	-	-	-	0.890
Plywood (1/2 inch)	PW03	0.067	0.042	1.600	0.625
Exterior Insulation		-	-	-	0.000
Insulation		0.025	0.291	0.086	11.632
Gyp Board (1/2 inch)	GP01	0.093	0.042	2.221	0.450
Int. Air Film		-	-	-	0.680
Total R-value					14.778

Table 4.8 Details of exterior wall thermal properties (Stud part)

Stud Part (25%)					
Material Description	Materials in DOE-2	Conductivity (Btu-ft/h-ft ² -F)	Thickness (ft)	Conductance (Btu/h-ft ² -F)	Resistance (h-ft ² -F/Btu)
Ext. Air Film					0.170
Brick (3 inch Face)	BK04	0.758	0.250	3.030	0.330
Air Layer	AL21				0.890
Plywood (1/2 inch)	PW03	0.067	0.042	1.600	0.625
Exterior Insulation					0.000
Stud		0.067	0.292	0.229	4.373
Gyp Board (1/2 inch)	GP01	0.093	0.042	2.221	0.450
Int. Air Film					0.680
Total R-value					7.518

The stud part area was calculated as 25% of the area minus the window area and the door area. Figure 4.84 shows an example of calculating the stud and non-stud areas.

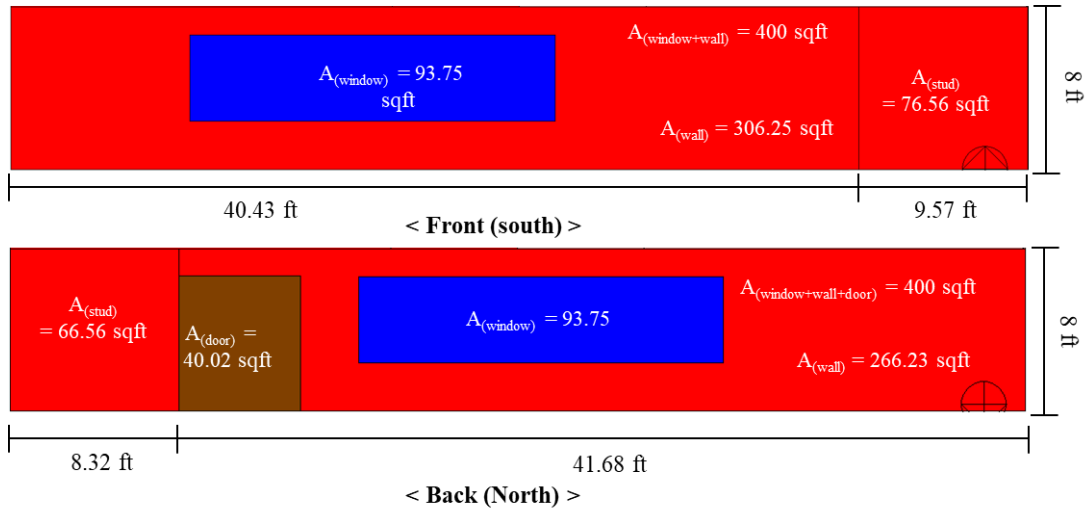


Figure 4.84 Calculation example for stud and non-stud portions of the exterior wall

4.2.2.2. Underground Surface

The heat transfer calculation through the underground surface was the same as the 2009 model. Since the floor of the slab-on-grade house directly contacts the ground, it is important to accurately calculate the heat transfer between the floor and the ground, and account the thermal mass of the surface. According to Winkelmann (2002), DOE-2 can over-calculate the heat transfer through the underground surface. This is because the heat transfer through the underground surface actually occurs mostly through the perimeter region. In other words, a large portion of the heat transfer occurs in the perimeter of the building floor, but not in the center of the building floor. However, in case of DOE-2, heat transfer is calculated without distinction between center and perimeter as shown in the equation below.

The DOE-2's default heat transfer calculation through underground surface is as below.

$$Q = U \times A (T_g - T_i) \quad \text{Equation 4.1}$$

Where,

Q the heat transfer through the underground surface (Btu/h)

U the conductance of the surface (Btu/h-F-ft²)

A is the area of the surface (ft²)

T_g is the ground temperature (F)

T_i is the indoor temperature (F)

To correct the ground heat transfer, Winkelmann (2002) introduced an effective U-value (U-effective) method to calculate the heat transfer through underground surface using DOE-2. The effective U-value method is a method that the correct U-value of the surface with perimeter conduction factor (F2), perimeter length, and floor area, and is expressed by the equation below. The base-case model has a floor area of 2,500 ft² and a perimeter length of 200 ft. In the base-case model, the foundation is a concrete slab-on-grade, and the floor is composed of 80% carpet 20% tiles according to IECC requirements.

$$R_{eff} = A / (F2 \times P_{exp}) \quad \text{Equation 4.2}$$

$$: 11.364 = 2500 / (1.10 \times 200)$$

$$U_{eff} = 1 / R_{eff} \quad \text{Equation 4.3}$$

$$: 0.088 = 1 / 11.364$$

$$Q = U_{eff} \times A (T_g - T_i) \quad \text{Equation 4.4}$$

Where,

R_{eff} is the effective resistance of the underground surface (h-F-ft²/Btu)

A is the area of the surface (2,500 ft²)

F2 is the perimeter conduction factor (1.10 Btu/h-F-ft) (see Table 4.9)

P_{exp} is the length of the surface's perimeter (200 ft)

U_{eff} is the effective U-value (Btu/h-F-ft²)

Q the heat transfer through the underground surface (Btu/h)

T_g is the ground temperature (F)

T_i is the inside air temperature (F)

In order to apply the U-effective method to DOE-2, it is possible to calculate and apply the fictitious resistance through the effective resistance with the underground surface layers. Figure 4.85 and the equation below present the calculation of the fictitious resistance.

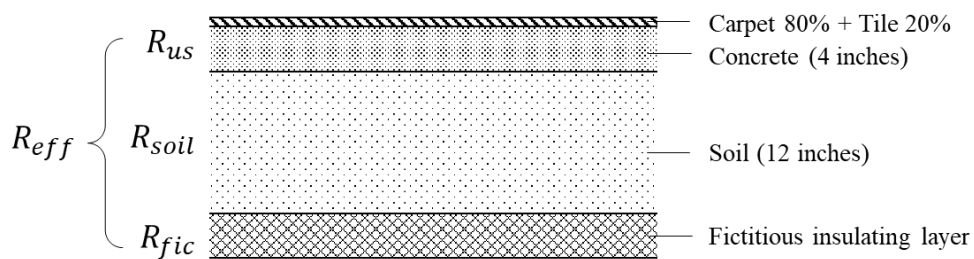


Figure 4.85 Layers of underground surface for the U-effective method (Winkelmann, 2002)

$$R_{eff} = R_{us} + R_{soil} + R_{fic} \quad \text{Equation 4.5}$$

$$R_{fic} = R_{eff} - R_{us} - R_{soil} \quad \text{Equation 4.6}$$

$$: 7.544 = 11.364 - 2.82 - 1$$

$$R_{us} = R_{concrete} + R_{carpet\ floor} + R_{air\ film} \quad \text{Equation 4.7}$$

$$: 2.82 = 0.44 + 1.61 + 0.77$$

$$R_{concrete} = \left(\frac{1}{\text{conductivity}} \right) \times \text{Thickness} \quad \text{Equation 4.8}$$

$$: 0.44 = (1/0.7576) \times (0.3333)$$

$$R_{carpet\ floor} = (0.8 \times R_{carpet}) + (0.2 \times R_{tile}) \quad \text{Equation 4.9}$$

$$: 1.61 = (0.8 \times 2) + (0.2 \times 0.05)$$

Where,

R_{soil} is the resistance of 1-ft soil (h-F-ft²/Btu),

R_{us} is the resistance of the floor, including carpeting, if present, and inside film resistance (h-F-ft²/Btu),

R_{fic} is the fictitious insulating layer (h-F-ft²/Btu),

$R_{carpet\ floor}$ is the resistance of 80% carpet and 20% tile (h-F-ft²/Btu),

$R_{concrete}$ is the 4-inch concrete resistance (0.44 h-F-ft²/Btu),

R_{carpet} is the carpet resistance (2 h-F-ft²/Btu), and

R_{tile} is the tile resistance (0.05 h-F-ft²/Btu).

Table 4.9 Perimeter conduction factors for concrete slab-on-grade (Winkelmann, 2002)

Foundation depth	Insulation Configuration	Perimeter Conduction Factor (F2) (Btu/hr-F-ft)	
		Uncarpeted	Carpeted
2ft	Uninsulated	1.10	0.70
	R-5 exterior	0.73	0.54
	R-10 exterior	0.65	0.49
4 ft	Uninsulated	1.10	0.77
	R-5 exterior	0.61	0.46
	R-10 exterior	0.50	0.37

4.2.2.3. Window

The base-case model computes the window heat transfer using the shading coefficient method (SC) in DOE-2. When using the SC method in DOE-2, the main input parameters are glass shading coefficient, glass conductance excluding outside air film coefficient, frame conductance, and frame width. All of these inputs were calculated based on a 3×5 window, as shown in Figure 4.86.

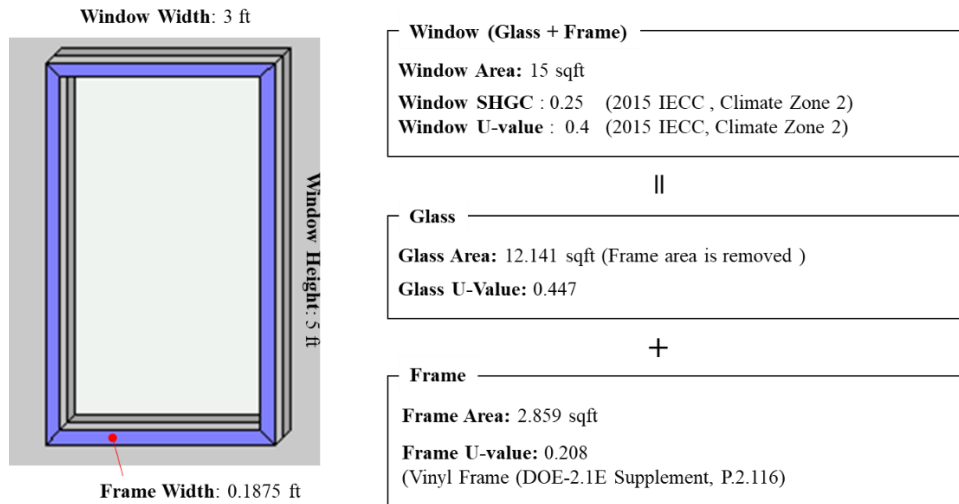


Figure 4.86 Reference window in the base-case model

DOE-2 uses the shading coefficient (SC) of the glass surface instead of the entire window as input. However, the IECC presents the Solar Heat Gain Coefficient (SHGC) of the entire window as a reference. According to the 2015 IECC, in College Station (Climate Zone 2), the window of the house must have a SHGC of 0.25 or less. Therefore, the window SHGC values were converted to glass SC values for use in DOE-2.

$$SC_{glass} = SHGC_{glass} / 0.87 \quad \text{Equation 4.10}$$

$$: 0.355 = 0.309 / 0.87$$

$$SHGC_{glass} = (SHGC_{window} \times A_{window}) / A_{glass} \quad \text{Equation 4.11}$$

$$: 0.309 = (0.25 \times 15) / 12.141$$

$$A_{glass} = (H_{window} - (2 \times W_{frame})) \times (W_{window} - (2 \times W_{frame}))$$

Equation 4.12 (see Figure 4.87)

$$: 12.141 = (5 - (2 \times 0.1875)) \times (3 - (2 \times 0.1875))$$

Where,

$SHGC_{window}$ is the solar heat gain coefficient for window (0.25 according to Table R402.1.2 in the 2015 IECC for Climate Zone 2),

H_{window} is the reference window height (5 ft),

W_{window} is the reference window Width (3 ft),

A_{window} is the reference window area (3ft \times 5ft = 15 sqft),

A_{glass} is the glass area for the reference window (sqft), and

W_{frame} is the window frame width (0.1875 ft).

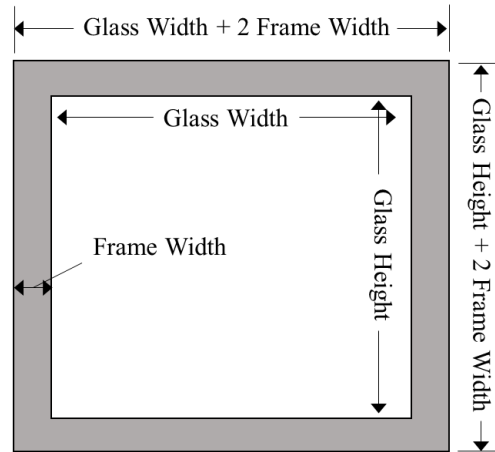


Figure 4.87 The dimensioning of a window with a frame

For DOE-2, the conductance value of the glass and frame needs to be input.

However, since the IECC presents the window U-value as the thermal performance of a window, it is necessary to convert the window U-value to glass conductance and frame conductance. The conversion process is as follows.

$$C_{glass} = \frac{1}{\left(\frac{1}{U_{glass}}\right) - 0.197} \quad \text{Equation 4.13}$$

$$: 0.462 = 1/(1/0.424)-0.197)$$

$$U_{glass} = UA_{glass}/A_{glass} \quad \text{Equation 4.14}$$

$$: 0.424 = 5.142/12.141$$

$$UA_{glass} = UA_{window} - UA_{frame} \quad \text{Equation 4.15}$$

$$: 5.142 = 6 - 0.858$$

$$UA_{window} = U_{window} \times A_{window} \quad \text{Equation 4.16}$$

$$: 6 = 0.4 \times 15$$

$$UA_{frame} = U_{frame} \times A_{frame} \quad \text{Equation 4.17}$$

$$: 0.858 = 0.300 \times 2.859$$

$$U_{frame} = \frac{1}{\left(\frac{1}{C_{frame}}\right) + 0.197} \quad \text{Equation 4.18}$$

$$: 0.300 = 1/((1/0.319)+0.197)$$

$$A_{frame} = A_{window} - A_{glass} \quad \text{Equation 4.19}$$

$$: 2.859 = 15 - 12.141$$

Where,

C_{glass} is the glass conductance (Btu/h-F-ft²),

U_{glass} is the glass U-value (Btu/h-F-ft²) (include outside air film at 15mph windspeed),

UA_{glass} is the glass UA (Btu/h-F),

UA_{window} is the window UA (Btu/h-F),

U_{window} is the window U-value (0.4 Btu/h-F-ft² according to Table R402.1.4 in the 2015 IECC for Climate Zone 2),

U_{frame} is the vinyl frame U-value (Btu/h-F-ft²) (include outside air film at 15mph windspeed),

C_{frame} is the vinyl frame conductance (0.319 Btu/h-F-ft² according to DOE-2.1E Supplement, P.2.116), and

A_{frame} is the frame area (ft²).

The width of the window frame was calculated based on the 3×5 reference window. In the simplified simulation model, several windows are expressed as one combined window rather than separate windows for each window in the case study house. In this case, the equivalent frame width was used since the frame width of the actual window was smaller than the combined window.

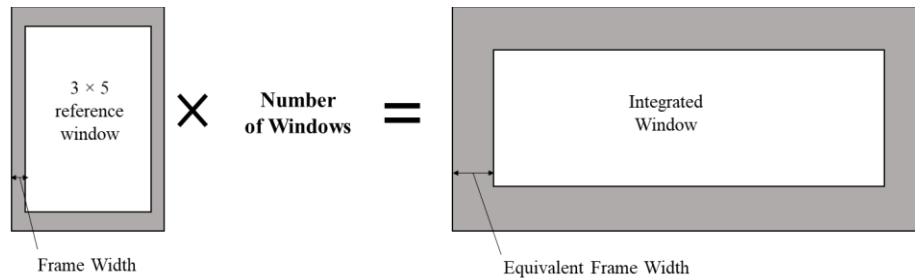


Figure 4.88 Concept of the equivalent frame width

4.2.2.4. Attic

The main differences between the 2015 IECC base-case model and the 2009 IECC base-case model are the roof types and the addition of an attic space. In the 2009 IECC model, the roof shape was a flat roof, but in the 2015 IECC model, the roof shape was changed to a gable roof with an unconditioned attic space. As the result of this change, the roof geometry was changed and a duct model was incorporated to the attic space.

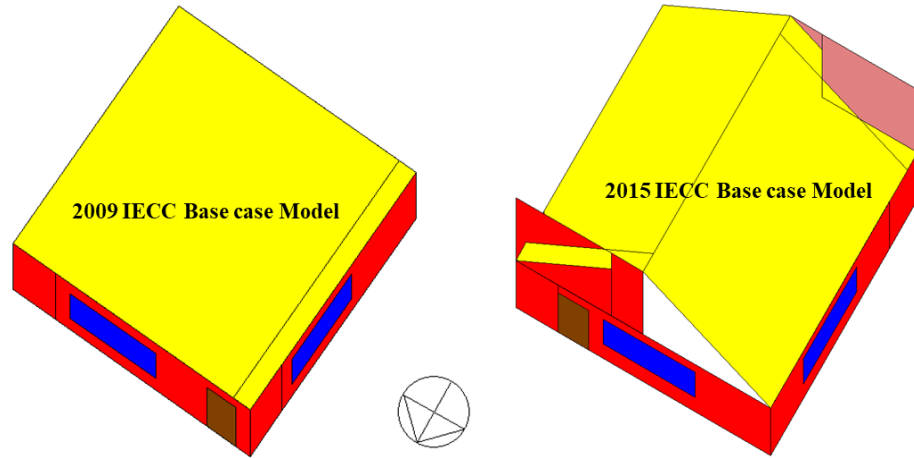


Figure 4.89 2009 IECC base case model Vs. 2015 IECC base case model

The duct model was incorporated to DOE-2.1e simulation program using FUNCTION commands in the DOE-2 program. The duct model for DOE-2 was developed based on ASHRAE 152-2004, and calculates the delivery efficiency of supply air and return air through the duct in consideration of conduction loss and air leakage of the duct (Kim, 2006). The equations for the duct model are as follows duct (Kim, 2006).

$$DE_{heating} = a_s B_s - a_s B_s (1 - B_r a_r) \frac{\Delta t_r}{\Delta t_e} - a_s (1 - B_s) \frac{\Delta t_s}{\Delta t_e} \quad \text{Equation 4.20}$$

$$DE_{cooling} = \frac{a_s Q_e \rho_{in}}{E_{cap}} \left(\frac{E_{cap}}{60 Q_e \rho_{in}} + (1 - a_r)(h_{amb,r} - h_{in}) + a_r C_p (B_r - 1) \Delta t_r \right. \\ \left. + C_p (B_s - 1)(t_{sp} - t_{amb,s}) \right) \quad \text{Equation 4.21}$$

Where,

$DE_{heating}$ is the delivery efficiency for heating,

$DE_{cooling}$ is the delivery efficiency for cooling,
 B_s is the conduction efficiency of supply duct ($\exp\left(\frac{-A_s}{60Q_e\rho_{in}C_pR_s}\right)$),
 B_r is the conduction efficiency of return duct ($\exp\left(\frac{-A_r}{60Q_e\rho_{in}C_pR_r}\right)$),
 a_s is the air leakage efficiency of the duct of supply duct ($\left(\frac{Q_e-Q_s}{Q_e}\right)$),
 a_r is the air leakage efficiency of the duct of return duct ($\left(\frac{Q_e-Q_r}{Q_e}\right)$),
 E_{cap} is the capacity of the equipment (Btu/h),
 Q_e is the system air flow (CFM),
 C_p is the specific heat (Btu/lb_m-F),
 Δt_e is the temperature rise across the equipment ($\left(\frac{E_{cap}}{60Q_e\rho_{in}C_p}\right)$ (F)),
 Δt_s is the temperature difference between the building and the ambient temperature surrounding the supply ($t_{in} - t_{amb,s}$) (F),
 Δt_r is the temperature difference between the building and the ambient temperature surrounding the return ($t_{in} - t_{amb,r}$) (F),
 t_{in} is the indoor air temperature (F),
 t_{sp} is the supply plenum air temperature (F),
 $t_{amb,s}$ is the ambient temperature for supply ducts (F),
 $t_{amb,r}$ is the ambient temperature for return ducts (F),
 $h_{amb,x}$ is the enthalpy of ambient air for return (Btu/h),
 h_{in} is the enthalpy of air inside conditioned space (Btu/h),
 A_s is the supply duct area (ft²),
 A_r is the return duct area (ft²),
 ρ_{in} is the density of air (lb/ft³),
 R_s is the thermal resistance of supply duct (h-ft²-F/Btu), and
 R_r is the thermal resistance of return duct (h-ft²-F/Btu).

4.2.2.5. *Schematic Procedure to Develop the 2015 IECC Residential Base Case Model*

Table 4.10 summarizes the development procedure to develop the 2015 IECC residential base-case model with a natural gas system for College Station, TX. The modified inputs for each simulation in the procedure are described as below.

- RUN 30 is the Simplified Residential ASHP Base case model for Houston, TX (Do et al., 2013)
- RUN 31 simulation redefined the cooling efficiency from SEER 13 to SEER 14.
- RUN 32 simulation redefined the heating efficiency from 7.7 HSPF to 0.78 AFUE.
- RUN 33 simulation modified the roof thermal insulation for Climate Zone 2 (College Station, TX). R-32.51 was used for the roof insulation based on Table R402.1.4 in the 2015 IECC. The U-0.030, ceiling U-factor, value was applied to use the DOE-2 layer input method, including a 7% of the framing factor that represents the percentage of stud or joist area.
- RUN 34 simulation modified the wall thermal insulation for Climate Zone 2. R-11.632 is used for the wall insulation based on Table R402.1.4 in the 2015 IECC. The U-0.084, frame wall U-factor, value is applied to use the layer input method, including 25% of the framing factor.

- RUN 35 simulation modified the door U-factor. U-0.4 is used for the door U-factor that is same as fenestration based on Table R402.1.4 in the 2015 IECC.
- RUN 36 simulation modified the window glass thermal conductance for Climate Zone 3. 0.462 Btu/ft²-F-h was used for the glass thermal conductance, and this value is from U-0.4, Fenestration U-factor, based on Table R402.1.4. in the 2015 IECC.
- RUN 37 simulation modified the Shading Coefficient (SC) for Climate Zone 2. 0.355 was used for the SC value, and this value is converted from 0.4, the Solar Heat Gain Coefficient (SHGC) in Table R402.1.2 of the 2015 IECC.
- RUN 38 simulation modified the fractional leakage area that was calculated with the inputs of a blower door test value (ACH50) and a mechanical ventilation value (CFM). 0.2 Air Changes per Hour (ACH) based on the calculated value based on Table R405.5.2(1) in the 2015 IECC. In order to input the infiltration, this study used 0.005212 of the Specific Leakage Area (SLA) value, which was calculated by the following equation (Do et al., 2013; ICC, 2015)

$$ACH = SLA \times 1,000 \times W \times NS^{0.3}$$

Equation 4.22

Where,

ACH is the air change per hour,
 SLA is the specific leakage area,

W is the weather factor, and

NS is the number of stories above grade.

- The RUN 39 simulation modified the interior shading schedule for summer and winter. The standard reference design based on Table R405.5.2(1) in the 2015 IECC requires that 0.8675 of the multiplier in the interior shading schedule is used for winter and summer interior shading.

Table 4.10 Development procedure for the 2015 IECC residential base case model from the 2009 IECC model (RUN 30)

IECC VERSION	RUN NAME	PROJECT									COOLING AND HEATING SYSTEM						
		# of Space	Area	Window-to-floor Ratios (WFR)	Overhang	Azimuth	# of People	Plenum	Return-Air-Path	Door Location	System Type	SEER	HSPF to AFUE	Fan Schedule	Thermostat Heat	Thermostat Cool	Air Flow Rate
IECC 2009	RUN30	1	2500	15%	No	0	0	Removed	Direct	Single (N)	RESYS	13	7.7	Always	72 F	75 F	1800 cfm
IECC 2015	RUN31	1	2500	15%	No	0	0	Removed	Direct	Single (N)	RESYS	14	7.7	Always	72 F	75 F	1800 cfm
	RUN32	1	2500	15%	No	0	0	Removed	Direct	Single (N)	RESYS	14	0.78	Always	72 F	75 F	1800 cfm
	RUN33	1	2500	15%	No	0	0	Removed	Direct	Single (N)	RESYS	14	0.78	Always	72 F	75 F	1800 cfm
	RUN34	1	2500	15%	No	0	0	Removed	Direct	Single (N)	RESYS	14	0.78	Always	72 F	75 F	1800 cfm
	RUN35	1	2500	15%	No	0	0	Removed	Direct	Single (N)	RESYS	14	0.78	Always	72 F	75 F	1800 cfm
	RUN36	1	2500	15%	No	0	0	Removed	Direct	Single (N)	RESYS	14	0.78	Always	72 F	75 F	1800 cfm
	RUN37	1	2500	15%	No	0	0	Removed	Direct	Single (N)	RESYS	14	0.78	Always	72 F	75 F	1800 cfm
	RUN38	1	2500	15%	No	0	0	Removed	Direct	Single (N)	RESYS	14	0.78	Always	72 F	75 F	1800 cfm
RUN39	1	2500	15%	No	0	0	Removed	Direct	Single (N)	RESYS	14	0.78	Always	72 F	75 F	1800 cfm	

Table 4.10 Development procedure for the 2015 IECC residential base case model from the 2009 IECC model (RUN30)
(Continued)

IECC VERSION	RUN NAME	CONSTRUCTION										INTERNAL GAIN		SCHEDULE			
		Floor U-Value (Slab-on-Grade)	Roof U-Value	Roof Absorptance	Wall U-Value	Door U-Value	Glazing U-Value	Window Frame	Glazing SHGC	Infiltration ACH	GND Reflec.	Lighting (w/sqft)	Equipment (w/sqft)	Lighting	Equipment	Infiltration	Interior Shading
IECC 2009	RUN30	0.088	0.035	0.75	0.082	0.65	0.65	Frame	0.3	0.35	0.24	0.1951	0.2632	Always	Always	Always	Schedule (Summer = 0.70, Winter=0.85)
IECC 2015	RUN31	0.088	0.035	0.75	0.082	0.65	0.65	Frame	0.3	0.35	0.24	0.1951	0.2632	Always	Always	Always	Schedule (Summer = 0.70, Winter=0.85)
	RUN32	0.088	0.035	0.75	0.082	0.65	0.65	Frame	0.3	0.35	0.24	0.1951	0.2632	Always	Always	Always	Schedule (Summer = 0.70, Winter=0.85)
	RUN33	0.088	0.03	0.75	0.082	0.65	0.65	Frame	0.3	0.35	0.24	0.1951	0.2632	Always	Always	Always	Schedule (Summer = 0.70, Winter=0.85)
	RUN34	0.088	0.03	0.75	0.084	0.65	0.65	Frame	0.3	0.35	0.24	0.1951	0.2632	Always	Always	Always	Schedule (Summer = 0.70, Winter=0.85)
	RUN35	0.088	0.03	0.75	0.084	0.4	0.65	Frame	0.3	0.35	0.24	0.1951	0.2632	Always	Always	Always	Schedule (Summer = 0.70, Winter=0.85)
	RUN36	0.088	0.03	0.75	0.084	0.4	0.4	Frame	0.3	0.35	0.24	0.1951	0.2632	Always	Always	Always	Schedule (Summer = 0.70, Winter=0.85)
	RUN37	0.088	0.03	0.75	0.084	0.4	0.4	Frame	0.25	0.35	0.24	0.1951	0.2632	Always	Always	Always	Schedule (Summer = 0.70, Winter=0.85)
	RUN38	0.088	0.03	0.75	0.084	0.4	0.4	Frame	0.25	0.2	0.24	0.1951	0.2632	Always	Always	Always	Schedule (Summer = 0.70, Winter=0.85)
	RUN39	0.088	0.03	0.75	0.084	0.4	0.4	Frame	0.25	0.2	0.24	0.1951	0.2632	Always	Always	Always	Fixed (0.8675)

As shown in Chapter 4.2.2.4, the roof type was changed from a flat roof to gable roof, and an attic space was created, and a duct model was applied.

4.3. Development of a Simplified Case-study House Simulation Model Analysis of the Simplified Uncalibrated House Simulation Model

This section provides the procedure to develop a simplified uncalibrated case-study house model in College Station, TX. The simplified uncalibrated case-study house model was developed using the 2015 IECC simplified house simulation in Chapter 4.2 and the information of the case-study house in Chapter 4.1.1.

4.4. Comparison of the Detailed and Simplified Model

In chapters 4.1 and 4.3, the simplified case-study house and detailed case-study house were developed. To analyze these two models they were compared to each other. The case-study house simulation models were analyzed to test the input values and calculation models of the simplified model. Building energy code compliance simulation has reduced the number of inputs displayed to users for ease of use. However, in order to calculate the building energy, numerous inputs and calculation models are required. For that reason, the large number of input values and calculation models are defined by developers instead of users. However, the pre-defined input values and calculation models may differ from the actual building and detailed building energy modeling. Therefore, with the detailed case-study house simulation model (detailed building energy model) developed in Ch.4.1, the elements of the simplified model were compared. Table

4.11 shows the input specifications of detailed and simplified case-study house simulation models and shows the limitations of the simplified model and the difference from the detailed model.

Table 4.11: Input Specifications of the Detailed and Simplified Case-study House Simulation Models

Component		Detailed Model (Calibrated)	Simplified Model
Envelope	Exterior Wall	Geometry	Detailed Geometry
		Wall Color	Dark
		Average Wall Height	9 ft
		Insulation R-Value	R-13
		Stud Spacing	16"
	Windows	Grass Area	303.5 ft ²
		Grazing Type	Clear Double Pane
		Frame Type	Aluminum
		U-Value	0.87
		SHGC	0.66
	Roof/Attic	Setback	3 inch
		Roof Color	Dark
		Roof Type	Hip Roof
		Ceiling Type	Ceiling with Attic Above
		Insulation R-Value	R-29.6 (8" insulation depth)
Slab Floor	Eaves	1.5 ft	
	Gross Area	2,391 ft ²	
	Slab Perimeter R-Value	R-0	
Systems	Heating	Fuel	Natural Gas
		System Type	Furnace
		Efficiency (AFUE or HSPF)	66%
		Manufacturer	Lennox
		System Location	Attic
	Cooling	Heating Set Temperature	67.7 F
		System Type	Air Conditioner, Air Cooled
		Efficiency (SEER)	8
		Manufacturer	Lennox
		System Location	Unconditioned Area
	Domestic Water Heater	Cooling Set Temperature	73.9 F
		Fuel	Gas
		Capacity	50 Gallon
		Energy Factor	0.594
		Burner Capacity	38,000 Btu/h
Type		Storage	
Tank Location		Unconditioned Area	
Manufacturer		Rheem	
Water Use		85 gal/day	
Etc.	Inlet Water Temperature	Measured	
	Tank Temperature	135.3 F	
Etc.	Light and Equipment	0.9 kw	
	Tree	Nine Trees	
	Fence	Yes	
	Garage	Yes	
	Ground Heat Transfer Method	Winkelmann and Huang	
	Weather	2019, College Station	
Unconditioned Zone	Calibrated		

5. RESULTS OF THE DETAILED CALIBRATED CASE STUDY HOUSE SIMULATION MODEL

This chapter presents the results of the detailed calibrated case-study house simulation model. The detailed calibrated case-study house simulation model was tested against the simplified model to determine the impact of specific calibrations.

5.1. Analysis of the Impact of Shading

In this section, the impact of shading of the case-study house was tested. To accomplish this, the window setback, eaves, trees, and surrounding fences were examined.

5.1.1. Window Setback

Window setback is often ignored in simplified simulation models. However, Buildings may have a window setback. In the case-study house of this study, there was a 3-inch window setback, which was analyzed.

5.1.2. Eaves

Most buildings have roof eaves. The eaves protrude the wall as the edge of the roof, usually over the sides of a building. In the case-study house, there were 1.5 ft eaves. These eaves are often ignored in building energy simulations, and the eaves are not present in building energy modeling in building energy simulations tests.

5.1.3. Trees

Most single-family houses are surrounded by trees. In a simulation for a new house, it may not be easy to add a tree, but in a simulation for an existing building, it is possible to add a tree to evaluate it. However, it is common not to consider the trees for building energy simulation.

5.1.4. Fences

A fence is a structure that usually surrounds an outdoor area and is usually made up of posts connected by boards, wires, rails, or nets. The typical height for backyard fences is between 6 and 8 feet.

5.1.5. Results of the Impact of Shading

In this section, shading impact on the annual energy usage was analyzed for the window setback, eaves, trees, and fences. Table 5.1 shows the list of cases for this shading analysis. Case 0 was the simplified uncalibrated model. Case 1 was a calibrated detailed model of a case-study house. Case 2 was the case where the 3-inch window setback was removed from Case 1 and was used to analyze how much the window setback affect the building energy. Case 3 was the case where the 1.5ft eaves were removed from Case 1 and was used to analyze how much the eaves affect the building energy. Case 4 was the case of removing trees from Case1 and was used to analyze how shading of the trees affects the building energy. Case 5 was the case where fences were removed from Case 1 and was used to analyze how shading of the fences affects the building energy. Finally, Case 6 was the case where all the shades described (i.e., 3-inch

window setback, 1.5 ft eaves, trees, fences) above have been removed from Case 1, and was used to analyze how much shading affects the building energy.

Table 5.1: List of Cases for Shading Analysis

Case	Characteristic
Case 0	Simplified Model: without All
Case 1 (Base-case)	Detailed Model (Calibrated): 3-inch Window Setback, 1.5ft Eaves, Trees, and Fences
Case 2	Case 1 + without 3-inch Window Setbacks
Case 3	Case 1 + without 1.5ft Eaves
Case 4	Case 1 + without Trees
Case 5	Case 1 + without Fences
Case 6	Case 1 + without All (Case 2 to Case 5)

Figure 5.1 and Table 5.2 show the building energy consumption results according to shading. When the window setback was removed from the base-case, heating energy consumption decreased by 2.4% and cooling increased by 4.1%. As a result, total energy consumption increased by 0.5%. When eaves were removed from the base-case, the heating energy consumption was almost the same compared to the base-case, and the cooling was increased by 0.4%. As a result, total energy consumption was the same compared to the base-case. When the trees were removed from the base-case, heating energy consumption decreased by 2% and cooling increased by 3.7%. Total energy use increased by 0.5%. When removing the fences from the base-case, the heating energy consumption decreased by 2%, and the cooling increased by 2.6%. When there was no fence, the total energy consumption increased by 0.3%. Finally, when all shades were removed from the base-case, heating energy consumption decreased by 6.3% and

cooling increased by 11.1%. Eventually, the total energy consumption increased by 1.6%.

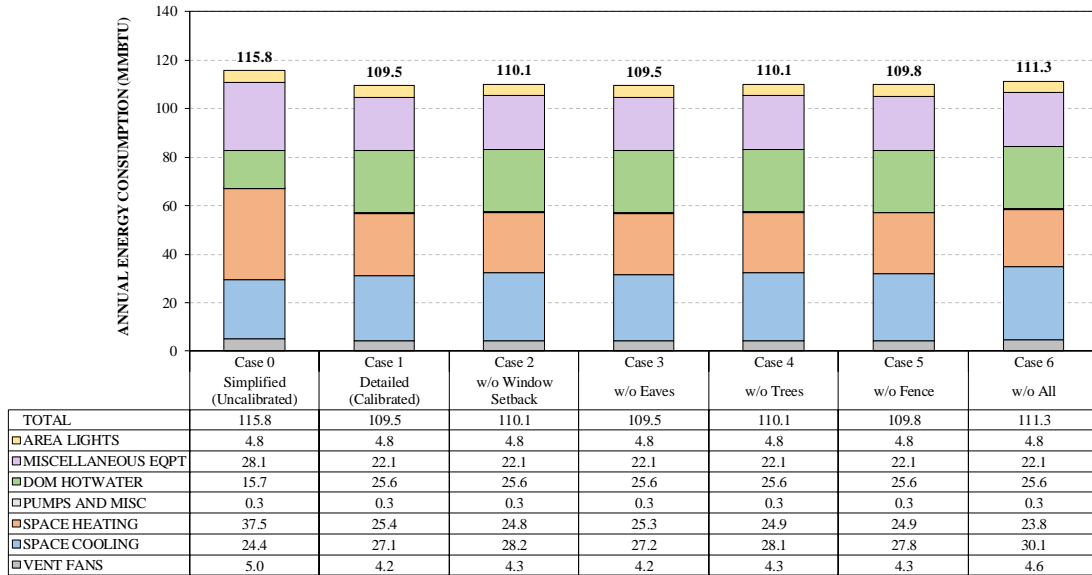


Figure 5.1: Shading Impact Analysis Result (MMBTu)

Table 5.2: Shading Impact Analysis Result (%)

% Difference	Case 0	Case 1	Case 2	Case 3	Case 4	Case 5	Case 6
	Simplified (Uncalibrated)	Detailed (Calibrated)	w/o Window Setback	w/o Eaves	w/o Trees	w/o Fence	w/o All
TOTAL	5.8%	-	0.5%	0.0%	0.5%	0.3%	1.6%
SPACE HEATING	47.6%	-	-2.4%	-0.4%	-2.0%	-2.0%	-6.3%
SPACE COOLING	-10.0%	-	4.1%	0.4%	3.7%	2.6%	11.1%
VENT FANS	19.0%	-	2.4%	0.0%	2.4%	2.4%	9.5%
DOM HOTWATER	-38.7%	-	0.0%	0.0%	0.0%	0.0%	0.0%

5.2. Analysis of the Impact of Unconditioned Space

In this section, the unconditioned space of the case-study house was tested. To accomplish this, a garage and roof type were analyzed.

5.2.1. Garage

Garages are classified as unconditioned spaces because they are not air-conditioned or heated. In building energy simulations, unconditioned space is usually not considered. This is because the garage is not included when defining the building thermal envelope. Figure 5.2 shows an example of a building thermal envelope. However, the presence of a garage can also affect the conditioned zone. The garage blocks direct solar radiation to the building and prevents the direct influence of wind and outdoor temperature. Therefore, it was analyzed whether the garage affects building energy consumption.

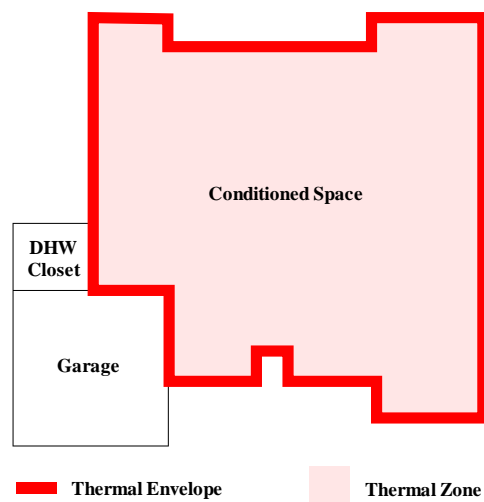


Figure 5.2: Example of Building Thermal Envelope

5.2.2. Roof Type

Roofs are often ignored in simplified building energy modeling. Figure 5.3 shows an example of the roof omission in a simplified building energy modeling. In ASHRAE Standard-140, which is used to evaluate building energy simulations, roof modeling is considered, but geometry differences according to roof types are not considered. Therefore, in this study, the difference according to the shape of the roof was analyzed.

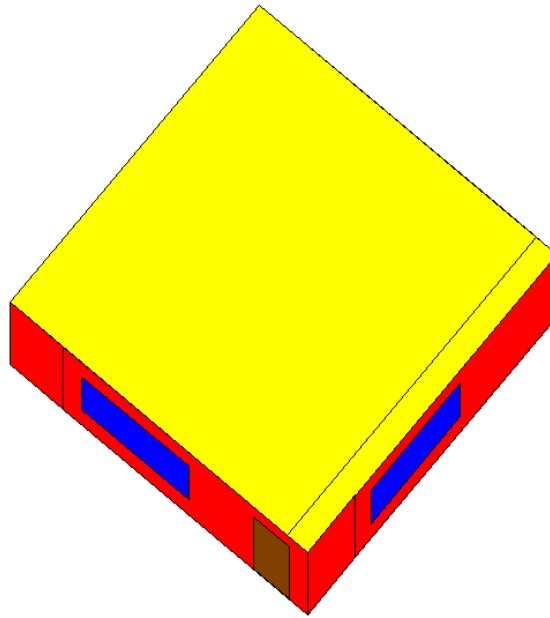


Figure 5.3: Example of the Roof Omission in a Simplified Building Energy Modeling

5.2.3. Results of the Impact of Unconditioned Space

In this chapter, how unconditioned space affects building energy use was analyzed. Case 1 is the detailed calibrated model of a case-study house with a garage and a hip roof. Case 1 is a base-case in this analysis. Case 2 is a house where the garage was

removed from Case 1. Case 3 is a house where the roof type in Case 1 was changed from gable to hip roof. Case 4 is a house where the garage was removed and changed the roof type from Case 1. Table 5.3 and Figure 5.4 show the list of cases of unconditioned space analysis.

Table 5.3: List of Cases for Unconditioned Space Analysis

Case	Characteristic
Case 0	Simplified Model: without a Garage, with a Gable Roof
Case 1 (Base-case)	Detailed Model (Calibrated): with a Garage, with a Hip Roof
Case 2	Case 1 + without a Garage
Case 3	Case 1 + with a Gable Roof
Case 4	Case 1 + without a Garage, with a Gable Roof

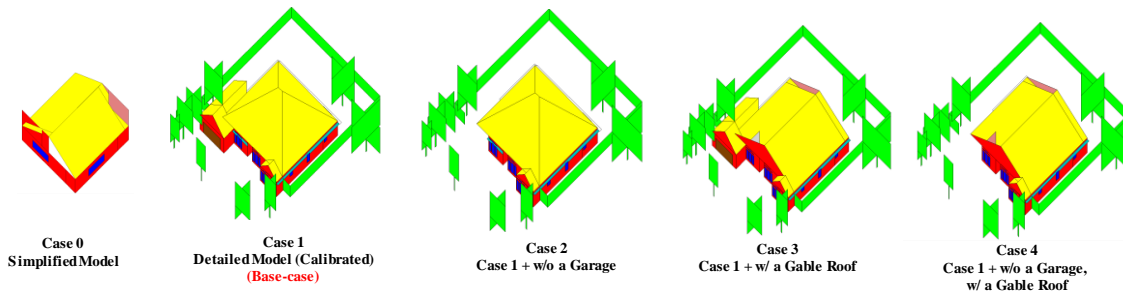


Figure 5.4: Example of Cases for Unconditioned Space Analysis

Figure 5.5 and Table 5.2 show the building energy consumption results according to unconditioned spaces. When the garage was removed from the base-case (Case 1), heating energy consumption increased by 3.5%, and cooling also increased by 2.2%. As a result, total energy consumption increased by 1.4%. When the roof type is changed from a gable roof to a hip roof, the heating energy consumption increased by 0%

compared to the Base-case, and the cooling was increased by 2.6%. As a result, total energy consumption increased by 0.7%. When the garage was removed and the roof type was changed from a gable roof to a hip roof, the heating energy consumption increased by 3.9% compared to the Base-case, and the cooling was increased by 4.1%. As a result, total energy consumption increased by 2.0%.

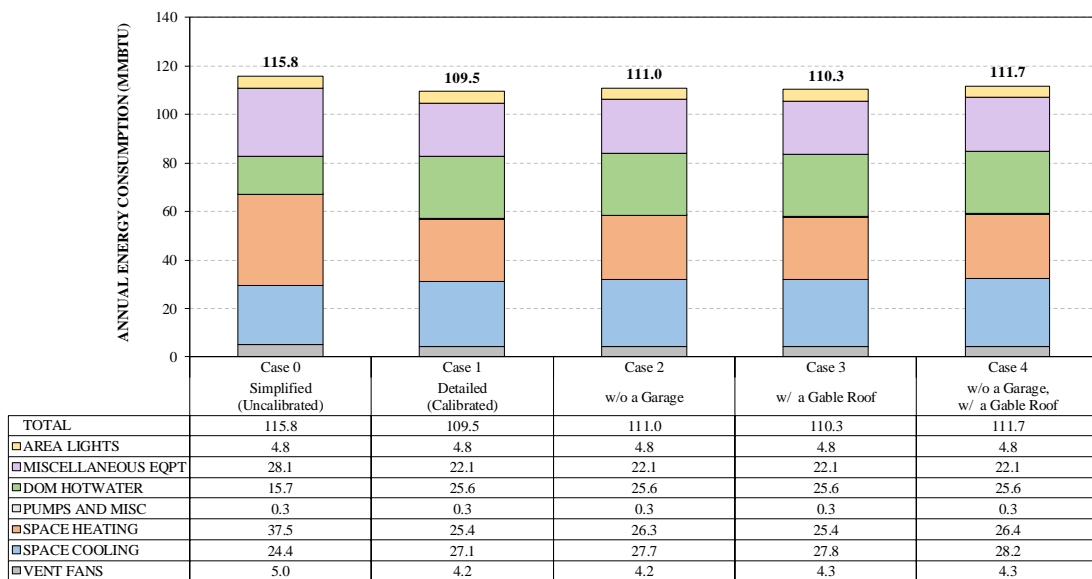


Figure 5.5: Unconditioned Space Analysis Results (MMBtu)

Table 5.4: Unconditioned Space Analysis Results (%)

	Case 0	Case 1	Case 2	Case 3	Case 4
	Simplified	Detailed (Case-Study)	w/o a Garage	w/ a Gable Roof	w/o a Garage, w/ a Gable Roof
TOTAL	5.8%	-	1.4%	0.7%	2.0%
SPACE HEATING	47.6%	-	3.5%	0.0%	3.9%
SPACE COOLING	-10.0%	-	2.2%	2.6%	4.1%
VENT FANS	19.0%	-	0.0%	2.4%	2.4%
DOM HOTWATER	-38.7%	-	0.0%	0.0%	0.0%

5.3. Analysis of the Impact of Domestic Hot Water Heater: Inlet and Outlet Water Temperatures

In this section, the domestic hot water heater of the case-study house was tested. To accomplish this, inlet and outlet water temperatures for domestic water heater were analyzed.

5.3.1. Inlet Water Temperature

Inlet water temperature represents the temperature of the water entering the domestic hot water system. Since it is not easy to accurately predict this temperature, some inlet water temperature calculation models are used for building energy simulation.

Among them, Building America's inlet water temperature model and Kusuda-Achenbach model are widely used in building energy simulation. The mains water temperature model from the 2014 Building America House Simulation Protocols is used in the building energy simulation. This model calculates the daily inlet water temperatures, the temperatures vary significantly depending on the location and time of year. Kusuda-Achenbach's Undisturbed Ground Temperature Model is a model that predicts ground temperature but is used as the inlet water temperature in many whole building energy simulation programs (e.g. DOE 2.1e and EnergyPlus).

In this study, these two inlet water temperature models were compared with the measured inlet water temperature model.

5.3.2. Outlet Water Temperature (Tank Temperature)

Outlet water temperature is the temperature of hot water supplied to the house from the domestic water heater. This temperature is the same as the water tank temperature. Outlet water temperature is a very important input to determine energy usage in a water heater, but in building energy simulation, 120 F is usually used as input.

In this study, how much the 120 F and the measured outlet water temperature affect the building energy consumption.

5.3.3. Results of the Impact of DHW Outlet Water Temperature

In this chapter, how the domestic hot water system affects building energy use was analyzed. Case 1 used a model made from data measured for the DHW outlet water temperature of 135.6F. The 135.6F was the average of the measured outlet water temperature of a case-study house. Case 2 is the case where the DHW outlet water temperature was changed to 120 F in Case 1. Table 5.5 shows the list of cases for this domestic hot water system analysis.

Table 5.5: List of Cases for DHW Outlet Water Temperature Analysis

Case	Characteristic
Case 0	Simplified Model: 120F
Case 1 (Base-case)	Detailed Model (Calibrated): 135.6 F
Case 2	Case 1 + 120 F (2008 Building America)

Figure 5.6 and Table 5.6 show the building energy consumption results according to the domestic hot water system. Case 1 is a base-case, and this base-case was

compared with Case 2. When the outlet water temperature in the base-case is changed to 120 F, domestic hot water system energy consumption decreased by 27.0%. As a result, total energy consumption decreased by 6.3%.

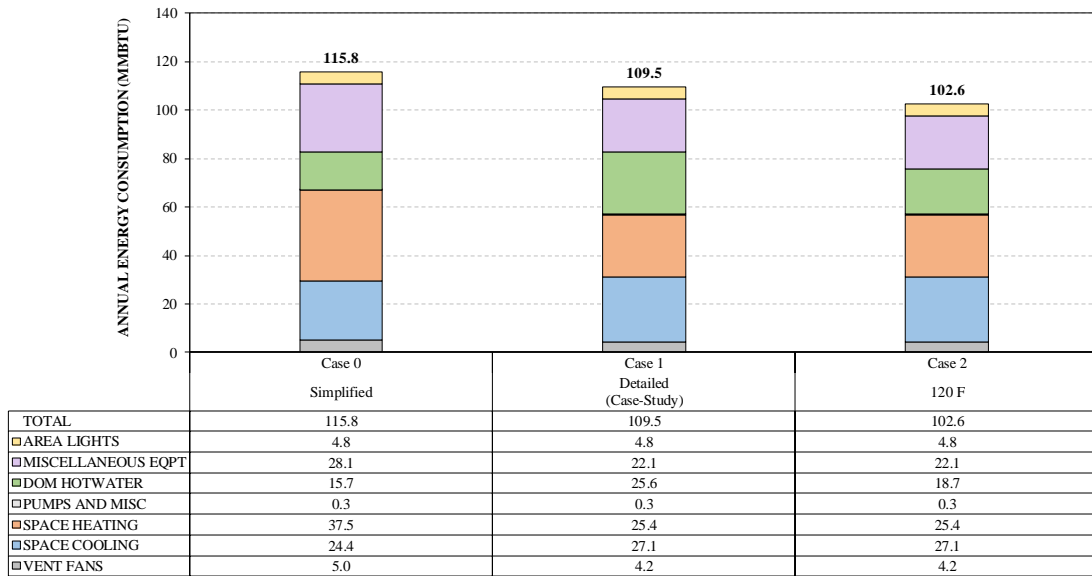


Figure 5.6: DHW Outlet Water Temperature Analysis Results (MMBtu)

Table 5.6: DHW Outlet Water Temperature Analysis Results (%)

	Case 0	Case 1	Case 2
	Simplified	Detailed (Case-Study)	120 F
TOTAL	5.8%	-	-6.3%
SPACE HEATING	47.6%	-	0.0%
SPACE COOLING	-10.0%	-	0.0%
VENT FANS	19.0%	-	0.0%
DOM HOTWATER	-38.7%	-	-27.0%

5.3.1. Results of the Impact of DHW Inlet Water Temperature

In this chapter, how the domestic hot water inlet water temperature affects building energy use was analyzed. Case 1 used a model made from data measured inlet water temperatures of a case-study house. Case 2 is a case using Building America's inlet water temperature model as the inlet water temperature. Case 3 is a case using Kusuda-Achenbach's model as the inlet water temperature. Case 4 is a case using measured inlet water temperatures from the college station pump station. Table 5.5 shows the list of cases for this DHW inlet water temperature analysis.

Table 5.7: List of Cases for DHW Inlet Water Temperature Analysis

Case	Characteristic
Case 0	Simplified Model: Building America Model
Case 1 (Base-case)	Detailed Model (Calibrated): Measured
Case 2	Case 1 + Building America Model
Case 3	Case 1 + DOE2.1e Default (Kusuda-Achenbach)
Case 4	Case 1 + College Station Pump Station

Figure 5.6 and Table 5.6 show the building energy consumption results according to the DHW inlet water temperatures. Case 1 is a base-case, and this base-case was compared with Case 2, Case 3, and Case 4. When the inlet water temperatures in the base-case were changed using the Building America Model, and domestic hot water system energy consumption was increased by 5.5%. As a result, total energy consumption increased by 1.3%. When the inlet water temperatures in the base-case were changed using the Kusuda-Achenbach Model, domestic hot water system energy consumption increased by 18.4%. Total energy use increased by 4.3%. When the inlet

water temperatures in the base-case were changed using the measured data of the college station pump station, domestic hot water system energy consumption decreased by 2.3%. Total energy use decreased by 0.5%.

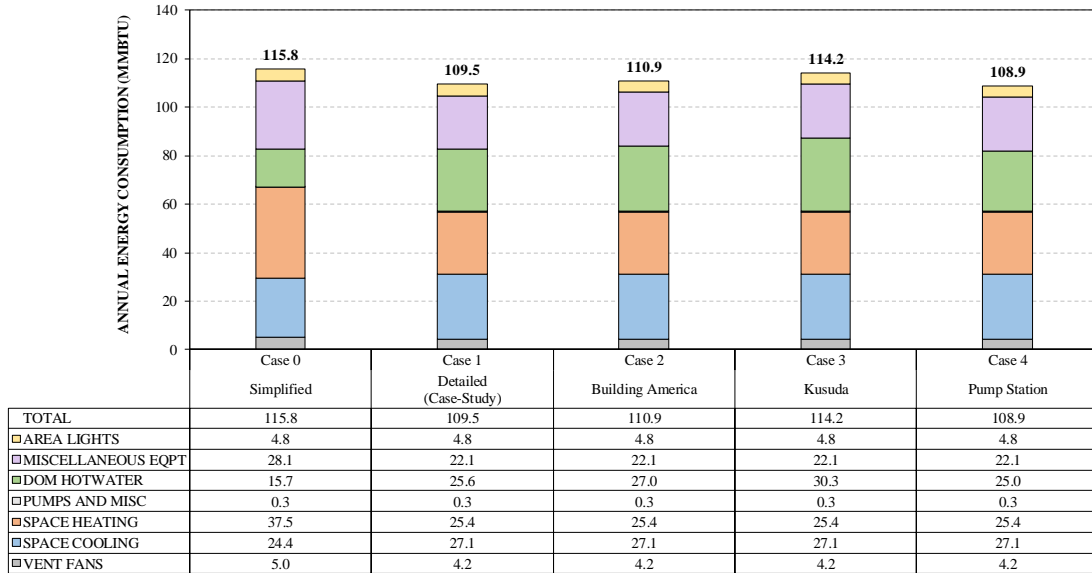


Figure 5.7: DHW Inlet Water Temperature Analysis Results (MMBtu)

Table 5.8: DHW Inlet Water Temperature Analysis Results (%)

	Case 0	Case 1	Case 2	Case 3	Case 4
	Simplified	Detailed (Case-Study)	Building America	Kusuda	Pump Station
TOTAL	5.8%	-	1.3%	4.3%	-0.5%
SPACE HEATING	47.6%	-	0.0%	0.0%	0.0%
SPACE COOLING	-10.0%	-	0.0%	0.0%	0.0%
VENT FANS	19.0%	-	0.0%	0.0%	0.0%
DOM HOTWATER	-38.7%	-	5.5%	18.4%	-2.3%

5.4. Analysis of the Impact of Ground Heat Transfer

In this section, the ground heat transfer of the case-study house was tested. To accomplish this, ground heat transfer methods were analyzed.

5.4.1. Winkelmann's Ground Heat Transfer

Ground heat transfer occurs mainly on the periphery of the building. To calculate this, Winkelmann's ground heat transfer calculation was developed to help to calculate a more accurate ground heat transfer in the DOE-2.1E simulation program. Therefore the case-study house computed the ground heat transfer using this method.

5.4.2. Ground Heat Transfer through the Entire Surface

The underground surface of DOE-2.1E is a wall or floor that comes into contact with the ground. Since DOE-2.1E assumes that the ground heat transfer takes place on the entire floor surface, it is over calculated compared to Winkelmann's method, where heat transfer occurs only at the outer periphery of the floor.

5.4.3. Without Ground Heat Transfer

The ground heat transfer calculation is sometimes ignored in the Simplified simulation model. The ASHRAE STANDARD-140 has test suites for easy simulation, but there is no detailed explanation for ground heat transfer here.

5.4.4. Results of the Impact of Ground Heat Transfer

In this chapter, how the ground heat transfer affects building energy use was analyzed. Case 1 is a model made with Winkelmann’s method and detailed perimeter length. Case 2 is a case using ground heat transfer through the entire surface (e.g. DOE2.1e’s default calculation) instead of Winkelmann’s method in Case 1. Case 3 is a case using without ground heat transfer in Case 1. Table 5.9 and Figure 5.8 shows the list of cases for this ground heat transfer analysis.

Table 5.9: List of Cases for Ground Heat Transfer Analysis

Case	Characteristic
Case 0	Simplified Model: Winkelmann Huang Method
Case 1 (Base-case)	Detailed Model (Calibrated): Winkelmann Huang Method
Case 2	Case 1 + DOE2.1E Default
Case 3	Case 1 + No Heat Transfer

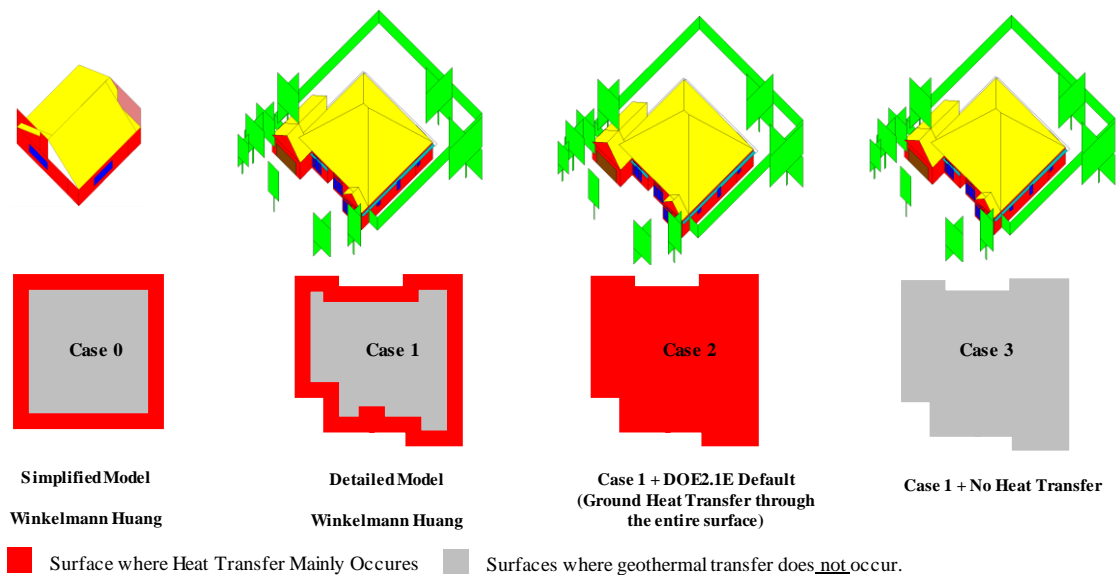


Figure 5.8: Example of Cases for Ground Heat Transfer Analysis

Figure 5.9 and Table 5.10 show the building energy consumption results according to the ground heat transfer. Case 1 was a base-case, and this base-case was compared with Case 2, and Case 3. When the ground heat transfer method was changed from the Winkelmann’s method to the ground heat transfer through the entire surface (e.g. DOE2.1e’s default calculation), the heating energy consumption increased by 34.6% compared to the Base-case, and the cooling energy consumption was decreased by 10.7%. As a result, total energy consumption increased by 5.2%. When the ground heat transfer method was removed from the Base-case, the heating energy consumption decreased by 19.7% compared to the Base-case, and the cooling energy consumption was increased by 9.6%. As a result, total energy consumption decreased by 2.0%.

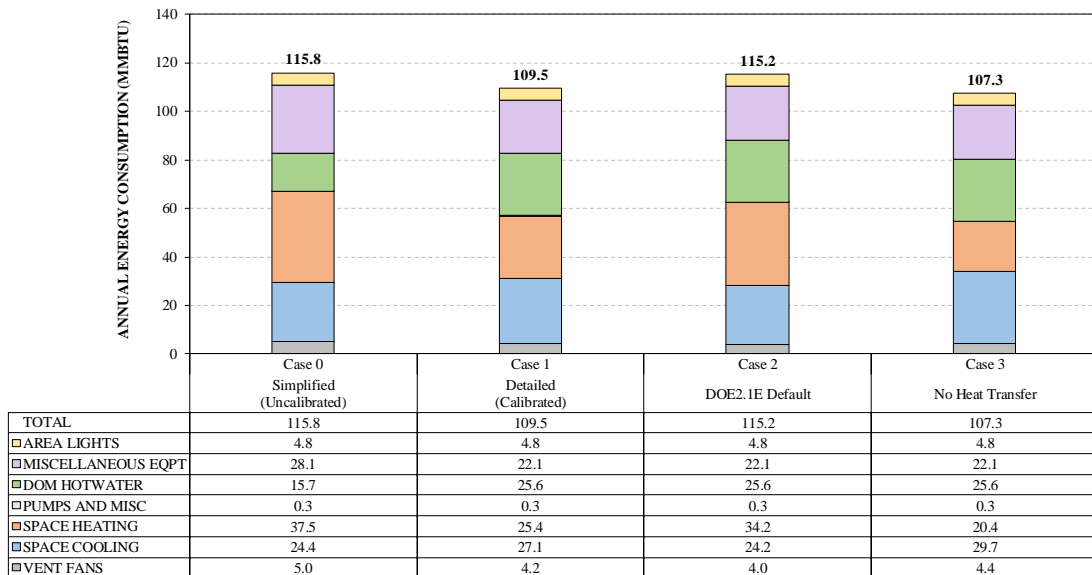


Figure 5.9: Ground Heat Transfer Analysis Results (MMBtu)

Table 5.10: Ground Heat Transfer Analysis Results (%)

	Case 0	Case 1	Case 2	Case 3
	Simplified	Detailed (Case-Study)	DOE2.1E Default	No Heat Transfer
TOTAL	5.8%	-	5.2%	-2.0%
SPACE HEATING	47.6%	-	34.6%	-19.7%
SPACE COOLING	-10.0%	-	-10.7%	9.6%
VENT FANS	19.0%	-	-4.8%	4.8%
DOM HOTWATER	-38.7%	-	0.0%	0.0%

5.5. Comparison of the Detailed Calibrated Model and the Simplified Uncalibrated Model

This section compares the results of the detailed calibrated model and the simplified uncalibrated model to predict the annual source energy savings resulting from changing selected parameters to approach the code compliance of the 2015 IECC. Table 5.11 shows the input specifications used to compare the detailed calibrated model and the simplified uncalibrated model.

Table 5.11: Input Specifications for the Comparison of the Detailed Calibrated Model and the Simplified Uncalibrated Model.

Component		Detailed (Calibrated)	Detailed (Calibrated) with IECC Code Compliance	Simplified (Uncalibrated)	Simplified (Uncalibrated) with IECC Code Compliance
Envelope	Exterior Wall	Geometry	Detailed Geometry	Detailed Geometry	<i>Simplified Geometry</i>
		Wall Color	Dark	Dark	Dark
		Average Wall Height	9 ft	9 ft	9 ft
		Insulation R-Value	R-13	R-13	R-13
	Windows	Stud Spacing	16"	16"	16"
		Grass Area	303.5 ft ²	303.5 ft ²	303.5 ft ²
		U-Value	0.87	0.4	0.87
		SHGC	0.66	0.25	0.66
	Roof/Attic	Setback	3 inch	3 inch	<i>No Setback</i>
		Roof Color	Dark	Dark	Dark
		Roof Type	Hip Roof	Hip Roof	Gable Roof
		Ceiling Type	Ceiling with Attic Above	Ceiling with Attic Above	Ceiling with Attic Above
	Slab Floor	Insulation R-Value	R-29.6 (8" insulation depth)	R-30	R-29.6 (8" insulation depth)
		Eaves	1.5 ft	1.5 ft	<i>No Eaves</i>
Gross Area		2,391 ft ²	2,391 ft ²	2,391 ft ²	
Slab Perimeter R-Value		R-0	R-0	R-0	
Systems	Heating	Fuel	Natural Gas	Natural Gas	Natural Gas
		System Type	Furnace	Furnace	Furnace
		Efficiency (AFUE or HSPF)	66%	80%	66%
		Manufacturer	Lennox	Lennox	Lennox
		System Location	Attic	Attic	Attic
		Heating Set Temperature	67.7 F	67.7 F	72 F
	Cooling	System Type	Air Conditioner, Air Cooled	Air Conditioner, Air Cooled	Air Conditioner, Air Cooled
		Efficiency (SEER)	8	14	10
		Manufacturer	Lennox	Lennox	Lennox
		System Location	Unconditioned Area	Unconditioned Area	Unconditioned Area
	Domestic Water Heater	Cooling Set Temperature	73.9 F	73.9 F	75 F
		Fuel	Gas	Gas	Gas
		Capacity	50 Gallon	50 Gallon	50 Gallon
		Energy Factor	0.594	0.594	0.594
		Burner Capacity	38,000 Btu/h	38,000 Btu/h	38,000 Btu/h
		Type	Storage	Storage	Storage
		Tank Location	Unconditioned Area	Unconditioned Area	Unconditioned Area
		Manufacturer	Rheem	Rheem	Rheem
		Water Use	85 gal/day	85 gal/day	50 gal/day
		Inlet Water Temperature	Measured	Measured	Building America Model
Etc.	Tank Temperature	135.3 F	135.3 F	120 F	
	Light and Equipment	0.9 kw	0.9 kw	1.1 kw	
Etc.	Tree	Nine Trees	Nine Trees	No Tree	
	Fence	Yes	Yes	No	
	Garage	Yes	Yes	No	
	Ground Heat Transfer Method	Winkelmann and Huang	Winkelmann and Huang	Winkelmann and Huang	
	Weather	2019, College Station	2019, College Station	2019, College Station	
	Unconditioned Zone	Calibrated	Calibrated	Uncalibrated	

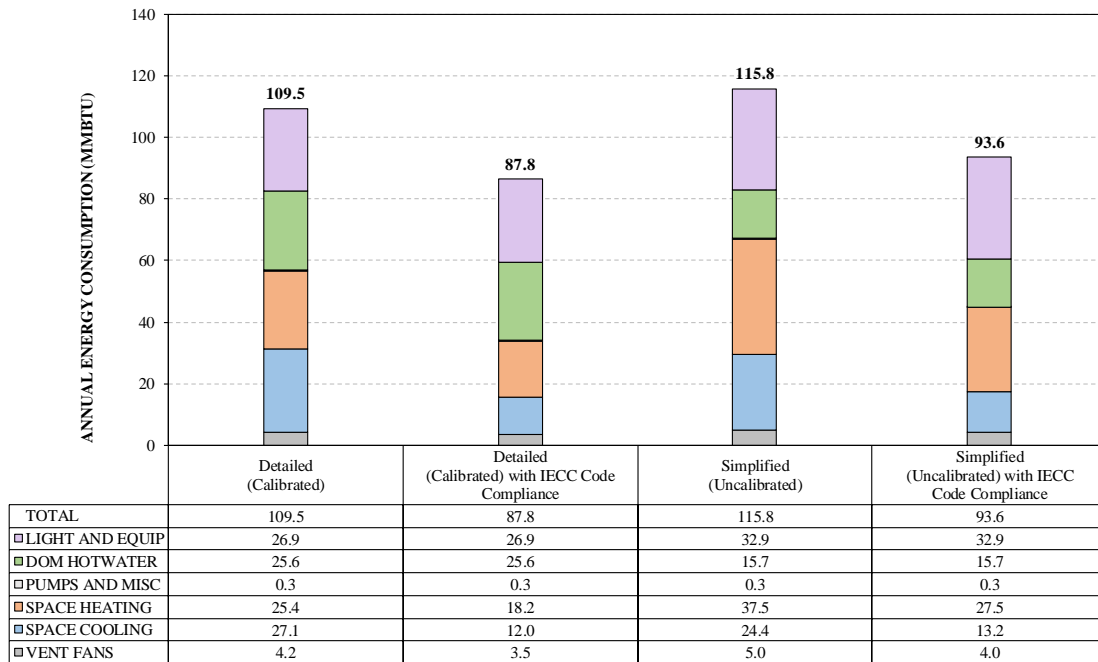


Figure 5.10: Site Energy Usage for the Comparison of the Detailed Calibrated Model and the Simplified Uncalibrated Model (MMBTu)

Table 5.12: Source Energy Usage for the Comparison of the Detailed Calibrated Model and the Simplified Uncalibrated Model (MMBTu)

	Detailed (Calibrated)	Detailed (Calibrated) with IECC Code Compliance	Simplified (Uncalibrated)	Simplified (Uncalibrated) with IECC Code Compliance
TOTAL	241.0	183.1	256.3	206.8
LIGHT AND EQUIP	85.0	85.0	104.0	104.0
SPACE HEATING	27.9	20.0	41.3	30.3
SPACE COOLING	85.6	37.9	77.1	41.7
PUMPS AND MISC	0.9	0.9	0.9	0.9
VENT FANS	13.3	11.1	15.8	12.6
DOM HOTWATER	28.2	28.2	17.3	17.3

Table 5.13: Source Energy Percentage Difference for the Comparison of the Detailed Calibrated Model and the Simplified Uncalibrated Model (%)

	Detailed (Calibrated)	Detailed (Calibrated) with IECC Code Compliance	Simplified (Uncalibrated)	Simplified (Uncalibrated) with IECC Code Compliance
TOTAL	-	-24.0%	-	-19.3%
LIGHT AND EQUIP	-	0.0%	-	0.0%
SPACE HEATING	-	-28.3%	-	-26.7%
SPACE COOLING	-	-55.7%	-	-45.9%
PUMPS AND MISC	-	0.0%	-	0.0%
VENT FANS	-	-16.7%	-	-20.0%
DOM HOTWATER	-	0.0%	-	0.0%

Figure 5.10 shows the simulated site energy usage results for the detailed model and for the simplified model of the case-study house. In the IECC, the annual energy cost or source energy usage is used when calculating the building energy code compliance. To calculate the source energy usage, according to the 2015 IECC, electricity energy use must be multiplied by 3.16, and non-electric fuel use (e.g., natural gas) must be multiplied by 1.1 (ICC, 2015). Using this calculation, Table 5.12 and Table 5.13 show the source energy usage and percentage difference of the source energy usage of the detailed model and simplified model, respectively. In this analysis, when selected parameters for the case-study house were replaced with IECC code-compliant parameters using the detailed calibrated model the total source energy usage was reduced by 24% compared to the detailed calibrated model of the case-study house without the parameters. This includes a decrease of 28.3% in the heating energy use, a decrease of 55.7% in the cooling energy use, and a decrease of 16% in the fan energy use. In contrast, when a simplified model was used on the same case-study house the total source energy use decreased by 19.3%, which included a 26.7% decrease in heating energy use, a 45.9% decrease in the cooling energy use, and a 20% decrease in the vent fan energy use.

5.6. Selected Calibrations for Improving the Accuracy of a Simplified Model

In this section several factors (e.g., zone temperatures, the energy usage of lighting and equipment, SEER, and hot water use, shading, unconditioned space, DHW, ground heat transfer) found in the case-study house from Chapters 4.1 to 5.4 were

specifically, found to impact the energy consumption of the case-study house simulation model. Unfortunately, although many of these parameters had an impact on the simulated energy use of the case-study house, requiring a builder or home owner to measure the factors is probably not reasonable for the average homeowner. Therefore a smaller subset of these parameters was chosen that could be easily obtained to determine how a selected calibration might improve the accuracy of the simplified simulation. The heating setpoint temperature, cooling setpoint temperature, and DHW outlet water temperature of the case-study house were applied to the simplified model to make the simplified model be more representative.

In this analysis, the uncalibrated heating setpoint of 72F was reduced to 67.7F, which was the measured average setpoint temperature. In addition, the uncalibrated cooling setpoint of 75F was decreased to 73.9F, and the DHW outlet temperature was changed from 120F to 135.3F. Table 5.14 shows the simplified model with the selected calibrations.

Table 5.14: Input Specifications for the Comparison of the Simplified Uncalibrated Model and the Simplified Selected Uncalibrated Model.

Component		Simplified (Uncalibrated)	Simplified (Selected Calibrated)	Simplified (Uncalibrated) with IECC Code Compliance	Simplified (Selected Calibrated) with IECC Code Compliance
Envelope	Exterior Wall	Geometry	Simplified Geometry	Simplified Geometry	Simplified Geometry
		Wall Color	Dark	Dark	Dark
		Average Wall Height	9 ft	9 ft	9 ft
		Insulation R-Value	R-13	R-13	R-13
		Stud Spacing	16"	16"	16"
	Windows	Gross Area	303.5 ft ²	303.5 ft ²	303.5 ft ²
		U-Value	0.87	0.87	0.4
		SHGC	0.66	0.66	0.25
		Setback	No Setback	No Setback	No Setback
	Roof/Attic	Roof Color	Dark	Dark	Dark
		Roof Type	Gable Roof	Gable Roof	Gable Roof
		Ceiling Type	Ceiling with Attic Above	Ceiling with Attic Above	Ceiling with Attic Above
		Insulation R-Value	R-29.6 (8" insulation depth)	R-29.6 (8" insulation depth)	R-30
	Slab Floor	Eaves	No Eaves	No Eaves	No Eaves
		Gross Area	2,391 ft ²	2,391 ft ²	2,391 ft ²
		Slab Perimeter R-Value	R-0	R-0	R-0
Systems	Heating	Fuel	Natural Gas	Natural Gas	Natural Gas
		System Type	Furnace	Furnace	Furnace
		Efficiency (AFUE or HSPF)	66%	66%	80%
		Manufacturer	Lennox	Lennox	Lennox
		System Location	Attic	Attic	Attic
	Heating Set Temperature	72 F	67.7 F	72F	
	Cooling	System Type	Air Conditioner, Air Cooled	Air Conditioner, Air Cooled	Air Conditioner, Air Cooled
		Efficiency (SEER)	10	10	14
		Manufacturer	Lennox	Lennox	Lennox
		System Location	Unconditioned Area	Unconditioned Area	Unconditioned Area
	Domestic Water Heater	Cooling Set Temperature	75 F	73.9 F	75F
		Fuel	Gas	Gas	Gas
		Capacity	50 Gallon	50 Gallon	50 Gallon
		Energy Factor	0.594	0.594	0.594
		Burner Capacity	38,000 Btu/h	38,000 Btu/h	38,000 Btu/h
		Type	Storage	Storage	Storage
		Tank Location	Unconditioned Area	Unconditioned Area	Unconditioned Area
		Manufacturer	Rheem	Rheem	Rheem
	Etc.	Water Use	50 gal/day	50 gal/day	50 gal/day
		Inlet Water Temperature	Building America Model	Building America Model	Building America Model
Etc.	Tank Temperature	120 F	135.3 F	120 F	
	Light and Equipment	1.1 kw	1.1 kw	1.1 kw	
	Tree	No Tree	No Tree	No Tree	
	Fence	No	No	No	
	Garage	No	No	No	
	Ground Heat Transfer Method	Winkelmann and Huang	Winkelmann and Huang	Winkelmann and Huang	
	Weather	2019, College Station	2019, College Station	2019, College Station	
Unconditioned Zone	Uncalibrated	Uncalibrated	Uncalibrated		

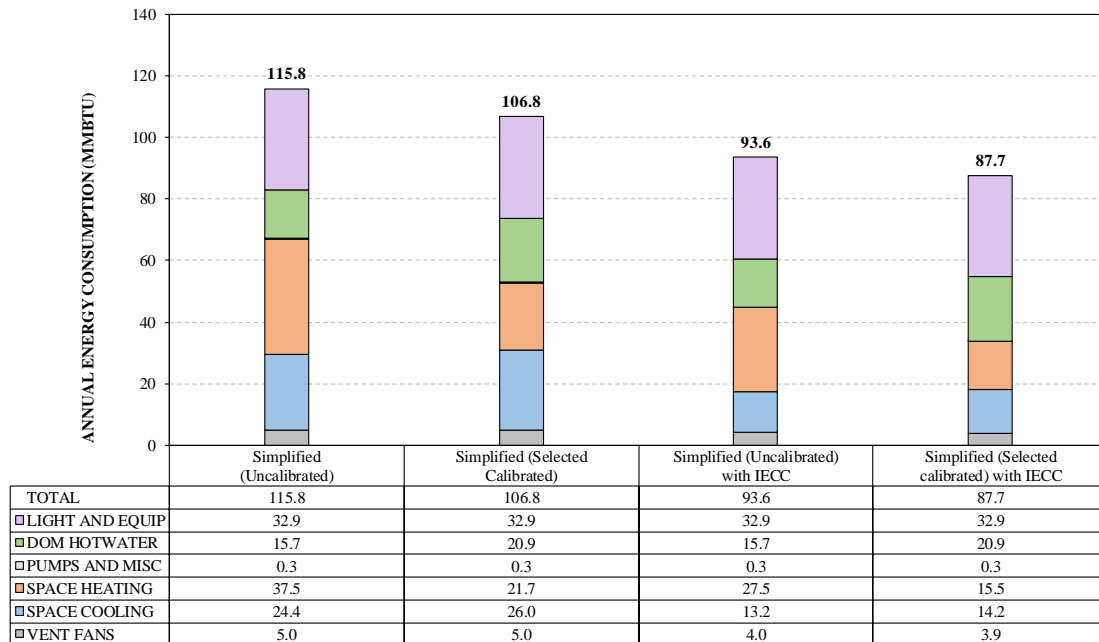


Figure 5.11: Site Energy Usage for the Comparison of the Simplified Uncalibrated Model and the Simplified Selected Calibrated Model (MMBTu)

Table 5.15: Source Energy Usage for the Comparison of the Simplified Uncalibrated Model and the Simplified Selected Calibrated Model (MMBTu)

	Simplified (Uncalibrated)	Simplified (Selected Calibrated)	Simplified (Uncalibrated) with IECC	Simplified (Selected calibrated) with IECC
TOTAL	256.3	249.7	206.8	202.1
LIGHT AND EQUIP	104.0	104.0	104.0	104.0
SPACE HEATING	41.3	23.9	30.3	17.1
SPACE COOLING	77.1	82.2	41.7	44.9
PUMPS AND MISC	0.9	0.9	0.9	0.9
VENT FANS	15.8	15.8	12.6	12.3
DOM HOTWATER	17.3	23.0	17.3	23.0

Table 5.16: Source Energy Percentage Difference for the Comparison of the Simplified Uncalibrated Model and the Simplified Selected Calibrated Model (%)

	Simplified (Uncalibrated)	Simplified (Selected Calibrated)	Simplified (Uncalibrated) with IECC	Simplified (Selected calibrated) with IECC
TOTAL	-	-2.6%	-	-2.2%
LIGHT AND EQUIP	-	0.0%	-	0.0%
SPACE HEATING	-	-42.1%	-	-43.6%
SPACE COOLING	-	6.6%	-	7.6%
PUMPS AND MISC	-	0.0%	-	0.0%
VENT FANS	-	0.0%	-	-2.5%
DOM HOTWATER	-	33.1%	-	33.1%

Figure 5.11 shows the site energy usage results of the uncalibrated, simplified model, the simplified model with selected calibration, the simplified model with parameters changed to match the IECC 2015; and the simplified model with selected parameters that included parameters changed to meet the IECC 2015. In this analysis, the source energy use was used in the comparison using the 3.16 multiplier for electricity and a 1.1 multiplier for the natural gas use. Table 5.15 and Table 5.16 show the source energy usage comparison and percentage difference of the source energy usage, respectively. The analysis showed the model with selected calibration reduced the total source energy usage by 2.6% compared to the simplified uncalibrated model. This includes a heating energy usage decreased by 42.1%, a cooling energy usage increased by 6.6%, and a DHW energy usage increased by 33.1%. The IECC code-compliant house model created by using the simplified, selected calibrated model reduced the total source energy usage by 2.2% compared to the IECC code-compliant house model created by using the simplified uncalibrated model, which included a heating energy usage decrease of 43.6%, a cooling energy usage increase of 7.6%, and a DHW energy usage increase of 33.1%.

6. RESULTS OF THE IECC-COMPLIANT HOUSE SIMULATION MODEL

This chapter presents the results of the IECC residential model simulation tests for fenestration, shading, ground heat transfer, and attic, and the duct model.

6.1. Analysis of the Impact of Fenestration

6.1.1. Window Glazing

Code-compliant building energy simulation programs usually take a simplified approach to window modeling to maintain ease-of-use. For example, the conduction and solar heat gains from windows are often calculated using constant heat conduction and shading coefficients. However, a more accurate analysis is needed to accurately assess the effects of today's Low-E windows.

Table A.1 describes the three window input methods of DOE-2.1E, which include: the shading coefficient method (SC) (Winkelmann et al., 1983), the glass type method, and the Window Library Method (WL) (Winkelmann et al., 1983). This study compared the results of the use of the shading coefficient (SC) method and the window library (WL) method. DOE-2.1E has a large number of glazing choices in the window library. Each glazing type provides information on the transmittance of the solar heat gain according to the angle of incidence of solar radiation and thermal conductance of glazing, for the prevailing temperature and wind speed. The window library produces different results than simply entering fixed glazing conduction and shading coefficient

values. In this study, results using the shading coefficient method and the window library method were compared.

Three types of glass were selected to test the impact of window glazing on building energy use. Table 6.1 shows the three glass types. The first glass was single-pane clear glass. Its U-value is 1.11 Btu/hr-ft²-F and SHGC is 0.86. The second glazing was double-pane clear glass. Its U-value is 0.57 Btu/hr-ft²-F and SHGC is 0.76. The third glazing was double-pane Low-E glass. Its U-value is 0.42 Btu/hr-ft²-F and SHGC is 0.31.

Table 6.1: Properties of the Selected Glazing (source: DOE-2 BDL Summary, Version 2.1E, P.126)

Type of Glazing	Properties					
	U-Value	SC	SHGC	% Transmittance	% Absorptance	% Reflectance
Single Pane Clear (1000)	1.11	1	0.86	86%	6%	8%
Double Pane Clear (2000)	0.57	0.88	0.76	70%	17%	13%
Double Pane Low-E (2666)	0.42	0.35	0.31	21%	65%	14%

In this study, the difference between the SC method and the WL method was analyzed for each glass type. The N,E,S,W glazing were analyzed, respectively, and solar heat gains were simulated at peak heating load (Jan 7th) and peak cooling load (Aug 3rd) conditions.

Figure 6.1 through Figure 6.4 shows the solar heat gain differences for the three glazing types according to SC and WL methods on January 7th. Table 6.2 shows the single-pane glazing summary of the solar heat gain differences between the simulation results of SC and WL methods for January 7th. Table 6.3 shows the double-pane clear

glazing summary of the solar heat gain differences between the simulation results of SC and WL methods for January 7th. Table 6.4 shows the double-pane Low-E glazing summary of the solar heat gain differences between the simulation results of SC and MLW methods for January 7th.

The use of single-pane clear glass at peak heating load makes a difference in solar heat gain when using the SC method were using the WL method. At the peak heating load, when using the WL method with a single-pane facing south, the solar heat gain was reduced from 2.69% to 3.87% compared to when using the SC method. For the glass facing north, the solar heat gain was reduced from 4.02% to 4.41% compared to when using the SC method. For the glass facing east, the solar heat gain was reduced from 2.31% to 3.93% compared to when using the SC method. For the glass facing west, the solar heat gain was reduced from 2.78% to 4.53% compared to when using the SC method.

The use of double-pane clear glass at peak heating load makes the difference in solar heat gain when using the SC method and when using the WL method. At peak heating load, when using the WL method with the double-pane clear glass facing south, the solar heat gain was reduced from 1.95% to 10.24% compared to when using the SC method. For the glass facing north, the solar heat gain was reduced from 6.74% to 7.20% compared to when using the SC method. For the glass facing east, the solar heat gain was reduced from 0.91% to 15.8% compared to when using the SC method. For the glass facing west, the solar heat gain was reduced from 1.99% to 16.59% compared to when using the SC method.

The use of double-pane Low-E glass at peak heating load makes the difference in solar heat gain when using the SC method and when using the WL method. At peak heating load, when using the WL method with the double-pane Low-E glass facing south, the solar heat gain was reduced from -4.33% to 3% compared to when using the SC method. For the glass facing north, the solar heat gain was reduced from 2.26% to 9.30% compared to when using the SC method. For the glass facing east, the solar heat gain was reduced from -5.88% to 6.2% compared to when using the SC method. For the glass facing west, the solar heat gain was reduced from -1.58% to 10.32% compared to when using the SC method.

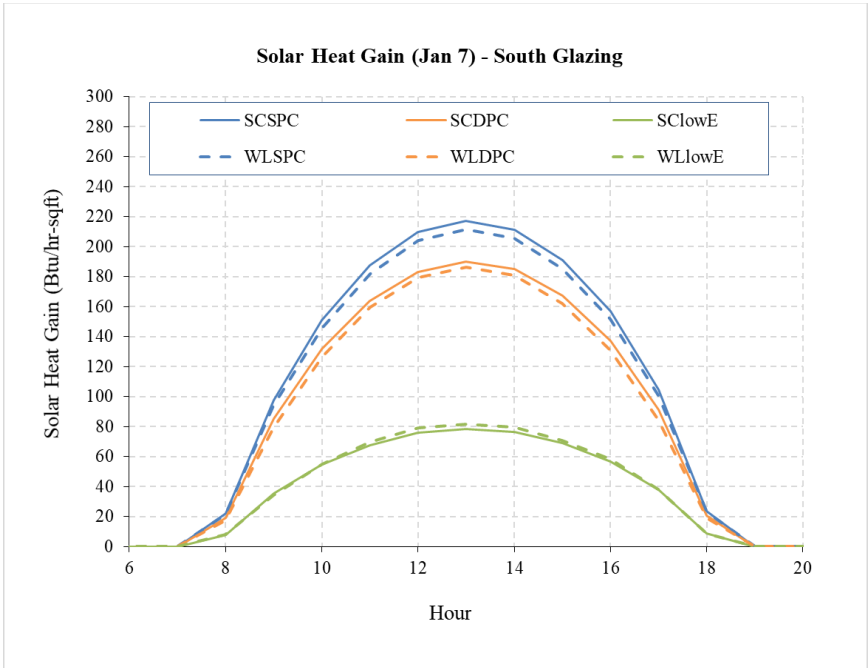


Figure 6.1: Solar heat gains for January 7 (south facing)

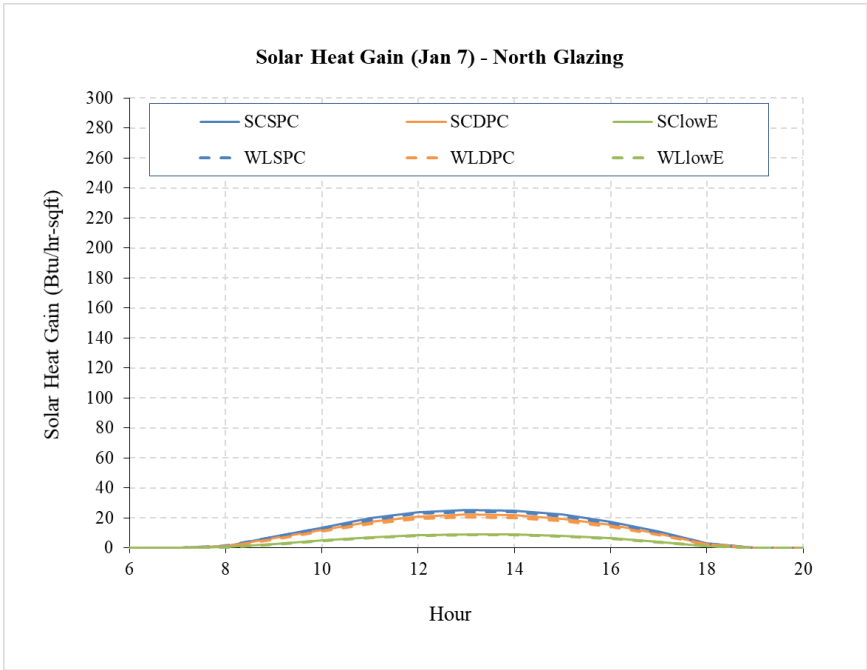


Figure 6.2: Solar heat gains for January 7 (north facing)

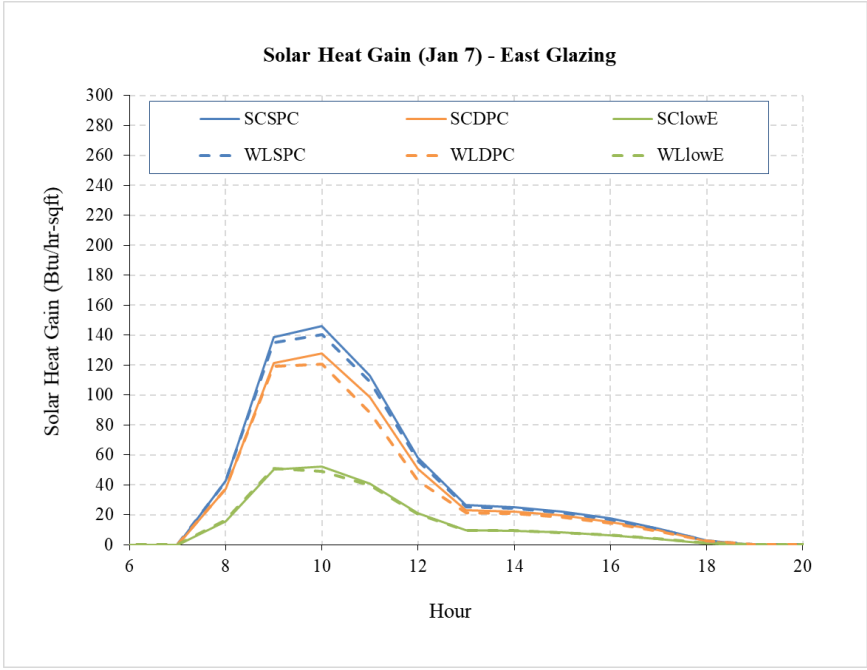


Figure 6.3: Solar heat gains for January 7 (east facing)

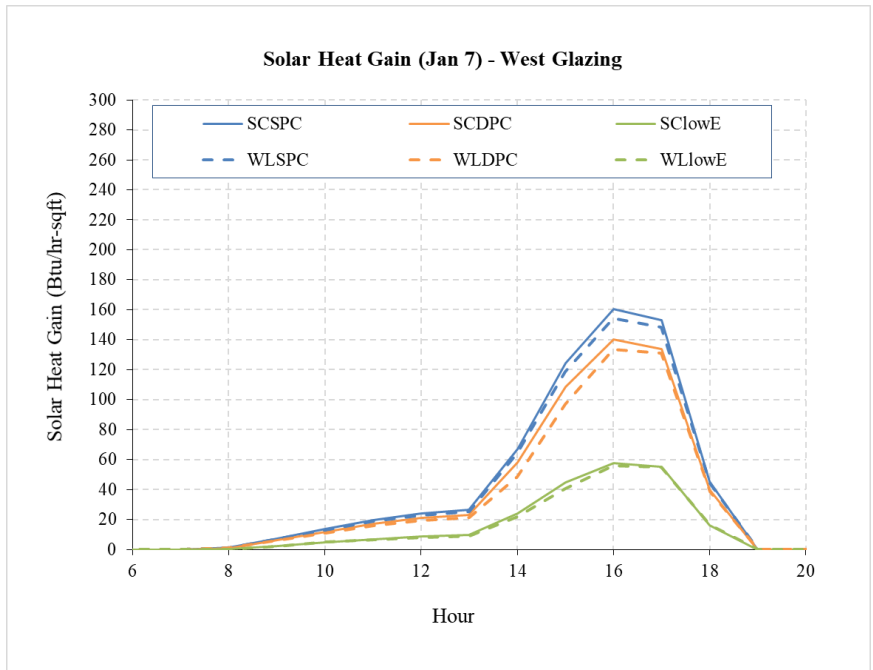


Figure 6.4: Solar heat gains for January 7 (west facing)

Figure 6.5 through Figure 6.8 shows the solar heat gain differences for the three glazing types according to SC and WL methods on August 3rd. Table 6.5 shows the single-pane glazing summary of the solar heat gain differences between the simulation results of SC and WL methods for August 3rd. Table 6.6 shows the double-pane clear glazing summary of the solar heat gain differences between the simulation results of SC and WL methods for August 3rd. Table 6.7 shows the double-pane Low-E glazing summary of the solar heat gain differences between the simulation results of SC and WL methods for August 3rd.

Table 6.2: Solar heat gain difference between the shading coefficient and the window library methods for January 7 (single clear window)

Hours	SC_SPC				WL_SPC				% Difference((WL_SPC-SC_SPC)/SC_SPC)			
	South	North	East	West	South	North	East	West	South	North	East	West
1	0.00	0.00	0.00	0.00	0.00	0.00	0.00	0.00	-	-	-	-
2	0.00	0.00	0.00	0.00	0.00	0.00	0.00	0.00	-	-	-	-
3	0.00	0.00	0.00	0.00	0.00	0.00	0.00	0.00	-	-	-	-
4	0.00	0.00	0.00	0.00	0.00	0.00	0.00	0.00	-	-	-	-
5	0.00	0.00	0.00	0.00	0.00	0.00	0.00	0.00	-	-	-	-
6	0.00	0.00	0.00	0.00	0.00	0.00	0.00	0.00	-	-	-	-
7	0.00	0.00	0.00	0.00	0.00	0.00	0.00	0.00	-	-	-	-
8	21.98	1.20	42.90	1.20	21.13	1.15	41.91	1.15	-3.87%	-4.19%	-2.31%	-4.19%
9	97.73	7.29	138.68	7.29	93.92	6.97	134.96	6.97	-3.90%	-4.41%	-2.68%	-4.39%
10	150.91	13.57	145.92	13.68	145.81	12.99	140.19	13.16	-3.38%	-4.29%	-3.93%	-3.80%
11	187.61	19.63	113.03	19.63	182.03	18.79	108.55	18.79	-2.97%	-4.24%	-3.96%	-4.24%
12	209.72	23.79	58.06	24.01	203.98	22.79	56.15	23.00	-2.74%	-4.19%	-3.30%	-4.19%
13	217.25	25.26	26.29	26.56	211.41	24.20	25.31	25.47	-2.69%	-4.20%	-3.75%	-4.11%
14	211.45	24.92	25.26	66.96	205.57	23.87	24.31	64.27	-2.78%	-4.21%	-3.75%	-4.03%
15	191.27	22.16	22.31	124.47	185.40	21.21	21.47	118.84	-3.07%	-4.27%	-3.80%	-4.53%
16	157.10	17.50	17.60	160.36	151.78	16.77	16.94	154.44	-3.39%	-4.14%	-3.71%	-3.70%
17	104.63	10.85	10.91	153.05	100.70	10.40	10.51	148.60	-3.75%	-4.13%	-3.70%	-2.91%
18	23.81	2.89	2.90	45.42	22.91	2.77	2.80	44.16	-3.77%	-4.02%	-3.63%	-2.78%
19	0.00	0.00	0.00	0.00	0.00	0.00	0.00	0.00	-	-	-	-
20	0.00	0.00	0.00	0.00	0.00	0.00	0.00	0.00	-	-	-	-
21	0.00	0.00	0.00	0.00	0.00	0.00	0.00	0.00	-	-	-	-
22	0.00	0.00	0.00	0.00	0.00	0.00	0.00	0.00	-	-	-	-
23	0.00	0.00	0.00	0.00	0.00	0.00	0.00	0.00	-	-	-	-
24	0.00	0.00	0.00	0.00	0.00	0.00	0.00	0.00	-	-	-	-
SUM	1573.45792	169.052117	603.867135	642.64133	1524.6373	161.923548	583.092938	618.85044	-3.10%	-4.22%	-3.44%	-3.70%

Table 6.3: Solar heat gain difference between the shading coefficient and the window library methods for January 7 (double clear window)

Hours	SC_DPC				WL_DPC				% Difference((WL_DPC-SC_DPC)/SC_DPC)			
	South	North	East	West	South	North	East	West	South	North	East	West
1	0.00	0.00	0.00	0.00	0.00	0.00	0.00	0.00	-	-	-	-
2	0.00	0.00	0.00	0.00	0.00	0.00	0.00	0.00	-	-	-	-
3	0.00	0.00	0.00	0.00	0.00	0.00	0.00	0.00	-	-	-	-
4	0.00	0.00	0.00	0.00	0.00	0.00	0.00	0.00	-	-	-	-
5	0.00	0.00	0.00	0.00	0.00	0.00	0.00	0.00	-	-	-	-
6	0.00	0.00	0.00	0.00	0.00	0.00	0.00	0.00	-	-	-	-
7	0.00	0.00	0.00	0.00	0.00	0.00	0.00	0.00	-	-	-	-
8	19.20	1.05	37.55	1.05	17.23	0.97	37.21	0.97	-10.24%	-6.94%	-0.91%	-6.93%
9	85.41	6.38	121.32	6.38	79.28	5.91	119.25	5.91	-7.19%	-7.40%	-1.71%	-7.40%
10	131.93	11.87	127.58	11.96	126.35	11.02	120.75	11.19	-4.23%	-7.20%	-5.35%	-6.47%
11	164.03	17.16	98.68	17.16	159.60	15.94	87.83	15.94	-2.70%	-7.12%	-11.00%	-7.13%
12	183.37	20.80	50.59	20.99	179.59	19.33	42.56	19.51	-2.06%	-7.05%	-15.88%	-7.05%
13	189.96	22.09	22.98	23.21	186.26	20.52	21.51	21.55	-1.95%	-7.07%	-6.39%	-7.18%
14	184.87	21.78	22.08	58.39	180.83	20.24	20.67	48.70	-2.19%	-7.08%	-6.40%	-16.59%
15	167.20	19.37	19.51	108.73	162.17	17.98	18.24	96.96	-3.01%	-7.20%	-6.49%	-10.82%
16	137.29	15.30	15.38	140.18	131.12	14.23	14.41	133.63	-4.50%	-6.97%	-6.32%	-4.67%
17	91.39	9.48	9.54	133.86	84.75	8.82	8.94	130.99	-7.26%	-6.94%	-6.30%	-2.14%
18	20.79	2.52	2.54	39.73	18.76	2.35	2.38	38.94	-9.75%	-6.74%	-6.13%	-1.99%
19	0.00	0.00	0.00	0.00	0.00	0.00	0.00	0.00	-	-	-	-
20	0.00	0.00	0.00	0.00	0.00	0.00	0.00	0.00	-	-	-	-
21	0.00	0.00	0.00	0.00	0.00	0.00	0.00	0.00	-	-	-	-
22	0.00	0.00	0.00	0.00	0.00	0.00	0.00	0.00	-	-	-	-
23	0.00	0.00	0.00	0.00	0.00	0.00	0.00	0.00	-	-	-	-
24	0.00	0.00	0.00	0.00	0.00	0.00	0.00	0.00	-	-	-	-
SUM	1375.44344	147.79293	527.742086	561.643972	1325.94015	137.315555	493.738721	524.297072	-3.60%	-7.09%	-6.44%	-6.65%

Table 6.4: Solar heat gain difference between the shading coefficient and the window library methods for January 7 (double low-E window)

Hours	SC_lowE				WL_lowE				% Difference((WL_lowE-SC_lowE)/SC_lowE)			
	South	North	East	West	South	North	East	West	South	North	East	West
1	0.00	0.00	0.00	0.00	0.00	0.00	0.00	0.00	-	-	-	-
2	0.00	0.00	0.00	0.00	0.00	0.00	0.00	0.00	-	-	-	-
3	0.00	0.00	0.00	0.00	0.00	0.00	0.00	0.00	-	-	-	-
4	0.00	0.00	0.00	0.00	0.00	0.00	0.00	0.00	-	-	-	-
5	0.00	0.00	0.00	0.00	0.00	0.00	0.00	0.00	-	-	-	-
6	0.00	0.00	0.00	0.00	0.00	0.00	0.00	0.00	-	-	-	-
7	0.00	0.00	0.00	0.00	0.00	0.00	0.00	0.00	-	-	-	-
8	8.00	0.43	15.60	0.43	7.89	0.41	16.52	0.41	-1.35%	-4.86%	5.88%	-4.86%
9	35.33	2.62	50.10	2.62	34.27	2.38	50.91	2.38	-3.00%	-9.30%	1.60%	-9.30%
10	54.57	4.90	52.44	4.97	55.05	4.56	49.19	4.97	0.89%	-6.84%	-6.20%	-0.05%
11	67.79	7.09	40.94	7.09	69.74	6.67	39.86	6.67	2.87%	-5.91%	-2.65%	-5.91%
12	75.78	8.60	21.22	8.68	78.98	8.18	20.54	8.26	4.22%	-4.90%	-3.25%	-4.90%
13	78.45	9.13	9.54	9.64	81.85	8.68	9.66	9.17	4.33%	-4.95%	1.27%	-4.91%
14	76.34	9.01	9.18	24.35	79.42	8.56	9.29	21.83	4.03%	-4.99%	1.23%	-10.32%
15	69.00	8.00	8.10	44.84	70.68	7.51	8.13	40.76	2.44%	-6.11%	0.39%	-9.11%
16	56.78	6.34	6.40	57.82	58.32	6.09	6.54	56.22	2.70%	-3.81%	2.06%	-2.78%
17	37.85	3.93	3.97	55.17	38.19	3.78	4.06	55.05	0.87%	-3.76%	2.16%	-0.22%
18	8.64	1.05	1.06	16.41	8.70	1.02	1.09	16.66	0.63%	-2.26%	3.37%	1.58%
19	0.00	0.00	0.00	0.00	0.00	0.00	0.00	0.00	-	-	-	-
20	0.00	0.00	0.00	0.00	0.00	0.00	0.00	0.00	-	-	-	-
21	0.00	0.00	0.00	0.00	0.00	0.00	0.00	0.00	-	-	-	-
22	0.00	0.00	0.00	0.00	0.00	0.00	0.00	0.00	-	-	-	-
23	0.00	0.00	0.00	0.00	0.00	0.00	0.00	0.00	-	-	-	-
24	0.00	0.00	0.00	0.00	0.00	0.00	0.00	0.00	-	-	-	-
SUM	568.55	61.09	218.56	232.03	583.08	57.85	215.78	222.38	2.56%	-5.31%	-1.27%	-4.16%

The use of single-pane clear glass at peak cooling load makes the difference in solar heat gain when using the SC method and when using the WL method. At peak cooling load, when using the WL method with a single-pane facing south, the solar heat gain was reduced from 2.59% to 4.43% compared to when using the SC method. For the glass facing north, the solar heat gain was reduced from 2.27% to 3.82% compared to when using the SC method. For the glass facing east, the solar heat gain was reduced from 2.14% to 4.43% compared to when using the SC method. For the glass facing west, the solar heat gain was reduced from 2.46% to 3.76% compared to when using the SC method.

The use of double-pane clear glass at peak cooling load makes the difference in solar heat gain when using the SC method and when using the WL method. At peak cooling load, when using the WL method with the double-pane clear glass facing south, the solar heat gain was reduced from 4.13% to 11.01% compared to when using the SC method. For the glass facing north, the solar heat gain was reduced from 5.34% to 11.22% compared to when using the SC method. For the glass facing east, the solar heat gain was reduced from 1.71% to 11.51% compared to when using the SC method. For the glass facing west, the solar heat gain was reduced from 2.47% to 11.08% compared to when using the SC method.

The use of double-pane Low-E glass at peak heating load makes the difference in solar heat gain when using the SC method and when using the WL method. At peak heating load, when using the WL method with the double-pane Low-E glass facing south, the solar heat gain was reduced from -24.2% to 11.02% compared to when using

the SC method. For the glass facing north, the solar heat gain was reduced from -23.18% to 5.11% compared to when using the SC method. For the glass facing east, the solar heat gain was reduced from -25.87% to 11.04% compared to when using the SC method. For the glass facing west, the solar heat gain was reduced from -24.2% to 1.67% compared to when using the SC method.

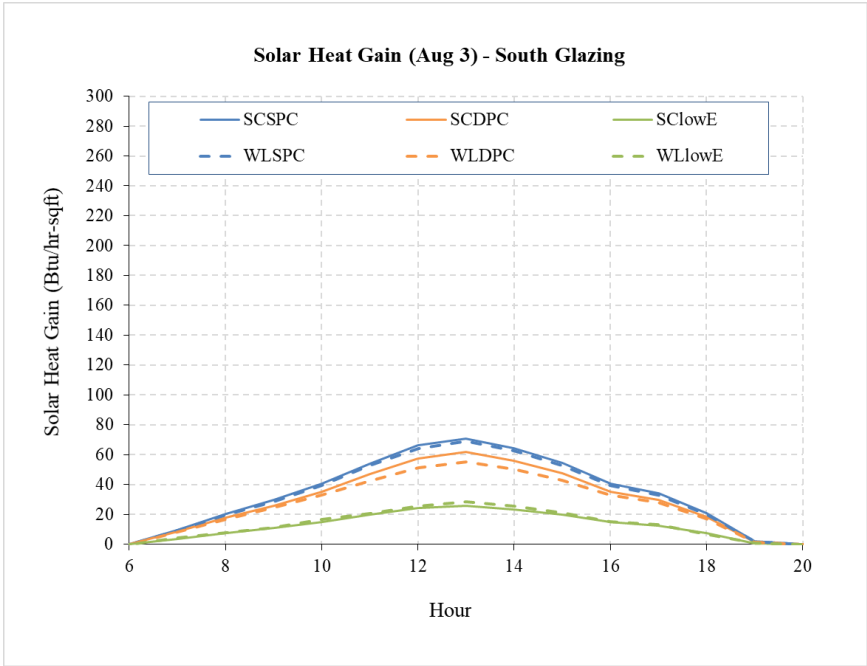


Figure 6.5: Solar heat gains for August 3 (south facing)

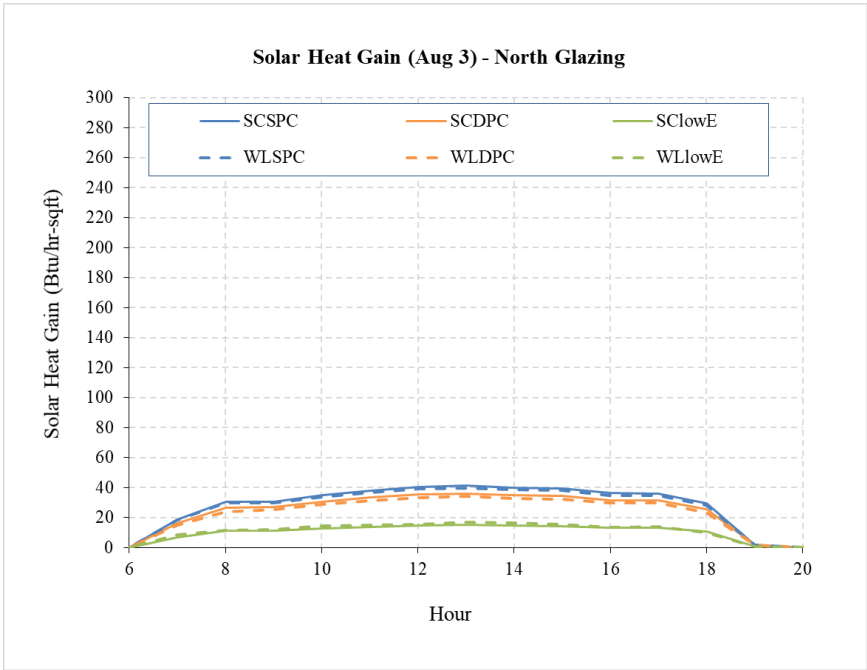


Figure 6.6: Solar heat gains for August 3 (north facing)

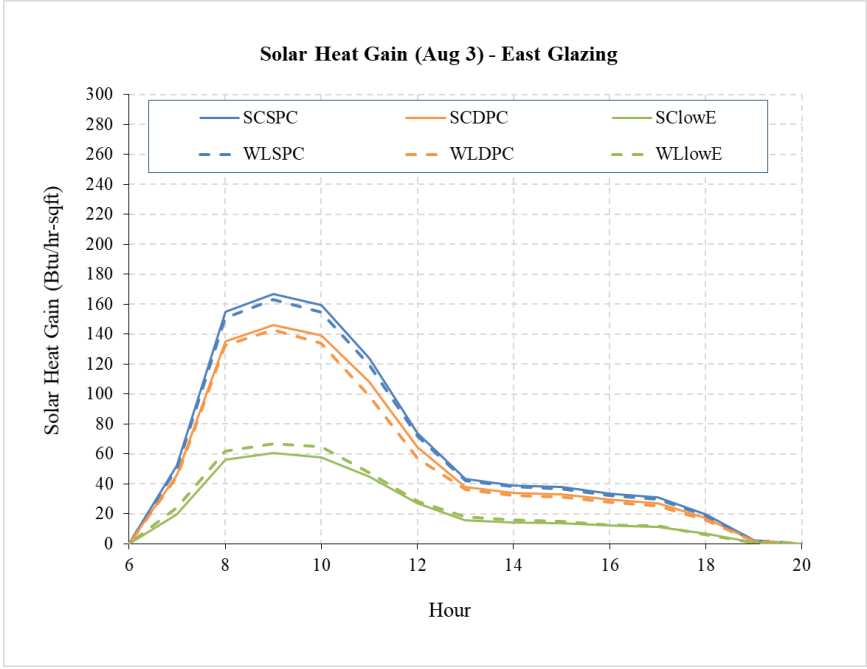


Figure 6.7: Solar heat gains for August 3 (east facing)

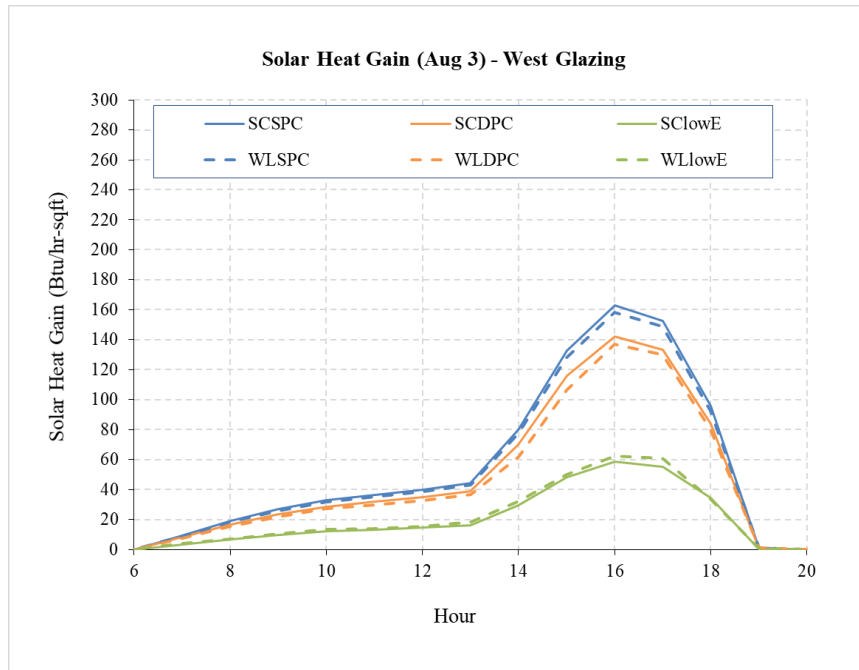


Figure 6.8: Solar heat gains for August 3 (west facing)

Table 6.5: Solar heat gain difference between the shading coefficient and the window library methods for August 3 (single clear window)

Hours	SC_SPC				WL_SPC				% Difference((WL_SPC-SC_SPC)/SC_SPC)			
	South	North	East	West	South	North	East	West	South	North	East	West
1	0.00	0.00	0.00	0.00	0.00	0.00	0.00	0.00	-	-	-	-
2	0.00	0.00	0.00	0.00	0.00	0.00	0.00	0.00	-	-	-	-
3	0.00	0.00	0.00	0.00	0.00	0.00	0.00	0.00	-	-	-	-
4	0.00	0.00	0.00	0.00	0.00	0.00	0.00	0.00	-	-	-	-
5	0.00	0.00	0.00	0.00	0.00	0.00	0.00	0.00	-	-	-	-
6	0.00	0.00	0.00	0.00	0.00	0.00	0.00	0.00	-	-	-	-
7	9.67	18.75	52.32	9.37	9.42	18.32	51.20	9.13	-2.59%	-2.27%	-2.14%	-2.57%
8	20.44	30.67	154.80	19.18	19.68	29.61	150.83	18.46	-3.75%	-3.43%	-2.56%	-3.74%
9	29.76	30.68	166.96	26.94	28.71	29.67	162.86	25.99	-3.52%	-3.30%	-2.46%	-3.52%
10	40.53	34.95	159.24	32.86	39.31	33.87	154.69	31.83	-3.00%	-3.10%	-2.86%	-3.14%
11	54.27	38.03	123.86	36.58	52.58	36.72	119.70	35.32	-3.10%	-3.43%	-3.36%	-3.43%
12	66.21	40.39	74.07	40.05	64.31	39.00	71.92	38.67	-2.87%	-3.44%	-2.91%	-3.44%
13	70.83	41.14	43.53	44.52	68.96	39.86	42.19	43.15	-2.64%	-3.10%	-3.07%	-3.07%
14	64.25	39.77	39.11	80.09	62.58	38.55	37.93	77.93	-2.59%	-3.06%	-3.02%	-2.70%
15	54.60	39.45	37.80	132.96	53.02	38.11	36.58	128.31	-2.88%	-3.38%	-3.21%	-3.49%
16	40.58	36.21	33.65	162.90	39.26	34.89	32.43	158.02	-3.24%	-3.64%	-3.64%	-3.00%
17	34.26	36.14	30.86	152.39	33.15	34.92	29.81	148.64	-3.24%	-3.37%	-3.41%	-2.46%
18	21.16	29.51	19.63	95.80	20.22	28.40	18.76	92.66	-4.43%	-3.75%	-4.43%	-3.28%
19	2.08	1.86	2.09	1.30	1.99	1.79	2.00	1.25	-4.19%	-3.82%	-4.22%	-3.76%
20	0.00	0.00	0.00	0.00	0.00	0.00	0.00	0.00	-	-	-	-
21	0.00	0.00	0.00	0.00	0.00	0.00	0.00	0.00	-	-	-	-
22	0.00	0.00	0.00	0.00	0.00	0.00	0.00	0.00	-	-	-	-
23	0.00	0.00	0.00	0.00	0.00	0.00	0.00	0.00	-	-	-	-
24	0.00	0.00	0.00	0.00	0.00	0.00	0.00	0.00	-	-	-	-
SUM	508.64	417.54	937.92	834.93	493.22	403.73	910.90	809.35	-3.03%	-3.31%	-2.88%	-3.06%

Table 6.6: Solar heat gain difference between the shading coefficient and the window library methods for August 3 (double clear window)

Hours	SC_DPC				WL_DPC				% Difference ((WL_DPC-SC_DPC)/SC_DPC)			
	South	North	East	West	South	North	East	West	South	North	East	West
1	0.00	0.00	0.00	0.00	0.00	0.00	0.00	0.00	-	-	-	-
2	0.00	0.00	0.00	0.00	0.00	0.00	0.00	0.00	-	-	-	-
3	0.00	0.00	0.00	0.00	0.00	0.00	0.00	0.00	-	-	-	-
4	0.00	0.00	0.00	0.00	0.00	0.00	0.00	0.00	-	-	-	-
5	0.00	0.00	0.00	0.00	0.00	0.00	0.00	0.00	-	-	-	-
6	0.00	0.00	0.00	0.00	0.00	0.00	0.00	0.00	-	-	-	-
7	8.46	16.38	45.79	8.19	8.11	15.12	45.01	7.85	-4.13%	-7.65%	-1.71%	-4.13%
8	17.87	26.74	135.40	16.77	16.73	23.74	132.64	15.70	-6.37%	-11.22%	-2.04%	-6.38%
9	26.02	26.81	145.94	23.55	24.44	25.22	142.94	22.12	-6.04%	-5.93%	-2.05%	-6.05%
10	35.39	30.55	139.11	28.73	32.86	28.92	133.94	27.18	-7.15%	-5.35%	-3.72%	-5.38%
11	47.33	33.24	108.12	31.97	42.41	31.25	98.75	30.06	-10.40%	-5.97%	-8.67%	-5.96%
12	57.74	35.30	64.58	35.00	51.39	33.19	57.15	32.91	-11.01%	-5.97%	-11.51%	-5.98%
13	61.77	35.96	38.03	38.92	55.12	34.03	36.00	36.80	-10.77%	-5.37%	-5.35%	-5.43%
14	56.03	34.77	34.19	69.88	50.17	32.91	32.37	62.14	-10.46%	-5.34%	-5.31%	-11.08%
15	47.61	34.48	33.03	116.10	43.00	32.43	31.15	106.62	-9.69%	-5.94%	-5.69%	-8.16%
16	35.42	31.65	29.41	142.35	32.85	29.63	27.53	136.79	-7.26%	-6.39%	-6.39%	-3.90%
17	29.94	31.58	26.97	133.20	28.23	29.60	25.37	129.91	-5.71%	-6.26%	-5.96%	-2.47%
18	18.51	25.77	17.17	83.79	17.08	23.36	15.84	80.21	-7.73%	-9.37%	-7.73%	-4.27%
19	1.82	1.63	1.83	1.13	1.68	1.52	1.69	1.06	-7.26%	-6.64%	-7.22%	-6.64%
20	0.00	0.00	0.00	0.00	0.00	0.00	0.00	0.00	-	-	-	-
21	0.00	0.00	0.00	0.00	0.00	0.00	0.00	0.00	-	-	-	-
22	0.00	0.00	0.00	0.00	0.00	0.00	0.00	0.00	-	-	-	-
23	0.00	0.00	0.00	0.00	0.00	0.00	0.00	0.00	-	-	-	-
24	0.00	0.00	0.00	0.00	0.00	0.00	0.00	0.00	-	-	-	-
SUM	443.91	364.84	819.58	729.57	404.07	340.92	780.39	689.36	-8.98%	-6.56%	-4.78%	-5.51%

Table 6.7: Solar heat gain difference between the shading coefficient and the window library methods for August 3 (double low-E window)

Hours	SC_lowE				WL_lowE				% Difference ((WL_lowE-SC_lowE)/SC_lowE)			
	South	North	East	West	South	North	East	West	South	North	East	West
1	0.00	0.00	0.00	0.00	0.00	0.00	0.00	0.00	-	-	-	-
2	0.00	0.00	0.00	0.00	0.00	0.00	0.00	0.00	-	-	-	-
3	0.00	0.00	0.00	0.00	0.00	0.00	0.00	0.00	-	-	-	-
4	0.00	0.00	0.00	0.00	0.00	0.00	0.00	0.00	-	-	-	-
5	0.00	0.00	0.00	0.00	0.00	0.00	0.00	0.00	-	-	-	-
6	0.00	0.00	0.00	0.00	0.00	0.00	0.00	0.00	-	-	-	-
7	3.59	7.00	19.41	3.48	4.46	8.62	24.43	4.32	24.20%	23.18%	25.87%	24.20%
8	7.46	11.31	56.30	7.00	7.72	11.47	61.65	7.24	3.41%	1.43%	9.49%	3.41%
9	10.89	11.26	60.53	9.85	11.53	12.15	66.94	10.43	5.86%	7.88%	10.58%	5.86%
10	15.06	12.83	57.82	12.10	16.73	14.35	65.05	13.51	11.07%	11.80%	12.52%	11.69%
11	19.96	13.89	44.91	13.36	20.77	14.70	47.54	14.14	4.06%	5.81%	5.85%	5.81%
12	24.27	14.73	27.03	14.61	25.64	15.59	28.47	15.46	5.64%	5.80%	5.33%	5.80%
13	26.03	15.09	15.88	16.38	28.51	16.82	17.72	18.25	9.52%	11.46%	11.59%	11.42%
14	23.61	14.59	14.33	29.52	25.86	16.24	15.96	32.15	9.52%	11.30%	11.36%	8.89%
15	20.01	14.38	13.79	48.26	21.24	15.20	14.84	50.20	6.14%	5.72%	7.64%	4.02%
16	14.82	13.14	12.21	58.88	15.48	13.34	12.40	62.36	4.47%	1.54%	1.54%	5.92%
17	12.49	13.23	11.26	55.18	13.45	13.97	11.90	60.73	7.68%	5.64%	5.74%	10.05%
18	7.57	10.65	7.02	34.38	6.73	10.11	6.25	33.81	-11.02%	-5.11%	-11.04%	-1.67%
19	0.75	0.67	0.75	0.47	0.71	0.67	0.71	0.47	-5.63%	0.00%	-5.60%	0.00%
20	0.00	0.00	0.00	0.00	0.00	0.00	0.00	0.00	-	-	-	-
21	0.00	0.00	0.00	0.00	0.00	0.00	0.00	0.00	-	-	-	-
22	0.00	0.00	0.00	0.00	0.00	0.00	0.00	0.00	-	-	-	-
23	0.00	0.00	0.00	0.00	0.00	0.00	0.00	0.00	-	-	-	-
24	0.00	0.00	0.00	0.00	0.00	0.00	0.00	0.00	-	-	-	-
SUM	186.51	152.77	341.24	303.48	198.82	163.22	373.86	323.07	6.60%	6.84%	9.56%	6.46%

Figure 6.9 and Table 6.8 show the monthly solar heat gains in south facing glazing. The monthly heat gains of single-pane clear glass when using the WL method were reduced from 3.3% to 4% compared to when using the SC method. The monthly heat gains of double-pane clear glass when using the WL method were reduced from 4.2% to 11% compared to when using the SC method. The monthly heat gains of double-pane Low-E glass when using the WL method were reduced from -6.8% to 2% compared to when using the SC method.

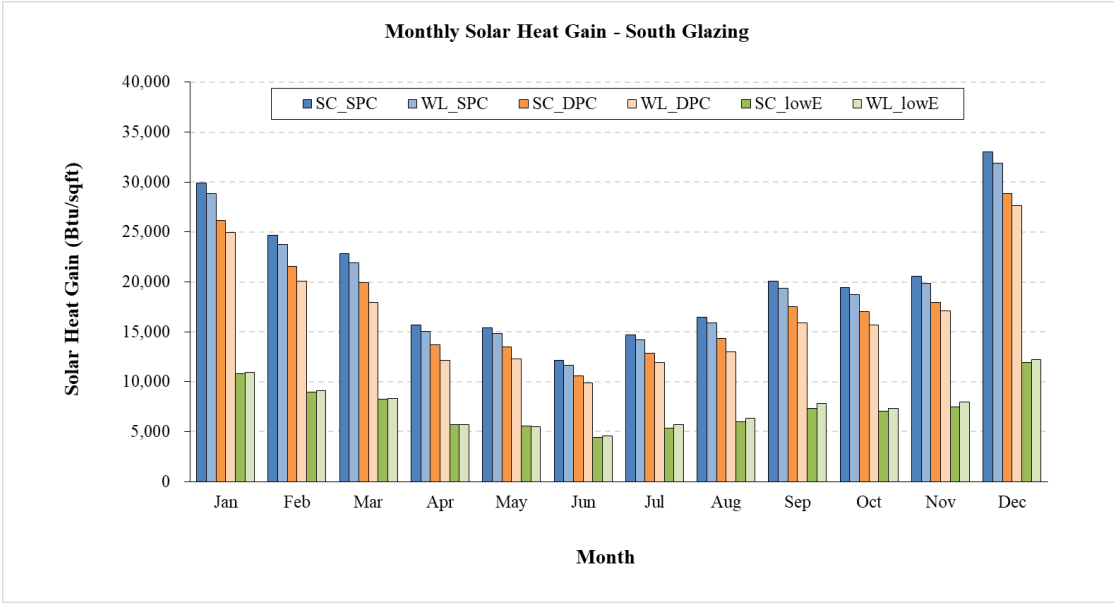


Figure 6.9: Monthly solar heat gain (south facing)

Table 6.8: Monthly solar heat gain difference between the shading coefficient and the window library methods (south facing)

Month	BTU/SQFT						Diff. (%) SPC (SC vs. WL)	Diff. (%) DPC (SC vs. WL)	Diff. (%) LowE (SC vs. WL)
	SC_SPC	WL_SPC	SC_DPC	WL_DPC	SC_lowE	WL_lowE			
Jan	29,914	28,880	26,147	24,963	10,814	10,973	-3.5%	-4.5%	1.5%
Feb	24,674	23,721	21,555	20,069	8,941	9,091	-3.9%	-6.9%	1.7%
Mar	22,832	21,908	19,935	17,984	8,288	8,292	-4.0%	-9.8%	0.0%
Apr	15,665	15,046	13,671	12,173	5,706	5,672	-3.9%	-11.0%	-0.6%
May	15,407	14,800	13,456	12,272	5,593	5,481	-3.9%	-8.8%	-2.0%
Jun	12,123	11,673	10,591	9,848	4,421	4,563	-3.7%	-7.0%	3.2%
Jul	14,719	14,215	12,857	11,950	5,384	5,703	-3.4%	-7.1%	5.9%
Aug	16,432	15,894	14,343	13,010	6,010	6,334	-3.3%	-9.3%	5.4%
Sep	20,082	19,387	17,530	15,895	7,330	7,823	-3.5%	-9.3%	6.7%
Oct	19,459	18,726	16,995	15,711	7,069	7,347	-3.8%	-7.6%	3.9%
Nov	20,557	19,870	17,964	17,122	7,468	7,979	-3.3%	-4.7%	6.8%
Dec	33,014	31,896	28,861	27,663	11,941	12,203	-3.4%	-4.2%	2.2%

Figure 6.10 and Table 6.9 show the monthly solar heat gains in north facing glazing. The monthly heat gains of single-pane clear glass when using the WL method were reduced from 3.3% to 4% compared to when using the SC method. The monthly heat gains of double-pane clear glass when using the WL method were reduced from 5.9% to 7.7% compared to when using the SC method. The monthly heat gains of double-pane Low-E glass when using the WL method were reduced from -9% to 0.4% compared to when using the SC method.

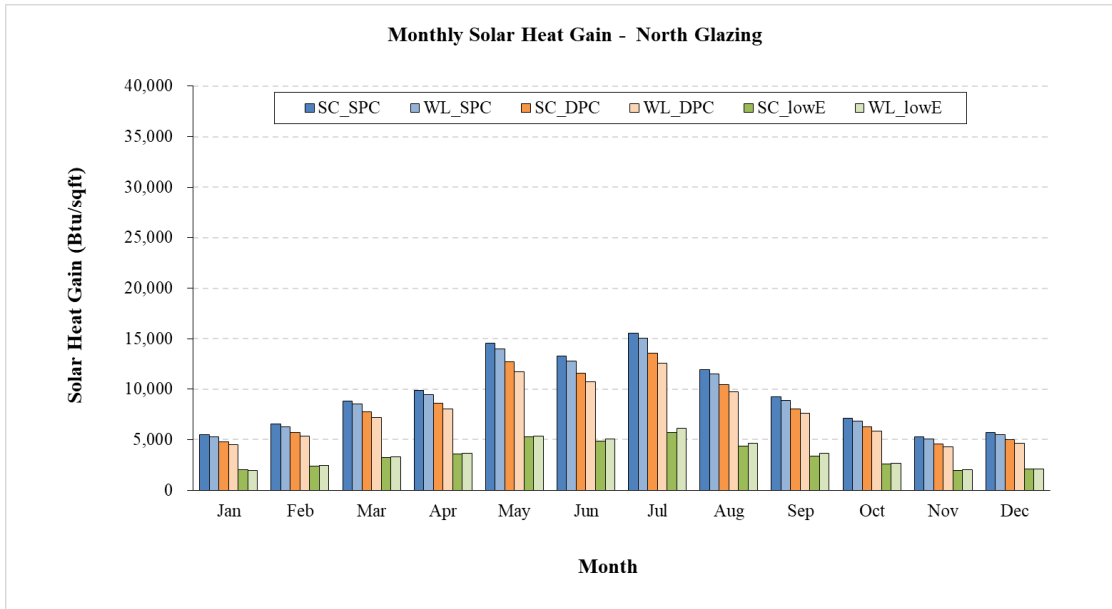


Figure 6.10: Monthly solar heat gain (north facing)

Table 6.9: Monthly solar heat gain difference between the shading coefficient and the window library methods (north facing)

Month	BTU/SQFT						Diff. (%) SPC (SC vs. WL)	Diff. (%) DPC (SC vs. WL)	Diff. (%) LowE (SC vs. WL)
	SC_SPC	WL_SPC	SC_DPC	WL_DPC	SC_lowE	WL_lowE			
Jan	5,496	5,274	4,805	4,477	1,996	1,988	-4.0%	-6.8%	-0.4%
Feb	6,554	6,296	5,728	5,350	2,388	2,457	-3.9%	-6.6%	2.9%
Mar	8,852	8,502	7,738	7,225	3,223	3,305	-3.9%	-6.6%	2.6%
Apr	9,849	9,457	8,607	8,007	3,587	3,651	-4.0%	-7.0%	1.8%
May	14,534	13,984	12,697	11,720	5,286	5,356	-3.8%	-7.7%	1.3%
Jun	13,266	12,798	11,588	10,736	4,843	5,101	-3.5%	-7.4%	5.3%
Jul	15,560	15,045	13,591	12,601	5,693	6,108	-3.3%	-7.3%	7.3%
Aug	11,941	11,536	10,434	9,765	4,367	4,678	-3.4%	-6.4%	7.1%
Sep	9,215	8,894	8,055	7,583	3,373	3,677	-3.5%	-5.9%	9.0%
Oct	7,151	6,872	6,250	5,840	2,606	2,686	-3.9%	-6.6%	3.1%
Nov	5,265	5,064	4,603	4,309	1,923	2,008	-3.8%	-6.4%	4.4%
Dec	5,697	5,469	4,980	4,644	2,072	2,086	-4.0%	-6.8%	0.7%

Figure 6.11 and Table 6.10 show the monthly solar heat gains in east facing glazing. The monthly heat gains of single-pane clear glass when using the WL method were reduced from 3.1% to 3.7% compared to when using the SC method. The monthly heat gains of double-pane clear glass when using the WL method were reduced from 5.1% to 6.7% compared to when using the SC method. The monthly heat gains of double-pane Low-E glass when using the WL method were reduced from -10% to -1% compared to when using the SC method.

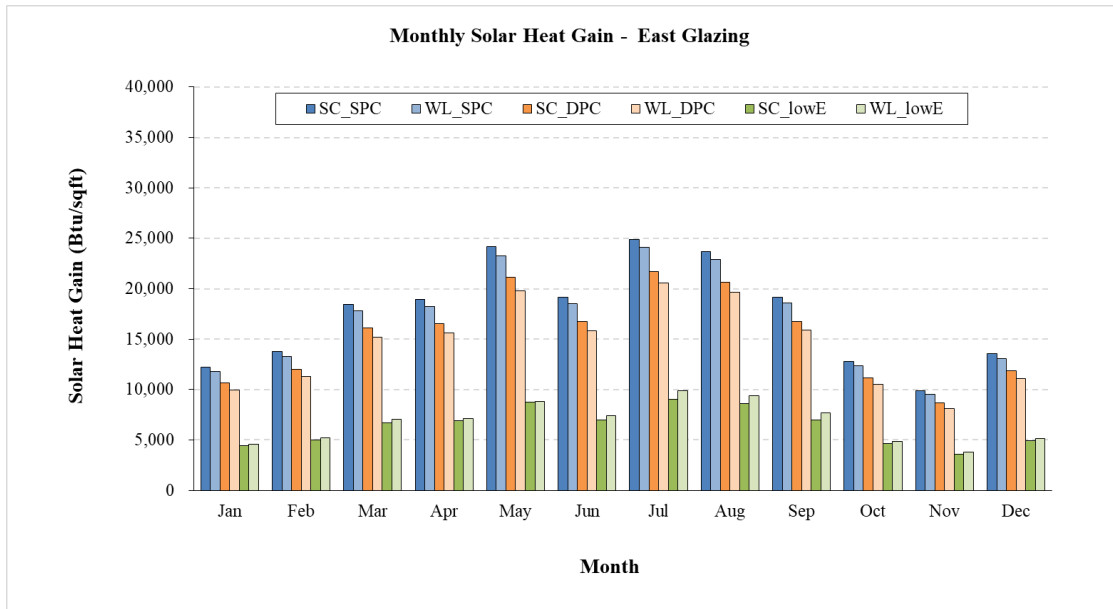


Figure 6.11: Monthly solar heat gain (east facing)

Table 6.10: Monthly solar heat gain difference between the shading coefficient and the window library methods (east facing)

Month	BTU/SQFT						Diff. (%) SPC (SC vs. WL)	Diff. (%) DPC (SC vs. WL)	Diff. (%) LowE (SC vs. WL)
	SC_SPC	WL_SPC	SC_DPC	WL_DPC	SC_lowE	WL_lowE			
Jan	12,194	11,765	10,657	9,957	4,434	4,543	-3.5%	-6.6%	2.5%
Feb	13,748	13,266	12,014	11,289	5,004	5,230	-3.5%	-6.0%	4.5%
Mar	18,465	17,815	16,139	15,209	6,714	7,017	-3.5%	-5.8%	4.5%
Apr	18,948	18,266	16,561	15,585	6,884	7,113	-3.6%	-5.9%	3.3%
May	24,145	23,254	21,101	19,789	8,746	8,830	-3.7%	-6.2%	1.0%
Jun	19,181	18,532	16,761	15,797	6,978	7,395	-3.4%	-5.8%	6.0%
Jul	24,860	24,089	21,723	20,591	9,058	9,869	-3.1%	-5.2%	9.0%
Aug	23,652	22,924	20,669	19,622	8,613	9,375	-3.1%	-5.1%	8.8%
Sep	19,170	18,556	16,752	15,876	6,991	7,692	-3.2%	-5.2%	10.0%
Oct	12,788	12,329	11,175	10,501	4,653	4,874	-3.6%	-6.0%	4.7%
Nov	9,904	9,559	8,655	8,096	3,616	3,827	-3.5%	-6.5%	5.9%
Dec	13,551	13,075	11,843	11,055	4,935	5,121	-3.5%	-6.7%	3.8%

Figure 6.12 and Table 6.11 show the monthly solar heat gains in west facing glazing. The monthly heat gains of single-pane clear glass when using the WL method were reduced from 3.1% to 3.8% compared to when using the SC method. The monthly heat gains of double-pane clear glass when using the WL method were reduced from 4.8% to 6.9% compared to when using the SC method. The monthly heat gains of double-pane Low-E glass when using the WL method were reduced from -9.6% to 1.5% compared to when using the SC method.

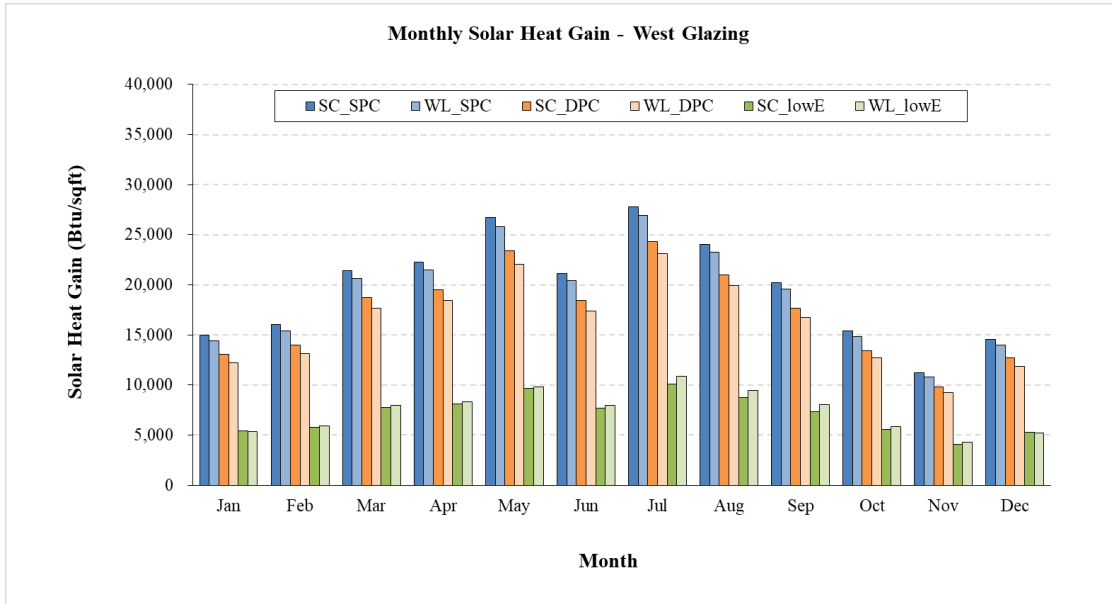


Figure 6.12: Monthly solar heat gain (west facing)

Table 6.11: Monthly solar heat gain difference between the shading coefficient and the window library methods (west facing)

Month	BTU/SQFT						Diff. (%) SPC (SC vs. WL)	Diff. (%) DPC (SC vs. WL)	Diff. (%) LowE (SC vs. WL)
	SC_SPC	WL_SPC	SC_DPC	WL_DPC	SC_lowE	WL_lowE			
Jan	14,972	14,406	13,085	12,218	5,418	5,343	-3.8%	-6.6%	-1.4%
Feb	16,007	15,422	13,988	13,151	5,807	5,950	-3.7%	-6.0%	2.5%
Mar	21,421	20,642	18,723	17,645	7,763	7,936	-3.6%	-5.8%	2.2%
Apr	22,295	21,493	19,485	18,410	8,083	8,296	-3.6%	-5.5%	2.6%
May	26,740	25,800	23,370	22,050	9,678	9,828	-3.5%	-5.6%	1.6%
Jun	21,132	20,413	18,467	17,416	7,673	7,990	-3.4%	-5.7%	4.1%
Jul	27,791	26,935	24,288	23,126	10,103	10,842	-3.1%	-4.8%	7.3%
Aug	24,036	23,292	21,006	19,934	8,741	9,421	-3.1%	-5.1%	7.8%
Sep	20,198	19,567	17,652	16,776	7,361	8,069	-3.1%	-5.0%	9.6%
Oct	15,381	14,842	13,441	12,679	5,591	5,841	-3.5%	-5.7%	4.5%
Nov	11,209	10,823	9,795	9,218	4,085	4,319	-3.4%	-5.9%	5.7%
Dec	14,557	13,999	12,722	11,841	5,272	5,194	-3.8%	-6.9%	-1.5%

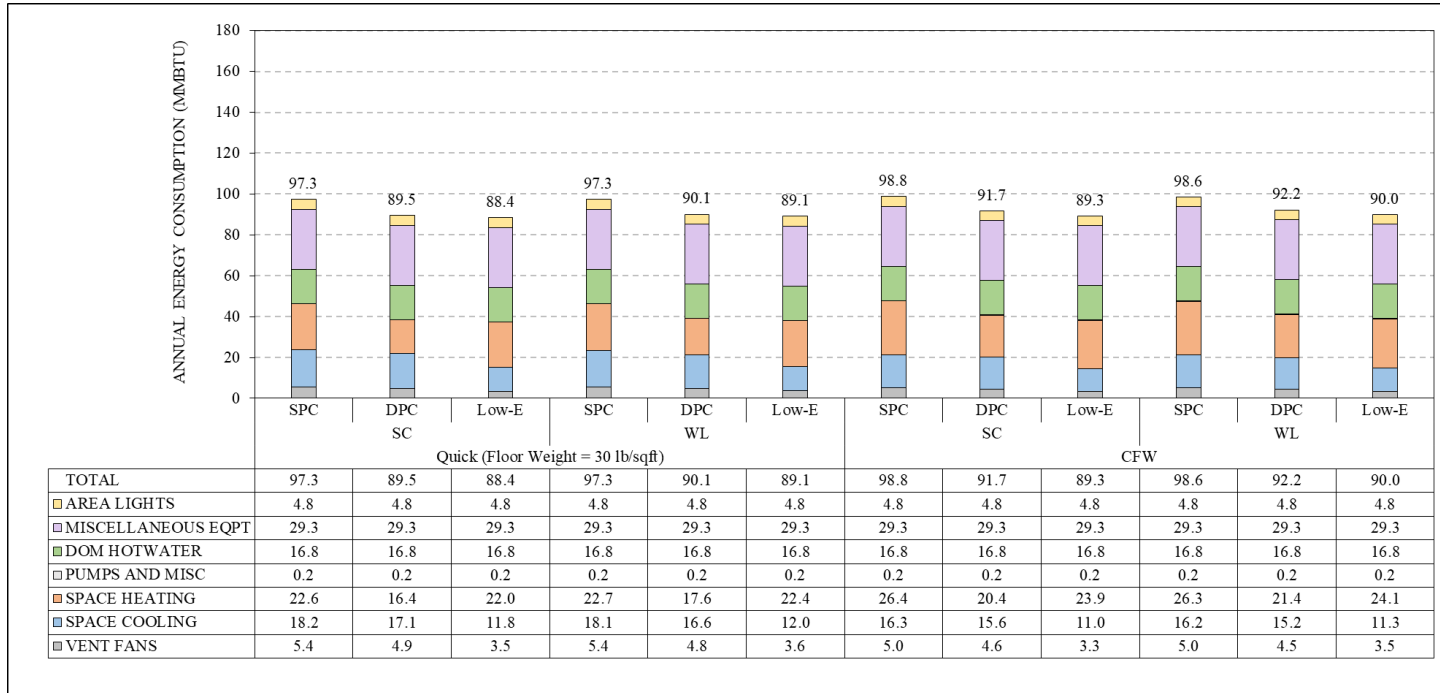


Figure 6.13: Annual building energy performance (BEPS) report

Table 6.12: Annual building energy performance (BEPS) report difference between the shading coefficient and the window library methods

	Glazing											
	Quick (Floor Weight = 30 lb/sqft)						CFW					
	SC			WL			SC			WL		
	SPC	DPC	Low-E	SPC	DPC	Low-E	SPC	DPC	Low-E	SPC	DPC	Low-E
AREA LIGHTS	-	-	-	0.0%	0.0%	0.0%	0.0%	0.0%	0.0%	0.0%	0.0%	0.0%
MISCELLANEOUS EQPT	-	-	-	0.0%	0.0%	0.0%	0.0%	0.0%	0.0%	0.0%	0.0%	0.0%
SPACE HEATING	-	-	-	0.4%	7.3%	1.8%	16.8%	24.4%	8.6%	16.4%	30.5%	9.5%
SPACE COOLING	-	-	-	-0.5%	-2.9%	1.7%	-10.4%	-8.8%	-6.8%	-11.0%	-11.1%	-4.2%
VENT FANS	-	-	-	0.0%	-2.0%	2.9%	-7.4%	-6.1%	-5.7%	-7.4%	-8.2%	0.0%
TOTAL	-	-	-	0.0%	0.7%	0.8%	1.5%	2.5%	1.0%	1.3%	3.0%	1.8%

Figure 6.13 and Table 6.12 show the annual building energy performance according to different glass types, glazing calculation methods, and weighting factors. When comparing the total energy consumption of the SC method using the Quick method and the WL method using the Quick method, for SPC, DPC, and Low-E there were 0%, 0.7%, and 0.8% differences when moving from the SC method option to the WL option, respectively. When comparing the total energy consumption of the SC method using the Quick method and the SC method using the CFW method, for SPC and DPC, there were 1.5%, 2.5%, and 1.0% differences when moving from the SC method option to the WL option, respectively. When comparing the total energy consumption of the SC method using the Quick method and the WL method using the CFW method, for SPC and DPC, there were 1.3%, 3.0%, and 1.8% differences when moving from the SC method option to the WL option, respectively.

When comparing the SC and WL methods, the differences in energy usage were very small (e.g. up to 0.8%). However, when comparing the Quick method and the CFW method, the differences in energy consumption were up to 3%.

6.1.2. Window Frame

The window frame is approximately 19% to 26% of the total window area, depending on the type and size of the window. However, in a simplified window model, it is easy to overlook the difference in window frame type, frame width, and frame area. Therefore, in this study, an analysis of the energy consumption according to the frame

area, frame type, frame width, and window type was performed. Table 6.13 shows the thermal properties of window frames, and Table 6.14 shows frame widths by frame types.

Table 6.13: Thermal properties of window frames

Frame Type	Thermal Performance (Btu/ft ² -F-h) ^a	
	Conductance (excludes OA film)	U-value ^b (includes OA film at 15mph windspeed)
Aluminum w/ thermal break	1.245	1.0
Wood	0.434	0.4
Vinyl	0.319	0.3
Fiberglass ^f	0.208	0.2

a. DOE-2 Supplement Version 2.1E, p.2.116

b. Conductance = ((U-value)⁻¹ - 0.197)⁻¹

Table 6.14: Frame width by frame type

Frame Type	Frame Width (inches)		
	IC3 ^a	LBNL Window v7.7 ^b	ASHRAE Std-140 ^c
Aluminum w/ thermal break	2.25	2.25	2.75
Wood	2.25	2.75	2.75
Vinyl	2.25	2.75	-
Fiberglass ^d	-	-	-

a. Frame width information in IC3

b. Frame width information in LBNL Window v7.7.10

c. Frame width information in ASHARE Std-140

d. ALPEN: https://www.thinkalpen.com/wp-content/uploads/2013/10/Alpen-HPP-X25-Total-Unit_Glass_Performance_101313.pdf

Table 6.15 shows the reference window size and the window shape, and Table 6.16 shows the test cases for window frame analysis. In this study, window frame analysis was conducted according to frame type, frame width, and window shape.

Table 6.15: Reference window size and window shape

Reference	Base Window	
	Single Window Size	Window Shape
IC3	Width: 3ft Height: 5ft	Single Vision
ASHRAE Std-140		Vertical Slider

Table 6.16: Test cases for window frame analysis

Case Number	Frame Type	Frame Width (inches)	Window Shape
Case1 (Base-case)	Vinyl	2.25	3x5, Single Vision
Case2	Vinyl	2.75	3x5, Single Vision
Case3	Aluminum w/ thermal break	2.25	3x5, Single Vision
Case4	Wood	2.75	3x5, Single Vision
Case5	Fiberglass	2.75	3x5, Single Vision
Case6	Vinyl	2.25	3x5, Vertical Slider
Case7	Vinyl	2.75	3x5, Vertical Slider
Case8	Aluminum w/ thermal break	2.25	3x5, Vertical Slider
Case9	Wood	2.75	3x5, Vertical Slider
Case10	Fiberglass	2.75	3x5, Vertical Slider

The analysis was conducted by carefully changing the frame type, frame width, and window shape. Figure 6.14 and Table 6.17 show the annual building energy performance according to different frame types, frame width, and window shape. Case 1 was compared one by one as the base-case. When the frame width was changed to 2.75 inch in Case 1, the difference in total energy consumption was 0.3%. When the frame type was changed to the aluminum with thermal break frame in Case 1, the difference in total energy consumption was 3.1%. When the frame type was changed to the wood frame in Case 1, the difference in total energy consumption was 1.2%. When the frame type was changed to the fiberglass frame in Case 1, the difference in total energy consumption was 0.4%. When the window shape was changed to the vertical slider in Case 1, the difference in total energy consumption was 0.3%. When the window shape

was changed to the vertical slider and the frame width was changed to 2.75 inch in Case 1, the difference in total energy consumption was 0.7%. When the window shape was changed to the vertical slider and the frame type was changed to the aluminum with thermal break frame in Case 1, the difference in total energy consumption was 3.9%. When the window shape was changed to the vertical slider and the frame type was changed to the wood frame in Case 1, the difference in total energy consumption was 1.6%. When the window shape was changed to the vertical slider and the frame type was changed to the fiberglass frame in Case 1, the difference in total energy consumption was 0.1%. In this analysis, it was found that there was a difference from 0.1% to 3.9% depending on the frame type, frame width, and window shape.

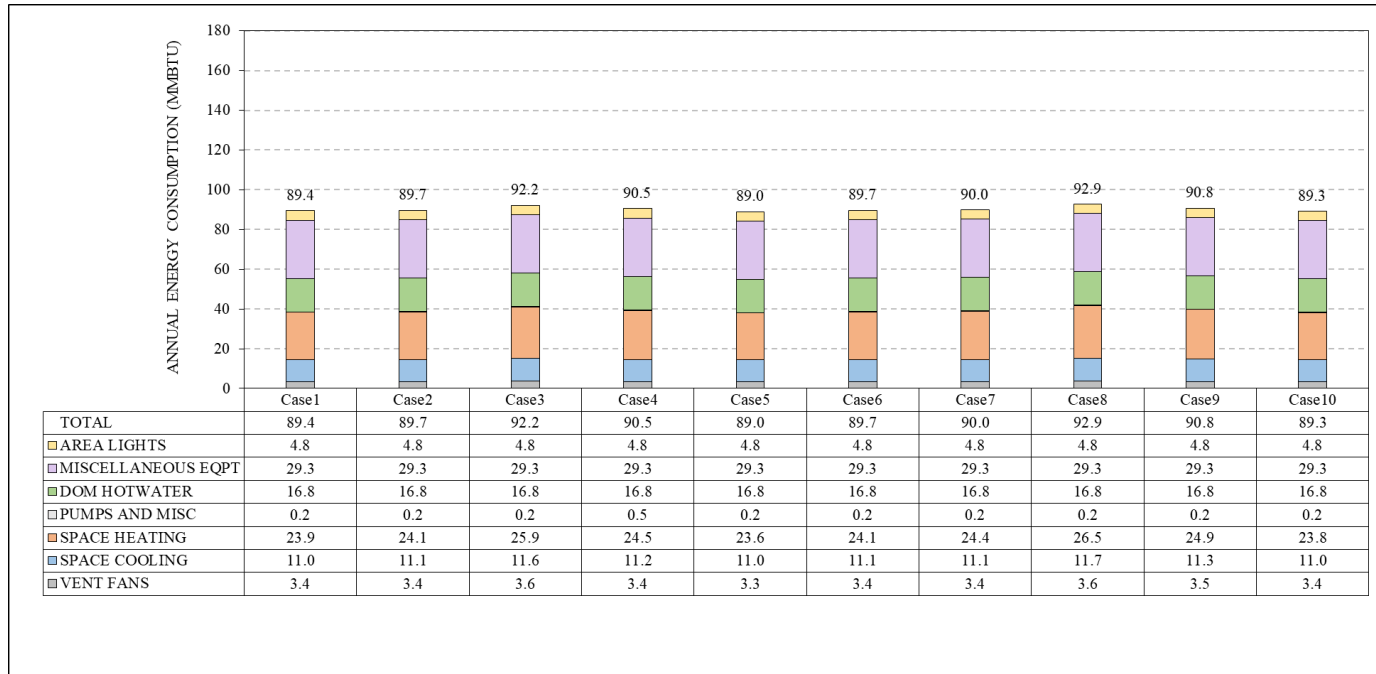


Figure 6.14: Annual building energy performance (BEPS) report

Table 6.17: Annual building energy performance (BEPS) report difference between the window frame type, width, and shape

	Case1	Case2	Case3	Case4	Case5	Case6	Case7	Case8	Case9	Case10
AREA LIGHTS	-	0.0%	0.0%	0.0%	0.0%	0.0%	0.0%	0.0%	0.0%	0.0%
MISCELLANEOUS EQPT	-	0.0%	0.0%	0.0%	0.0%	0.0%	0.0%	0.0%	0.0%	0.0%
SPACE HEATING	-	0.8%	8.4%	2.5%	-1.3%	0.8%	2.1%	10.9%	4.2%	-0.4%
SPACE COOLING	-	0.9%	5.5%	1.8%	0.0%	0.9%	0.9%	6.4%	2.7%	0.0%
VENT FANS	-	0.0%	5.9%	0.0%	-2.9%	0.0%	0.0%	5.9%	2.9%	0.0%
TOTAL	-	0.3%	3.1%	1.2%	-0.4%	0.3%	0.7%	3.9%	1.6%	-0.1%

6.2. Shading (Roof Eave and Window Setback)

In studying the case study house, it was discovered that the roof eave and window setback were present. However, in most residential building energy code-compliance simulation models, the roof eaves and window setback are not represented. This can also be seen in the residential building simulation test models of ASHRAE Standard-140 (ASHRAE, 2017) and RESNET (RESNET, 2020b). For this reason, the impact of the roof eaves and window setbacks were analyzed on the case-study house.

6.2.1. Roof Eave

Table 6.18 shows the test cases for roof eave analysis. In this study, window roof analysis was conducted according to eave depth and height above window head

Table 6.18: Test cases for roof eave analysis

Case Number	Eave Length (ft)	Height Above Window Head (ft)
Case1 (Base-case)	No Shadings	-
Case2	1	1
Case3	1.5	1
Case4	2	1
Case5	1	0
Case6	1.5	0
Case7	2	0

Figure 6.15 and Table 6.19 show the annual building energy performance according to different eave depths, and heights above window head. When the eave length was changed to 1ft and the height above window head was changed to 1ft in Case

1 and, the difference in total energy consumption was 0.1%. When the eave length was changed to 1.5ft and the height above window head was changed to 1ft in Case 1 and, the difference in total energy consumption was 0.2%. When the eave length was changed to 2ft and the height above window head was changed to 1ft in Case 1 and, the difference in total energy consumption was 0.4%. When the eave length was changed to 1ft and the height above window head was changed to 0ft in Case 1 and, the difference in total energy consumption was 0.3%. When the eave length was changed to 1.5ft and the height above window head was changed to 0ft in Case 1 and, the difference in total energy consumption was 0.6%. When the eave length was changed to 2ft and the height above window head was changed to 0ft in Case 1 and, the difference in total energy consumption was 0.8%. Through this analysis, it was found that roof eaves did not make a significant difference in building energy use.

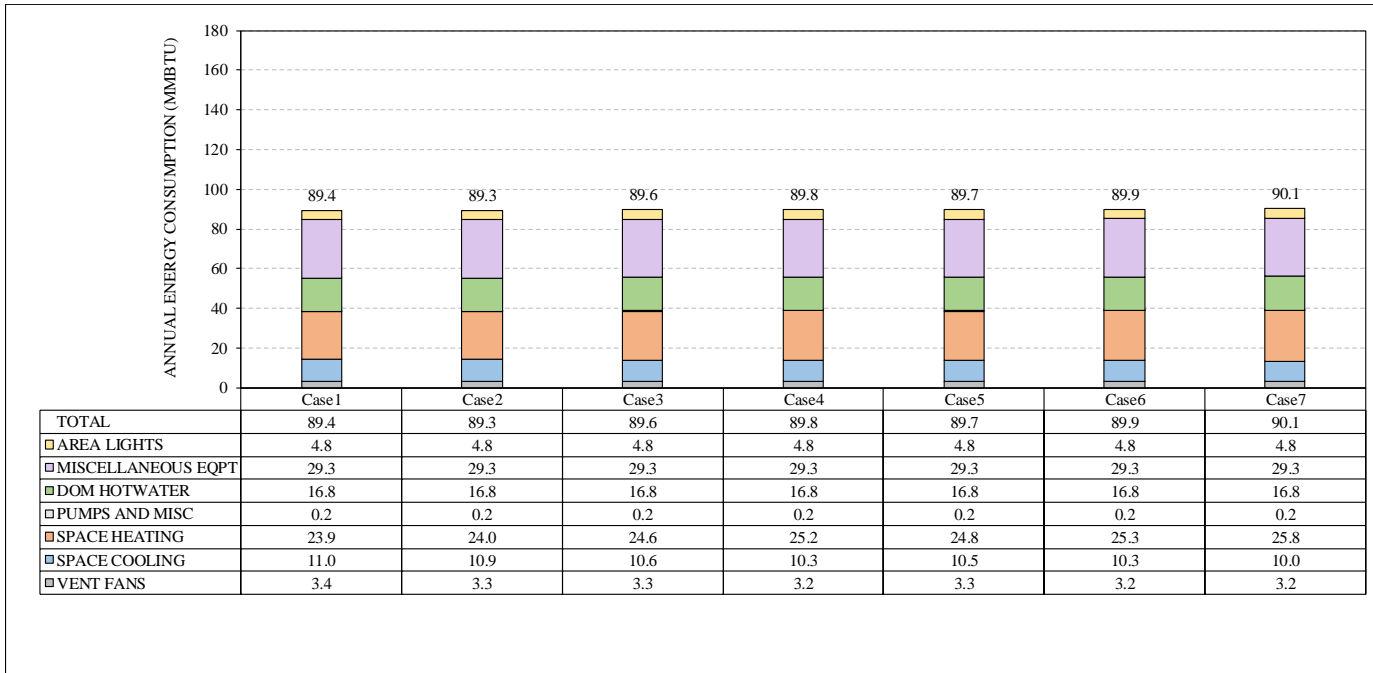


Figure 6.15: Annual building energy performance (BEPS) report

Table 6.19: Annual building energy performance (BEPS) report difference between the roof eaves

	Case1	Case2	Case3	Case4	Case5	Case6	Case7
AREA LIGHTS	-	0.0%	0.0%	0.0%	0.0%	0.0%	0.0%
MISCELLANEOUS EQPT	-	0.0%	0.0%	0.0%	0.0%	0.0%	0.0%
SPACE HEATING	-	0.4%	2.9%	5.4%	3.8%	5.9%	7.9%
SPACE COOLING	-	-0.9%	-3.6%	-6.4%	-4.5%	-6.4%	-9.1%
VENT FANS	-	-2.9%	-2.9%	-5.9%	-2.9%	-5.9%	-5.9%
TOTAL	-	-0.1%	0.2%	0.4%	0.3%	0.6%	0.8%

6.2.2. Window Setback

Table 6.20 shows the test cases for window setback analysis. In this study, window setback analysis was conducted according to window modeling methods (e.g. single window method and multiple window method) and setback depth.

Table 6.20: Test cases for window setback analysis

Case Number	Window Modeling Method	Setback Length (ft)
Case1 (Base-case)	Single	0
Case2	Single	0.25
Case3	Mutiple	0.25

Figure 6.16 and Table 6.21 show the annual building energy performance according to different window modeling methods, and setback depths. When the window setback was changed to 0.25 ft in Case 1 and, the difference in total energy consumption was 0.2%. When the window setback was changed to 0.25 ft and the window modeling method was changed to multiple windows in Case 1 and, the difference in total energy consumption was 0.1%. Through this analysis, it was found that window setbacks did not make a significant difference in building energy use.

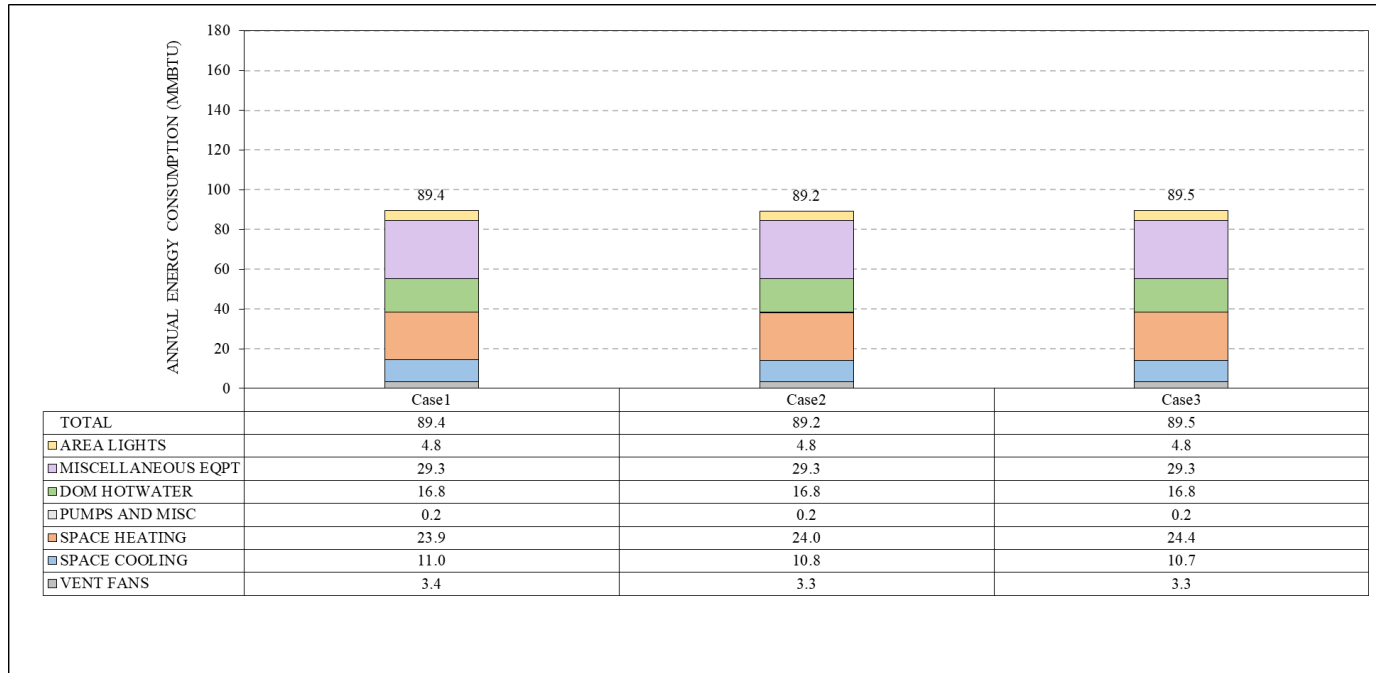


Figure 6.16: Annual building energy performance (BEPS) report

Table 6.21: Annual building energy performance (BEPS) report difference between the window frame type, width, and shape

	Case1	Case2	Case3
AREA LIGHTS	-	0.0%	0.0%
MISCELLANEOUS EQPT	-	0.0%	0.0%
SPACE HEATING	-	0.4%	2.1%
SPACE COOLING	-	-1.8%	-2.7%
VENT FANS	-	-2.9%	-2.9%
TOTAL	-	-0.2%	0.1%

6.3. Ground Heat Transfer

To investigate a more accurate method of calculating ground heat transfer, several tests were prepared using the DOE-2.1E program. As mentioned in Chapter 4.1.2.2, in actual buildings, ground heat transfer occurs mostly in the perimeter of the floor. However, DOE-2's ground heat transfer calculations resulted in the heat transfer through the whole floor including the perimeter zone. This causes more ground heat transfer than it is when using the DOE-2 program. To resolve this, the U-effective method was used in this analysis, which calculates the ground heat transfer around the perimeter of the building in the DOE-2 program. Since the ground heat transfer plays a major role in the energy use of a slab-on-grade residence, this adjustment was expected to have a large impact.

Since the floor of the slab-on-grade house directly contacts the ground, it is important to accurately calculate the heat transfer between the floor and the ground, to account the thermal mass of the surface. To analyze the ground heat transfer, tests were conducted according to the thermal mass, carpet, and floor insulation.

Table 6.22 shows the preliminary test cases for ground heat transfer analysis. In this study, ground heat transfer analysis was conducted according to ground heat transfer methods (e.g. Winklemann (U-effective) method and without the Winklemann method), and floor types (e.g. carpeted and uncarpeted).

Table 6.22: Preliminary tests for ground heat transfer analysis

Case Number	GC Method	Floor Type	Insulation Configuration
Case1 (Base-case)	with U-Effective (Perimeter Method)	Carpeted	Uninsulated
Case2		Uncarpeted	
Case3	without U-Effective	Carpeted	
Case4		Uncarpeted	

Figure 6.17 and Table 6.24 show the annual building energy performance according to different ground heat transfer methods and floor types. Table 6.23 shows the test cases for ground heat transfer analysis. In this study, ground heat transfer analysis was conducted according to slab constructions (e.g. thermal mass and without thermal mass), floor types (e.g. carpeted and uncarpeted floors), and insulation configurations (e.g. uninsulated, R-5 exterior, and R-10 exterior floors). Figure 6.18 and Table 6.25 show the annual building energy performance according to different slab constructions, floor types, and insulation configurations.

When the floor type was changed to the uncarpeted floor in Case 1 and, the difference in total energy consumption was 1.8%. When the floor type was changed to the carpeted floor without U-effective method in Case 1 and, the difference in total energy consumption was 18.1%. When the floor type was changed to the uncarpeted floor without U-effective method in Case 1 and, the difference in total energy consumption was 36.9%. Through this analysis, it was found that the use of U-effective method and the use of carpet have a great influence on energy consumption.

Table 6.23: Test cases for ground heat transfer analysis

Case Number	Slab Construction	Floor Type	Insulation Configuration
Case1 (Base-case)	With Thermal Mass Effect	Carpeted	Uninsulated
Case2		Uncarpeted	
Case3		Carpeted	R-5 exterior
Case4		Uncarpeted	
Case5		Carpeted	R-10 exterior
Case6		Uncarpeted	
Case7	Without Thermal Mass Effect	Carpeted	Uninsulated
Case8		Uncarpeted	
Case9		Carpeted	R-5 exterior
Case10		Uncarpeted	
Case11		Carpeted	R-10 exterior
Case12		Uncarpeted	

Figure 6.18 and Table 6.25 show the annual building energy performance according to different slab construction, floor type, and insulation configuration. When the floor type was changed to the uncarpeted floor with uninsulated insulation in Case 1 and, the difference in total energy consumption was 1.8%. When the insulation configuration was changed to R-5 exterior insulation in Case 1 and, the difference in total energy consumption was 1.9%. When the floor type was changed to the uncarpeted floor with R-5 exterior insulation in Case 1 and, the difference in total energy consumption was 4.1%. When the insulation configuration was changed to R-10 exterior insulation in Case 1 and, the difference in total energy consumption was 2.3%. When the floor type was changed to the uncarpeted floor with R-10 exterior insulation in Case 1 and, the difference in total energy consumption was 4.6%. When the insulation slab construction was changed to without thermal mass effect in Case 1 and, the difference in total energy consumption was 3.4%. When the insulation slab construction was changed to without thermal mass effect and the floor type was changed to the uncarpeted floor in

Case 1 and, the difference in total energy consumption was 4.2%. When the insulation slab construction was changed to without thermal mass effect and the floor type was changed to the carpeted floor with R-5 exterior floor insulation in Case 1 and, the difference in total energy consumption was 1.8%. When the insulation slab construction was changed to without thermal mass effect and the floor type was changed to the uncarpeted floor with R-5 exterior floor insulation in Case 1 and, the difference in total energy consumption was 2.1%. When the insulation slab construction was changed to without thermal mass effect and the floor type was changed to the carpeted floor with R-10 exterior floor insulation in Case 1 and, the difference in total energy consumption was 1.4%. When the insulation slab construction was changed to without thermal mass effect and the floor type was changed to the uncarpeted floor with R-10 exterior floor insulation in Case 1 and, the difference in total energy consumption was 1.7%. From this analysis, it was found that depending on the slab construction, floor type, and floor insulation configuration, the total building energy consumption could vary from 1.4% to 4.6%.

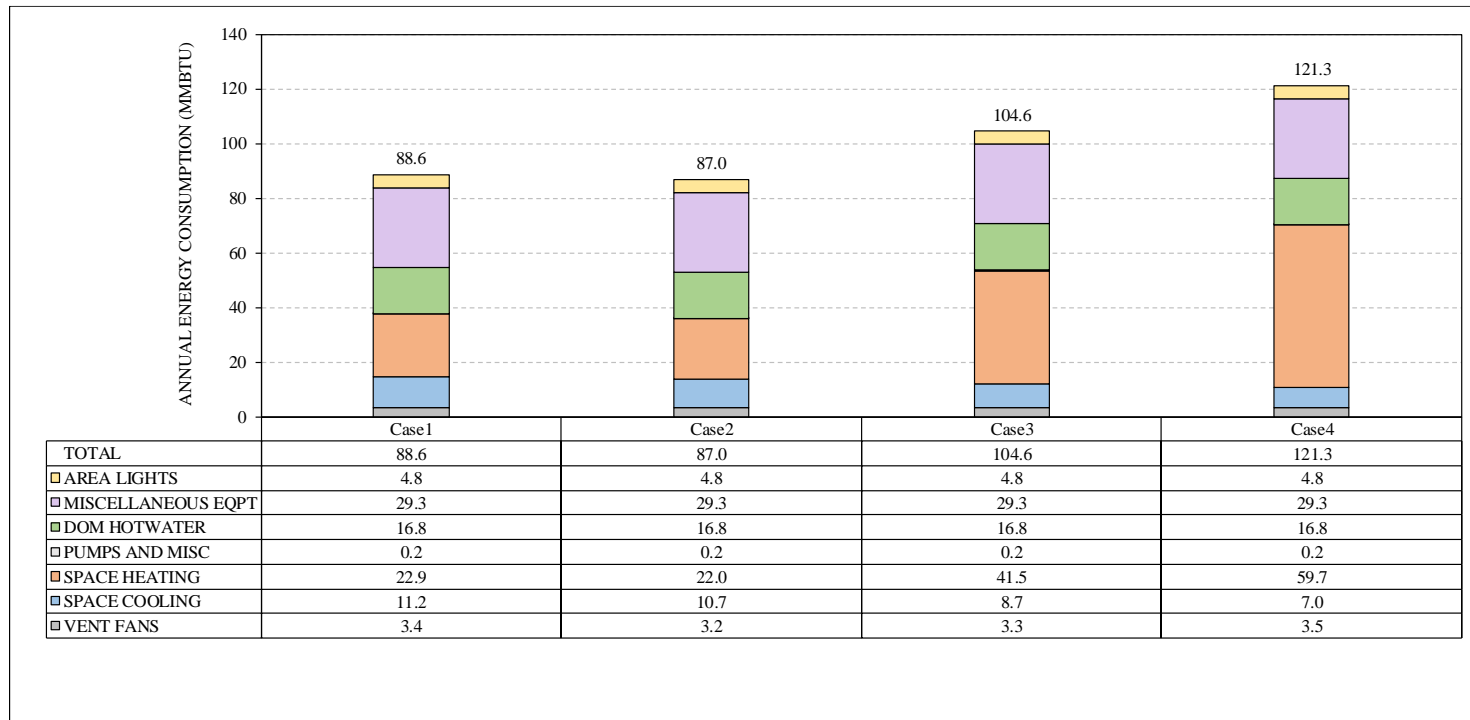


Figure 6.17: Annual building energy performance (BEPS) report

Table 6.24: Annual building energy performance (BEPS) report difference between ground heat transfer analysis

	Case1	Case2	Case3	Case4
AREA LIGHTS	-	0.0%	0.0%	0.0%
MISCELLANEOUS EQPT	-	0.0%	0.0%	0.0%
SPACE HEATING	-	-3.9%	81.2%	160.7%
SPACE COOLING	-	-4.5%	-22.3%	-37.5%
VENT FANS	-	-5.9%	-2.9%	2.9%
TOTAL	-	-1.8%	18.1%	36.9%

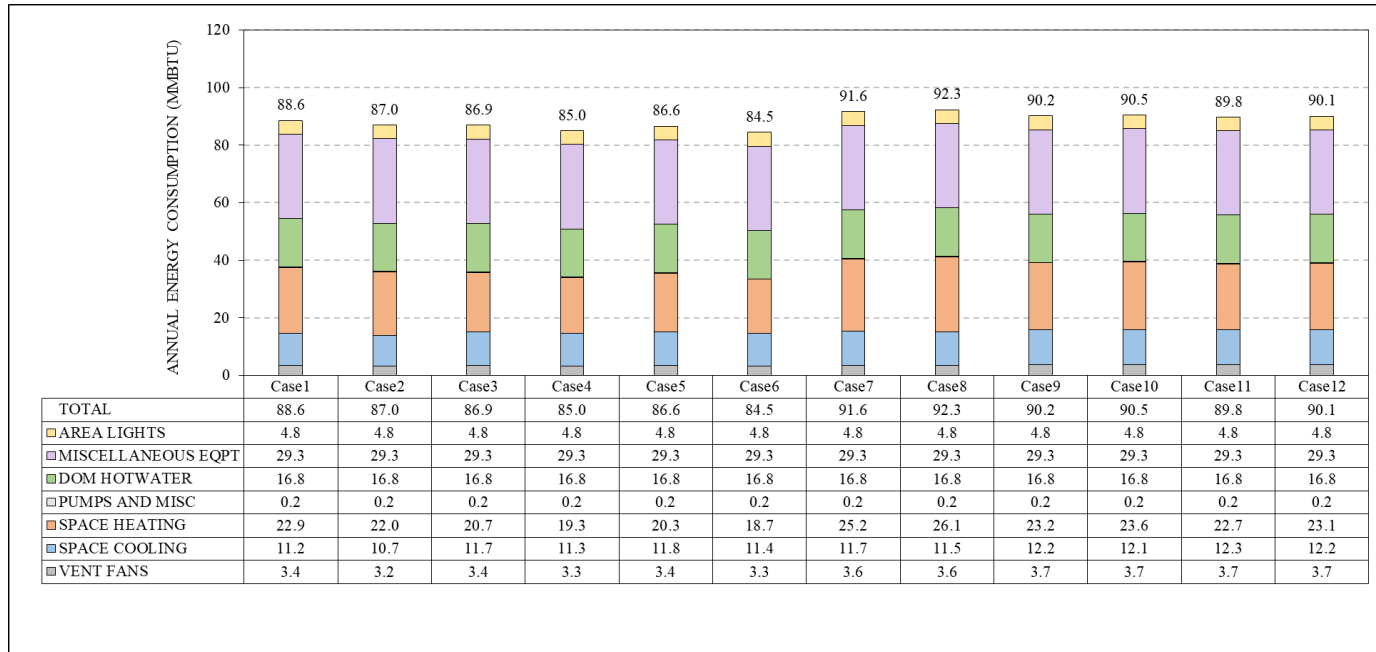


Figure 6.18: Annual building energy performance (BEPS) report

Table 6.25: Annual building energy performance (BEPS) report difference between ground heat transfer analysis

	Case1	Case2	Case3	Case4	Case5	Case6	Case7	Case8	Case9	Case10	Case11	Case12
AREA LIGHTS	-	0.0%	0.0%	0.0%	0.0%	0.0%	0.0%	0.0%	0.0%	0.0%	0.0%	0.0%
MISCELLANEOUS EQPT	-	0.0%	0.0%	0.0%	0.0%	0.0%	0.0%	0.0%	0.0%	0.0%	0.0%	0.0%
SPACE HEATING	-	-3.9%	-9.6%	-15.7%	-11.4%	-18.3%	10.0%	14.0%	1.3%	3.1%	-0.9%	0.9%
SPACE COOLING	-	-4.5%	4.5%	0.9%	5.4%	1.8%	4.5%	2.7%	8.9%	8.0%	9.8%	8.9%
VENT FANS	-	-5.9%	0.0%	-2.9%	0.0%	-2.9%	5.9%	5.9%	8.8%	8.8%	8.8%	8.8%
TOTAL	-	-1.8%	-1.9%	-4.1%	-2.3%	-4.6%	3.4%	4.2%	1.8%	2.1%	1.4%	1.7%

6.4. Attic and the Duct Model

Unconditioned attic spaces change temperature often depending on the ambient temperature, solar radiation, and thermal mass in the attic. In these attic spaces, ducts are often located, and these ducts exchange heat depending on the attic temperature, the duct insulation, and the leakage of the ducts. Therefore, in this study variation of the attic parameters was analyzed.

Table 6.26 shows the test cases for duct model analysis. In this study, duct model analysis was conducted according to attic thermal mass weighting factors, duct insulation values, and duct tightnesses.

Table 6.26: Test cases for duct model analysis

Case Number	Attic Thermal Mass	Duct R-value	Duct Tightness for Total Leakage
Case1 (Base-case)	Custom Weighting Factor	R-8	4 cfm/100sqft
Case2	9 lb/sqft		
Case3	30 lb/sqft		
Case4	Custom Weighting Factor	R-11	
Case5	9 lb/sqft		
Case6	30 lb/sqft		
Case7	Custom Weighting Factor	R-8	3.5 cfm/100sqft
Case8	9 lb/sqft		
Case9	30 lb/sqft		
Case10	Custom Weighting Factor	R-11	
Case11	9 lb/sqft		
Case12	30 lb/sqft		

Figure 6.19 and Table 6.27 show the annual building energy performance according to different attic thermal mass weighting factors, duct insulation values, and duct tightnesses. When the parameters for the duct model were changed to 9 lb/sqft attic thermal mass with R-8 duct insulation and 4 cfm/100sqft duct tightness in Case 1 and,

the difference in total energy consumption was 1.1%. When the parameters for the duct model were changed to 9 lb/sqft attic thermal mass with R-8 duct insulation and 4 cfm/100sqft duct tightness in Case 1 and, the difference in total energy consumption was 2.0%. When the parameters for the duct model were changed to the custom weighting factor for attic thermal mass with R-11 duct insulation and 4 cfm/100sqft duct tightness in Case 1 and, the difference in total energy consumption was 0.9%. When the parameters for the duct model were changed to 9 lb/sqft for attic thermal mass with R-11 duct insulation and 4 cfm/100sqft duct tightness in Case 1 and, the difference in total energy consumption was 1.8%. When the parameters for the duct model were changed to 30 lb/sqft for attic thermal mass with R-11 duct insulation and 4 cfm/100sqft duct tightness in Case 1 and, the difference in total energy consumption was 2.7%. When the parameters for the duct model were changed to the custom weighting factor for attic thermal mass with R-8 duct insulation and 3.5 cfm/100sqft duct tightness in Case 1 and, the difference in total energy consumption was 0.4%. When the parameters for the duct model were changed to 9 lb/sqft for attic thermal mass with R-8 duct insulation and 3.5 cfm/100sqft duct tightness in Case 1 and, the difference in total energy consumption was 1.5%. When the parameters for the duct model were changed to 30 lb/sqft for attic thermal mass with R-8 duct insulation and 3.5 cfm/100sqft duct tightness in Case 1 and, the difference in total energy consumption was 2.2%. When the parameters for the duct model were changed to the custom weighting factor for attic thermal mass with R-11 duct insulation and 3.5 cfm/100sqft duct tightness in Case 1 and, the difference in total energy consumption was 1.1%. When the parameters for the duct model were changed to

9 lb/sqft for attic thermal mass with R-11 duct insulation and 3.5 cfm/100sqft duct tightness in Case 1 and, the difference in total energy consumption was 2.2%. When the parameters for the duct model were changed to 30 lb/sqft for attic thermal mass with R-11 duct insulation and 3.5 cfm/100sqft duct tightness in Case 1 and, the difference in total energy consumption was 2.9%. In this analysis, it was found that depending on the attic thermal mass, duct R-value, and duct tightness, the total building energy consumption could vary from 0.4% to 2.9%.

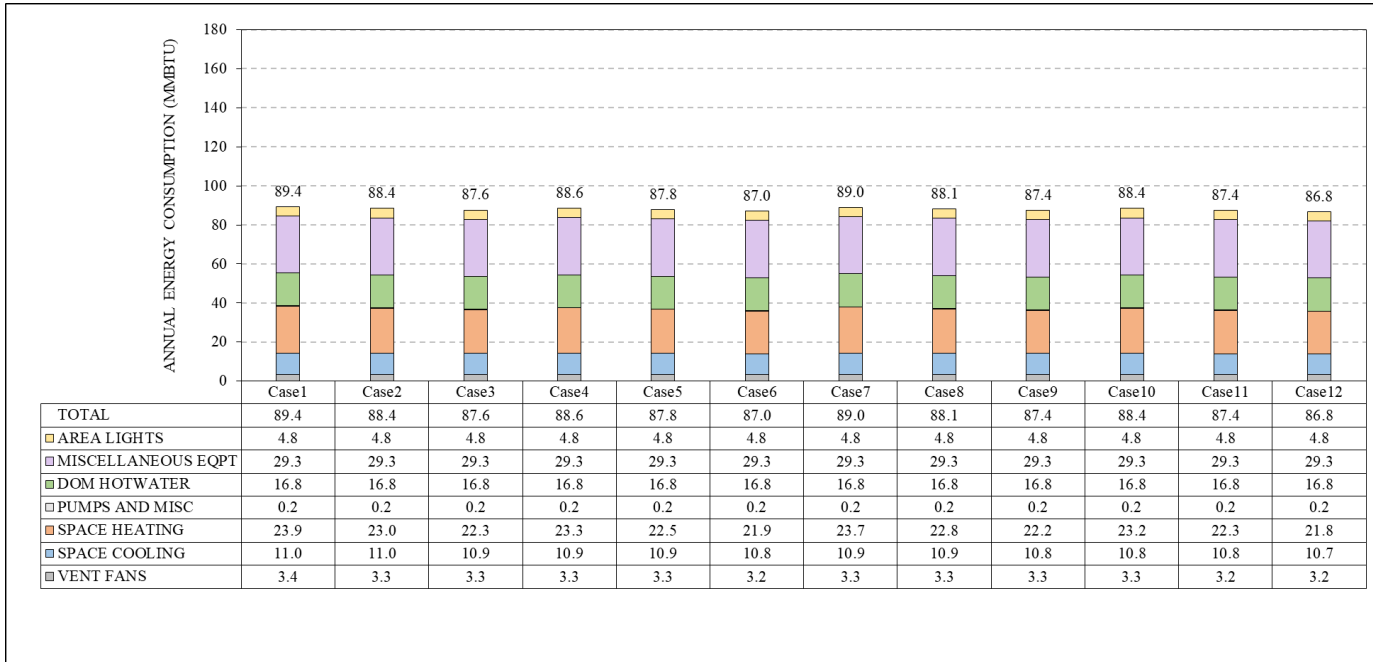


Figure 6.19: Annual building energy performance (BEPS) report

Table 6.27: Annual building energy performance (BEPS) report difference between duct model analysis

	Case1	Case2	Case3	Case4	Case5	Case6	Case7	Case8	Case9	Case10	Case11	Case12
AREA LIGHTS	-	0.0%	0.0%	0.0%	0.0%	0.0%	0.0%	0.0%	0.0%	0.0%	0.0%	0.0%
MISCELLANEOUS EQPT	-	0.0%	0.0%	0.0%	0.0%	0.0%	0.0%	0.0%	0.0%	0.0%	0.0%	0.0%
SPACE HEATING	-	-3.8%	-6.7%	-2.5%	-5.9%	-8.4%	-0.8%	-4.6%	-7.1%	-2.9%	-6.7%	-8.8%
SPACE COOLING	-	0.0%	-0.9%	-0.9%	-0.9%	-1.8%	-0.9%	-0.9%	-1.8%	-1.8%	-1.8%	-2.7%
VENT FANS	-	-2.9%	-2.9%	-2.9%	-2.9%	-5.9%	-2.9%	-2.9%	-2.9%	-2.9%	-5.9%	-5.9%
TOTAL	-	-1.1%	-2.0%	-0.9%	-1.8%	-2.7%	-0.4%	-1.5%	-2.2%	-1.1%	-2.2%	-2.9%

7. SUMMARY AND FUTURE RECOMMENDATIONS

7.1. Summary of the Case-Study House Simulation Analysis

For the case-study house simulation analysis, the simplified building energy models were tested using on-site measurements and calibrated simulation.

The results of the case-study house analysis are as follows.

- a. The annual building energy performance according to window setbacks, eaves, trees, and fences was analyzed. The difference in total energy consumption ranged from 0.0% to 1.6%.
- b. The annual building energy performance according of an attached garage and different roof types was analyzed. The difference in total energy consumption ranged from 0.7% to 2.0%.
- c. The annual building energy performance of different DHW inlet and outlet water temperatures was analyzed. The difference in total energy consumption ranged from 0.5% to 6.3%.
- d. The annual building energy performance according to different ground heat transfer methods was analyzed. The difference in total energy consumption ranged from 2.0% to 5.2%.

Simplified code-compliance models have helped building energy simulation to be more widely used in building energy code analysis. Moreover, it is very important to include important inputs in the user interface. Finally, for simulation of building energy

code compliance, care must be taken when selecting input and calculation methods for domestic hot water heaters and ground heat transfer.

7.2. Summary of the IECC House Simulation Analysis

For the IECC house simulation analysis, the impact of an improved fenestration, shading, ground heat transfer, and duct model was tested. The results of the IECC house analysis are as follows.

- a. The annual building energy performance according of different glass types, glazing calculation methods, and weighting factors was analyzed. The difference in total energy consumption ranged from 0% to 3%.
- b. The annual building energy performance according to different window frame types, frame width, and window shape was analyzed. The difference in total energy consumption ranged from -0.4% to 3.9%.
- c. The annual building energy performance according to different eave depths and the height above the window header was analyzed. The difference in total energy consumption ranged from -0.1% to 0.8%.
- d. The annual building energy performance according to different window modeling methods and setback depths was analyzed. The difference in total energy consumption ranged from -0.2% to 0.1%.
- e. The annual building energy performance according to different ground heat transfer models and floor types was analyzed. The difference in total energy consumption ranged from -1.8% to 36.9%.

- f. The annual building energy performance according of different slab construction, floor types, and insulation configurations was analyzed. The difference in total energy consumption ranged from -4.6% to 4.2%.

7.3. Summary of the Comparison of the Detailed Calibrated Model and the Simplified Uncalibrated Model

For the this analysis, the detailed calibrated model and the simplified uncalibrated model were compared. The results of the comparison of the detailed calibrated model and the simplified uncalibrated model are as follows.

- a. In this analysis, when selected parameters for the case-study house were replaced with IECC code-compliant parameters using the detailed calibrated model the total source energy usage was reduced by 24% compared to the detailed calibrated model of the case-study house without the parameters.
- b. When the simplified model was used on the same case-study house the total source energy use decreased by 19.3%.

7.4. Summary of the Selected Calibrations for Improving the Accuracy of a Simplified Model

For the this analysis, the selected calibrations were analyzed for improving the accuracy of a simplified model. In this analysis, the uncalibrated heating setpoint of 72F was reduced to 67.7F, which was the measured average setpoint temperature. In addition,

the uncalibrated cooling setpoint of 75F was decreased to 73.6F, and the DHW outlet temperature was changed from 120F to 135.3F. The results of the comparison of the selected calibrations are as follows.

- a. The analysis showed the model with selected calibration reduced the total source energy usage by 2.6% compared to the simplified uncalibrated model.
- b. The IECC code-compliant house model created by using the simplified, selected calibrated model reduced the total source energy usage by 2.2% compared to the IECC code-compliant house model created by using the simplified uncalibrated model.

7.5.Recommendations for Future Research

The purpose of this study is to compare analyzed results from the detailed building energy simulation model of an existing single-family residence versus the results from the simplified building energy simulation model of the same residence to determine which parameters that represent an existing house. To achieve this purpose, this study tested the influential input parameters and calculation models. The tests in this study were limited to the following:

- a. This study was focused on a single-family residential building code-compliance simulation;
- b. This study was performed using one single-family, IECC code-compliant detached case-study house in Texas (a hot and humid climate);

- c. This study was focused on a one-story, slab-on-grade house with a gas furnace for the heating and domestic water heating and an electric air-conditioner for cooling;
- d. This study used many of the simplifications in the ESL's IC3 simulation model; and
- e. This study was focused on the DOE-2.1e, ver 119 building energy simulation program.

The recommendations for future research as follow.

- a. Recommended future study for single-family residential building with several case-study houses: This study was limited to develop one detailed house model using a case-study house. It is recommended to develop additional detailed house simulation models using several case-study houses.
- b. Recommended future study for single-family residential buildings in different climate zones: This study was limited to houses in central Texas (a hot and humid climate). Therefore, it is recommended to conduct a detailed model analysis using case-study houses in different climate zones.
- c. Recommended future study for improved ground heat transfer: This study utilized the Winkelmann and Huang (W-H) ground heat transfer method for a slab-on-grade house as the detailed simulation model. Therefore, it is recommended to analyze a more detailed ground heat transfer models such as KIVA (Horowitz et al., 2016; Kruis & Karati, 2015). In addition, measurements

of underground temperatures and floor temperatures are recommended to help verify the ground heat transfer models.

- d. Recommended future study for DHW water usage. This study calibrated the DHW water usage using utility bills. For more accurate analysis, the DHW water usage (i.e., gallons/her) will be measured.
- e. Recommended future study using the NREL window model (Booten et al., 2012). This study utilized simplified input parameters of DOE-2.1e. Therefore, it is recommended to analyze with NREL window model to fix for DOE-2.1e ver 119.

REFERENCES

- Adelman, M. A. (2004). *The Real Oil Problem*. Regulation, 27, 16-21.
- AEC. (2016). *REM/Rate Simulation Software by Architectural Energy Corporation (AEC)*. Retrieved from www.homeinnovation.com/~media/Files/.../REMrate.pdf
- ANL. (2019). *Uncertainty Analysis and Bayesian Calibration*. Retrieved from <https://www.anl.gov/es/uncertainty-analysis-and-bayesian-calibration>
- ASHRAE. (2011). *ANSI/ASHRAE Standard 140-2011 : Standard Method of Test for the Evaluation of Building Energy Analysis Computer Programs*: American Society of Heating, Refrigerating and Air-Conditioning Engineers, Inc.
- ASHRAE. (2017). *ANSI/ASHRAE Standard 140-2017 : Standard Method of Test for the Evaluation of Building Energy Analysis Computer Programs*: American Society of Heating, Refrigerating and Air-Conditioning Engineers, Inc.

- Bartlett, R., Schultz, R., Connell, L., Taylor, Z., Wiberg, J., & Lucas, R. (2012). *Methodology for Developing the REScheck™ Software through Version 4.4.3*.
- Birru, D., Wen, T.-J., Rubinstein, F. M., & Clear, R. D. (2013). *Energy-Efficient and Comfortable Buildings through Multivariate Integrated Control (ECoMIC)*. Retrieved from <https://flexlab.lbl.gov/publications/energy-efficient-and-comfortable>
- Booten, C., Kruis, N., & Christensen, C. (2012). *Identifying and Resolving Issues in EnergyPlus and DOE-2 Window Heat Transfer Calculations*. Retrieved from <https://pdfs.semanticscholar.org/cd9b/6c3792a5d71a14f204cb62d8838c4b13fa82.pdf>
- Christensen, D. (2014). *HVAC Performance Maps - 2014 Building Technologies Office Peer Review*.
- Crowder, H., & Foster, C. (1998). *Building Energy Codes: New Trends*. *ACEEE*, 10, 31-40.
- CTTC. (2020). *The Incredible Shedding Live Oak*. Retrieved from <https://centraltexastreecare.com/2016/04/20/the-incredible-shedding-live-oak/>
- Determan, K. (2014). *Sustainability and Residential Development: A Guide to Cost-Efficient Green Building Technologies*. (Master), Massachusetts Institute of Technology.
- Do, S., & Choi, J. (2013). *A Simplified Residential Base-Case Model*. Retrieved from <https://oaktrust.library.tamu.edu/handle/1969.1/152122>
- DOE. (2012). *Choosing an Energy Code Compliance Path*: U.S. Department of Energy.
- DOE. (2013). *Choose a Compliance Path Within the Applicable Energy Code*. Retrieved from <https://www.energycodes.gov/resource-center/ace/compliance/step2>
- DOE. (2015a). *About Building Energy Codes*. Retrieved from <https://www.energycodes.gov/about>
- DOE. (2015b). *Commercial Compliance Using COMcheck™*. Retrieved from <https://www.energycodes.gov/comcheck>

- DOE. (2015c). *Residential Compliance Using REScheck™*. Retrieved from <https://www.energycodes.gov/rescheck>
- DOE. (2016). *Status of State Energy Code Adoption*. Retrieved from <https://www.energycodes.gov/status-state-energy-code-adoption>
- Duffie, J., & Beckman, W. (2014). *Solar Engineering of Thermal Processes* (4th ed.). New York: Wiley.
- EERE. (2017). *Test Procedures for Building Energy Simulation Tools*. Retrieved from <https://www.energy.gov/eere/buildings/downloads/test-procedures-building-energy-simulation-tools>
- ekotrope. (2016). *Energy Decisions That Drive Bussiness*. Retrieved from <http://www.ekotrope.com/>
- ESL. (2016). *International Code Compliance Calculator V4.2 User's Manual - Sep. 2016*: Energy Systems Laboratory.
- Fairey, P., Vieira, R. K., Parker, D. S., Hanson, B., Broman, P. A., Grant, J. B., . . . Gu, L. (2012). *EnergyGauge USA: A Residential Building Energy Simulation Design Tool*. Retrieved from <http://hdl.handle.net/1969.1/4562>
- Haddad, K. H., & Beausoleil-Morrison, I. (2001). *Results of the HERS BESTEST on an Energy Simulation Computer Program*. *ASHRAE Transactions*, 107, 713.
- Halverson, M., Johnson, J., Weitz, D., Majette, R., & Laliberte, M. (2002). *Making Residential Energy Codes More Effective: Building Science, Beyond Code Programs, and Effective Implementation Strategies*. *ACEEE*, 2, 111-122. Retrieved from https://www.aceee.org/files/proceedings/2002/data/papers/SS02_Panel2_Paper10.pdf
- Heldenbrand, J. L. (2001). *NBS Research and ASHRAE's 90 Series Standards*.
- Henninger, R., Witte, M., & Crawley, D. (2004). *Analytical and comparative testing of EnergyPlus using IEA HVAC BESTEST E100-E200 test suite*. *Energy and Buildings*, 36, 855-863.

- Historian, O. o. t. (2016). *Oil Embargo, 1973-1974*. Retrieved from <https://history.state.gov/milestones/1969-1976/oil-embargo>
- Horner, B. (2011). *Putting Energy Back Into the Energy Code*. *Lighting Design & Application*, 41(7), 34-36. Retrieved from <http://lib-ezproxy.tamu.edu:2048/login?url=http://search.ebscohost.com/login.aspx?direct=true&db=aci&AN=502024637&site=eds-live>
- Horowitz, S., Maguire, J., Tabares-Velasco, P. C., Winkler, J., & Christensen, C. (2016). *EnergyPlus and SEEM Modeling Enhancements via Software-to-Software Comparison Using NREL's BEopt Test Suite*. Retrieved from <https://www.nrel.gov/docs/fy16osti/65858.pdf>
- Huang, Y. J., Shen, L. S., Bull, J. C., & Goldberg, L. F. (1988). *Whole-House Simulation of Foundation Heat Flows Using the DOE-2.1C Program*. *ASHRAE Transactions*, 94. Retrieved from https://www.techstreet.com/standards/ot-88-02-2-whole-house-simulation-of-foundation-heat-flows-using-the-doe-2-1c-program?product_id=1714582
- Hui, S. (2003). *Effective Use of Building Energy Simulation for Enhancing Building Energy Codes*. Paper presented at the Eighth International IBPSA Conference, Eindhoven, Netherlands. <http://citeseerx.ist.psu.edu/viewdoc/download?doi=10.1.1.523.3573&rep=rep1&type=pdf>
- Hunn, B. D. (2010). *35 Years of Standard 90.1*. ASHRAE.
- IBHS. (2015). *Insurance Institute for Business & Home Safety's Building Code Resources: The Benefits of Statwide Building Codes*: Insurance Institute for Business & Home Safety.
- ICC. (2009). *2009 International Energy Conservation Code*: International Code Council.
- ICC. (2012). *2012 International Energy Conservation Code*: International Code Council.
- ICC. (2015). *2015 International Energy Conservation Code*: International Code Council.
- ICC. (2016). *About ICC*. Retrieved from <http://www.iccsafe.org/about-icc/overview/about-international-code-council/>

- ICC. (2018). *2018 International Energy Conservation Code*: International Code Council.
- Im, P. (2003). *A Methodology to Evaluate Energy Savings and NOx Emissions Reductions from the Adoption of the 2000 International Energy Conservation Code (IECC) to New Residences in Non-attainment and Affected Counties in Texas*. Texas A&M University.
- Im, P., Bhandari, M., & New, J. (2016). *Multi-Year Plan for Validation of EnergyPlus Multi-Zone HVAC System Modeling Using ORNL's Flexible Research Platform*. Retrieved from <https://info.ornl.gov/sites/publications/Files/Pub68267.pdf>
- Judkoff, R. (2008). *A methodology for validating building energy analysis simulations*. Retrieved from <http://purl.access.gpo.gov/GPO/LPS114415>
- Judkoff, R., & Neymark, J. (1995a). *Home Energy Rating System Building Energy Simulation Test (HERS BESTEST)* (Vol. 1).
- Judkoff, R., & Neymark, J. (1995b). *Home Energy Rating System Building Energy Simulation Test (HERS BESTEST)* (Vol. 2).
- Judkoff, R., & Neymark, J. (1995). *International Energy Agency Building Energy Simulation Test (BESTEST) and Diagnostic Method*.
- Judkoff, R., & Neymark, J. (1997a). *Home Energy Rating System Building Energy Simulation Test for Florida (Florida-HERS BESTEST)* (Vol. 1).
- Judkoff, R., & Neymark, J. (1997b). *Home Energy Rating System Building Energy Simulation Test for Florida (Florida-HERS BESTEST)* (Vol. 2).
- Judkoff, R., Neymark, J., & Kennedy, M. (2011). *Building Energy Simulation Test for Existing Homes (BESTEST-EX): Instructions for Implementing the Test Procedure, Calibration Test Reference Results, and Example Acceptance-Range Criteria*.
- Judkoff, R., Polly, B., & Bianchi, M. (2017). *Building Energy Simulation Test for Existing Homes (BESTEST-EX): Instructions for Implementing the Test Procedure, Calibration Test Reference Results, and Example Acceptance-Range Criteria*. Retrieved from <https://www.nrel.gov/docs/fy11osti/52414.pdf>

- Kim, K. H., & Baltazar, J.-C. (2010). *Procedure for Packing Weather Files for DOE-2.1e* (ESL-TR-10-09-03). Retrieved from <https://oaktrust.library.tamu.edu/handle/1969.1/187107>
- Kim, S. (2006). *An Analysis of International Energy Conservation Code (IECC) - Compliant Single-Family Residential Energy Use*. (Ph.D.), Texas A&M University.
- Kneifel, J. (2012). *Prototype Residential Building Designs for Energy and Sustainability Assessment*: National Institute of Standards and Technology.
- Kruis, N., & Karati, M. (2015). *Three-dimensional Accuracy with Two-dimensional Computation Speed: Using the KivaTM Numerical Framework to Improve Foundation Heat Transfer Calculations*. *Journal of Building Performance Simulation*, 10, 2017(2), 161-182.
- Lyons, R. K., Owens, K. M., & Machen, R. V. (2020). *Juniper Biology and Management in Texas*. Retrieved from <https://agrillifeextension.tamu.edu/library/ranching/juniper-biology-and-management-in-texas/>
- Mann, J. (2013). *A reassessment of the 1967 Arab oil embargo*. *Israel Affairs*, 19(iv), 693-703. Retrieved from <http://lib-ezproxy.tamu.edu:2048/login?url=http://search.ebscohost.com/login.aspx?direct=true&db=ich&AN=ICHA954267&site=eds-live>
- McNeil, A., Kohler, C., Lee, E., & Selkowitz, S. (2014). *High Performance Building Mockup in FLEXLAB* (LBNL-1005151). Retrieved from
- Mukhopadhyay, J., Baltazar, J. C., Haberl, J. S., & Yazdani, B. (2013). *Comparison of the Performance Predictions of a 2009 IECC Code-Compliant House Using IC3 (Ver.3.12.1), REM/Rate (Ver.13.00), EnergyGauge (Ver. 2.8.05) and ResCHECK (Ver. 4.4.3.1)*. Retrieved from <https://oaktrust.library.tamu.edu/handle/1969.1/152123>
- Neymark, J., & Judkoff, R. (2002). *International Energy Agency Building Energy Simulation Test and Diagnostic Method for Heating, Ventilating, and Air-Conditioning Equipment Models (HVAC BESTEST)* (Vol. 1).

- Neymark, J., & Judkoff, R. (2004). *International Energy Agency Building Energy Simulation Test and Diagnostic Method for Heating, Ventilating, and Air-Conditioning Equipment Models (HVAC BESTEST)* (Vol. 2).
- Neymark, J., & Judkoff, R. (2008). *International Energy Agency Building Energy Simulation Test and Diagnostic Method (IEA BESTEST) Multi-Zone Non-Airflow In-Depth Diagnostic Cases: MZ320 - MZ360*.
- NORESCO. (2016a). *NORESCO Completes Architectural Energy Corp. and Dome-Tech Intergration, Expands Energy and Sustainability Services*. Retrieved from <http://www.noresco.com/energy-services/en/us/news/news-article/noresco-completes-architectural-energy-corp-and-dome-tech-integration-expands-energy-and-sustainability-services.aspx>
- NORESCO. (2016b). *REM/RATETM*. Retrieved from <http://www.remrate.com/home/desktop>
- ORNL. (2019). *Flexible Research Platforms*. Retrieved from <https://www.ornl.gov/content/flexible-research-platforms>
- Patterson, S. (2020). *What are Deciduous Trees and Shrubs: Types of Deciduous Trees and Shrubs*. Retrieved from <https://www.gardeningknowhow.com/ornamental/trees/tgen/what-are-deciduous-plants.htm>
- Peng, J., Goudey, H., Thanachareonkit, A., Curcija, C., & Lee, E. (2017). *Measurement & Verification of the Performance of Solaria BIPV in Flexbla Test Facility*: Lawrence Berkeley National Laboratory.
- Polly, B., Kruis, N., & Roberts, D. (2011). *Assessing and Improving the Accuracy of Energy Analysis for Residential Buildings*. Retrieved from <http://www.nrel.gov/docs/fy11osti/50865.pdf>
- Raslan, R., & Davies, M. (2010). *An Analysis of Industry Capability for the Implementation of a Software-based Compliance Approach for the UK Building Regulations*. *Building Services Engineering Research and Technology*, 31 (2), 141-162.
- Raslan, R., Davies, M., & Doylend, N. (2009). *An Analysis of Results Variability in Energy Performance Compliance Verification Tools*. Paper presented at the Eleventh International IBPSA Conference.

- RESNET. (2013). *Mortgage Industry National Home Energy Rating Systems Standards*. Retrieved from https://12eliy2nfgkv28dsuc43nr17-wpengine.netdna-ssl.com/wp-content/uploads/RESNET-Mortgage-Industry-National-HERS-Standards_3-8-17.pdf
- RESNET. (2016a). *ANSI/RESNET/ICC 301-2014 Standard for the Calculation and Labeling of the Energy Performance of Low-Rise Residential Buildings using an Energy Rating Index*: Residential Energy Services Network.
- RESNET. (2016b). *Energy Rating Index Performance Path - Overview of the ERI Performance Path in the 2015 IECC*. Retrieved from http://www.resnet.us/uploads/documents/EnergyRatings_FactSheet1_Final.pdf
- RESNET. (2016c). *National Registry of Accredited IECC Performance Verification Software Tools*. Retrieved from http://www.resnet.us/professional/programs/iecc_programs
- RESNET. (2016d). *Procedures for Verification of International Energy Conservation Code (IECC) Performance Path Calculation Tools (003-16 ed.)*: Residential Energy Services Network.
- RESNET. (2017). *Procedures for Verification of RESNET Accredited HERS Software Tools (002-2017 ed.)*: Residential Energy Services Network.
- RESNET. (2020a). *Accredited HERS Software Tools*. Retrieved from <https://www.resnet.us/providers/accredited-providers/hers-software-tools/>
- RESNET. (2020b). *Procedures for Verification of RESNET Accredited HERS Software Tools (002-2020 ed.)*: Residential Energy Services Network.
- Schwartz, Y., & Raslan, R. (2013). *Variations in Results of Building Energy Simulation Tools, and Their Impact on BREEAM and LEED Ratings: A Case Study*. *Energy and Buildings*, 62(July 2016), 350-359.
- Taylor, Z., & Lucas, R. (2010). *An Estimate of Residential Energy Savings From IECC Change Proposals Recommended for Approval at the ICC's Fall, 2009, Initial Action Hearings*.
- TPDDL. (2020). *Live Oak Dropping Leaves in Early Spring*. Retrieved from <https://plantclinic.tamu.edu/factsheets/live->

[oak/#:~:text=Live%20oaks%2C%20also%20known%20as,leaves%20emerge%20in%20the%20spring.](#)

Wilson, E., Engerbrecht Metzger, C., Horowitz, S., & Hendron, R. (2014). *2014 Building America House Simulation Protocols*: National Renewable Energy Laboratory.

Winkelmann, F. C. (2002). *Underground Surface: How to Get a Better Underground Surface Heat Transfer Calculation in DOE-2.1E*. *Building Energy Simulation User News*, 19(1).

Winkelmann, F. C., Birdsall, B. E., Buhl, W. F., Erdem, A. E., Hirsch, J. J., & Gates, S. (1983). *DOE-2 Supplement Version 2.1E* (pp. 2.99): Lawrence Berkely Laboratory and Hirsch & Associates.

APPENDIX A

WINDOW PROPERTIES IN DOE-2.1E WINDOW LIBRARY

(Source: DOE-2 Supplement Version 2.1E (1993); pp.2.98 – 2.114)

DOE-2.1E has a large number of glazings in the Window Library. Each glazing provides information on transmittance according to the angle of incidence of solar radiation and thermal conductance of glazing according to temperature and wind speed. If glazing is specified in this window library in the DOE-2 simulation, the information described above is applied to the simulation. There are three methods in DOE-2.1E, but in this study, the shading coefficient method and the window library method are compared.

Table A.1 Differences between DOE-2.1E Window Glazing Calculation Methods

Method	Advantage	Disadvantage
Shading Coefficient	1) Convenient to use	1) Inaccurate angular dependence transmittance for multipane glazing 2) Inaccurate conductance calculation for glazing
GLASS-TYPE-CODE \leq 11	1) More accurate angular dependence transmittance for glazing	1) Inaccurate conductance calculation for glazing
Window Library	1) More accurate angular dependence transmittance for glazing 2) More accurate conductance calculation for glazing	1) Increase the required computer resource 2) Increase the simulation time

In this study, three glazings were selected from the window library. The information on the library used for the selected glazing is shown in Figure A.1, Figure A.2, and Figure A.3. Also, what each line of the library information describes is as follows.

<i>Line</i>	<i>Description</i>
3.	Units type. All units in this library are SI.
5.	Short description of glazing; same descriptor appears in the Index to the Window Library, Table 2.12. "Single Band Calculation" means that the optical properties of the glazing system were calculated by WINDOW-4 using the total (wavelength-integrated) optical properties of the glass layers. "Multiple Band Calculation" means that the properties of the glazing system were calculated wavelength by wavelength using the spectral properties of the layers, and then averaged to give the total properties over the solar, visible, and thermal infrared spectral ranges (see WINDOW-4 documentation).
6.	GLASS-TYPE-CODE
7.	Tilt angle in degrees for which the U-values, lines 52-55, were calculated; tilt = 90 corresponds to vertical glazing. DOE-2 recalculates U-value for actual tilt of glazing.
8.	Number of panes.
9.	Frame type ID, frame descriptor, and U-value of frame (which was used to calculate the frame contribution to the overall U-values in lines 52-55). Other frame U-values besides the one indicated can be specified in the DOE-2 input.
10.	SPACER-TYPE-CODE, spacer descriptor, and spacer coefficients. Used to calculate the edge-of-glass contribution to the overall U-values in lines 52-55. Other SPACER-TYPE-CODEs can be entered in the DOE-2 input.
11-14.	Overall height and width of window including frame; height and width of glazed portion of window, excluding frame. Used to calculate overall U-values in lines 52-55, but not used by DOE-2. Actual frame and glazing dimensions must be separately specified in the DOE-2 input for the window.
17-21.	Thermophysical properties of the gap gas fill. For double glazing, only gap 1 (line 17) is relevant. For triple glazing, only gaps 1 and 2 are relevant. In this example there is one gap and the gas fill is argon. Given are gap width (mm), conductivity ($W/m-K$), temperature derivative of conductivity ($W/m-K^2 \times 10^{-5}$), viscosity ($kg/m-s \times 10^{-5}$), temperature derivative of viscosity ($kg/m-s-K \times 10^{-7}$), density (kg/m^3), temperature derivative of density (kg/m^3-K), Prandtl number, and temperature derivative of Prandtl number ($1/K$).

- 23-35. Center-of-glass solar-optical properties of the glazing for angles of incidence between 0° (normal incidence) and 90° , and for hemispherical diffuse radiation:
- Tsol = overall solar transmittance of glazing assembly.
 - Abs N = solar absorptance of pane N , i.e., the fraction of incident solar absorbed in pane N .
 - Rfsol = overall solar reflectance of the glazing assembly for radiation incident from the front, i.e., from the outside. Not used by DOE-2.
 - Rbsol = overall solar reflectance for radiation incident from the back, i.e., from the inside.
 - Tvis = overall visible transmittance of the glazing assembly.
 - Rfvis, Rbvis = the overall visible reflectance for radiation incident from the front and back, respectively.
 - SHGC = the solar heat gain coefficient, which is the fraction of the solar radiation incident on the glazing that enters the room as heat. Calculated by WINDOW-4 for ASHRAE summer conditions (95F outside temperature, 75F room temperature, 7.5 mph windspeed, and near-normal incident solar radiation of 248 Btu/h-ft²). Not used by DOE-2.
36. Center-of-glass shading coefficient, which is the solar heat gain through the center of the glazing divided by the solar heat gain through 1/8-in, double-strength clear glass. Calculated by WINDOW-4 for ASHRAE summer conditions. (Note: the version of WINDOW-4 available at the time of this writing (Feb 1993) calculates this as the *overall* shading coefficient [glazing plus frame], rather than the center-of-glass shading coefficient. This has no effect on DOE-2 results since DOE-2 does not use the shading coefficient value from the Window Library.)
- 40-46. Thermophysical data for each pane. Layer ID# = identification number from the WINDOW-4 Glass Layer Library, Appendix D.
- Tir = thermal infrared transmittance.
 - Emis F, Emis B = thermal emissivity of front and back surface, respectively.
 - Cond = conductance (W/m²-K),
 - Spectral File = name of file containing transmittance and reflectance values at different wavelengths for each glass layer for multiband calculation of overall solar-optical properties of the glazing assembly (see WINDOW-4 documentation).
- 48-51. Headings for the table in lines 52-55.
- 52-55. Summary table of U-values for overall window (including edge of glass and frame) and for center of glass, as a function of incident solar radiation, windspeed, and outdoor temperature. All values shown are as calculated by WINDOW-4. (These values are recalculated each hour by DOE-2.) hcout and hrout are convective and radiative outside air film conductances, respectively (hrout assumes the outside surface radiates to a black body). hin is the combined convective plus radiative inside air film conductance (assuming the inside surface radiates to a black body). Column pairs beneath each outside temperature give overall and center-of-glass U-values.
- For example, 1.46W/m²-K is the center-of-glass U-value for outdoor temperature = -17.8°C (0°F), incident solar radiation = 0, and windspeed = 6.71 m/s (15 mph). The bold faced quantities here are used only in the DOE-2 Custom Weighting Factor calculation.

WINDOW 3.2 Data File : Single Band Calculation											
Unit System: SI											
Name	: DOE2 WINDOW LIB										
Desc	: SINGLE CLEAR										
Window ID	: 1000										
Tilt	: 90.0										
Glazings	: 1										
Frame	: 3 Alum, flush			3.970							
Spacer	: 1 Aluminum			1.310			0.736		0.000		
Total Height: 1828.8 mm											
Total Width: 1219.2 mm											
Glass Height: 1714.5 mm											
Glass Width: 1104.9 mm											
Mullion : None											
Gap	Thick	Cond	dCond	Vis	dVis	Dens	dDens	Pr	dPr		
1 Air	0.	0.	0.	0.	0.	0.	0.	0.	0.		
2 Air	0.	0.	0.	0.	0.	0.	0.	0.	0.		
3 Air	0.	0.	0.	0.	0.	0.	0.	0.	0.		
4 Air	0.	0.	0.	0.	0.	0.	0.	0.	0.		
5 Air	0.	0.	0.	0.	0.	0.	0.	0.	0.		
Angle	0.	10.	20.	30.	40.	50.	60.	70.	80.	90. Hemis	
Tsol	0.837	0.836	0.835	0.830	0.821	0.800	0.752	0.639	0.390	0.000 0.756	
Abs1	0.088	0.089	0.090	0.093	0.097	0.101	0.105	0.108	0.105	0.000 0.098	
Abs2	0.	0.	0.	0.	0.	0.	0.	0.	0.	0.	
Abs3	0.	0.	0.	0.	0.	0.	0.	0.	0.	0.	
Abs4	0.	0.	0.	0.	0.	0.	0.	0.	0.	0.	
Abs5	0.	0.	0.	0.	0.	0.	0.	0.	0.	0.	
Abs6	0.	0.	0.	0.	0.	0.	0.	0.	0.	0.	
Rfsol	0.075	0.075	0.075	0.077	0.083	0.099	0.143	0.253	0.505	1.000 0.136	
Rbsol	0.075	0.075	0.075	0.077	0.083	0.099	0.143	0.253	0.505	1.000 0.136	
Tvis	0.898	0.898	0.897	0.895	0.887	0.868	0.820	0.703	0.439	0.000 0.820	
Rfvis	0.081	0.081	0.081	0.083	0.090	0.107	0.154	0.270	0.534	1.000 0.146	
Rbvis	0.081	0.081	0.081	0.083	0.090	0.107	0.154	0.270	0.534	1.000 0.146	
SHGC	0.860	0.860	0.858	0.855	0.846	0.826	0.779	0.668	0.418	0.000 0.782	
SC:	1.00										
Layer ID#	2		0	0	0	0	0	0			
Tir	0.000		0.	0.	0.	0.	0.	0.			
Emis F	0.840		0.	0.	0.	0.	0.	0.			
Emis B	0.840		0.	0.	0.	0.	0.	0.			
Thickness(mm)	3.0		0.	0.	0.	0.	0.	0.			
Cond(W/m2-C)	300.0		0.	0.	0.	0.	0.	0.			
Spectral File	None		None	None	None	None	None	None			
Overall and Center of Glass Window U-values (W/m2-C)											
Outdoor Temperature						-17.8 C		15.6 C		26.7 C 37.8 C	
Solar	WdSpd	hcout	hroun	hin							
(W/m2)	(m/s)	(W/m2-C)									
0	0.00	12.25	3.43	8.23	5.10	5.30	4.83	4.98	4.82	4.97	5.33 5.57
0	6.71	25.47	3.33	8.30	5.95	6.31	5.49	5.76	5.46	5.72	6.13 6.51
783	0.00	12.25	3.48	8.17	5.09	5.28	4.56	4.66	5.06	5.25	5.43 5.69
783	6.71	25.47	3.37	8.27	5.94	6.29	5.34	5.58	5.67	5.97	6.22 6.61

Figure A.1 Single-pane Clear Glazing (ID: 1000)

WINDOW 3.2 Data File : Single Band Calculation												
Unit System: SI												
Name	: DOE2 WINDOW LIB											
Desc	: DOUBLE CLEAR IG											
Window ID	: 2000											
Tilt	: 90.0											
Glazings	: 2											
Frame	: 3	Alum, flush										3.970
Spacer	: 1	Aluminum	1.310	0.736	0.000							
Total Height: 1828.8 mm												
Total Width : 1219.2 mm												
Glass Height: 1714.5 mm												
Glass Width : 1104.9 mm												
Mullion : None												
Gap	Thick	Cond	dCond	Vis	dVis	Dens	dDens	Pr	dPr			
1 Air	6.3	0.02410	7.600	1.730	10.000	1.290	-0.0044	0.720	0.00180			
2 Air	0.	0.	0.	0.	0.	0.	0.	0.	0.			
3 Air	0.	0.	0.	0.	0.	0.	0.	0.	0.			
4 Air	0.	0.	0.	0.	0.	0.	0.	0.	0.			
5 Air	0.	0.	0.	0.	0.	0.	0.	0.	0.			
Angle	0.	10.	20.	30.	40.	50.	60.	70.	80.	90.	Hemis	
Tsol	0.705	0.704	0.700	0.693	0.678	0.646	0.577	0.436	0.204	0.000	0.601	
Abs1	0.094	0.094	0.096	0.099	0.103	0.109	0.117	0.127	0.133	0.000	0.108	
Abs2	0.074	0.074	0.076	0.078	0.080	0.081	0.081	0.074	0.055	0.000	0.076	
Abs3	0.	0.	0.	0.	0.	0.	0.	0.	0.	0.	0.	
Abs4	0.	0.	0.	0.	0.	0.	0.	0.	0.	0.	0.	
Abs5	0.	0.	0.	0.	0.	0.	0.	0.	0.	0.	0.	
Abs6	0.	0.	0.	0.	0.	0.	0.	0.	0.	0.	0.	
Rfsol	0.128	0.128	0.128	0.130	0.139	0.164	0.226	0.363	0.608	1.000	0.205	
Rbsol	0.128	0.128	0.128	0.130	0.139	0.164	0.226	0.363	0.608	1.000	0.205	
Tvis	0.812	0.811	0.810	0.806	0.794	0.763	0.690	0.533	0.270	0.000	0.709	
Rfvis	0.147	0.147	0.147	0.150	0.161	0.189	0.260	0.415	0.678	1.000	0.235	
Rbvis	0.147	0.147	0.147	0.150	0.161	0.189	0.260	0.415	0.678	1.000	0.235	
SHGC	0.760	0.760	0.757	0.752	0.739	0.708	0.640	0.497	0.255	0.000	0.660	
SC: 0.88												
Layer ID#		2	2	0	0	0	0	0				
Tir		0.000	0.000	0.	0.	0.	0.	0.				
Emis F		0.840	0.840	0.	0.	0.	0.	0.				
Emis B		0.840	0.840	0.	0.	0.	0.	0.				
Thickness(mm)		3.0	3.0	0.	0.	0.	0.	0.				
Cond(W/m2-C)		300.0	300.0	0.	0.	0.	0.	0.				
Spectral File		None	None	None	None	None	None	None				
Overall and Center of Glass Window U-values (W/m2-C)												
Outdoor Temperature				-17.8 C		15.6 C		26.7 C		37.8 C		
Solar	WdSpd	hcout	hrout	hin								
(W/m2)	(m/s)	(W/m2-C)										
0	0.00	12.25	3.31	7.96	3.19	2.96	3.23	3.00	3.27	3.06	3.48	3.32
0	6.71	25.47	3.25	8.00	3.41	3.23	3.44	3.27	3.49	3.32	3.73	3.62
783	0.00	12.25	3.41	7.68	3.20	2.97	3.34	3.14	3.48	3.32	3.61	3.47
783	6.71	25.47	3.31	7.80	3.42	3.24	3.51	3.35	3.70	3.58	3.85	3.77

Figure A.2 Double-pane Clear Glazing (ID: 2000)

WINDOW 3.2 Data File : Single Band Calculation

Unit System: SI
Name : DOE2 WINDOW LIB
Desc : DOUBLE LOW-E (e2=.04) TINT IG
Window ID : 2666
Tilt : 90.0
Glazings : 2
Frame : 3 Alum, flush 3.970
Spacer : 1 Aluminum 1.310 0.736 0.000
Total Height: 1828.8 mm
Total Width : 1219.2 mm
Glass Height: 1714.5 mm
Glass Width : 1104.9 mm
Mullion : None

Gap	Thick	Cond	dCond	Vis	dVis	Dens	dDens	Pr	dPr
1 Air	6.3	0.02410	7.600	1.730	10.000	1.290	-0.0044	0.720	0.00180
2 Air	0.	0.	0.	0.	0.	0.	0.	0.	0.
3 Air	0.	0.	0.	0.	0.	0.	0.	0.	0.
4 Air	0.	0.	0.	0.	0.	0.	0.	0.	0.
5 Air	0.	0.	0.	0.	0.	0.	0.	0.	0.

Angle	0.	10.	20.	30.	40.	50.	60.	70.	80.	90.	Hemis
Tsol1	0.208	0.209	0.205	0.201	0.194	0.183	0.161	0.118	0.054	0.000	0.171
Abs1	0.606	0.612	0.617	0.618	0.613	0.607	0.598	0.560	0.413	0.001	0.587
Abs2	0.041	0.042	0.042	0.042	0.043	0.044	0.043	0.038	0.027	0.000	0.041
Abs3	0.	0.	0.	0.	0.	0.	0.	0.	0.	0.	0.
Abs4	0.	0.	0.	0.	0.	0.	0.	0.	0.	0.	0.
Abs5	0.	0.	0.	0.	0.	0.	0.	0.	0.	0.	0.
Abs6	0.	0.	0.	0.	0.	0.	0.	0.	0.	0.	0.
Rfsol1	0.145	0.138	0.136	0.139	0.149	0.166	0.199	0.284	0.505	0.999	0.191
Rbsol1	0.325	0.321	0.319	0.318	0.320	0.330	0.357	0.429	0.596	1.000	0.352
Tvis	0.407	0.409	0.403	0.396	0.385	0.364	0.318	0.230	0.106	0.000	0.338
Rfvis	0.077	0.069	0.067	0.070	0.082	0.102	0.140	0.236	0.475	0.999	0.130
Rbvis	0.111	0.105	0.104	0.108	0.122	0.152	0.216	0.360	0.629	1.000	0.192
SHGC	0.304	0.306	0.303	0.299	0.293	0.281	0.257	0.206	0.119	0.000	0.265
SC:	0.35										




Layer ID#	550	3	0	0	0	0
Tir	0.000	0.000	0.	0.	0.	0.
Emis F	0.840	0.840	0.	0.	0.	0.
Emis B	0.040	0.840	0.	0.	0.	0.
Thickness(mm)	6.0	6.0	0.	0.	0.	0.
Cond(W/m2-C)	150.0	150.0	0.	0.	0.	0.
Spectral File	None	None	None	None	None	None

Overall and Center of Glass Window U-values (W/m2-C)

Outdoor Temperature	-17.8 C						15.6 C		26.7 C		37.8 C	
Solar (W/m2)	WdSpd (m/s)	hcout (W/m2-C)	hrout (W/m2-C)	hin								
0	0.00	12.25	3.28	7.81	2.57	2.19	2.58	2.21	2.61	2.23	2.71	2.36
0	6.71	25.47	3.23	7.84	2.69	2.34	2.69	2.34	2.71	2.37	2.83	2.51
783	0.00	12.25	3.80	6.50	2.54	2.16	2.76	2.42	2.81	2.49	2.86	2.55
783	6.71	25.47	3.53	7.23	2.69	2.34	2.83	2.51	2.89	2.59	2.95	2.66

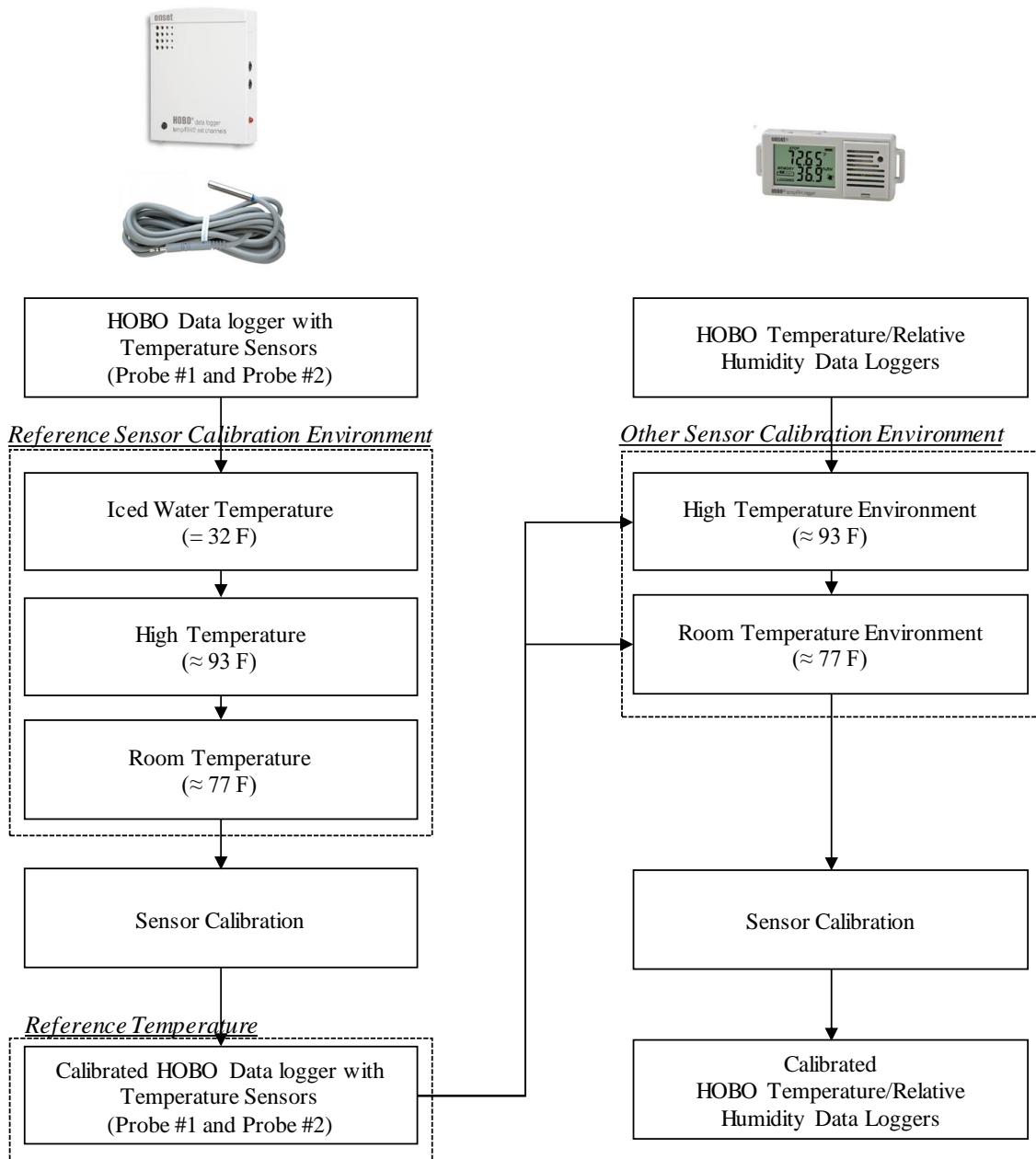
Figure A.3 Double-pane Low-E Glazing (ID: 2666)

APPENDIX B
SPECIFICATIONS OF MEASURING INSTRUMENTS FOR DHW

Product	Company	Model	Measurement Range	Accuracy	# of Devices	Cost
 <p>HOBO Temperature/Relative Humidity/2 External Channel Data Logger</p>	ONSET	U12-13	a. Temperature: -4° to 158°F b. RH: 5% to 95% RH	a. Temperature: ±0.63°F from 32° to 122°F b. RH: ±2.5% from 10% to 90% RH (typical), to a maximum of ±3.5% , see Plot B in manual c. External input channel: ± 2 mV ± 2.5% of absolute reading	1	\$140 USD/EA
 <p>Air/Water/Soil Temperature Sensor - 6' cable</p>	ONSET	TMCx-HD	a. Temperature: -40° to 122°F in water; -40° to 212°F in air	a. Temperature: with U12: ±0.45°F from 32° to 122°F	2	\$39 USD/EA
 <p>HOBO Temperature/Relative Humidity 3.5% Data Logger</p>	ONSET	UX100-003	a. Temperature: -4° to 158°F b. RH: 15% to 95% RH	a. Temperature: ±0.38°F from 32° to 122°F b. RH: ±3.5% from 25% to 85% including hysteresis at 77°F; below 25% and above 85% ±5% typical	3	\$89 USD/EA

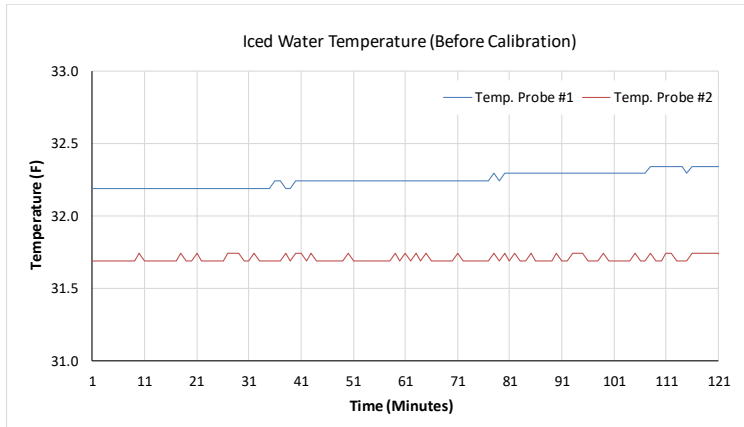
APPENDIX C
CALIBRATION OF MEASURING INSTRUMENTS FOR DHW

Calibration Procedure Diagram

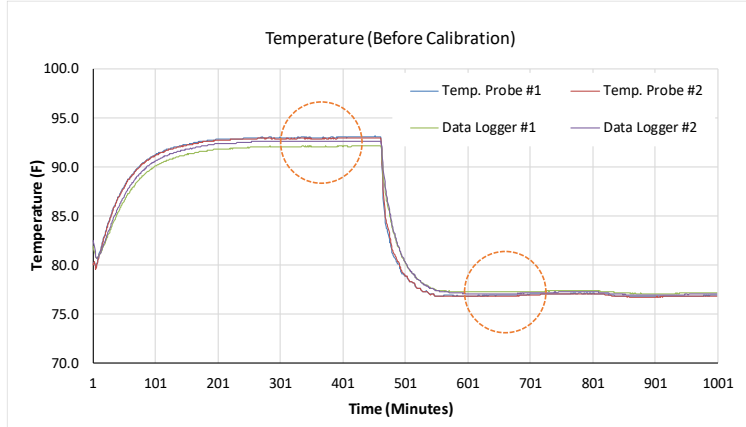


Reference Sensor Calibration (Before Calibration)

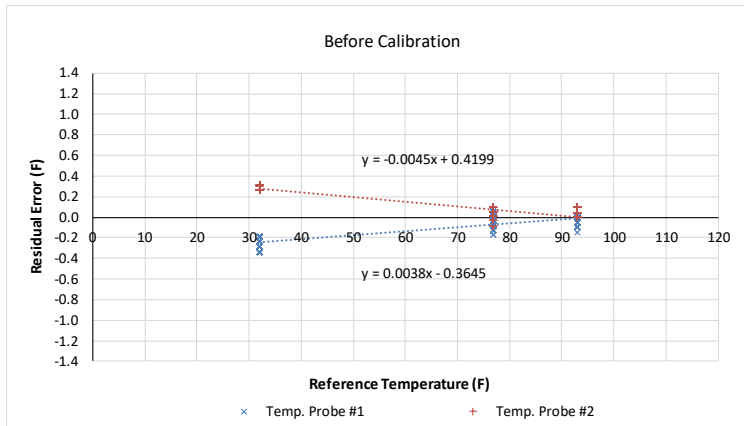
Iced Water Temperature Environment



High and Room Temperature Environments



Residual Plot

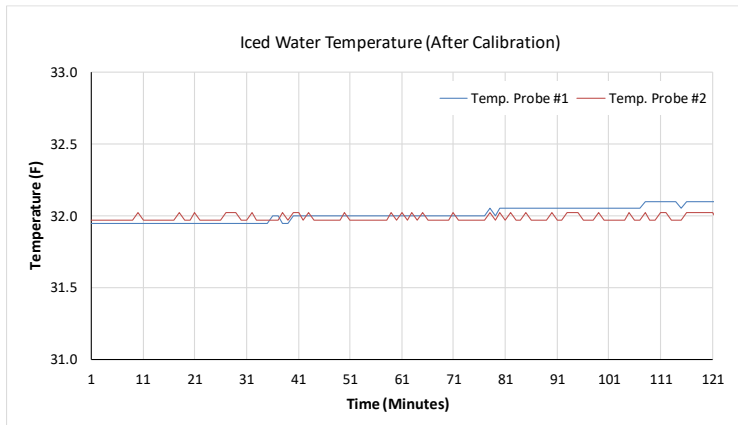


Scale and Offset

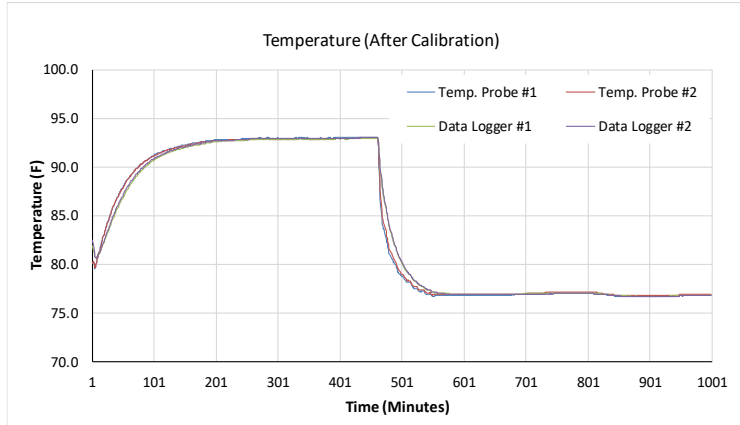
Sensor	Calibration	
	Scale	Offset
Temperature Probe #1	0.0038	-0.3645
Temperature Probe #2	-0.0045	0.4199

Reference Sensor Calibration (After Calibration)

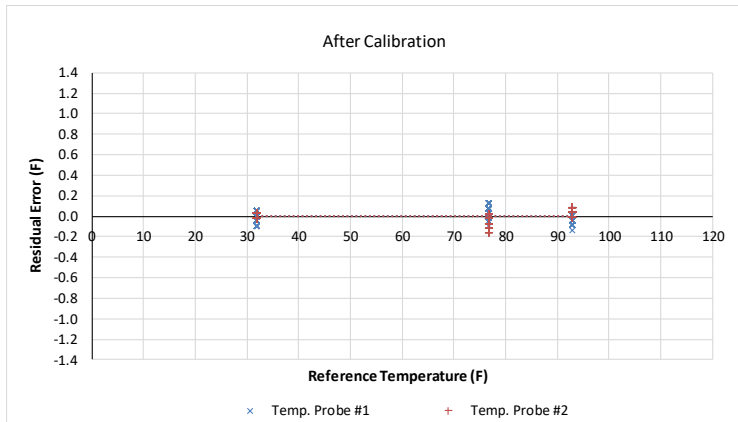
Iced Water Temperature Environment



High and Room Temperature Environments



Residual Plot

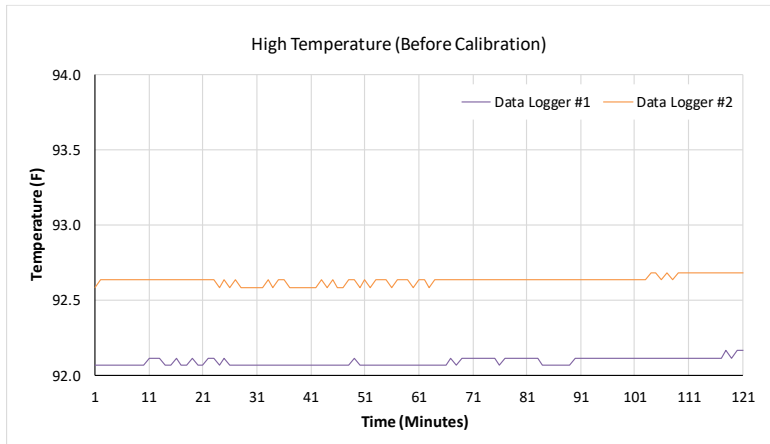


Scale and Offset

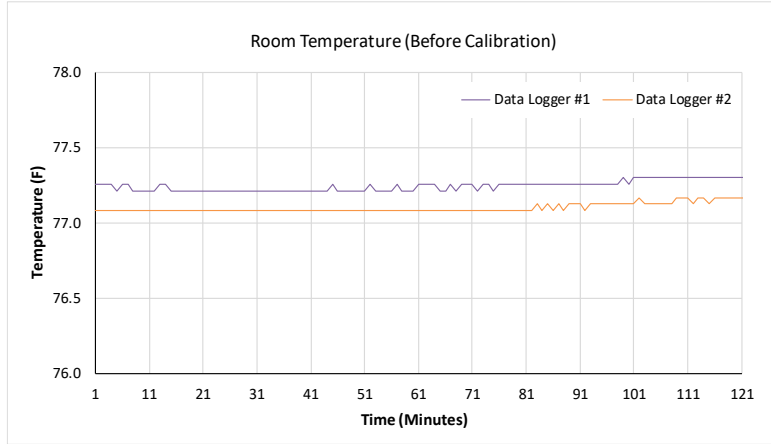
Sensor	Calibration	
	Scale	Offset
Temperature Probe #1	0.0038	-0.3645
Temperature Probe #2	-0.0045	0.4199

Other Sensor Calibration (Before Calibration)

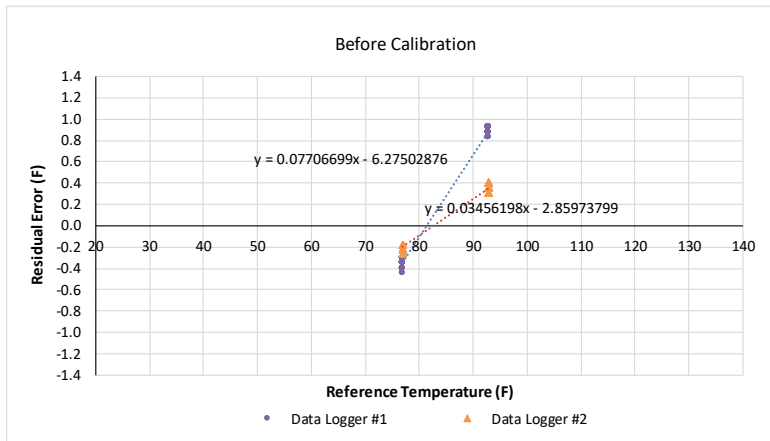
High Temperature Environment



Room Temperature Environment



Residual Plot

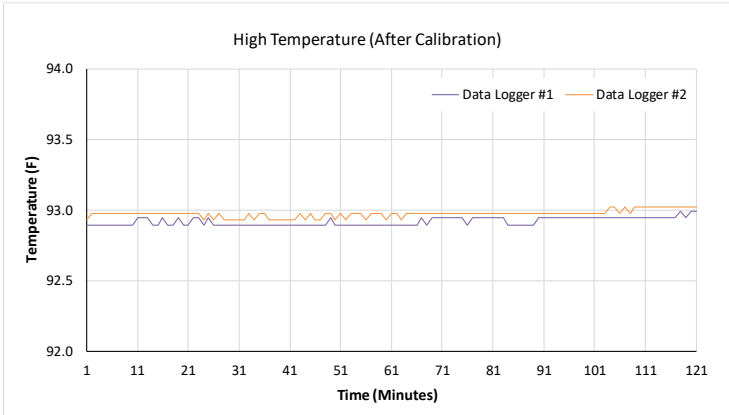


Scale and Offset

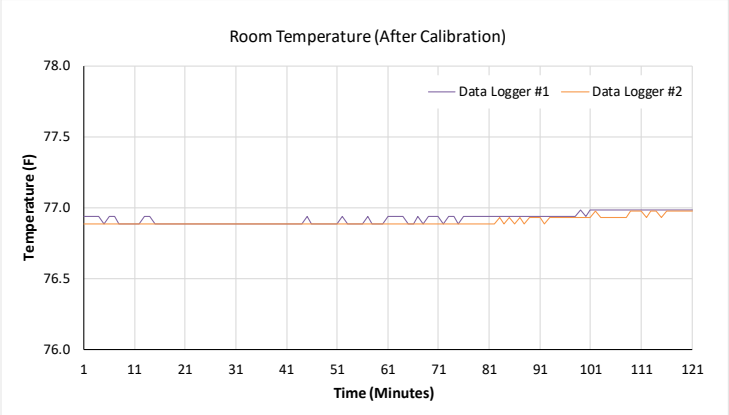
Sensor	Calibration	
	Scale	Offset
Data Logger #1	0.0771	-6.2750
Data Logger #2	0.0346	-2.8597

Other Sensor Calibration (After Calibration)

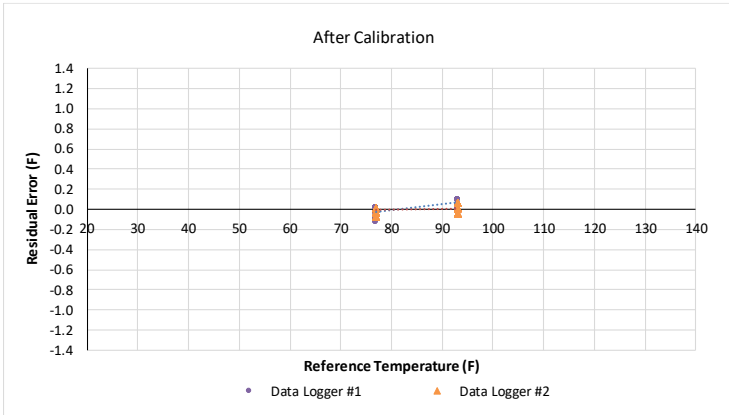
High Temperature Environment



Room Temperature Environment



Residual Plot



Scale and Offset

Sensor	Calibration	
	Scale	Offset
Data Logger #1	0.0771	-6.2750
Data Logger #2	0.0346	-2.8597